

Polypyridylruthenium(II) complexes as therapeutic agents

Author:

Gorle, Anil Kumar

Publication Date:

2015

DOI:

<https://doi.org/10.26190/unsworks/18565>

License:

<https://creativecommons.org/licenses/by-nc-nd/3.0/au/>

Link to license to see what you are allowed to do with this resource.

Downloaded from <http://hdl.handle.net/1959.4/55233> in <https://unsworks.unsw.edu.au> on 2024-05-04

Polypyridylruthenium(II) complexes as therapeutic agents

Anil K. Gorle

A thesis in fulfilment of the requirements for the degree of

Doctor of Philosophy



School of Physical, Environmental and Mathematical Sciences

University of New South Wales Canberra

August 2015

The University of New South Wales
Thesis/Dissertation Sheet

Surname or Family name: **Gorle**First name: **Anil Kumar**Abbreviation for degree as given in the University calendar: **PhD**School: **Physical, Environmental and Mathematical Sciences** Faculty: **UNSW Canberra**Title: **Polypyridylruthenium(II) Complexes as Therapeutic Agents.**

Abstract

A series of dinuclear ruthenium(II) complexes containing labile chlorido ligands (Cl-Rubb_n) have been synthesised and their potential as anticancer agents examined. Some of the Cl-Rubb_n species showed good anticancer activity against breast cancer cell lines, with the Cl-Rubb₁₂ complex being four-times more active than cisplatin. The results of this study suggest that the cytotoxicity of the dinuclear ruthenium complexes is a combination of covalent and reversible binding with DNA. A series of inert mono-, tri- and tetra-nuclear polypyridylruthenium(II) complexes have been synthesised and their potential as antimicrobial agents examined. Geometric isomers of the mononuclear complexes were separated. The minimum inhibitory concentrations (MIC) of the ruthenium(II) complexes were determined against a range of Gram positive and Gram negative bacteria. The linear tetranuclear complexes were generally more active, with MIC values < 1 μM against Gram positive bacteria. Of particular note, the cellular accumulation of the oligonuclear ruthenium complexes was greater in the Gram negative strains compared to that in the Gram positive strains. The mononuclear complexes [Ru(phen)(bb_n)]²⁺ (phen=1,10-phenanthroline) exhibited excellent activity against Gram positive bacteria, but only the *cis*-α-[Ru(phen)(bb₁₂)]²⁺ species showed good activity against Gram negative species. In particular, the *cis*-α-[Ru(phen)(bb₁₂)]²⁺ complex was two to four times more active than the *cis*-β-[Ru(phen)(bb₁₂)]²⁺ complex against the Gram negative strains. The *cis*-α- and *cis*-β-[Ru(phen)(bb₁₂)]²⁺ complexes readily accumulated in the bacteria, but significantly, showed the highest level of uptake in *P. aeruginosa*. The antimicrobial activities of a series of di-, tri- and tetra-nuclear ruthenium complexes against a wider range of clinically relevant pathogenic bacteria were examined. The toxicity of some of these complexes against eukaryotic cells was also investigated. Results of this study indicate that these complexes are highly active against Gram positive bacteria but they were less active against Gram negative bacteria. The dinuclear Rubb₁₂ complex exhibits less toxicity to liver and kidney cells when compared to the tri- and tetra-nuclear complexes. In addition, *in vivo* experiments demonstrate serum level concentrations for both Rubb₁₆ and Rubb₁₂-tetra were lower than the MIC values against Gram positive and Gram negative bacteria, with both complexes accumulating mainly in the liver and kidney after dosing.

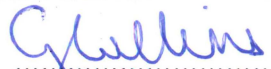
Declaration relating to disposition of project thesis/dissertation

I hereby grant to the University of New South Wales or its agents the right to archive and to make available my thesis or dissertation in whole or in part in the University libraries in all forms of media, now or here after known, subject to the provisions of the Copyright Act 1968. I retain all property rights, such as patent rights. I also retain the right to use in future works (such as articles or books) all or part of this thesis or dissertation.

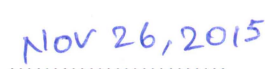
I also authorise University Microfilms to use the 350 word abstract of my thesis in Dissertation Abstracts International (this is applicable to doctoral theses only).



Signature



Witness



Date


The University recognises that there may be exceptional circumstances requiring restrictions on copying or conditions on use. Requests for restriction for a period of up to 2 years must be made in writing. Requests for a longer period of restriction may be considered in exceptional circumstances and require the approval of the Dean of Graduate Research.

FOR OFFICE USE ONLY

Date of completion of requirements for Award:

Originality Statement

ORIGINALITY STATEMENT 'I hereby declare that this submission is my own work and to the best of my knowledge it contains no materials previously published or written by another person, or substantial proportions of material which have been accepted for the award of any other degree or diploma at UNSW or any other educational institution, except where due acknowledgement is made in the thesis. Any contribution made to the research by others, with whom I have worked at UNSW or elsewhere, is explicitly acknowledged in the thesis. I also declare that the intellectual content of this thesis is the product of my own work, except to the extent that assistance from others in the project's design and conception or in style, presentation and linguistic expression is acknowledged.'

Signed 

Date NOV 26, 2015

Copyright Statement

'I hereby grant the University of New South Wales or its agents the right to archive and to make available my thesis or dissertation in whole or part in the University libraries in all forms of media, now or here after known, subject to the provisions of the Copyright Act 1968. I retain all proprietary rights, such as patent rights. I also retain the right to use in future works (such as articles or books) all or part of this thesis or dissertation.

I also authorise University Microfilms to use the 350 word abstract of my thesis in Dissertation Abstract International (this is applicable to doctoral theses only).

I have either used no substantial portions of copyright material in my thesis or I have obtained permission to use copyright material; where permission has not been granted I have applied/will apply for a partial restriction of the digital copy of my thesis or dissertation.'

Signed *G. Anil Kumar*

Date *NOV 26, 2015*

Authenticity Statement

‘I certify that the Library deposit digital copy is a direct equivalent of the final officially approved version of my thesis. No emendation of content has occurred and if there are any minor variations in formatting, they are the result of the conversion to digital format.’

Signed *G. Sridhar*

Date *NOV 26, 2015*

Acknowledgements

It gives me immense pleasure in expressing my gratitude to all the people without whom this thesis would not have been possible to accomplish. Firstly, I would like to acknowledge my supervisor Prof. Grant Collins for his incredible guidance, encouragement and advice over the past few years, without which I would not have reached this far. I am extremely grateful to him for his patience, support and lots of ideas throughout my tenure at UNSW. He has been the constant source of inspiration and encouragement. It has been wonderful working with a supervisor like him who is very excited towards science. I greatly appreciate him for generously sharing his time and expertise, as well as many long insightful discussions. I am indebted to him for his endless support professionally as well as personally.

Sincere thanks to my honorary co-supervisor Emeritus Prof. Richard Keene for his constructive suggestions during the course of my research. His dedication towards research has been a great inspiration to me and working with him was a complete privilege. His scientific advice on the synthesis and isomer separation of ruthenium metal complexes as well as his support with the writing and reviewing of the publication manuscripts and this thesis has greatly improved the quality of the outcome. I would like to thank him for his generosity, support and encouragement throughout my PhD. I can't thank him enough for all his contributions to my research.

Thanks must go to the group members at the James Cook University for their contribution to the completion of this project. Thanks to A/Prof. Jeff Warner for providing me with the lab space, equipment, technical advice and suggestions with the antimicrobial studies. Thanks to Dr. Marshall Feterl for showing me how to run *in vitro*

antimicrobial assays and *in vivo* animal studies. Thanks to Dr. Robert Kinobe for technical advice in designing the pharmacokinetic assays. Thanks also to Sebastian Primrose and Constantin Constantinoiu for their help with some assays.

The contribution of several colleagues at the University of Technology Sydney is greatly acknowledged. Thanks to Prof. Liz Harry for providing me with the lab space, equipment, technical advice and suggestions for the microscopic studies on some of my compounds. Thanks to Dr. Amy Bottomley for helping me with the design of the microscopic experiments and showing me how to run the high-magnification wide-field fluorescent microscope and process the results. Thanks to Dr. Lynne Turnbull who generously helped with the high-magnification DeltaVision OMX SIM microscopic studies. Prof. Alaina Ammit at the University of Sydney is also greatly acknowledged for her help in investigating the anticancer activity of several of my compounds.

The academic and technical members of the School of PEMS at UNSW Canberra have been tremendously helpful, in particular, thanks to A/Prof. Cliff Woodward for his valuable contributions, analysis and discussions with the microscopic studies. Thanks to Dr. Lynne Wallace for generously sharing her time and expertise in electrochemical measurements of the metal complexes. Thanks to Dr. Anthony Day for his advice and suggestions during our group meetings. I am very thankful to Dr. Barry Gray for his excellent assistance with NMR and building related matters. Thanks to Dr. Damian Buck for his help with HyperChem Software. The support and contributions from my fellow PhD student colleagues is also greatly acknowledged. I would like to thank them for the wonderful time I had in both the lab and office.

I would like to take this opportunity to thank the UNSW Canberra for the PhD scholarship and travel grants to support my research carried out at James Cook University and University of Technology Sydney. I would also like to thank the University for a PRSS travel grant to present my research at ICBIC 2013 conference in Grenoble, France.

Finally, and most importantly, I would like to express my deepest thanks to my parents, family, friends and my wife Siji for their unconditional love and support as I would not have come this far without their support. I hope they would feel proud with my accomplishments.

Abbreviations and Acronyms

AMR	Antimicrobial resistance
bb_n	bis[4(4'-methyl-2,2'-bipyridyl)]-1,n-alkane
BL	bridging ligand
bpy	2,2'-bipyridine
CAMHB	Cation-adjusted Mueller-Hinton broth
cfu/mL	Colony forming units per mL
CLSI	Clinical and Laboratory Standards Institute
COSY	Correlation spectroscopy
CT-DNA	Calf thymus deoxyribonucleic acid
DNA	Deoxyribonucleic acid
ESI-MS	Electrospray ionisation mass spectrometry
<i>fac</i>	facial
GMP	guanosine 5'-monophosphate disodium salt
HC₅₀	Concentration causing 50% haemolysis
HPLC	High-performance liquid chromatography
ICP-MS	Inductively coupled plasma mass spectrometer
IC₅₀	Concentration required to inhibit growth by 50%
IDSA	Infectious Diseases Society of America
Log P	The partition coefficient
LPS	lipopolysaccharide
MBC	Minimum bactericidal concentration
Me₂bpy	4,4'-dimethyl-2,2'-bipyridine
Me₄phen	3, 4, 7, 8-tetra-methyl-1,10-phenanthroline
<i>mer</i>	meridional

MIC	Minimum inhibition concentration
MTD	Maximum tolerated dose
mV	milli volts
NMR	Nuclear magnetic resonance
2D NMR	Two-dimensional nuclear magnetic resonance
PBS	Phosphate-buffered saline
phen	1,10-phenanthroline
ppm	parts per million
PTA	1,3,5-triaza-7-phosphatricyclo-[3.3.1.1]decane
RNA	Ribonucleic acid
ROE	Rotating frame overhauser effect
ROESY	Rotating frame overhauser spectroscopy
rpm	Revolutions per minute
Rubb_n	$[\{\text{Ru}(\text{phen})_2\}_2\{\mu\text{-bb}_n\}]\text{Cl}_4$
TLC	Thin layer chromatography
tpy	2,2':6',2''-Terpyridine
UV	Ultraviolet
UV-Vis	Ultraviolet-visible spectrophotometry
V	Volts
WHO	World Health Organisation
μM	micro molar

Citations

The research work in this thesis has been published in the following Journals:

Peer reviewed papers in international journals

1. “Multinuclear ruthenium(II) complexes as anticancer agents.” **Anil K. Gorle**, Alaina J. Ammit, Lynne Wallace, F. Richard Keene and J. Grant Collins. *New Journal of Chemistry*. 2014, 38, 4049-4059. Selected as **Front Cover** of the issue.
2. “Tri- and tetra-nuclear polypyridyl ruthenium(II) complexes as antimicrobial agents.” **Anil K. Gorle**, Marshall Feterl, Jeffrey M. Warner, Lynne Wallace, F. Richard Keene and J. Grant Collins. *Dalton Transactions*. 2014, 43, 16713-16725.
3. “RNA and DNA binding of inert oligonuclear ruthenium(II) complexes in live eukaryotic cells.” Xin Li, **Anil K. Gorle**, Tracy D. Ainsworth, Kirsten Heimann, Clifford E. Woodward, J. Grant Collins and F. Richard Keene. *Dalton Transactions*. 2015, 44, 3594-3603. {Invited contribution to the themed issue on '*Metal Interactions with Nucleic Acids*'}. Selected as **Front Cover** of the issue.
4. “Mononuclear polypyridyl ruthenium(II) complexes with high membrane permeability in Gram negative bacteria: in particular *Pseudomonas aeruginosa*.” **Anil K. Gorle**, Marshall Feterl, Jeffrey M. Warner, Sebastian Primrose, Constantin C. Constantinoiu, F. Richard Keene and J Grant Collins. *Chemistry-A European Journal*. 2015, 21, 10472-10481.

Manuscripts in preparation

1. “Polypyridyl ruthenium(II) complexes as antimicrobial agents against clinically relevant bacteria.” **Anil K. Gorle**, Xin Li, Marshall Feterl, Jeffrey M. Warner, F. Richard Keene and J. Grant Collins. Manuscript in preparation for publication.

2. “Pharmacokinetic studies of free Cucurbit(7)uril and a dinuclear ruthenium antimicrobial complex encapsulated in Cucurbit(10)uril.” F.Li, **Anil K. Gorle**, Anthony Day, F. Richard Keene and J Grant Collins. Manuscript in preparation for publication.

Conference abstract

1. “The effect of cucurbituril encapsulation on the antimicrobial properties of ruthenium(II) polypyridyl complexes.” **Anil K Gorle**, F. Li, Anthony Day, J Grant Collins and F. Richard Keene. Conference abstract published in ***Journal of Biological Inorganic Chemistry***. 2014, 19, S581-S581.

Abstract

Cancer and infectious diseases remain leading causes of death worldwide and the World Health Organisation (WHO) has identified both cancer and microbial resistance to drugs as the most important problems affecting human health. Transition-metal complexes have been widely studied for their use as anticancer and antimicrobial agents. Based upon their versatile physical and chemical properties, ruthenium complexes have been widely studied for biological applications. This thesis is aimed towards the development of polypyridylruthenium(II) complexes containing the flexible bridging ligand 'bb_n' (where bb_n = bis[4(4'-methyl-2,2'-bipyridyl)]-1,n-alkane {n = 7, 10, 12, 14 or 16}) and an investigation of their use as antimicrobial and anticancer agents.

A series of dinuclear ruthenium(II) complexes that contain labile chlorido ligands, $[\{\text{Ru}(\text{tpy})\text{Cl}\}_2\{\mu\text{-bb}_n\}]^{2+}$ (designated Cl-Rubb_n; tpy = 2,2':6',2''-terpyridine) and derivatives containing nitro substituents on the tpy ligand and/or secondary amines within the bb_n linking chain have been synthesised and their potential as anticancer agents examined. Some of the Cl-Rubb_n species showed good anticancer activity against MCF-7 and MDA-MB-231 breast cancer cell lines, with the Cl-Rubb₁₂ complex being four-times more active than cisplatin. Inclusion of nitro substituents on the tpy ligands of Cl-Rubb₁₂ resulted in significantly decreased anticancer activity. The incorporation of amine groups into the linking ligand did not increase the anticancer activity of the Cl-Rubb_n complexes. The Cl-Rubb_n complexes and those containing amine groups in the linking chain aquated at approximately the same rate, with 50% aquation within 120 minutes. By comparison, the complexes containing nitro substituents on the tpy ligand aquated extremely slowly. Cyclic voltammetry with the

model mononuclear complex $[\text{Ru}\{(\text{NO}_2)_3\text{tpy}\}(\text{Me}_2\text{bpy})\text{Cl}]^+$ $\{(\text{NO}_2)_3\text{tpy} = 4,4',4''\text{-trinitro-2,2':6',2''-terpyridine}\}$ showed that the nitro substituents exerted a strong effect on the ruthenium centre, with the anodic peak corresponding to the Ru(III/II) couple shifted positively by 300 mV compared to that from the non-nitrated parent complex $[\text{Ru}(\text{tpy})(\text{Me}_2\text{bpy})\text{Cl}]^+$. ^1H NMR studies of the reaction of the Cl-Rubb_n complexes with GMP indicated that the ruthenium complexes covalently bound the nucleotide slowly, with 33% bound in 24 hours. However, the results of this study suggest that the cytotoxicity of the dinuclear ruthenium complexes is a combination of covalent and reversible binding with DNA.

A series of inert tri- and tetra-nuclear polypyridylruthenium(II) complexes that are linked by the “bb_n” ligand (for n = 10, 12 and 16) have been synthesised and their potential as antimicrobial agents examined. The minimum inhibitory concentrations (MIC) of the ruthenium(II) complexes were determined against a range of Gram positive and Gram negative bacteria. In order to gain an understanding of the relative antimicrobial activities, the cellular uptake and water–octanol partition coefficients (log P) were determined for a selection of the ruthenium complexes. Although the trinuclear complexes were the most lipophilic based upon log P values and showed the greatest cellular uptake, the linear tetranuclear complexes were generally more active, with MIC values < 1 µM against the Gram positive bacteria. Similarly, although the non-linear tetranuclear complexes were slightly more lipophilic and were taken up to a greater extent by the bacteria, they were consistently less active than their linear counterparts. Of particular note, the cellular accumulation of the oligonuclear ruthenium complexes was greater in the Gram negative strains compared to that in the Gram positive strains. The results demonstrate that the lower antimicrobial activity of polypyridylruthenium(II) complexes towards Gram negative bacteria, particularly

Pseudomonas aeruginosa (*P. aeruginosa*), is not strongly correlated to the cellular accumulation but rather to a lower intrinsic ability to kill the Gram negative cells.

The antimicrobial activities of a series of di-, tri- and tetra-nuclear ruthenium complexes against a wider range of clinically relevant pathogenic bacteria were examined. The toxicity of some of these complexes against eukaryotic cells was also investigated. Results of this study confirmed that these complexes are highly active against Gram positive bacteria but they were less active against Gram negative bacteria. The dinuclear Rubb_{12} complex exhibits less toxicity to liver and kidney cells when compared to the tri- and tetra-nuclear complexes. In addition, the *in vivo* pharmacokinetic profiles and tissue accumulation of the highly active complexes Rubb_{16} and Rubb_{12} -tetra were established using a healthy animal model. The *in vivo* experiments demonstrate lower serum level concentrations of both Rubb_{16} and Rubb_{12} -tetra than the MIC values against Gram positive and Gram negative bacteria, and both the complexes accumulated mainly in the liver and kidneys after dosing.

Mononuclear ruthenium(II) complexes containing “ bb_n ” as a tetradentate ligand, rather than as a linking ligand for the oligonuclear complexes, (for $n = 10$ and 12) have been synthesised and their geometric isomers separated. All $[\text{Ru}(\text{phen})(\text{bb}_n)]^{2+}$ ($\text{phen}=1,10\text{-phenanthroline}$) complexes exhibited excellent activity against Gram positive bacteria, but only the *cis- α* - $[\text{Ru}(\text{phen})(\text{bb}_{12})]^{2+}$ species showed good activity against Gram negative species. In particular, the *cis- α* - $[\text{Ru}(\text{phen})(\text{bb}_{12})]^{2+}$ complex was two to four times more active than the *cis- β* - $[\text{Ru}(\text{phen})(\text{bb}_{12})]^{2+}$ complex against the Gram negative strains. The *cis- α* - and *cis- β* - $[\text{Ru}(\text{phen})(\text{bb}_{12})]^{2+}$ complexes readily accumulated in the bacteria, but significantly, showed the highest level of uptake in *P. aeruginosa*. Furthermore, the accumulation of the *cis- α* - and *cis- β* - $[\text{Ru}(\text{phen})(\text{bb}_{12})]^{2+}$ complexes in *P. aeruginosa* was considerably greater than in *Escherichia coli* (*E. coli*).

The uptake of the *cis*- α -[Ru(phen)(bb₁₂)]²⁺ complex into live *P. aeruginosa* was confirmed by fluorescence microscopy. The water/octanol partition coefficients (log P) were determined to gain an understanding of the relative cellular uptake. The *cis*- α - and *cis*- β -[Ru(phen)(bb₁₂)]²⁺ complexes exhibited relatively strong binding to DNA ($K_b \approx 10^6 \text{ M}^{-1}$), but no significant difference between the geometric isomers was observed.

Table of Contents

<i>Thesis/Dissertation Sheet</i>	<i>ii</i>
<i>Originality Statement</i>	<i>iii</i>
<i>Copyright Statement</i>	<i>iv</i>
<i>Authenticity Statement</i>	<i>v</i>
<i>Acknowledgements</i>	<i>vi</i>
<i>Abbreviations and Acronyms</i>	<i>ix</i>
<i>Citations</i>	<i>xi</i>
<i>Abstract</i>	<i>xiii</i>
<i>Table of Contents</i>	<i>xvii</i>
CHAPTER 1	1
1. Introduction	1
1.1. Metals in medicine	2
1.2. Platinum-based drugs	3
1.3. Ruthenium-based drugs	8
1.3.1. Labile ruthenium complexes	9
1.3.2. Inert polypyridylruthenium(II) complexes	13
1.3.2.1. Mononuclear polypyridylruthenium(II) complexes	13
1.3.2.2. Oligonuclear polypyridylruthenium(II) complexes	19
1.4. Aims of the project	25
1.5. Thesis outline	28
1.6. References	30
CHAPTER 2	39
2. Multinuclear ruthenium(II) complexes as anticancer agents	39

2.1.	Introduction.....	40
2.2.	Experimental.....	43
2.2.1.	Physical measurements	43
2.2.2.	Materials and methods	43
2.2.3.	Cyclic voltammetry	43
2.2.4.	Cytotoxicity assays	44
2.2.5.	Synthesis	44
2.3.	Results.....	54
2.3.1.	Synthesis	54
2.3.2.	Anticancer activity	56
2.3.3.	Aquation and GMP binding	59
2.3.4.	Cyclic voltametry of $[\text{Ru}\{(\text{NO}_2)_3\text{tpy}\}(\text{Me}_2\text{bpy})\text{Cl}]^+$	63
2.4.	Discussion.....	65
2.5.	Conclusions.....	68
2.6.	References.....	68
CHAPTER 3.....		73
3.	Tri- and tetra-nuclear polypyridylruthenium(II) complexes as antimicrobial agents.....	73
3.1.	Introduction.....	74
3.2.	Experimental.....	77
3.2.1.	Physical measurements	77
3.2.2.	Materials and methods	77
3.2.3.	Bacterial strains	78
3.2.4.	MIC and MBC determination	78
3.2.5.	Cellular uptake	79

3.2.6.	Lipophilicity (log P) determination.....	80
3.2.7.	Time-kill curve studies	80
3.2.8.	Electrochemistry	81
3.2.9.	Wide-field fluorescent microscopy	81
3.2.10.	Synthesis of metal complexes	82
3.3.	Results.....	93
3.3.1.	Synthesis	93
3.3.2.	Electrochemistry	97
3.3.3.	Antimicrobial activity	98
3.3.4.	Log P	103
3.3.5.	Cellular accumulation	105
3.3.6.	Time-kill curve examination	106
3.3.7.	Intra-bacterium localisation by wide-field fluorescent microscopy....	108
3.4.	Discussion.....	110
3.5.	Conclusions.....	113
3.6.	References.....	114
CHAPTER 4.....		119
4.	Clinical potential of polypyridylruthenium(II) complexes.....	119
4.1.	Introduction.....	120
4.2.	Experimental	122
4.2.1.	Selection of bacteria	122
4.2.2.	Minimum inhibitory concentration (MIC) determination.....	124
4.2.3.	Eukaryotic cell culture	124
4.2.4.	Cytotoxicity	124
4.2.5.	Animals	125

4.2.6.	Pharmacokinetic studies	125
4.2.7.	Sampling	125
4.2.8.	Sample preparation and digestion	126
4.2.9.	Concentration determination of ruthenium metal by ICP-MS	126
4.3.	Results.....	127
4.3.1.	Antimicrobial activity	127
4.3.2.	Toxicity against eukaryotic cells.....	131
4.3.3.	Time-course cytotoxicity assays	132
4.3.4.	Pharmacokinetic studies.....	134
4.3.5.	Tissue distribution and accumulation of Rubb ₁₆ and Rubb ₁₂ -tetra as a function of time.	135
4.4.	Discussion	137
4.5.	Conclusions.....	142
4.6.	References.....	143
CHAPTER 5		145
5. Mononuclear polypyridylruthenium(II) complexes with high membrane permeability in Gram negative bacteria - in particular Pseudomonas aeruginosa.....		145
5.1.	Introduction.....	146
5.2.	Experimental	150
5.2.1.	Physical measurements	150
5.2.2.	Materials and methods	150
5.2.3.	Bacterial strains	151
5.2.4.	MIC determination	151
5.2.5.	DNA binding studies.....	151

5.2.6.	Cellular uptake	151
5.2.7.	Epifluorescent microscopy	152
5.2.8.	Lipophilicity (log P) determination.....	152
5.2.9.	Syntheses.....	152
5.3.	Results.....	156
5.3.1.	Synthesis	156
5.3.2.	Geometric isomers	157
5.3.3.	Antimicrobial activity	160
5.3.4.	Log P	161
5.3.5.	Cellular accumulation	162
5.3.6.	Epifluorescence microscopy	164
5.3.7.	Interaction with DNA.....	166
5.4.	Discussion.....	168
5.5.	Conclusions.....	171
5.6.	References.....	172
CHAPTER 6.....		175
6.	Conclusions and Future Perspectives.....	175
6.1.	Conclusions.....	176
6.2.	Future perspectives	180
6.3.	References.....	182
APPENDIX		183

CHAPTER 1

Introduction

1.1. *Metals in medicine*

Despite of all the advances in modern medicine, cancer and microbial infections still remain major causes of death worldwide. The World Health Organisation (WHO) has identified both cancer and microbial resistance to drugs as the most important problems affecting human health.¹⁻³

According to WHO,

- Cancer is a leading cause of death worldwide accounting for 8.2 million deaths in 2012 and it is expected that the number of new cases will rise by about 70% over the next two decades (from 14 million in 2012 to 22 million within the next two decades).¹
- Antimicrobial resistance (AMR) threatens the effective prevention and treatment of an ever-increasing range of infections caused by bacteria.⁴ AMR is present in all parts of the world and new mechanisms of resistance are emerging and spreading globally.² WHO indicates antimicrobial resistance is an increasingly serious threat to global health that requires action across all government sectors and society.²

Although organic drugs have been traditionally used for the majority of diseases, medicinal inorganic chemistry offers real possibilities for the discovery of truly novel drugs with new mechanisms of action. Precious metals have been used for medicinal purposes for at least 3500 years, where for example, records show that gold was included in a variety of medicines in Arabia and China.^{5,6} An organoarsenic compound, arsphenamine (salvarsan) – as shown in Figure 1.1 – developed by Ehrlich and co-workers in 1909, was the first chemotherapeutic agent for the treatment of syphilis.⁷

Metals – in particular, transition metals – offer potential advantages over the more common organic-based drugs, including a wide range of coordination numbers, geometries, accessible redox states, 'tune-ability' of the thermodynamics and kinetics of ligand substitution, and a wide structural diversity.⁸ Many metal-based drugs have been approved for clinical use and currently there are a significant number of metal-based drugs that are undergoing clinical trials.⁹

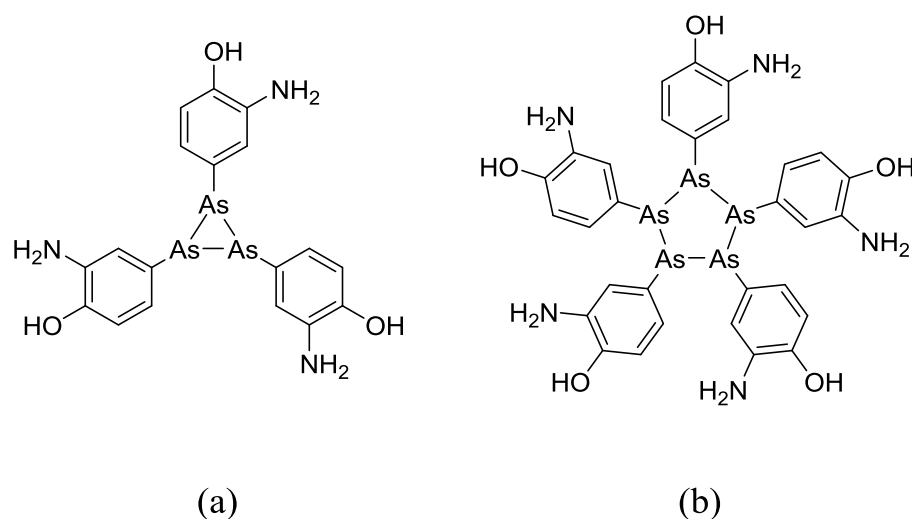


Figure 1.1. Mixture of (a) and (b) found in the crystal structure of the metal-based therapeutic agent arsphenamine.

1.2. *Platinum-based drugs*

In 1844, the Italian chemist Michele Peyrone reported the discovery of a chemical substance which later become known as Peyrone's salt.¹⁰ The molecular structure of the salt was then determined by another chemist Alfred Werner, in 1893, as part of his 1913 Nobel Prize-winning work.^{10,11} However, it was not until 1965 that the biological activity of Peyrone's salt was discovered by the physicist, Barnett Rosenberg, after

which the substance became known as cisplatin, *cis*-diamminedichloridoplatinum(II) (see Figure 1.2).¹²⁻¹⁴ Rosenberg reported that treatment of *Escherichia coli* (*E. coli*) bacteria with cisplatin resulted in continued bacterial growth; however, cell division was stopped resulting in long filaments of bacteria, indicating that the platinum complex affected the growth of bacteria.¹³ The platinum complex was subsequently introduced into clinical practice and became one of the most successful anticancer drugs of all time.¹⁵⁻¹⁸ Cisplatin was the first platinum-based drug to be approved by the U.S Food and Drug Administration for the clinical use in 1978.¹⁶

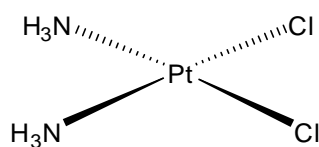


Figure 1.2. Anticancer platinum complex cisplatin.

Even after 30 years of clinical use, cisplatin is still one of the best and most widely-used anticancer drugs in the clinic and it can be used alone or in combination with other drugs to treat different types of cancer.^{16,17} Cisplatin is mainly used in the treatment of ovarian, testicular, head and neck, bladder, lung, cervical and lymphoma cancers.^{16,18} Cisplatin, as shown in Figure 1.2, is a square planar complex that forms adducts with DNA, through a covalent reaction. Formation of cisplatin-DNA adducts results in inhibition of DNA replication, blocks transcription by RNA polymerase II and triggers programmed cell death or apoptosis.¹⁹ Despite the success of cisplatin, it has several disadvantages that include severe toxicity such as nephrotoxicity, neurotoxicity and emetogenesis.²⁰⁻²⁵ The toxic side effects of cisplatin limit the dose that can be given to patients.²⁶ The majority of human cancers have a natural resistance to treatment with

cisplatin, while others respond to the treatment initially but become resistant after a period of time.^{27,28} Furthermore because of its limited solubility in aqueous solutions, cisplatin is administered intravenously, which is another disadvantage of the drug. These drawbacks have been the driving force for the development of improved platinum-based antitumour drugs.²⁹

Over the last thirty years much interest has focused on developing cisplatin analogues that are less toxic and/or are active against cisplatin-resistant cell lines.²⁷ Since the introduction of cisplatin, hundreds of platinum complexes have been synthesised and screened as potential antitumour agents.³⁰ Many complexes have entered human clinical trials, but of these only two derivatives – known as carboplatin and oxaliplatin, shown in Figure 1.3 – have been approved by the U.S. FDA for worldwide clinical use.^{16,17,27,31-33} In addition to these two complexes, another platinum complex, nedaplatin, has also been approved for clinical use in Japan (see Figure 1.3 c).³⁴

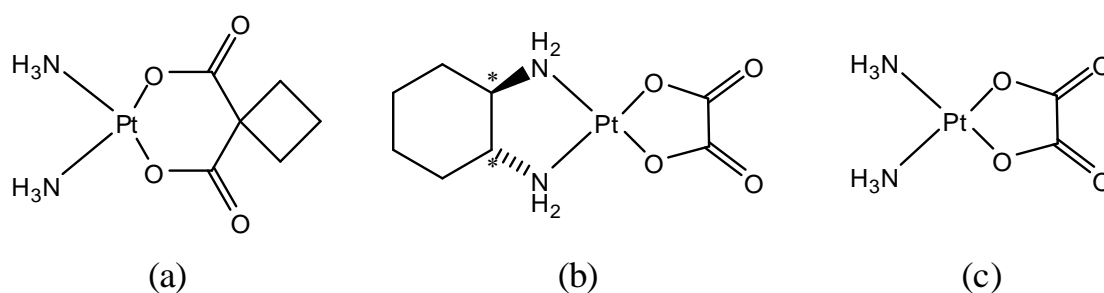


Figure 1.3. Platinum-based anticancer drugs, (a) carboplatin, (b) oxaliplatin and (c) nedaplatin.

Although carboplatin has shown lower toxicity levels than cisplatin and it can be used at much higher doses, it is still only active in the same range of tumours as cisplatin.³⁴ Despite the success of cisplatin and its analogues there are still some

problems with these mononuclear platinum complexes; in particular, drug resistance and side effects have limited their clinical utility.³² These limitations have prompted a search for more effective and less toxic metal-based antitumour agents. In order to achieve anticancer activity in a wide range of cell lines, and also to overcome both natural and acquired resistance in human cancer cell lines, research has focused on the development of multinuclear platinum complexes that can bind to DNA in a fundamentally different manner to cisplatin.³⁵⁻³⁹ Multinuclear platinum complexes, as shown in Figure 1.4, contain two or more platinum centres that can covalently bind to DNA to give a different range of adducts, and represent a completely new paradigm for platinum-based anticancer complexes. These platinum complexes are capable of forming a different range of DNA adducts and can therefore display an alternate spectrum of anticancer activity compared to cisplatin and its analogues.^{35,36}

Several multinuclear platinum complexes have been synthesised and tested for their activity in a range of cancer cell lines. Of all the complexes tested, the trinuclear complex BBR3464 entered clinical trials based on successful *in vitro* and *in vivo* trials. The dinuclear complexes BBR3571, BBR3610 and BBR3611 were also found to be highly cytotoxic.^{35,40,41} BBR3464 is much more active than cisplatin in most cancer cell lines and is also capable of overcoming cisplatin resistance.^{40,42,43} However, because of its degradation in the blood stream by thiol-containing proteins, BBR3464 was removed from clinical trials.^{40,41,43-45}

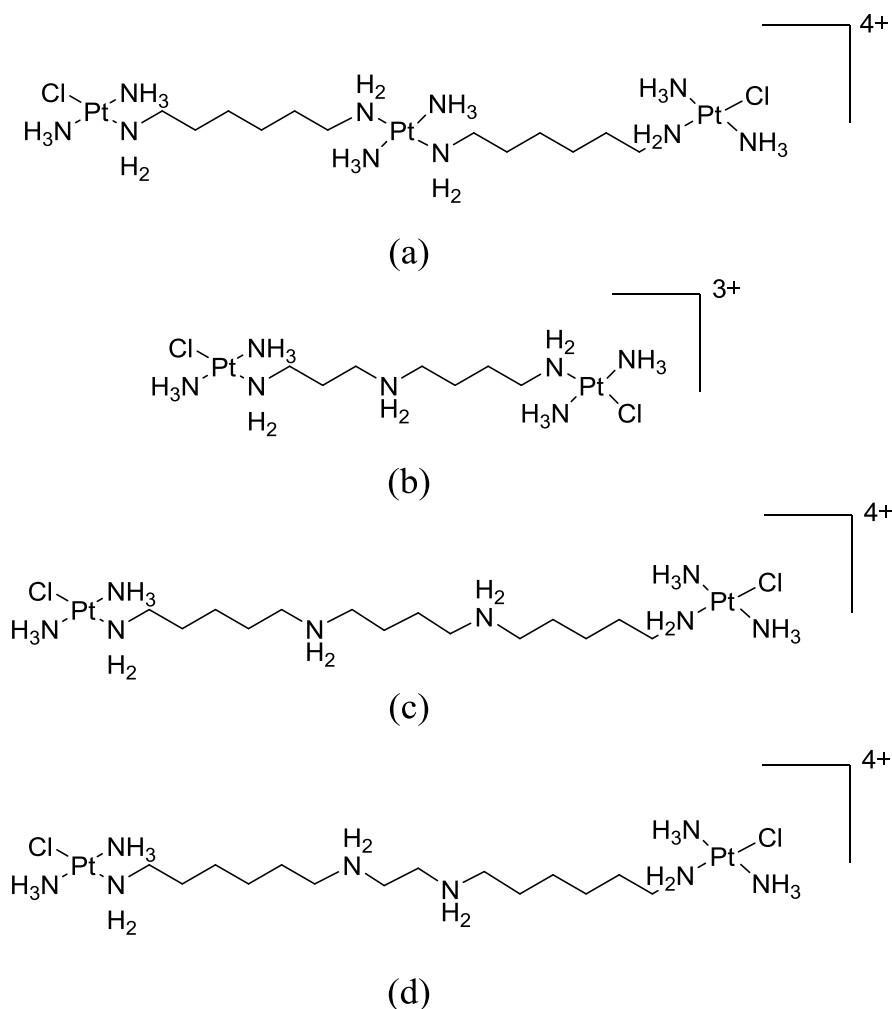


Figure 1.4. Multinuclear platinum complexes, (a) BBR3464, (b) BBR3571, (c) BBR3610 and (d) BBR3611.

Although platinum-based drugs have been used successfully for the treatment of many types of cancer, the problems associated with these drugs have limited their clinical use. Hence there is a need for the development of metal complexes that have different modes of action compared to platinum-based therapeutic drugs. As a consequence, complexes based on other metals such as gold, iron, titanium, gallium, osmium, ruthenium etc., have been investigated for their possible applications as antitumour drugs.⁴⁶⁻⁵¹ One of the most promising metals is ruthenium, and there has recently been significant interest in using ruthenium as an alternative to platinum.⁵⁰⁻⁵⁶

1.3. Ruthenium-based drugs

Efforts were made to break the "cisplatin design rule" and explore other transition metal-based antitumour agents. Ruthenium complexes have attracted much interest, due in part to the stable, well characterised and predictable structures that can be produced through judicious choice of ligands.^{49,50,53,56-58} The three main properties that potentially make ruthenium compounds well suited for medicinal applications are:

- i. The rate of ligand exchange.
- ii. The range of accessible oxidation states.
- iii. The ability of ruthenium to mimic iron in binding to certain biological molecules.

Ligand exchange can be an important determinant of biological activity. Ruthenium complexes have been increasingly recognised as alternative drugs to cisplatin for cancer chemotherapy as they demonstrate similar ligand exchange kinetics to the clinically approved platinum(II) drugs, and display low toxicity.⁵⁹ Ruthenium offers a range of oxidation states (Ru^{II} , Ru^{III} and Ru^{IV}) which are accessible under physiological conditions, a significant feature which can be exploited to increase the activity of the drugs.^{55,58} The potential ability of ruthenium to mimic iron in binding to various biomolecules, such as human serum albumin and the iron-transport protein transferrin, may aid a more effective delivery of ruthenium complexes to cancer cells without being modified.^{55,60} Alternatively, the biochemical changes that accompany cancer alter the physiological environment, enabling ruthenium complexes to be selectively activated in cancer tissues – for example, the Ru^{III} complex, NAMI-A, is converted into the more active Ru^{II} complex *in vivo*.^{49,60,61} Due to the differing ligand geometry compared to

the square-planar platinum complexes, ruthenium compounds can bind to DNA in a different manner to cisplatin and its analogues.^{60,62} Thus, ruthenium compounds could offer significant potential over the platinum(II) complexes that are currently used in the clinic, possessing unique features such as reduced toxicity, a novel mechanism of action, the prospect of non-cross-resistance, and a different spectrum of activity.^{56-58,63} In other words, the chemical properties could make ruthenium compounds well suited for medicinal applications.

1.3.1. *Labile ruthenium complexes*

Many ruthenium complexes have been evaluated for the treatment of both cancer and bacterial infectious diseases.^{61,64-68} After the discovery of the antitumour potential of ruthenium red, complexes containing chlorido and ammine ligands such as *cis*-[RuCl₂(NH₃)₄]Cl, *fac*-[RuCl₃(NH₃)₃] and *trans*-[RuCl₄(Im)₂](HIm) were the first ruthenium complexes to be studied for anticancer activity.^{69,70} However, while this class of complexes showed good activity, the water solubility of *fac*-[RuCl₃(NH₃)₃] was not sufficient for the pharmaceutical use.^{49,71} The tetrachlorido ruthenium complex, *trans*-[RuCl₄(Im)₂](HIm) (where Im = imidazole), exhibited good *in vivo* activity against platinum-resistant colorectal tumours.⁷² Another class of ruthenium complexes with dimethyl sulfoxide and chlorido ligands, particularly, *cis*- and *trans*-[RuCl₂(DMSO)₄] demonstrated lower levels of toxicity than the platinum complexes.^{60,72} The dimethyl sulfoxide ligands enhanced their selectivity for solid tumour metastases but also lowered their activity compared to cisplatin.

The first real breakthrough for ruthenium complexes as therapeutic agents was the discovery of two ruthenium(III) complexes, *trans*-[Ru(Im)(DMSO)Cl₄](HIm) (NAMI-A) and *trans*-[Ru(Ind)₂Cl₄](HInd) (KP1019, where Ind = Indazole; see Figure

1.5 a, b), which have entered clinical trials based on their excellent anticancer properties. Both NAMI-A and KP1019 are active against a number of tumour models, in particular against platinum-resistant colorectal autochthonous tumours.^{61,64,73,74} It is believed that the activity of these ruthenium(III) compounds is dependent on the *in vivo* reduction to the more reactive ruthenium(II) species.^{61,64,75} Much work has also focused on the anticancer potential of the well known “half-sandwich” Ru(II)-arene and RAPTA-C complexes (see Figure 1.5 c, d). The half-sandwich Ru(II)-arene complexes offer much scope for design with the potential to change the ligands and enable modifications of thermodynamic and kinetic parameters of the ligands to obtain better activity. Some of these complexes display promising *in vitro* and *in vivo* anticancer activity.⁷⁶ Although the RAPTA-C complex has low *in vitro* cytotoxicity, it shows selectivity towards tumours *in vivo*.^{77,78} In general, RAPTA-C complexes contain a face-capping arene, two labile chlorido ligands and a PTA ligand (where PTA = 1,3,5-triaza-7-phosphatricyclo-[3.3.1.1]decane) which imparts biologically favourable aqueous solubility to the compounds.⁵⁶

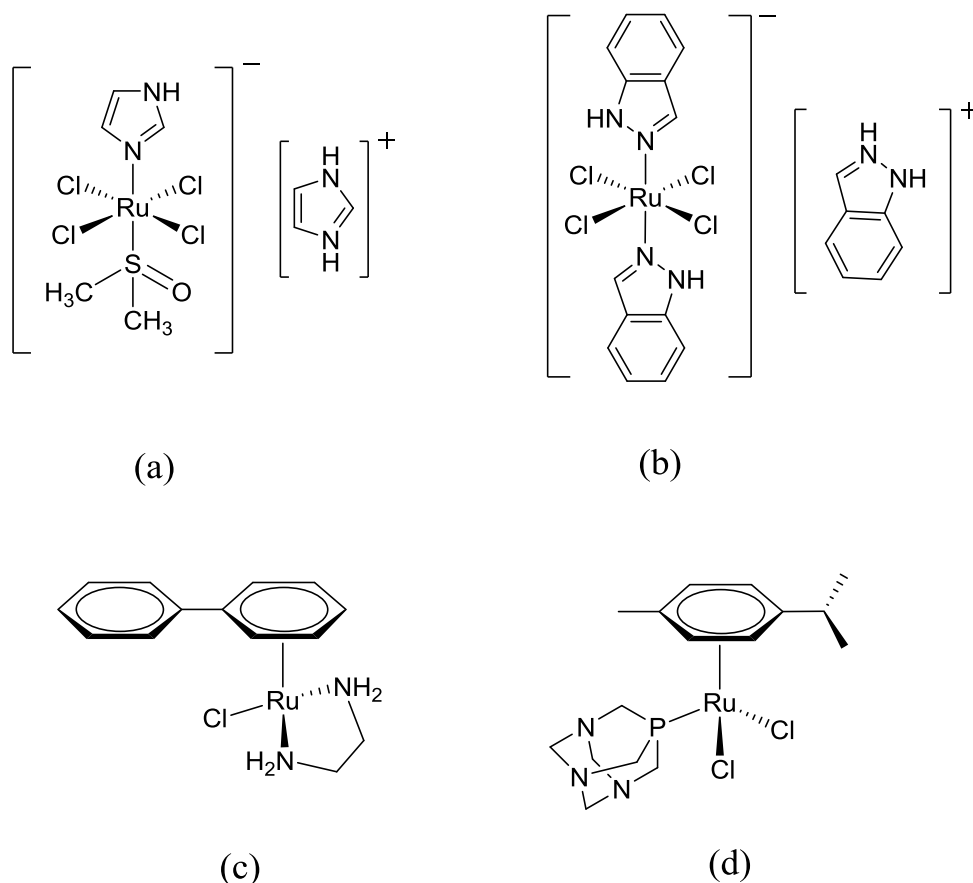


Figure 1.5. Anticancer ruthenium complexes, (a) NAMI-A, (b) KP1019, (c) half-sandwich Ru(II)-arene complex and (d) RAPTA-C.

Due to the success of ruthenium-based complexes as anticancer agents, there has been a significant interest towards the investigation of ruthenium complexes as antimicrobial agents. The chlorido and the corresponding aqua derivatives of mononuclear half-sandwich complexes, $[(p\text{-cymene})\text{RuCl}(\text{bpmo})](\text{ClO}_4)$ and $[(p\text{-cymene})\text{RuCl}(\text{bpms})](\text{PF}_6)$ containing bpmo and bpms ligands {where bpmo = 2-methoxyphenyl-bis(3,5-dimethylpyrazol-1-yl)methane and bpms = 2-methylthiophenyl-bis(3,5-dimethylpyrazol-1-yl)methane} have been tested for their antimicrobial activity against *E. coli* and *Bacillus subtilis* (*B. subtilis*).⁶⁷ The observed activity was higher for the aqua derivatives when compared to the chlorido derivatives. In addition, the aqua complexes have shown good activities against kanamycin-, ampicillin- and

chloramphenicol-resistant *E. coli* strains.⁶⁷ Hacıoglu and co-workers have developed ruthenium(II) complexes containing cyclotriphosphazene ligands bearing 3-pyridyloxy moieties.^{79,80} These complexes showed moderate to good activities (MIC = 6.25 to 50 µg/ml, where MIC = minimum inhibitory concentration) against Gram positive and Gram negative bacteria. More encouragingly, the complex containing a methyl substituent (2-CH₃, 3-pyridyloxy) exhibited promising activities against Gram negative bacteria with MICs of 6.25 µg/ml against both *E. coli* and *Klebsiella pneumonia* (*K. pneumonia*).⁸⁰ Furthermore, these complexes showed good antifungal activities with MICs of 3.1 to 12.5 µg/ml. In all the cases, ruthenium complexation enhanced the activities of the free ligands. Organometallic ruthenium(II) complexes, [Ru(HL)(CH₃CN)(CO)(EPh₃)₂] (where HL = 4-oxo-4*H*-pyran-2,6-dicarboxylic acid) developed by Natarajan and co-workers have been examined for antibacterial and antifungal activities. Although these complexes displayed better activities than some of the previously reported organometallic compounds, they only showed moderate activities against Gram positive and Gram negative bacteria.⁸¹

Some of the above ruthenium complexes have shown promising *in vitro* and *in vivo* activity.^{61,64,76-80} However, the study of their mode of action with biomolecules like DNA, RNA and protein is at an early stage. Since all the above complexes have labile ligands (e.g. chlorido) on the ruthenium centre, they could react with DNA or other biomolecules through a covalent reaction to form an adduct. However, ruthenium complexes without labile ligands (inert ruthenium complexes) can also interact with biomolecules through a range of intermolecular forces.

1.3.2. *Inert polypyridylruthenium(II) complexes*

Recently there has been growing interest in the potential of inert (i.e. they do not contain labile ligands) polypyridyl ruthenium(II) complexes as therapeutic agents.^{54,82-84} These complexes are chemically inert and do not change their structure under physiological conditions and are kinetically stable in strong acids and bases. Inert ruthenium complexes, for example, see Figure 1.6, have been shown to interact with DNA reversibly.⁶² Due to the intermolecular interactions between DNA and the ruthenium complex, the complex could bind to DNA for a period of time, potentially blocking the cancer cell growth by stopping its replication.^{62,84} These polypyridylruthenium(II) complexes are readily synthesised and in many cases can be resolved into their enantiomeric forms (Δ and Λ isomers) if they are chiral and can consequently exhibit enantiomeric differences in their binding to chiral biological receptors like DNA, RNA and proteins.⁸⁵ For example, Dwyer and his co-workers first identified the different biological activity for the Δ and Λ isomers of $[\text{Ru}(\text{phen})_3]^{2+}$.⁸⁶ Many inert ruthenium(II) complexes also have useful luminescence spectroscopic properties which make them ideal diagnostic agents.⁸⁷ Barton and co-workers reported the first example of using a ruthenium complex, $[\text{Ru}(\text{phen})_2(\text{dppz})]^{2+}$ (where dppz = dipyrido[3,2-*a*:2',3'-*c*]phenazine) as a light-switching DNA probe.⁸⁸ Although extensive research has been carried out on polypyridylruthenium(II) complexes as DNA binding agents, a focus on their biological properties is becoming an area of interest.

1.3.2.1. *Mononuclear polypyridylruthenium(II) complexes*

There has been considerable recent interest in the anticancer properties of mononuclear polypyridylruthenium(II) complexes. Promising anticancer properties of mononuclear

polypyridylruthenium(II) complexes containing a β -carboline ligand (β -carboline is an alkaloid with broad spectrum of biological functions and can intercalate with DNA; see Figure 1.6 a) were reported by Xu and co-workers.⁸⁹ These complexes were tested against HepG2, HeLa, MCF-7 and MCF-10 cell lines, and one of the complexes was found to have better antiproliferative activity than cisplatin. Dyson and co-workers have reported the anticancer activities of mononuclear ruthenium complexes containing substituted 2,2'-bipyridyl ligands against A2780 and cisplatin-resistant A2780cisR cell lines. The more lipophilic complex, $[\text{Ru}(\{4,4'\text{-diethylamine}\}_2\text{bpy})_3]^{2+}$, (see Figure 1.6 b) was found to be highly active with an $\text{IC}_{50} < 1 \mu\text{M}$, whereas the less lipophilic complexes (see Figure 1.6 c, d) were inactive with $\text{IC}_{50}\text{s} > 150 \mu\text{M}$.⁹⁰ A mononuclear ruthenium complex containing an extended aromatic ligand, $[\text{Ru}(\text{bpy})_2(\text{dppn})]^{2+}$ (where $\text{dppn} = \text{benzo}[i]\text{dipyrido}[3,2\text{-}a:2',3'\text{-}c]\text{phenazine}$, see Figure 1.7 a) developed by Wolf and co-workers has shown promising anticancer activity with an IC_{50} of $3.3 \mu\text{M}$ against the breast cancer cell line MCF-7, with the high activity of this complex related to its ability to make modifications to cell membrane function and cell adhesion properties.⁹¹ In another study, Wong and co-workers have developed a potent antiproliferative agent, $[\text{Ru}(\text{phen})_2(p\text{-MOPIP})]^{2+}$ (where $p\text{-MOPIP} = 2\text{-(4-methoxyphenyl)-1}H\text{-imidazo}[4,5\text{-}f][1,10]\text{phenanthroline}$, see Figure 1.7 b) that was able to induce mitochondria-mediated and caspase-dependent apoptosis in human cancer cells.⁹² Recently, Thomas and co-workers have demonstrated the multifunctional ability of mononuclear polypyridylruthenium(II) complexes (see Figure 1.7 c, d), as cellular DNA imaging agents and also as active compounds against cancer cell lines.⁹³ The activity of these complexes was comparable with cisplatin. Furthermore, the complex with the 1,10-phenanthroline ligand displayed an *in vitro* DNA light-switch effect through an intercalative DNA binding mode.⁹³

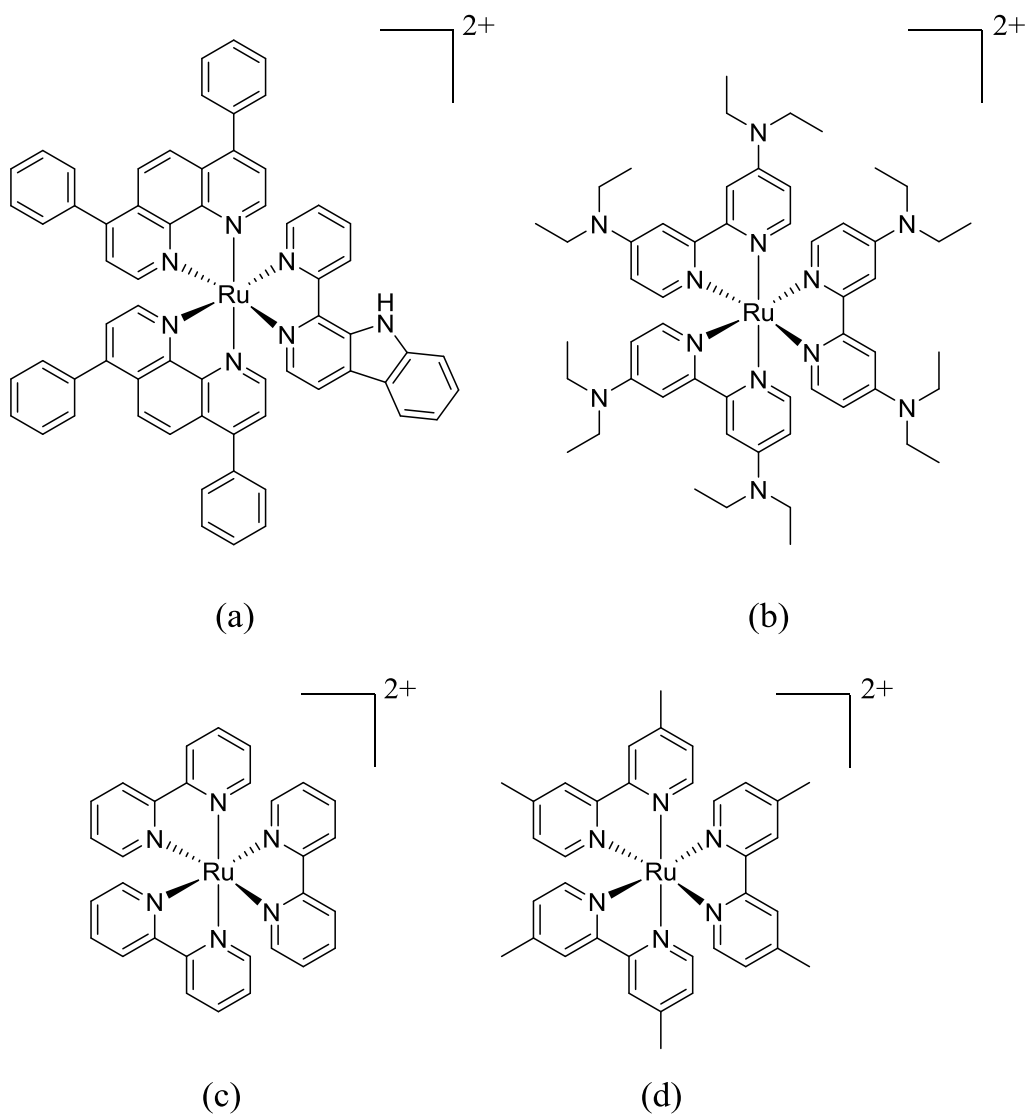


Figure 1.6. Mononuclear polypyridylruthenium(II) complexes, (a) $[\text{Ru}(4,9\text{-Ph}_2\text{phen})_2(\beta\text{-carboline})]^{2+}$, (b) $[\text{Ru}(\{4,4'\text{-diethylamine}\}_2\text{bpy})_3]^{2+}$, (c) $[\text{Ru}(\text{bpy})_3]^{2+}$ and (d) $[\text{Ru}(4,4'\text{-Me}_2\text{bpy})_3]^{2+}$.

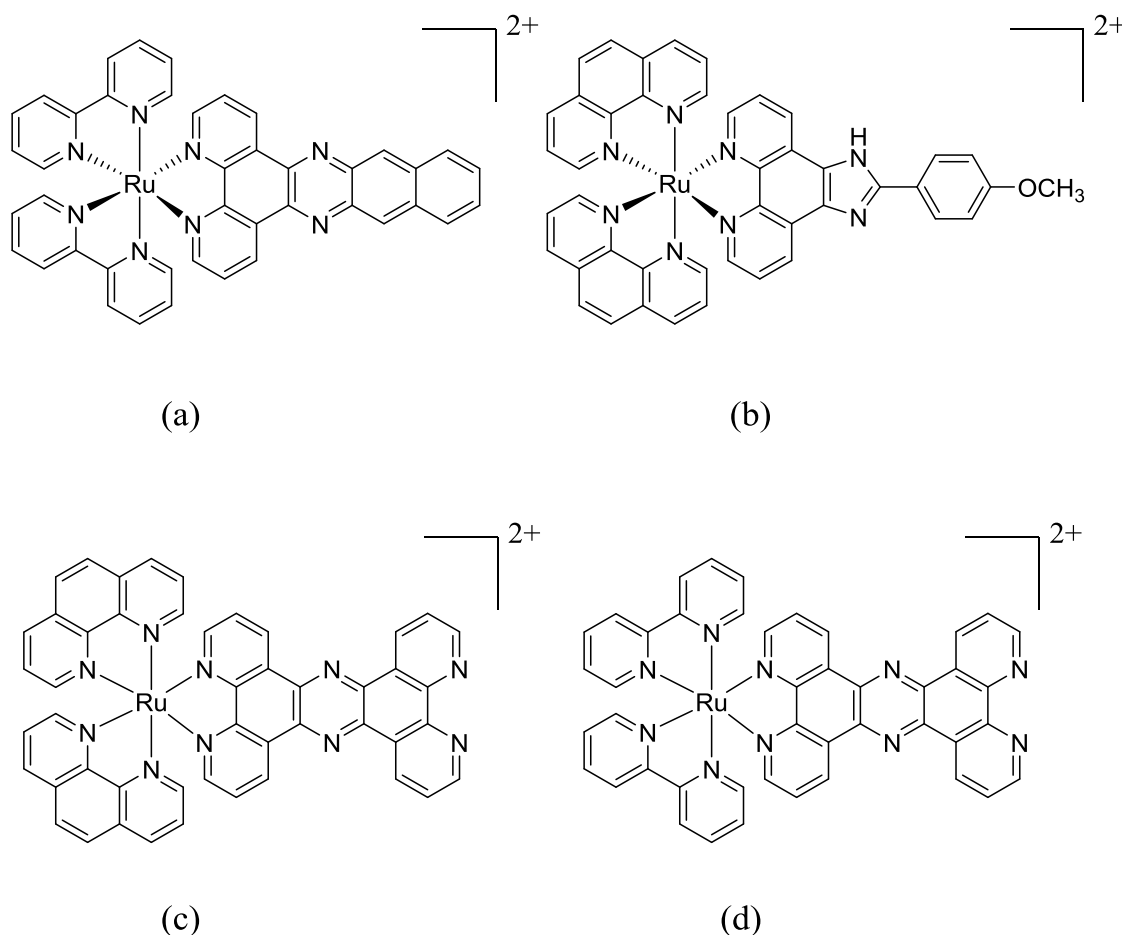


Figure 1.7. Mononuclear polypyridylruthenium(II) complexes, (a) $[\text{Ru}(\text{bpy})_2(\text{dppn})]^{2+}$, (b) $[\text{Ru}(\text{phen})_2(p\text{-MOPIP})]^{2+}$, (c) $[\text{Ru}(\text{phen})_2(\text{tpphz})]^{2+}$ and (d) $[\text{Ru}(\text{bpy})_2(\text{tpphz})]^{2+}$.

Along with anticancer studies, mononuclear polypyridylruthenium(II) complexes have also been well studied for their antimicrobial properties.⁹⁴⁻⁹⁸ Over 60 years ago, Dwyer and his co-workers first reported the antimicrobial potential of mononuclear iron and ruthenium complexes containing polypyridyl ligands.^{99,100} A series of metal complexes containing the 1,10-phenanthroline ligand (and derivatives) – see Figure 1.8 a, b, c – were synthesised and their bacteriostatic activities against Gram positive, Gram negative and acid-fast bacteria were determined. The parent complex, $[\text{Ru}(\text{phen})_3]^{2+}$, showed only slight activity against Gram positive and *Mycobacterium tuberculosis* (MTB) and no activity against Gram negative pathogens. It was observed

that the activity of the metal complexes against Gram positive and MTB increased with progressive alkylation of the phenanthroline ligands (e.g. 3, 5, 6, 8-tetramethyl-1,10-phenanthroline) - indicating the importance of the lipophilicity on the activity of metal complexes. Dwyer and his co-workers also carried out studies with other ligands (e.g. 2,2'-bipyridine) and other metals {Ni(II), Cu(II), Fe(II) and Co(II)}, and tested these complexes on a larger library of bacteria, with the ruthenium complexes generally showing slightly higher activities than the complexes with other metals.^{86,100} These complexes were more active against Gram positive bacteria than Gram negative bacteria. More interestingly, pathogenic bacteria such as MTB, *Erysipelothrix rhusiopathiae*, *S. aureus* and *E. coli*, as well as the fungi such as *Candida albicans* and *Trichophyton mentagrophytes*, did not develop resistance of any significance to the metal complexes with phenanthroline-based ligands.¹⁰¹ *In vivo* experiments using mice and guinea pig models with intraperitoneal and subcutaneous administrations, showed that these mononuclear complexes were ineffective. However, some of these complexes have been shown to be useful in the topical treatment of bacterial infections.^{100,101}

More recently, Aldrich-Wright and co-workers reported the antibacterial activities of a number of polypyridylruthenium(II) complexes that are capable of binding DNA through intercalation.⁹⁴ These complexes with the general structure $[\text{Ru}(\text{P}_\text{L})_2(\text{I}_\text{L})]^{2+}$ (where P_L = peripheral ligand and I_L = intercalating ligand) showed good activity against Gram positive bacteria, including drug-resistant strains such as methicillin-resistant *Staphylococcus aureus* (denoted as MRSA), and they also showed antifungal activity against *Neurospora crassa*; however, they were inactive against Gram negative bacteria. The activity of these complexes was attributed to the affinity of the intercalating ligands for DNA. In addition, the highly active complex, $[\text{Ru}(2,9-$

$\text{Me}_2\text{phen})_2(\text{dppz})]^{2+}$ (see Figure 1.8 d), also showed *in vivo* efficacy by increasing the survival population of MRSA-infected *Caenorhabditis elegans*, indicating the lower toxicity of the complex to the healthy eukaryotic cells.⁹⁴ Even though promising results have been reported on the development of mononuclear polypyridylruthenium(II) complexes as therapeutic agents, their biological properties and clinical potential are still to be extensively explored.

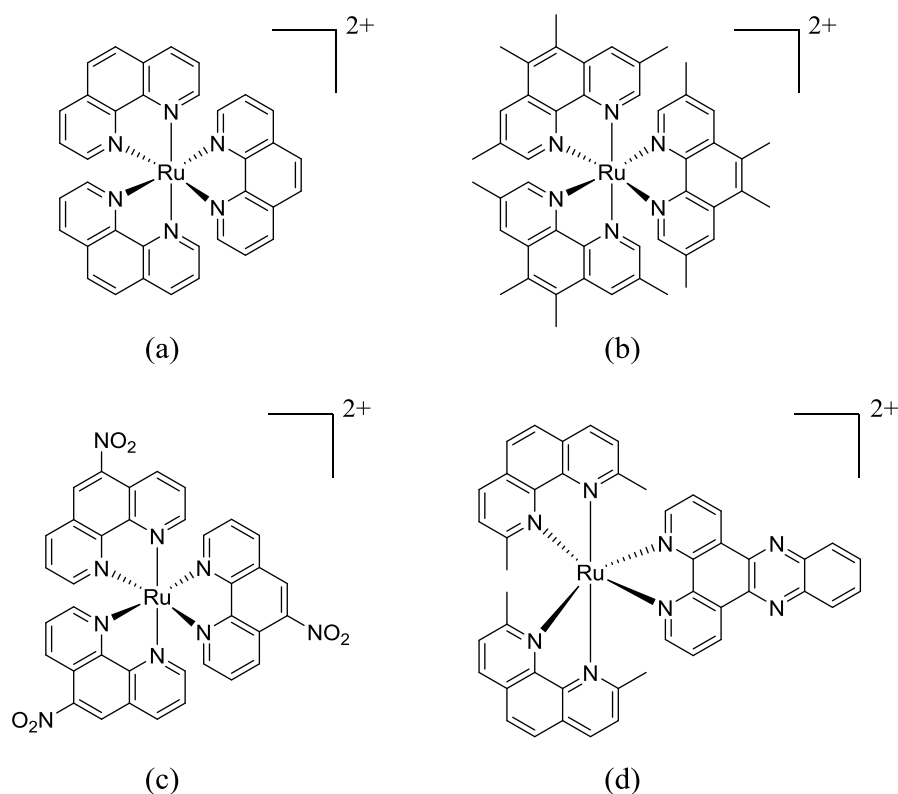


Figure 1.8. Mononuclear polypyridylruthenium(II) complexes, (a) $[\text{Ru}(\text{phen})_3]^{2+}$, (b) $[\text{Ru}(\text{Me}_4\text{phen})_3]^{2+}$, (c) $[\text{Ru}(5\text{-NO}_2\text{phen})_3]^{2+}$ and (d) $[\text{Ru}(2,9\text{-Me}_2\text{phen})_2(\text{dppz})]^{2+}$.

Although various mechanisms were proposed for the activity of mononuclear polypyridylruthenium(II) complexes, affinity of these complexes to negatively-charged nucleic acids, in particular DNA, is generally considered as the mechanism of biological activity.^{62,82,84,102,103} To increase the biological activity, the DNA-binding affinity of these complexes could be increased and this has proved to be driving force for the

investigation of higher-nuclearity inert ruthenium complexes as therapeutic agents. Given their higher affinity for DNA, it could be expected that dinuclear and polynuclear complexes with relatively larger size and higher charge would be better candidates as therapeutic agents when compared to their mononuclear counterparts.

1.3.2.2. *Oligonuclear polypyridylruthenium(II) complexes*

Dinuclear and polynuclear complexes were designed and developed mainly to improve the DNA binding properties compared to mononuclear complexes, which could potentially enhance the biological significance of these complexes when compared to the corresponding mononuclear complexes. The higher nuclearity complexes offer considerable advantages over the mononuclear complexes as probes for structural recognition of DNA. Kelly and co-workers first reported the improvement in DNA binding affinity of a dinuclear complex $[\{\text{Ru}(\text{bpy})_2\}_2\{\mu\text{-bb}_n\}]^{4+}$, {where $\text{bb}_n = \text{bis}[4(4'\text{-methyl-2,2'-bipyridyl})]\text{-1,n-alkane}$ for $n = 5$ and 7 } when compared to the mononuclear analogues $[\text{Ru}(\text{bpy})_3]^{2+}$ and $[\text{Ru}(\text{bpy})_2(\text{Me}_2\text{bpy})]^{2+}$.¹⁰⁴ These results indicate that the dinuclear species bound with a much higher affinity and were more efficient in photosensitising DNA strand breaks than the mononuclear analogues. Similarly Aldrich-Wright and co-workers also reported a 1000-fold increase in DNA binding affinity of a dinuclear complex, $[\{\text{Ru}(\text{dpq})_2\}_2\text{-(phen-x-SOS-x-phen)}]^{4+}$ ($\text{dpq} = \text{dipyrido}[3,2\text{-}d':2'3'\text{-}f]\text{quinoxaline}$; $\text{SOS} = 2\text{-mercaptoethyl ether}$; $x = 3, 4$ or 5), ($K_b = 6 \times 10^7 \text{ M}^{-1}$) when compared to its mononuclear analogue $[\text{Ru}(\text{dpq})_2(\text{phen})]^{2+}$ ($K_b = 5.4 \times 10^4 \text{ M}^{-1}$).¹⁰⁵ The research carried out in the Keene and Collins group has also focused on the development of dinuclear complexes that are capable of binding to DNA with greater affinity than the mononuclear analogues. The ruthenium(II) complexes with

rigid bridging ligands, such as 2,2'-bipyrimidine (bpm) and 1,4,5,8,9,12-hexaazatriphenylene (HAT) were used to probe non-duplex DNA structures. However, dinuclear complexes bridged by a rigid planar ligand cannot follow the curvature of the minor groove unless the groove is significantly straightened by a non-duplex structural feature.^{106,107} Hence, although this class of dinuclear complex shows potential as a probe for destabilised DNA sites, they are limited by their rigidity.¹⁰⁸ It was proposed that introducing flexibility into the bridging ligand could enhance the binding ability, as the flexible linking chain can follow the curvature of the DNA minor groove.¹⁰⁹ Consequently, ruthenium complexes containing the flexible bridging ligand bb_n , $[\{\text{Ru}(\text{phen})_2\}_2\{\mu\text{-bb}_n\}]^{4+}$ {"Rubb_n"; for $n = 5, 7, 10, 12$ and 16 }, were studied and it was shown that these Rubb_n complexes have improved DNA binding affinity when compared to the complexes with rigid bridging ligands.¹⁰⁹

The biological properties of a number of dinuclear ruthenium complexes have been examined. Recently, the anticancer activities of dinuclear complexes, $[\{\text{Ru}(\text{bpy})_2\}_2\{\mu\text{-L}\}]^{4+}$ and $[\{\text{Ru}(\text{phen})_2\}_2\{\mu\text{-L}\}]^{4+}$ (where L denotes the bis(pyridyl)imine ligand with a diphenylmethane spacer), were investigated by Hannon and co-workers.¹¹⁰ These flexible dinuclear complexes were designed to induce DNA binding modes analogous to other metallocupramolecular cylinders developed by the same group.^{111,112} It was observed that IC_{50} of these complexes were approximately 80–100 μM against HBL100 cells. Furthermore, the complex $[\{\text{Ru}(\text{phen})_2\}_2\{\mu\text{-L}\}]^{4+}$ was also tested in SKOV-3 cells, where a modest antiproliferative activity was determined. Onfelt and co-workers developed a dinuclear ruthenium complex, $\Delta\Delta\text{-}[\text{Ru}_2(\text{phen})_4\{\mu\text{-C4}(\text{cpdppz})_2\}]^{4+}$ (where $\text{C4}(\text{cpdppz})_2 = \text{N,N'-bis}(\text{cpdppz})\text{-1,4-diaminobutane}$ and $\text{cpdppz} = 12\text{-cyano-12,13-dihydro-11H-cyclopenta}[b]\text{dipyrido}[3,2\text{-}a:2',3'\text{-}c]\text{phenazine-12-carbonyl}$), with low toxicity which can be used as an excellent fluorescent marker for

DNA in live cells.¹¹³ Thomas and co-workers have also demonstrated the DNA imaging potential of a dinuclear polypyridylruthenium(II) complex, $[\{\text{Ru}(\text{phen})_2\}_2(\mu\text{-tpphz})]^{4+}$ (see Figure 1.9 a), that is well tolerated by both eukaryotic and prokaryotic cells.¹¹⁴ Interestingly, the bpy analogue, $[\{\text{Ru}(\text{bpy})_2\}_2(\mu\text{-tpphz})]^{4+}$ (see Figure 1.9 c), showed no staining of live cells.¹¹⁴ The same group recently reported the more lipophilic dinuclear ruthenium complex, $[\{\text{Ru}(\text{DIP})_2\}_2(\mu\text{-tpphz})]^{4+}$ (see Figure 1.9 b) specifically targets the lipid-dense endoplasmic reticulum of eukaryotic cells and acts as an *in cellulo* imaging agent for that organelle. Furthermore, the anticancer activity of this complex against MCF-7 and HeLa cell lines was 2-3 fold better than the anticancer drug cisplatin.¹¹⁵

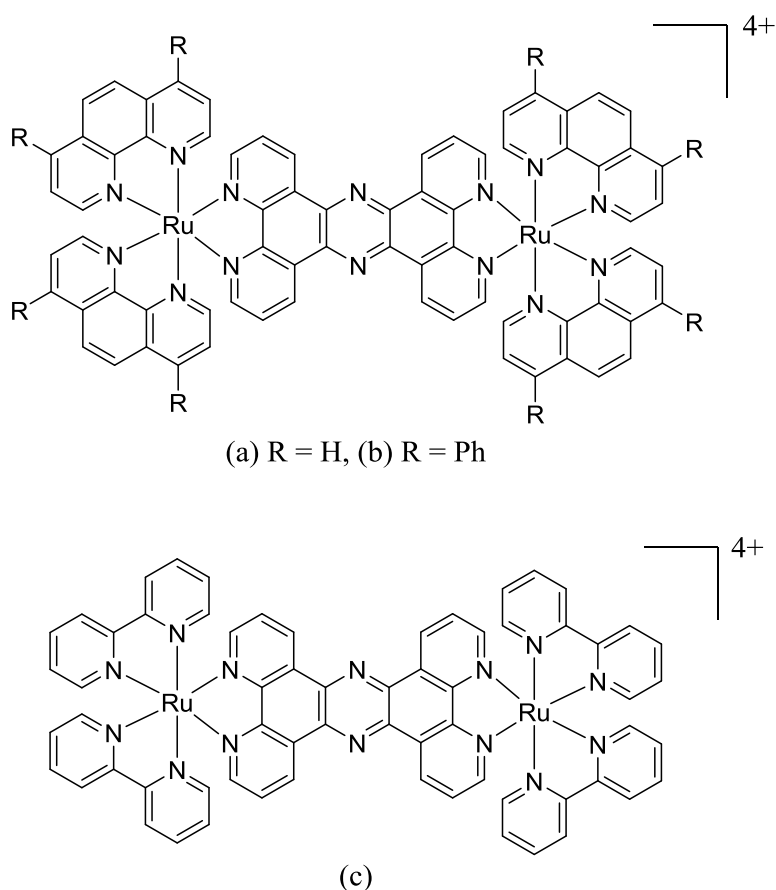


Figure 1.9. Dinuclear polypyridylruthenium(II) complexes, (a) $[\{\text{Ru}(\text{phen})_2\}_2(\mu\text{-tpphz})]^{4+}$, (b) $[\{\text{Ru}(\text{DIP})_2\}_2(\mu\text{-tpphz})]^{4+}$ and (c) $[\{\text{Ru}(\text{bpy})_2\}_2(\mu\text{-tpphz})]^{4+}$.

The research carried out by the Keene and Collins group has mainly focused on the development of inert dinuclear polypyridylruthenium(II) complexes, $[\{\text{Ru}(\text{phen})_2\}_2\{\mu\text{-bb}_n\}]^{4+}$ {"Rubb_n"; for $n = 5, 7, 10, 12$ and 16 , see Figure 1.10}, as therapeutic agents.^{68,96-98,116-118} The Rubb_n complexes have been examined for their potential as both anticancer and antibacterial agents. Cytotoxicity tests in L1210 cells revealed that the Rubb₁₆ complex showed the best anticancer activity, with an IC₅₀ of 5 μM , comparable to carboplatin.¹¹⁶ Studies on the cellular uptake mechanisms showed that these complexes were predominantly taken up by passive diffusion through the cell membrane with a minor contribution from an active structure-specific, non-endocytic mechanism. Interestingly, the complexes with $n = 12, 14$ and 16 (i.e. Rubb₁₂, Rubb₁₄ and Rubb₁₆) were shown to accumulate exclusively in mitochondria.¹¹⁶

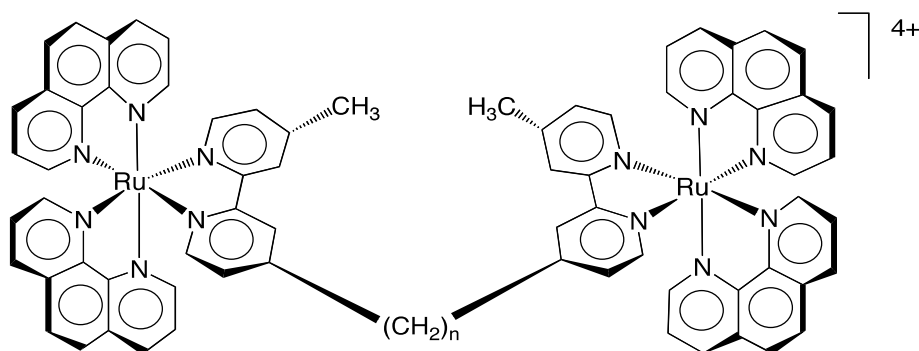


Figure 1.10. The structure of the dinuclear polypyridylruthenium(II) complexes, Rubb_n, where $n = 2, 5, 7, 10, 12, 14$ or 16 .

Along with their anticancer activity, Rubb_n complexes were also highly active against a range of pathogenic bacteria, particularly Gram positive strains.^{96,97} The MICs for Rubb₁₂ and Rubb₁₆ are 1 and 2 $\mu\text{g/mL}$ against a range of Gram positive and Gram negative bacterial strains and they maintained the activity against drug-resistant strains such as MRSA. Furthermore, preliminary toxicity assays against human red blood cells

and a human monocytic leukemia cell line (THP-1) indicated that the Rubb_n complexes were not toxic to human cells at the concentrations required to kill bacteria.⁹⁷ Consistent with the anticancer activities, the Rubb_n complexes with a longer alkane linking chain (Rubb₁₂, Rubb₁₄ and Rubb₁₆) were the most active against the bacterial strains, and the complexes with a shorter linking chain (Rubb₂, Rubb₅ and Rubb₇) showed very little or no activity against any of the bacterial strains.⁹⁷

The observed antimicrobial activity of the Rubb_n complexes was attributed to their ability to accumulate readily in bacterial strains. Consistent with the trend in lipophilicity of the dinuclear complexes (log P = -1.9, -2.7 and -3.4 for Rubb₁₆, Rubb₁₂ and Rubb₇, respectively), cellular uptake studies of these complexes revealed that Rubb₁₆ exhibited the highest level of uptake, followed by Rubb₁₂ and then Rubb₇.⁹⁶ The uptake into Gram negative bacteria was significantly less than that into Gram positive species, and was correlated with the observed MIC/MBC (MBC = minimum bactericidal concentration) values of the ruthenium complexes.⁹⁶ It was shown that the dinuclear Rubb_n complexes significantly depolarise and permeabilise the cellular membrane and enter bacterial cells in an energy-independent manner.¹¹⁹ Furthermore, cellular localisation studies showed that the most active compound, Rubb₁₆, condensed ribosomes (see Figure 1.11) when they existed as polysomes, and it was postulated that the condensation of polysomes would halt protein production and thereby inhibit bacterial growth.¹²⁰

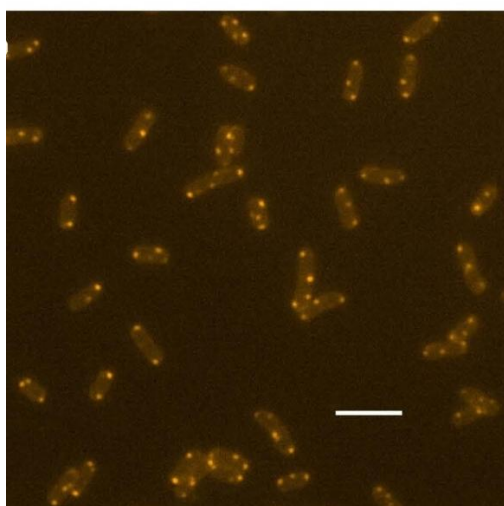


Figure 1.11. Fluorescence microscopy image of Rubb₁₆ localisation in *E. coli*

(Figure reproduced from the PhD thesis of F. Li, UNSW, 2013).

Based on their highly promising *in vitro* anticancer and antibacterial properties, there was a strong possibility that the manipulation of the structure of ruthenium complexes linked by the bb_n ligand could result in a suitable compound for clinical use.

1.4. Aims of the project

The purpose of this project was to further develop polypyridylruthenium(II) complexes as anticancer and antimicrobial agents. The following strategies were employed to achieve the desired aims.

It has been postulated that the inert dinuclear ruthenium complexes, Rubb_n , exhibit their biological activity through a combination of nucleic acid binding and membrane permeabilization. Based upon the excellent *in vitro* anticancer activity of the multinuclear platinum complexes, it was proposed to synthesise a series of analogous dinuclear ruthenium complexes (Cl-Rubb_n , see Figure 1.12) and examine their anticancer activity. Compared to the Rubb_n complexes, the Cl-Rubb_n complexes could covalently bind nucleic acids, and thereby, induce a stronger biological response.

Aim 1:

- Synthesis and biological evaluation of a series of chlorido containing dinuclear ruthenium complexes, $[\{\text{Ru}(\text{tpy})\text{Cl}\}_2\{\mu\text{-bb}_n\}]^{2+}$, (Cl-Rubb_n , where $\text{tpy} = 2,2':6',2''\text{-terpyridine}$, see Figure 1.12).

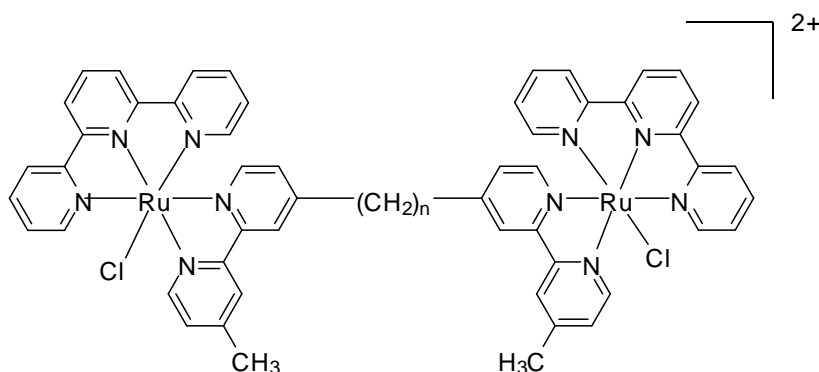


Figure 1.12. Structure of chlorido-containing dinuclear ruthenium(II) complexes, Cl-Rubb_n .

As an alternative means to increase nucleic acid binding, and consequently induce a stronger biological response, it was proposed to synthesise a series of tri- and tetra-nuclear complexes using bb_n as a bridging ligand (see Figure 1.13). These complexes will be more positively charged, 6+ and 8+ respectively, but they will also be more lipophilic than the corresponding dinuclear $Rubb_n$ complexes due to the additional bb_n ligands. The greater lipophilicity could allow greater cellular uptake, while the greater cationic charge could allow stronger interactions with nucleic acids.

Aim 2:

- Synthesis and biological evaluation of tri- and tetra-nuclear polypyridylruthenium(II) complexes (see Figure 1.13).

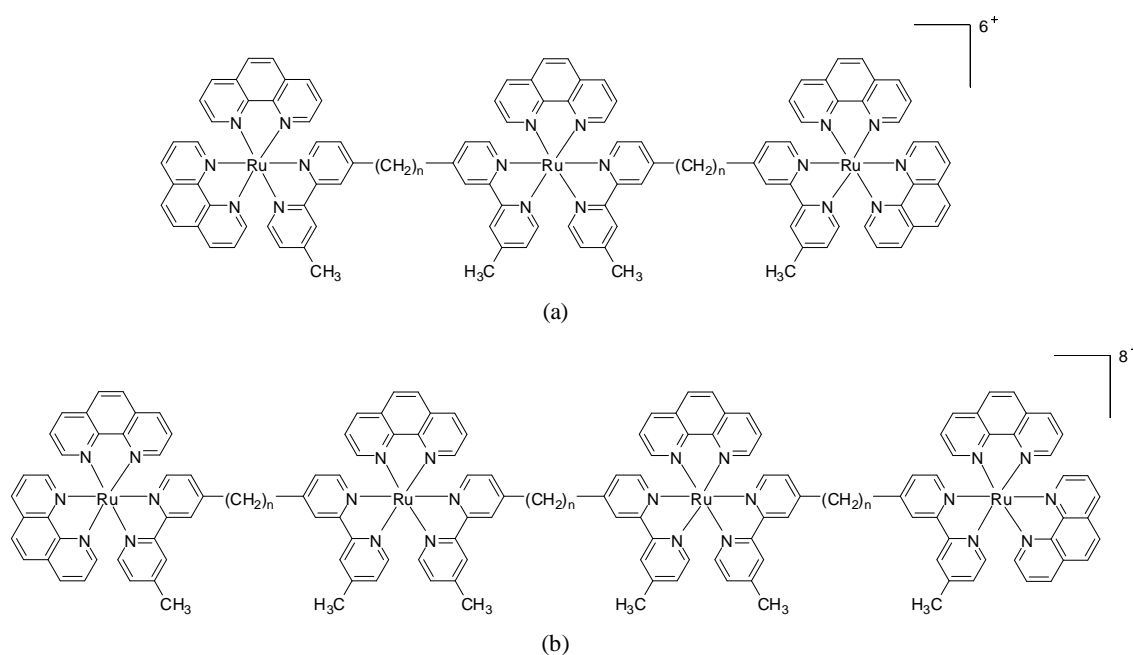


Figure 1.13. Structure of the inert tri- and tetra-nuclear polypyridylruthenium(II) complexes, (a) $Rubb_n$ -tri and (b) $Rubb_n$ -tetra.

While the biological activities of a range of mononuclear ruthenium complexes have been examined, the antimicrobial properties of mononuclear complexes that incorporate the bb_n ligand as a tetradentate ligand are yet to be explored. Such complexes would be expected to of similar lipophilicity to $[Ru(Me_4phen)_3]^{2+}$, but would represent a new type of structure that consequently may have significantly different antimicrobial properties.

Aim 3:

- Synthesis and biological evaluation of a family of mononuclear polypyridylruthenium(II) complexes using the bb_n ligand as a tetradentate ligand (see Figure 1.14).

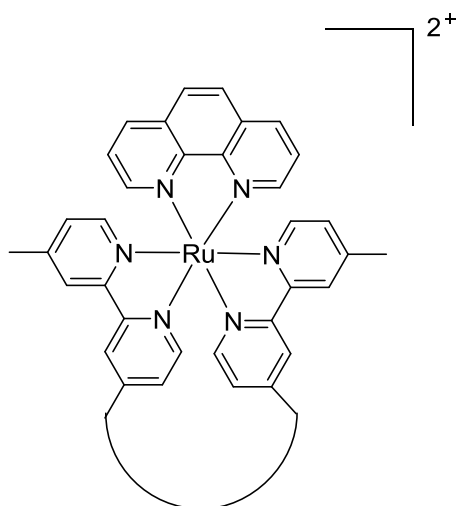


Figure 1.14. Structure of the mononuclear polypyridylruthenium(II) complex, *cis*- α - $[Ru(phen)(bb_n)]^{2+}$.

1.5. Thesis outline

Cancer and infectious diseases are leading causes of death worldwide. There is clearly a need for the development of new therapeutic agents; but more importantly, there is the need for the development of new *classes* of drugs.

- ❖ Chapter 2 discusses the synthesis of a series of dinuclear ruthenium(II) complexes that contain labile chlorido ligands, $[\{\text{Ru}(\text{tpy})\text{Cl}\}_2\{\mu\text{-bb}_n\}]^{2+}$ {designated Cl-Rubb_n; tpy = 2,2':6',2''-terpyridine} and their derivatives containing nitro substituents on the tpy ligand and/or secondary amines within the bb_n linking chain. The potential of these ruthenium complexes as anticancer agents against MCF-7 and MBA-MB-231 breast cancer cell lines has been examined to establish the structure-activity relationship of these chlorido containing dinuclear ruthenium complexes.
- ❖ Chapter 3 concentrates on the synthesis of a series of inert tri- and tetra-nuclear polypyridylruthenium(II) complexes that are linked by the bb_n ligand (for n = 10, 12 and 16) and an examination of their potential as antimicrobial agents against Gram positive and Gram negative bacterial strains. In order to gain an understanding of the relative antimicrobial activities, the cellular uptake and water-octanol partition coefficients (log P) were determined for the ruthenium complexes.

- ❖ Chapter 4 deals with the further development of inert tri- and tetra-nuclear polypyridylruthenium(II) complexes as antimicrobial agents. Given the good antimicrobial activities of tri- and tetra-nuclear $\text{Ru}(\text{bb})_n$ complexes, these complexes were assessed for their clinical potential against a wider range of bacteria, in particular, clinical isolates that are of current concern. In addition, the toxicity to eukaryotic cells and an healthy animal model was also established.

- ❖ Chapter 5 investigates the synthesis and antimicrobial properties of mononuclear ruthenium(II) complexes containing the tetradentate ligand bb_n (for $n = 10$ and 12) against Gram positive and Gram negative species. In order to gain an understanding of relative antimicrobial activities, cellular uptake and the water-octanol partition coefficients ($\log P$) were determined.

- ❖ Chapter 6 summarises the results and make suggestions for future studies in the development of polypyridylruthenium(II) complexes as therapeutic agents.

Taken together, the results of these studies suggest inert polypyridylruthenium(II) complexes have potential as a new class of therapeutic agents, but more work needs to be carried out.

1.6. References

1. World Health Organisation. Fact sheet on Cancer, 2015.
(<http://www.who.int/mediacentre/factsheets/fs297/en/>)
2. World Health Organisation. Fact sheet on Antimicrobial resistance, 2015.
(<http://www.who.int/mediacentre/factsheets/fs194/en/>)
3. WHO's first global report on antibiotic resistance, 2014.
(<http://www.who.int/mediacentre/news/releases/2014/amr-report/en/>)
4. H. W. Boucher, G. H. Talbot, J. S. Bradley, J. E. Jr Edwards, D. Gilbert, L. B. Rice, M. Scheld, B. Spellberg and J. Bartlett, *IDSA Report on Development Pipeline*, 2009, **48**, 1.
5. C. Orvig and M. J Abrams, *Chem. Rev.*, 1999, **99**, 2201.
6. C. X. Zhang and S. J. Lippard, *Curr. Opin. Chem. Biol.*, 2003, **7**, 481.
7. R. I. Aminov, *Front Microbiol.*, 2010, **1**, 134.
8. T. W. Hambley, *Science*, 2007, **318**, 1392.
9. S. H. van Rijt and P. J. Sadler, *Drug Discovery Today*, 2009, **14**, 1089.
10. G. B. Kauffman, R. Pentimalli, S. Doldi and M. D. Hall, *Platin. Met. Rev.*, 2010, **54**, 250.
11. G. B. Kauffman, *Alfred Werner: Founder of Coordination Chemistry*, Springer-Verlag, Berlin/Heidelberg/New York, 1966.
12. B. Rosenberg and L. V. Camp, *Nature*, 1969, **222**, 385.
13. B. Rosenberg, L. V. Camp and T. Krigas, *Nature*, 1965, **205**, 698.
14. B. Rosenberg, L. V. Camp, E. B. Grimley and A. J. Thomson, *J. Biol. Chem.*, 1967, **242**, 1347.

15. D. J. Higby, H. J. Wallace, D. J. Albert and J. F. Holland, *Cancer*, 1974, **33**, 1219.
16. R. B. Weiss and M. C. Christian, *Drugs*, 1993, **46**, 360.
17. L. Kelland, *Nat. Rev. Cancer*, 2007, **7**, 573.
18. S. J. Lippard, *Progress in Inorganic Chemistry: Bioinorganic Chemistry*, Wiley, Sydney, 1995, 48.
19. N. J. Wheate and J. G. Collins, *Curr. Med. Chem.: Anti - Cancer Agents*, 2005, **5**, 267.
20. R. P. Miller, R. K. Tadagavadi, G. Ramesh and W. B. Reeves, *Toxins*, 2010, **2**, 2490.
21. X. Yao, K. Panichpisal, N. Kurtzman and K. Nugent, *Am. J. Med. Sci.*, 2007, **334**, 115.
22. D. Screnci and M. J. McKeage, *J. Inorg. Biochem.*, 1999, **77**, 105.
23. S. R. McWhinney, R. M. Goldberg and H. L. McLeod, *Mol. Cancer Ther.*, 2009, **8**, 10.
24. R. L. Brown, R. C. Nuss, R. Patterson and J. Irey, *Gynecol. Oncol.*, 1983, **16**, 254.
25. S. S. More, O. Akil, A. G. Ianculescu, E. G. Geier, L. R. Lustig and K. M. Giacomini, *J. Neurosci.*, 2010, **30**, 9500.
26. J. Reedijk, *Chem. Commun.*, 1996, 801.
27. B. Lippert, *Cisplatin: Chemistry and Biochemistry of a Leading Anticancer Drug*, Verlag Helvetica Chimica Acta, Zurich; Wiley-VCH, Weinheim, Germany, 1999.
28. J. M. Ford and W. N. Hait, *Cytotechnology*, 1993, **12**, 171.
29. E. Wong and C. M. Giandomenico, *Chem. Rev.*, 1999, **99**, 2451.

30. N. P. Barry and P. J. Sadler, *Chem. Commun.*, 2013, **49**, 5106.
31. D. Lebwohl and R. Canetta, *Eur. J. Cancer*, 1998, **34**, 1522.
32. I. Romero-Canelón and P. J. Sadler, *Inorg. Chem.*, 2013, **52**, 12276.
33. E. Gallerani, J. Bauer, D. Hess, S. Boehm, C. Droege, S. Jeckelmann, M. Miani, R. Herrmann, S. Marsoni, S. Sperka and C. Sessa, *Acta Oncol.*, 2011, **50**, 1105.
34. K. D. Mjos and C. Orvig, *Chem. Rev.*, 2014, **114**, 4540.
35. N. Farrell and L. R. Kelland, *Platinum-based drugs in cancer therapy*, Humana Press, Totowa, 2000.
36. N. Farrell, *Comm. Inorg. Chem.*, 1995, **16**, 373.
37. E. Schuhmann, J. Altman, K. Karaghiosoff and W Beck, *Inorg. Chem.*, 1995, **34**, 2316.
38. P. Di Blasi, A. Bernareggi, G. Beggiolin, L. Piazzoni, E. Menta and M. L. Formento, *Anticancer Res.*, 1997, **18**, 3113.
39. U. Bierbach, T. W. Hambley and N. Farrell, *Inorg. Chem.*, 1998, **37**, 708.
40. G. Pratesi, P. Perego, D. Polizzi, S. C. Righetti and N. Farrell, *Brit. J. Cancer*, 1999, **80**, 1912.
41. J. D. Roberts, J. Peroutka, G. Beggiolin and N. Farrell, *J. Inorg. Biochem.*, 1999, **77**, 47.
42. G. Pratesi, F. C. Giuliani, D. Polizzi, S. Righetti, C. Pezzoni, N. Farrell and F. Zunino, *Proc. Am. Assoc. Cancer Res.*, 1997, **38**, 3310.
43. P. Perego, C. Caserini, L. Gatti, N. Carenini, S. Romanelli, R. Supino, D. Colangelo, L. Viano, R. Leone, S. Spinelli, G. Pezzoni, C. Mazotti, N. Farrell and F. Znino, *Mol. Pharm.*, 1999, **55**, 528.
44. V. Brabec, J. Kašpárková, O. Vrána, O. Nováková, J. W. Cox, Y. Qu and N. Farrell, *Biochemistry*, 1999, **38**, 6781.

45. C. Manzotti, G. Pratesi, E. Menta, R. Di Domenico, E. Cavalletti, H. H. Fiebig, L. R. Kelland, N. Farrell, D. Polizzi, R. Supino, G. Pezzoni and F. Zunino, *Clin. Cancer Res.*, 2000, **6**, 2626.
46. M. J. Clarke, B. K. Keppler, In *Metal complexes in cancer chemotherapy*, B. K. Keppler, Ed., VCH: Weinheim, 1993, 129.
47. C. G. Hartinger, N. Metzler-Nolte and P. J. Dyson, *Organometallics*, 2012, **31**, 5677.
48. P. Collery, J. Domingo and B. Keppler, *Anticancer Res.*, 1995, **16**, 687.
49. M. J. Clarke, F. Zhu and D. R. Frasca, *Chem. Rev.*, 1999, **99**, 2511.
50. M. J. Clarke, *Ruthenium and Other Non-Platinum Metal Complexes in Cancer Chemotherapy*, Springer, Heidelberg, Germany, 1989.
51. G. Gasser, I. Ott and N. Metzler-Nolte, *J. Med. Chem.*, 2010, **54**, 3.
52. S. B. Fricker, *Dalton Trans.*, 2007, 4903.
53. G. Süss-Fink, *Dalton Trans.*, 2010, **39**, 1673.
54. M. R. Gill and J. A. Thomas, *Chem. Soc. Rev.*, 2012, **41**, 3179.
55. C. S. Allardyce and P. J. Dyson, *Platin. Met. Rev.*, 2001, **45**, 62.
56. W. H. Ang and P. J. Dyson, *Eur. J. Inorg. Chem.*, 2006, 4003.
57. A. Bergamo, C. Gaiddon, J. H. M. Schellens, J. H. Beijnen and G. Sava, *J. Inorg. Biochem.*, 2012, **106**, 90.
58. I. Kostova, *Current Medicinal Chemistry*, 2006, **13**, 1085.
59. J. Reedijk, *Platinum Met. Rev.*, 2008, **52**, 2.
60. V. Brabec and O. Novakova, *Drug Resistance Updates*, 2006, **9**, 111.
61. J. M. Rademaker-Lakhai, D. Van Den Bongard, D. Pluim, J. H. Beijnen and J. H. M. Schellens, *Clin. Cancer Res.*, 2004, **10**, 3717.

62. B. J. Pages, D. L. Ang, E. P. Wright and J. R. Aldrich-Wright, *Dalton Trans.*, 2015, **44**, 3505.
63. M. J. Clarke, *Coord. Chem. Rev.*, 2003, **236**, 209.
64. C. G. Hartinger, S. Zorbas-Seifried, M. A. Jakupiec, B. Kynast, H. Zorbas and B. K. Keppler, *J. Inorg. Biochem.*, 2006, **100**, 891.
65. O. Novakova, J. Kasparkova, O. Vrana, P. M. Vanvliet, J. Reedijk and V. Brabec, *Biochemistry*, 1995, **34**, 12369.
66. P. M. Vanvliet, S. M. S. Toekimin, J. G. Haasnoot, J. Reedijk, O. Novakova, O. Vrana and V. Brabec, *Inorg. Chim. Acta*, 1995, **231**, 57.
67. S. K. Tripathy, A. C. Taviti, N. Dehury, A. Sahoo, S. Pal, T. K. Beuria and S. Patra, *Dalton Trans.*, 2015, **44**, 5114.
68. M. Pandrala, F. Li, M. Feterl, Y. Mulyana, J. M. Warner, L. Wallace, F. R. Keene and J. G. Collins, *Dalton Trans.*, 2013, **42**, 4686.
69. L. J. Anghileri and Z. Krebsforsch, *Cancer Res. Clin. Oncol.*, 1975, **83**, 213.
70. M. J. Clarke, *Met. Ions Biol. Syst.*, 1980, **11**, 231.
71. E. Alessio, G. Mestroni, A. Bergamo and G. Sava, *Curr. Top. Med. Chem.*, 2004, **4**, 1525.
72. K. M. Hindi, M. J. Panzner, C. A. Tessier, C. L. Cannon and W. J. Young, *Chem. Rev.*, 2009, **109**, 3859.
73. H. Keller and B. Keppler, *US Patent*, 1989, 4843069.
74. B. K. Keppler, K. G. Lipponer, B. Stenzel and F. Kratzin, *Metal Complexes in Cancer Chemotherapy*, VCH, Weinheim, 1993, p. 187.
75. G. Sava, A. Bergamo, S. Zorzet, B. Gava, C. Casrsa, M. Cocchietto, A. Furlani, V. Scarcia, B. Serli, E. Iengo, E. Alessio and G. Mestroni, *Eur. J. Cancer*, 2002, **38**, 427.

76. R. E. Aird, J. Cummings, A. A. Ritchie, M. Muir, R. E. Morris, H. Chen, P. J. Sadler and D. I. Jodrell, *Br. J. Cancer*, 2002, **86**, 1652.
77. P. J. Dyson, *Chimia*, 2007, **61**, 698.
78. C. Scolaro, A. Bergamo, L. Brescacin, R. Delfino, M. Cocchietto, G. Laurenczy, T. J. Geldbach, G. Sava and P. J. Dyson, *J. Med. Chem.*, 2005, **48**, 4161.
79. D. E. Cıralı, Z. Uyar, I. Koyuncu and N. Hacıoglu, *Appl. Organometal. Chem.*, 2015, **29**, 536.
80. D. E. Cıralı, O. Dayan, N. Ozdemir and N. Hacıoglu, *Polyhedron*, 2015, **88**, 170.
81. T. S. Kamatchi, P. Kalaivani, P. Poornima, V. V. Padma, F. R. Fronczek and K. Natarajan, *RSC Adv.*, 2014, **4**, 2004.
82. A. Bolhuis and J. R. Aldrich-Wright, *Bioorg. Chem.*, 2014, **55**, 51.
83. L. Salassa, *Eur. J. Inorg. Chem.*, 2011, **2011**, 4931.
84. F. R. Keene, J. A. Smith and J. G. Collins, *Coord. Chem. Rev.*, 2009, **253**, 2021.
85. H. Xu, Y. Lang, P. Zhang, F. Du, B.-R. Zhou, J. Wu, J.-H. Liu, Z.-G. Liu and L.-N. Ji, *J. Biol. Inorg. Chem.*, 2005, **10**, 529.
86. F. P. Dwyer, C. E. Gyarfas, W. P. Rogers and J. H. Koch, *Nature*, 1952, **170**, 190.
87. J. G. Vos and J. M. Kelly, *Dalton Trans.*, 2006, 4869.
88. R. M. Hartshorn and J. K. Barton, *J. Am. Chem. Soc.*, 1992, **114**, 5919.
89. C. Tan, S. Lai, S. Wu, S. Hu, L. Zhou, Y. Chen, M. Wang, Y. Zhu, W. Lian, W. Peng, L. Ji and A. Xu, *J. Med. Chem.*, 2010, **53**, 7613.
90. O. Zava, S. M. Zakeeruddin, C. Danelon, H. Vogel, M. Gratzel, and P. J. Dyson, *ChemBioChem*, 2009, **10**, 1796.
91. U. Schatzschneider, J. Niesel, I. Ott, R. Gust, H. Alborzinia and S. Wolf, *ChemMedChem*, 2008, **3**, 1104.

92. T. Chen, Y. Liu, W. Zheng, J. Liu, and Y. S. Wong, *Inorg. Chem.*, 2010, **49**, 6366.
93. M. R. Gill, H. Derrat, C. G. W. Smythe, G. Battaglia and J. A. Thomas, *ChemBioChem*, 2011, **12**, 877.
94. A. Bolhuis, L. Hand, J. E. Marshall, A. D. Richards, A. Rodger and J. Aldrich-Wright, *Eur. J. Pharm. Sci.*, 2011, **42**, 313.
95. C. S. Devi, D. A. Kumar, S. S. Singh, N. Gabra, N. Deepika, Y. P. Kumar and S. Satyanarayana, *Eur. J. Med. Chem.*, 2013, **64**, 410.
96. F. Li, M. Feterl, Y. Mulyana, J. M. Warner, J. G. Collins and F. R. Keene, *J. Antimicrob. Chemother.*, 2012, **67**, 2686.
97. F. Li, Y. Mulyana, M. Feterl, J. M. Warner, J. G. Collins and F. R. Keene, *Dalton Trans.*, 2011, **40**, 5032.
98. F. Li, J. G. Collins and F. R. Keene, *Chem. Soc. Rev.*, 2015, **44**, 2529.
99. F. P. Dwyer and D. P. Mellor, *Chelating Agents and Metal Chelates*, Academic Press, New York, 1964.
100. F. P. Dwyer, I. K. Reid, A. Shulman, G. M. Laycock and S. Dixon, *Aust. J. Exp. Biol. Med. Sci.*, 1969, **47**, 203.
101. *Lancet*, 1971, **297**, 72.
102. N. W. Luedtke, J. S. Hwang, E. Nava, D. Gut, M. Kol and Y. Tor, *Nucleic Acids Res.*, 2003, **31**, 5732.
103. C. Metcalfe and J. A. Thomas, *Chem. Soc. Rev.*, 2003, **32**, 215.
104. F. M. O'Reilly and J. M. Kelly, *New J. Chem.*, 1998, **22**, 215.
105. J. Aldrich-Wright, C. Brodie, E. C. Glazer, N. W. Luedtke, L. Elson-Schwab and Y. Tor, *Chem. Commun.*, 2014, 1018.

106. J. A. Smith, J. L. Morgan, A. G. Turley, J. G. Collins and F. R. Keene, *Dalton Trans.*, 2006, 3179.
107. D. P. Buck, C. B. Spillane, J. G. Collins and F. R. Keene, *Mol. Biosyst.*, 2008, **4**, 851.
108. J. L. Morgan, D. P. Buck, A. G. Turley, J. G. Collins and F. R. Keene, *Inorg. Chim. Acta*, 2006, **359**, 888.
109. J. L. Morgan, D. P. Buck, J. G. Collins and F. R. Keene, *Dalton Trans.*, 2007, 4333.
110. U. McDonnell, J. Kerchoffs, R. P. M. Castineiras, M. R. Hicks, A. C. G. Hotze, M. J. Hannon and A. Rodger, *Dalton Trans.*, 2008, 667.
111. A. C. G. Hotze, B. M. Kariuki and M. J. Hannon, *Angew. Chem.*, 2006, **118**, 4957.
112. G. I. Pascu, A. C. G. Hotze, C. Sanchez-Cano, B. M. Kariuki and M. J. Hannon, *Angew. Chem.*, 2007, **119**, 4452.
113. B. Onfelt, L. Gostring, P. Lincoln, B. Nordén and A. Onfelt, *Mutagenesis*, 2002, **17**, 317.
114. M. R. Gill, J. Garcia-Lara, S. J. Foster, C. Smythe, G. Battaglia and J. A. Thomas, *Nat. Chem.*, 2009, **1**, 662.
115. M. R. Gill, D. Cecchin, M. G. Walker, R. S. Mulla, G. Battaglia, C. Smythe and J. A. Thomas, *Chem. Sci.*, 2013, **4**, 4512.
116. M. J. Pisani, P. D. Fromm, R. J. Clarke, Y. Mulyana, H. Körner, K. Heimann, J. G. Collins and F. R. Keene, *ChemMedChem*, 2011, **6**, 848.
117. Y. Mulyana, J. G. Collins and F. R. Keene, *J. Incl. Phenom. Macrocycl. Chem.*, 2011, **71**, 371.

118. Y. Mulyana, D. K. Weber, D. P. Buck, C. A. Motti, J. G. Collins and F. R. Keene, *Dalton Trans.*, 2011, **40**, 1510.
119. F. Li, M. Feterl, J. M. Warner, F. R. Keene and J. G. Collins, *J. Antimicrob. Chemother.*, 2013, **68**, 2825.
120. F. Li, E. J. Harry, A. L. Bottomley, M. D. Edstein, G. W. Birrell, C. E. Woodward, F. R. Keene and J. G. Collins, *Chem. Sci.*, 2014, **5**, 685.

CHAPTER 2

***Multinuclear ruthenium(II) complexes as
anticancer agents***

2.1. Introduction

As mentioned in the previous chapter, multinuclear platinum-based drugs (see Figure 2.1) have been well studied for their anticancer properties.¹⁻¹⁴ Based on their high *in vitro* and *in vivo* activities, a trinuclear platinum complex, BBR3464, entered clinical trials.¹⁵⁻¹⁷ While these multinuclear platinum complexes are highly cytotoxic, they are also highly toxic.^{7,17-20} Although BBR3464 was withdrawn from clinical trials because of its high toxicity, there has been recent interest in “transferring the concept of multinuclearity to ruthenium complexes”.²¹

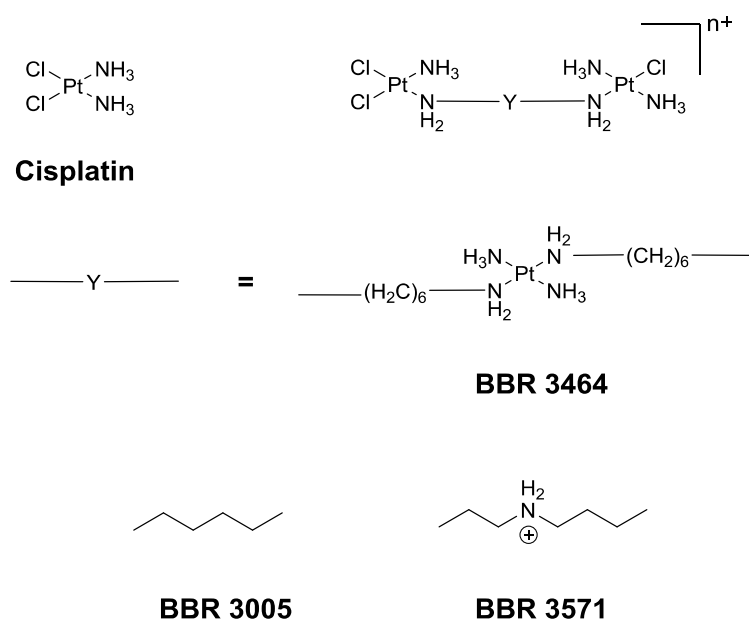


Figure 2.1. Cisplatin, and the structure of a generic dinuclear platinum complex (top right) with the linking ligands (Y) shown for BBR3464, BBR3005 and BBR3571.

Mendoza-Ferri *et al.* synthesised a series of dinuclear ruthenium(II)-arene compounds containing a bis(pyridinone)alkane linking ligand that incorporated 3, 6 or 12 methylene groups in the alkane chain.²¹ The ruthenium-arene complexes showed

good activity in a variety of cancer cell lines, with the activity increasing with the length of the alkane linker, and were more active than a similar mononuclear analogue. In addition, Yamada *et al.* synthesised $[\{Ru(bpy)_2Cl\}_2\{\mu-BL\}]^{2+}$ complexes {where bpy = 2,2'-bipyridine and BL = 1,6-diaminohexane or 1,12-diaminododecane} and examined their cytotoxicity.²² While the chlorido complexes showed little activity, replacement of the chlorido ligand by DMSO in the 1,12-diaminododecane-bridged complex resulted in good activity against L1210 cells. Corral *et al.* have recently demonstrated that the mononuclear ruthenium(II) complexes $[Ru(apy)(tpy)X]^{n+}$ (where apy = 2,2'-azobipyridine, tpy = 2,2':6',2''-terpyridine and X = a labile ligand such as Cl^- or H_2O) had good activity against a variety of cancer cell lines, but were significantly less active than cisplatin.²³ In an attempt to increase the activity of mononuclear $[Ru(tpy)(L)(Cl)]^+$ complexes (where L = a non-labile bidentate ligand), our group has previously synthesised the dinuclear ruthenium complexes $[\{Ru(tpy)Cl\}_2\{\mu-bb_n\}]^{2+}$ {Cl-Rubb_n, see Figure 2.2 a} containing bb_n as the bridging ligand between ruthenium centres.²⁴ The Cl-Rubb_n complexes showed good activity against the highly sensitive L1210 cell line ($IC_{50} \approx 5 - 10 \mu M$) and were ten-times more active than the corresponding mononuclear complex $[Ru(tpy)(Me_2bpy)Cl]^+$ {Me₂bpy = 4,4'-dimethyl-2,2'-bipyridine}.²⁴ Furthermore, Cl-Rubb_n complexes showed excellent antimicrobial activities against a range of bacterial strains, with MIC values for the Cl-Rubb₁₂ complex of 1 $\mu g/ml$ against Gram positive bacteria.³⁸

In this chapter the aim was to extend the family of Cl-Rubb_n dinuclear complexes by using a similar approach to that of Farrell and co-workers for the multinuclear platinum complexes.^{1,3-5} Consequently, a series of Cl-Rubb_n complexes that contain cationic groups (NH_2^+) in the chain of the bb_n linking ligand (Cl-RubbN_n, see Figure 2.2 c) have been synthesised and their anticancer activities, rates of

hydrolysis and GMP binding ability examined. Furthermore, in order to determine the effect of changes in charge distribution (and hence, the rate of ligand exchange) on the ruthenium(II) complexes, several Cl-Rubb_n and Cl-RubbN_n complexes that contain three electron-withdrawing NO₂ groups on the tpy ligands (Cl-Rubb_nNO₂ and Cl-RubbN_nNO₂, see Figure 2.2 b, d) were prepared. Since it was previously shown that the ability of the Cl-Rubb_n complexes to kill bacteria decreased due to the presence of chlorido group on each metal centre compare to the inert Rubb_n complexes, further antimicrobial studies were not carried out in the present study.³⁸

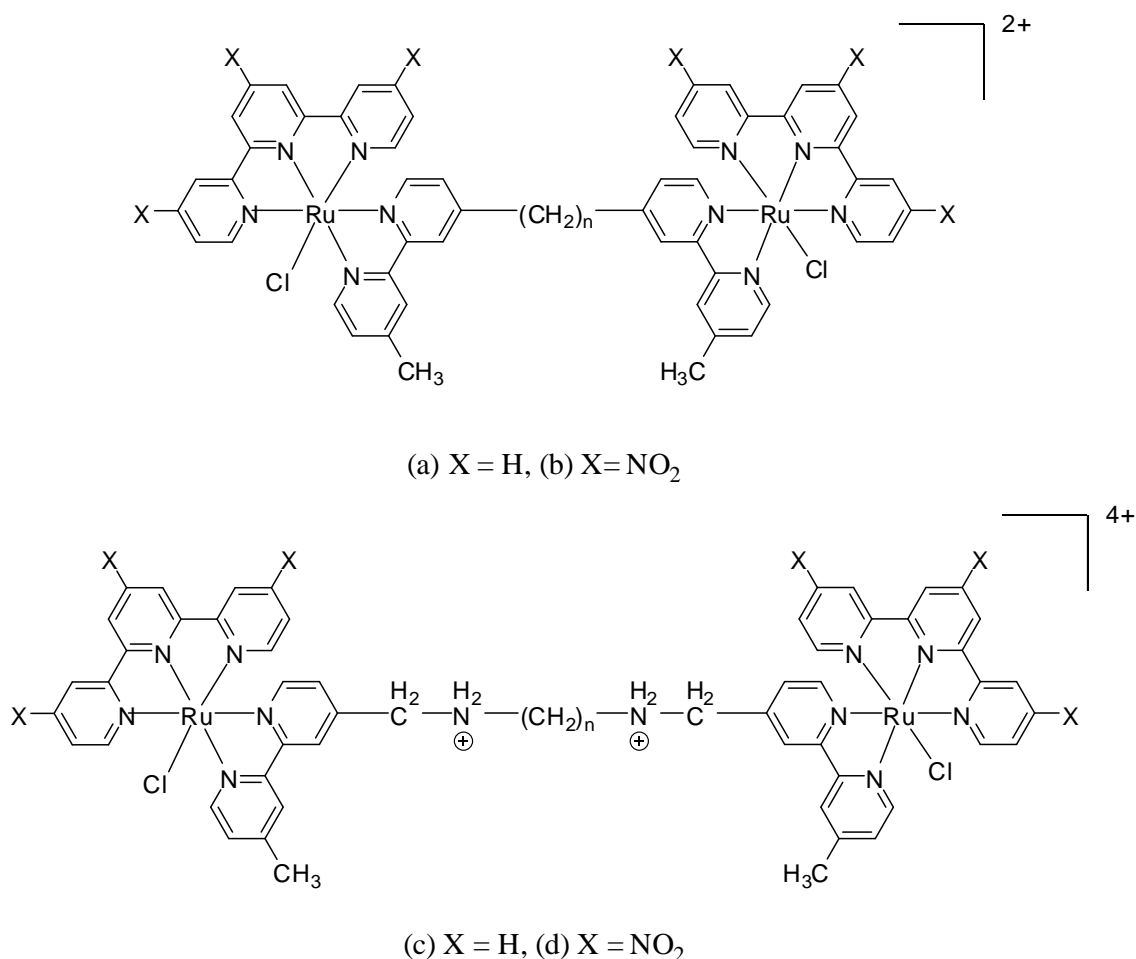


Figure 2.2. Chlorido-containing dinuclear ruthenium(II) complexes, (a) Cl-Rubb_n, (b) Cl-Rubb_nNO₂, (c) Cl-RubbN_n and (d) Cl-RubbN_nNO₂.

2.2. Experimental

2.2.1. Physical measurements

1D and 2D ^1H NMR spectra were recorded on a Varian Advance 400 MHz spectrometer at room temperature in D_2O {99.9%, Cambridge Isotope Laboratories (CIL)}, CDCl_3 (99.8%, CIL), or CD_3CN (>99.8%, Aldrich). Microanalyses were performed by the Microanalytical Unit, Research School of Chemistry, Australian National University, Canberra.

2.2.2. Materials and methods

4,4'-Dimethyl-2,2'-bipyridine (Me_2bpy), 2,2':6',2''-terpyridine (tpy), sodium borohydride, phosphorus trichloride, 1,3-diaminopropane, 1,12-diaminopropane, guanosine 5'-monophosphate disodium salt (5'-GMP), ammonium hexafluorophosphate (NH_4PF_6), potassium hexafluorophosphate (KPF_6) and Amberlite[®] IRA-400 (chloride form) anion-exchange resin were purchased from Aldrich and used as supplied; Sephadex[®] LH-20 was obtained from GE health care bioscience, $\text{RuCl}_3 \cdot 3\text{H}_2\text{O}$ was obtained from American elements, SeO_2 was obtained from Ajax chemicals. The syntheses of ligands bb_n ($n = 7, 10, 12, 14$ and 16)²⁵ and $[\text{Ru}(\text{tpy})\text{Cl}_3]$ ²⁶ were performed according to reported literature methods.

2.2.3. Cyclic voltammetry

Cyclic voltammetry was carried out using an eDAQ EA161 potentiostat operated via an eDAQ ED401 e-corder. A glassy carbon working electrode, platinum wire counter electrode and Ag/AgCl reference electrode were used. The data was normalised against the known standard Ferrocene.⁴² HPLC grade acetonitrile was used as solvent and the

supporting electrolyte was 0.1 mol/L tetra-*n*-butyl ammonium hexafluorophosphate (Aldrich).

2.2.4. Cytotoxicity assays

The cytotoxicity assays were carried out by Prof. Alaina J. Ammit at the University of Sydney. Cytotoxicity data was obtained using the mitochondrial-dependent reduction of 3-(3,4-dimethylthiazol-2yl)-5-diphenyl tetrazolium bromide (MTT) to formazan as described by Guh *et al.*³⁷ Metal complex solutions, including the control platinum complexes cisplatin and carboplatin, were made to the required concentrations in warm Milli-Q water. Growth inhibition assays were carried out over a 72 h continuous exposure period.

2.2.5. Synthesis

All newly synthesised materials were characterised by ¹H NMR, ¹³C NMR and microanalyses. All known materials were characterised by ¹H NMR and were found to be consistent with that previously reported in the literature.

Trinitro-terpyridine

4,4',4''-trinitro-2,2':6',2''-terpyridine was synthesised in three steps according to previously reported method as described below.³⁹ The intermediate compounds were characterised by ¹H NMR.

2,2':6',2''-Terpyridine trioxide

A solution of 2,2':6',2''-terpyridine (4.0 g, 17.1 mmol) in glacial acetic acid (21 mL) and 30% hydrogen peroxide (14 mL) was heated for 2 h at 80 °C after addition of

further hydrogen peroxide (14 mL) the temperature was raised to 90 °C and maintained for 18 h. The mixture was then poured into acetone (200 mL). After standing for 4-6 h, the precipitate was filtered and washed with acetone (2 × 40 mL) to obtain 4.2 g of product with high purity (yield 88%). ¹H NMR (400 MHz, CDCl₃): δ 8.35 (t, *J* = 9.3 Hz, 2H); 7.81 (d, *J* = 6.9 Hz, 2H); 7.77 (t, *J* = 5.2 Hz, 2H); 7.45 (t, *J* = 7.25 Hz, 1H); 7.36 (m, 4H).

4,4',4''-Trinitro-2,2':6',2''-terpyridine trioxide

Fuming nitric acid (90%, 7.2 mL) was added slowly to a cooled mixture of 2,2':6',2''-terpyridine trioxide (4.2 g, 15.1 mmol), conc. sulfuric acid (15 mL) and fuming sulfuric acid (30%, 3.6 mL) at 0-5 °C. The mixture was then stirred at 100 °C for 1 h and at 120 °C for 4 h. The contents of the flask were then poured into ice water and filtered. The precipitate, after washing first with sodium bicarbonate solution (40 mL) and then with water (40 mL), was dried and crystallised from 50% aqueous pyridine (50 mL) to yield 1.3 g of a light yellow coloured product (yield 21%). ¹H NMR (400 MHz, CDCl₃): δ 8.66 (s, 2H); 8.55 (d, *J* = 3.0 Hz, 2H); 8.39 (d, *J* = 7.4 Hz, 2H); 8.25 (dd, *J* = 2.9 Hz, 3.2 Hz, 2H).

4,4',4''-Trinitro-2,2':6',2''-terpyridine

A mixture of 4,4',4''-trinitro-2,2':6',2''-terpyridine trioxide (1.3 g) and phosphorus trichloride (15 mL) was refluxed for 18 h under an Ar atmosphere, and the hot solution was then poured on ice and made alkaline with 40% ammonium hydroxide solution. The precipitate was filtered, dried under vacuum, and crystallised from benzene to obtain 0.64 g of the product with high purity (yield 56%). ¹H NMR (400 MHz, CDCl₃):

δ 9.30 (s, 2H); 9.28 (d, $J = 2.0$ Hz, 2H); 9.08 (d, $J = 5.2$ Hz, 2H); 8.18 (dd, $J = 2.0$ Hz, 1.9 Hz, 2H).

bbN_n ligands

The bbN_n ligands were prepared according to previously reported methods.²⁵

4-formyl-4'-methyl-2,2'-bipyridine.

4-formyl-4'-methyl-2,2'-bipyridine was synthesised using a slight modification of previously reported methods and the ¹H NMR characterisation was found to be consistent with that previously reported.^{40,41} 4,4'-dimethyl-2,2'-bipyridine (2.0 g, 10.8 mmol) and SeO₂ (1.8 g, 16.7 mmol) were refluxed in 1,4-dioxane (45 mL) under a N₂ atmosphere for 24 h. The solution was filtered while hot to remove the solid selenium and the filtrate allowed to stand at room temperature for 1 h and then evaporated to obtain a pale pink powder. This crude product was redissolved in ethyl acetate (150 mL), the undissolved solid was removed by filtration and the filtrate was evaporated to obtain a pale yellow solid. The crude product was dissolved in a minimal volume of dichloromethane (DCM) and impregnated with silica gel (230-400 mesh, 5 g) the impregnated mixture was then loaded on a silica gel column (230-400 mesh; 3cm diam. \times 15 cm), the unreacted Me₂bpy was eluted with 5% (v/v) ethyl acetate in *n*-hexane and the product was eluted using 20-30% (v/v) ethyl acetate in *n*-hexane. The purity of each fraction was monitored by TLC, using 30% (v/v) ethyl acetate in *n*-hexane as the mobile phase. The purest fractions were combined and the solvent was evaporated *in vacuo* to obtain a white solid. A final recrystallisation with *n*-pentane gave 0.82 g of the product with high purity as a white powder (yield 38 %). ¹H NMR (400 MHz, CDCl₃): δ 10.17

(s, 1H); 8.89 (d, $J = 5.1$ Hz, 1H); 8.85 (s, 1H); 8.57 (d, $J = 4.9$ Hz, 1H); 8.28 (s, 1H); 7.72 (d, $J = 5.0$ Hz, 1H); 7.20 (d, $J = 4.2$ Hz, 1H); 2.46 (s, 3H).

bbN₇

A mixture of 4-formyl-4'-methyl-2,2'-bipyridine (0.74 g 3.76 mmol) and the 1,3-diaminopropane (0.16 mL, 1.88 mmol) was stirred in methanol (50 mL) at room temperature under an N₂ atmosphere for 4 h. Sodium borohydride (0.57 g, 15.07 mmol) was then added to the reaction mixture and stirred at 65 °C for 1-2 h. The solvent was evaporated from the reaction mixture and water (10 mL) added to the crude residue. The organic component was extracted with DCM (3 × 50 mL), and the organic phase was then washed with water (20 mL) and brine (20 mL). After removing the solvent, the crude residue was purified by column chromatography using silica gel, the unreacted starting material and other impurities were eluted with 1-2 % (v/v) MeOH in DCM and the *bbN₇* was eluted with 5-8 % (v/v) MeOH and 0.1% (v/v) triethylamine in DCM. Yield: 0.38 g, 23%. ¹H NMR (400 MHz, CDCl₃): δ 8.59 (d, $J = 6.2$ Hz, 2H); 8.53 (d, $J = 7.9$ Hz, 2H); 8.32 (s, 2H); 8.22 (s, 2H); 7.30 (bs, 2H); 7.13 (d, $J = 3.9$ Hz, 2H); 3.89 (s, 4H); 2.74 (t, $J = 10.9$ Hz, 4H); 2.44 (s, 6H); 1.66-1.52 (m, 2H).

bbN₁₆

This compound was prepared analogously to the above method from 4-formyl-4'-methyl-2,2'-bipyridine (0.81 g 4.10 mmol) and 1,12-diaminopropane (0.41 g, 2.05 mmol). Yield: 0.56 g, 24%. ¹H NMR (400 MHz, CDCl₃): δ 8.61 (d, $J = 5.0$ Hz, 2H); 8.52 (d, $J = 4.9$ Hz, 2H); 8.30 (s, 2H); 8.21 (s, 2H); 7.36 (bs, 2H); 7.12 (d, $J = 5.1$ Hz, 2H); 3.90 (s, 4H); 2.63 (dd, $J = 7.1$ Hz, 4H); 2.42 (s, 6H); 1.33-1.21 (m, 20H).

$[\{Ru(tpy)Cl\}_2 \{\mu-bb_n\}]^{2+}$ (Cl-Rubb_n)

The ruthenium(II) complexes Cl-Rubb_n were synthesised using a slight modification of methods previously described.²⁴ ¹H NMR and ¹³C NMR of these complexes are consistent with those previously reported.²⁴

$[\{Ru(tpy)Cl\}_2 (\mu-bb_7)](PF_6)_2$ Anal. Calcd. for $[\{Ru(tpy)Cl\}_2 (\mu-bb_7)](PF_6)_2 \cdot C_3H_6O$: C, 48.9%; H, 3.97%; N, 9.2%. Found: C, 49.1%; H, 4.11%; N, 9.3%.

$[\{Ru(tpy)Cl\}_2 (\mu-bb_{10})](PF_6)_2$ Anal. Calcd. for $[\{Ru(tpy)Cl\}_2 (\mu-bb_{10})](PF_6)_2 \cdot 2C_3H_6O$: C, 50.3%; H, 4.47%; N, 8.6%. Found: C, 50.4%; H, 4.4%; N, 8.8%.

$[\{Ru(tpy)Cl\}_2 (\mu-bb_{12})](PF_6)_2$ Anal. Calcd. for $[\{Ru(tpy)Cl\}_2 (\mu-bb_{12})](PF_6)_2 \cdot C_3H_6O$: C, 50.5%; H, 4.43%; N, 8.8%. Found: C, 50.6%; H, 4.65%; N, 8.5%.

$[\{Ru(tpy)Cl\}_2 (\mu-bb_{14})](PF_6)_2$ Anal. Calcd. for $[\{Ru(tpy)Cl\}_2 (\mu-bb_{14})](PF_6)_2$: C, 50.7%; H, 4.38%; N, 8.9%. Found: C, 50.8%; H, 4.56%; N, 9.0%.

$[Ru\{(NO_2)_3tpy\}Cl_3]$

4,4',4''-Trinitro-2,2':6',2''-terpyridine (0.44 g, 1.7 mmol) was stirred in absolute ethanol (EtOH, 220 mL) with gentle heating until dissolution. RuCl₃·3H₂O (0.63 g, 1.7 mmol) was added and the solution refluxed for 3 h with stirring under a nitrogen atmosphere. After the mixture was cooled to room temperature, the violet brown precipitate was filtered, washed with excess ethanol and ether, and dried under vacuum to yield 0.58 g of the product (yield 59%). ¹H NMR (400 MHz, DMSO-d₆): δ 9.91 (s, 2H); 9.73 (d, *J* = 2.5 Hz, 2H); 9.70 (d, *J* = 6.3 Hz, 2H); 8.30 (dd, *J* = 2.5 Hz, 2.4 Hz, 2H). ¹³C NMR (DMSO-d₆): δ 160.0, 158.1, 157.3, 154.2, 153.2, 120.8, 117.9, 117.5, 56.4, 19.0.

[Ru{(NO₂)₃tpy}(Me₂bpy)Cl]Cl

A solution of [Ru{(NO₂)₃tpy}Cl₃] (0.10 g, 0.17 mmol) and Me₂bpy (0.032 g, 0.17 mmol) in EtOH/H₂O (4:1; 20 mL) was refluxed under an N₂ atmosphere for 5 h. After cooling, the solvent mixture was evaporated to approximately half of the original volume and saturated aqueous NH₄PF₆ was added slowly to precipitate a dark violet-purple material, which was filtered and washed with ethanol (2 × 15 mL) followed by diethyl ether (2 × 15 mL). The crude product was dissolved in a minimum amount of acetone and loaded onto a column of Sephadex LH-20 (2 cm diam. × 30 cm), and using acetone as the eluent, the major first band was collected and acetone was evaporated to obtain [Ru{(NO₂)₃tpy}(bpy)Cl]PF₆ complex as a dark violet-brown material and was crystallised using acetonitrile/toluene. Anal. Calcd. for [Ru{(NO₂)₃tpy}(Me₂bpy)Cl]PF₆: C, 38.9%; H, 2.42%; N, 13.4%. Found: C, 39.0%; H, 2.22%; N, 13.2%. ¹H NMR (400 MHz, CD₃CN): δ 9.90 (d, *J* = 5.4 Hz, 1H); 9.57 (s, 2H); 9.35 (t, *J* = 2.5 Hz, 2H); 8.56 (s, 1H); 8.23 (s, 1H); 8.07-8.05 (m, 4H); 7.92 (d, *J* = 5.7 Hz, 1H); 6.88 (d, *J* = 5.9 Hz, 1H); 6.80 (d, *J* = 6.0 Hz, 1H); 2.82 (s, 3H); 2.34 (s, 3H). ¹³C NMR (CD₃CN): δ 160.8, 159.9, 157.7, 155.6, 154.9, 154.4, 152.35, 152.28, 152.20, 151.3, 150.9, 129.4, 128.2, 125.6, 125.4, 122.2, 118.9, 118.7, 21.4 and 20.8.

The chloride salt was obtained by stirring the PF₆⁻ salt in water with Amberlite IRA- 400 (chloride form) anion-exchange resin. The resin was removed by filtration, and the dark violet-brown solution was freeze-dried to obtain a fluffy dark violet-brown [Ru{(NO₂)₃tpy}(bpy)Cl]Cl. Yield: 65 mg, 51%.

$[\{\text{Ru}\{(\text{NO}_2)_3\text{tpy}\}(\text{Cl})\}_2(\mu\text{-bb}_n)]\text{Cl}_2$

The syntheses of $[\{\text{Ru}\{(\text{NO}_2)_3\text{tpy}\}(\text{Cl})\}_2(\mu\text{-bb}_n)]\text{Cl}_2$ ($n = 12, 16$) complexes were adapted from literature methods.^{24,26} $[\text{Ru}\{(\text{NO}_2)_3\text{tpy}\}\text{Cl}_3]$ (70 mg, 0.12 mmol) was dissolved in EtOH/H₂O (4:1; 15 mL), the appropriate bb_n ligand (0.06 mmol) added and the mixture was refluxed under an N₂ atmosphere for 5-6 h. After cooling, the solvent from the reaction mixture was evaporated to approximately half of the original volume and then cooled, after which a saturated aqueous NH₄PF₆ solution was slowly added until no further precipitation occurred. The dark violet-purple precipitate was then filtered and washed with ethanol (2 × 20 mL) followed by diethyl ether (2 × 20 mL). The crude product was dissolved in a minimum amount of acetone and loaded onto a column of Sephadex LH-20 (2 cm diam. × 30 cm); on elution with acetone the major first band collected. The $[\{\text{Ru}\{(\text{NO}_2)_3\text{tpy}\}\text{Cl}\}_2(\mu\text{-bb}_n)](\text{PF}_6)_2$ complex was isolated with high purity as dark violet-purple material. **$[\{\text{Ru}\{(\text{NO}_2)_3\text{tpy}\}(\text{Cl})\}_2(\mu\text{-bb}_{16})](\text{PF}_6)_2$.** Anal. Calcd. for $[\{\text{Ru}\{(\text{NO}_2)_3\text{tpy}\}(\text{Cl})\}_2(\mu\text{-bb}_{16})](\text{PF}_6)_2 \cdot \text{C}_3\text{H}_6\text{O}$: C, 44.4%; H, 3.78%; N, 11.7%. Found: C, 44.3%; H, 3.67%; N, 11.3%. ¹H NMR (400 MHz, CD₃CN): δ 9.91 (d, $J = 5.8$ Hz, 2H); 9.56 (s, 4H); 9.37-9.33 (m, 4H); 8.56 (dd, $J = 3.8$ Hz, 3.5 Hz, 2H); 8.24 (dd, $J = 3.3$ Hz, 4.7 Hz, 2H); 8.08-8.06 (m, 8H); 7.93-7.90 (m, 2H); 6.88 (m, 2H); 6.83-6.79 (m, 2H); 3.08-3.07 (m, 2H); 2.82 (s, 3H); 2.61-2.60 (m, 2H); 2.34 (s, 3H); 1.60-1.10 (m, 28H). ¹³C NMR (CD₃CN): δ 160.8, 159.9, 157.90, 157.85, 156.7, 155.8, 154.96, 154.92, 154.5, 152.4, 152.33, 152.29, 152.25, 151.3, 150.9, 129.4, 128.7, 128.2, 127.5, 125.7, 125.4, 124.9, 124.7, 122.2, 119.0, 118.7, 36.0, 35.4, 31.1, 30.7, 30.6, 30.46, 30.42, 30.39, 30.30, 30.1, 29.96, 29.92, 29.6, 21.5 and 20.9. **$[\{\text{Ru}\{(\text{NO}_2)_3\text{tpy}\}(\text{Cl})\}_2(\mu\text{-bb}_{12})](\text{PF}_6)_2$.** Anal. Calcd. for $[\{\text{Ru}\{(\text{NO}_2)_3\text{tpy}\}\text{Cl}\}_2(\mu\text{-bb}_{12})](\text{PF}_6)_2$: C, 42.6%; H, 3.24%; N, 12.4%. Found: C, 42.8%; H, 3.33%; N, 12.2%. ¹H NMR (400 MHz, CD₃CN): δ 9.91 (d, $J = 5.3$ Hz, 2H); 9.56 (s, 4H); 9.36-9.32 (m, 4H);

8.55 (dd, $J = 5.8$ Hz, 6.6 Hz, 2H); 8.23 (dd, $J = 5.4$ Hz, 7.0 Hz, 2H); 8.07 (m, 8H); 7.92-7.89 (m, 2H); 6.88 (d, $J = 5.6$ Hz, 2H); 6.81 (m, 2H); 3.07-3.06 (m, 2H); 2.81 (s, 3H); 2.60-2.59 (m, 2H); 2.34 (s, 3H); 1.61-1.08 (m, 20H). ^{13}C NMR (CD_3CN): δ 160.8, 159.9, 157.8, 156.6, 155.7, 154.95, 154.90, 154.4, 152.4, 152.33, 152.29, 152.24, 151.3, 150.9, 129.4, 128.7, 128.2, 127.5, 125.6, 125.4, 124.9, 124.7, 122.2, 118.9, 118.7, 36.0, 35.3, 31.1, 30.76, 30.73, 30.4, 30.3, 30.19, 30.13, 30.09, 29.99, 29.96, 29.89, 29.72, 29.66, 21.4 and 20.9.

The chloride salts were obtained by stirring the PF_6^- salt in water using Amberlite IRA- 400 (chloride form) anion-exchange resin. The resin was removed by filtration, and the solution was freeze-dried to obtain a fluffy dark violet-purple powder of $[\{\text{Ru}\{(\text{NO}_2)_3\text{tpy}\}(\text{Cl})\}_2(\mu\text{-bb}_n)]\text{Cl}_2$ in 30-35% yield.

$[\{\text{Ru}(\text{tpy})\text{Cl}\}_2(\mu\text{-bbH}_2\text{N}_n)]\text{Cl}_4$

To the bbN_7 ligand (53 mg, 0.122 mmol) dissolved in EtOH/ H_2O (4:1; 15 mL), solid $[\text{Ru}(\text{tpy})\text{Cl}_3]$ (108 mg, 0.245 mmol) was added at 60 °C and the reaction mixture was refluxed under an N_2 atmosphere for 5-6 h. After cooling, half of the solvent was evaporated from the reaction mixture and saturated aqueous NH_4PF_6 was added to obtain the PF_6^- salt as a dark purple-brown material, which was filtered and washed with ethanol (2×20 mL) followed by diethyl ether (2×20 mL). The crude product was dissolved in a minimum amount of acetone and loaded onto a column of Sephadex LH-20 (2 cm diam. \times 30 cm); and eluted with acetone, the major first band (dark purple coloured) was collected, the acetone evaporated to obtain $[\{\text{Ru}(\text{tpy})\text{Cl}\}_2(\mu\text{-bbH}_2\text{N}_n)](\text{PF}_6)_2\text{Cl}_2$ complex as a dark purple-brown material. **$[\{\text{Ru}(\text{tpy})\text{Cl}\}_2(\mu\text{-bbH}_2\text{N}_7)](\text{PF}_6)_2\text{Cl}_2$** . Anal. Calcd. for $[\{\text{Ru}(\text{tpy})\text{Cl}\}_2(\mu\text{-bbH}_2\text{N}_7)](\text{PF}_6)_2\text{Cl}_2$: C, 44.4%; H, 3.53%; N, 10.9%. Found: C, 44.6%; H, 3.75%; N, 10.6%. ^1H NMR (400 MHz,

CD₃CN): δ 10.16 (dd, $J = 5.0$ Hz, 5.4 Hz, 1H); 10.00 (d, $J = 5.7$ Hz, 1H); 8.50-8.46 (m, 4H); 8.37-8.29 (m, 6H); 8.12-8.05 (m, 4H); 7.82 (m, 6H); 7.66-7.62 (m, 4H); 7.24-7.6 (m, 6H); 7.05 (d, $J = 6.3$ Hz, 1H); 6.80 (bs, Hz, 1H); 4.50 (bs, 2H); 4.07 (bs, 2H); , 3.10-3.03 (m, 2H); 2.93-2.87 (m, 2H); 2.68 (s, 3H); 2.33 (s, 3H); 1.70-1.64 (m, 2H). ¹³C NMR (CD₃CN): δ 159.5, 158.8, 158.6, 153.5, 153.1, 152.6, 152.2, 149.8, 149.1, 137.9, 134.6, 128.9, 128.1, 127.2, 125.4, 124.4, 123.4, 51.3, 46.0, 21.5 and 20.8.

[{Ru(tpy)Cl}₂](μ -bbH₂N₁₆)](PF₆)₂Cl₂ Anal. Calcd. for [{Ru(tpy)Cl}₂](μ -bbH₂N₁₆)](PF₆)₂Cl₂.3H₂O: C, 46.0%; H, 4.57%; N, 9.8%. Found: C, 45.6%; H, 4.28%; N, 9.4%. ¹H NMR (400 MHz, CD₃CN): δ 10.27 (d, $J = 5.2$ Hz, 1H); 10.03 (d, $J = 5.6$ Hz, 1H); 8.59 (bs, 1H); 8.50 (dd, $J = 1.1$ Hz, 1.8 Hz, 4H); 8.43 (bs, 1H); 8.39 (dd, $J = 1.7$ Hz, 2.6 Hz, 4H); 8.30 (bs, 1H); 8.15 (bs, 1H); 8.11 (t, $J = 8.1$ Hz, 2H); 7.98-7.95 (m, 1H); 7.92-7.87 (m, 4H); 7.85 (dd, $J = 2.5$ Hz, 2.3 Hz, 1H); 7.67-7.63 (m, 4H); 7.37 (bs, 1H); 7.31-7.28 (m, 4H); 7.17 (d, $J = 5.7$ Hz, 1H); 6.95 (d, $J = 5.8$ Hz, 1H); 6.86 (d, $J = 5.2$ Hz, 1H); 4.49 (bs, 2H); 4.06 (bs, 2H); 3.23-3.16 (m, 2H); 2.94-2.86 (m, 2H); 2.78 (s, 3H); 2.36 (s, 3H); 1.61-1.20 (m, 20H). ¹³C NMR (CD₃CN): δ 160.1, 159.6, 159.5, 158.9, 158.7, 158.4, 157.5, 156.2, 153.6, 153.1, 153.0, 152.9, 152.6, 152.2, 149.9, 149.1, 137.9, 134.7, 134.5, 128.9, 128.2, 128.1, 127.8, 126.8, 125.1, 124.45, 124.42, 124.1, 123.4, 123.3, 51.2, 50.7, 49.5, 49.3, 30.0, 29.9, 29.6, 29.5, 27.3, 27.0, 26.9, 21.4 and 20.9.

The chloride salt was obtained by stirring the PF₆⁻ salt in water with Amberlite IRA- 400 (chloride form) anion-exchange resin. The resin was removed by filtration, and the solution was freeze-dried to obtain a fluffy dark purple-brown powder of [{Ru(tpy)Cl}₂](μ -bbH₂N_n)]Cl₄. Yield: 20-25%.

$[\{\text{Ru}\{(\text{NO}_2)_3\text{tpy}\}(\text{Cl})\}_2(\mu\text{-bbH}_2\text{N}_{16})]\text{Cl}_4$

The synthesis of $[\{\text{Ru}\{(\text{NO}_2)_3\text{tpy}\}(\text{Cl})\}_2(\mu\text{-bbH}_2\text{N}_{16})]\text{Cl}_4$ complex was prepared as described for $[\{\text{Ru}(\text{tpy})\text{Cl}\}_2(\mu\text{-bbH}_2\text{N}_n)]\text{Cl}_4$. Typical yield ~ 20%.

$[\{\text{Ru}\{(\text{NO}_2)_3\text{tpy}\}(\text{Cl})\}_2(\mu\text{-bbH}_2\text{N}_{16})](\text{PF}_6)_2\text{Cl}_2$ Anal. Calcd. for $[\{\text{Ru}\{(\text{NO}_2)_3\text{tpy}\}(\text{Cl})\}_2(\mu\text{-bbH}_2\text{N}_{14})](\text{PF}_6)_2\text{Cl}_2 \cdot 1.5\text{C}_3\text{H}_6\text{O}$: C, 41.8%; H, 3.73%; N, 12.5%. Found: C, 41.7%; H, 3.48%; N, 12.1%. ^1H NMR (400 MHz, CD_3CN): δ 9.92-9.91 (m, 2H); 9.57 (s, 2H); 9.48 (s, 1H); 9.36 (s, 2H); 9.31 (dd, $J = 1.6$ Hz, 2.1 Hz, 2H); 8.71 (m, 1H); 8.56-8.55 (m, 2H); 8.40-8.37 (m, 1H); 8.26-8.25 (m, 1H); 8.17 (d, $J = 2.5$ Hz, 1H); 8.07-8.05 (m, 8H); 7.43 (t, $J = 10.2$ Hz, 1H); 6.97-6.95 (m, 4H); 4.28 (dd, $J = 5.8$ Hz, 5.0 Hz, 2H); 3.84-3.82 (m, 2H); 2.96-2.95 (m, 2H); 2.82 (s, 3H); 2.79-2.77 (m, 2H); 2.35 (s, 3H); 1.74-1.05 (m, 20H). ^{13}C NMR (CD_3CN): δ 160.79, 160.74, 159.8, 159.7, 155.4, 154.9, 154.4, 153.0, 152.2, 151.6, 151.1, 129.5, 128.44, 128.32, 126.9, 125.6, 125.0, 124.3, 122.2, 119.3, 118.9, 118.6, 115.5, 112.8, 51.0, 49.4, 29.8, 29.6, 28.1, 27.2, 21.4, 20.9 and 14.4.

$[\text{Ru}\{(\text{NO}_2)_3\text{tpy}\}(\text{Cl})(\text{bbH}_2\text{N}_{16})]\text{Cl}_3$

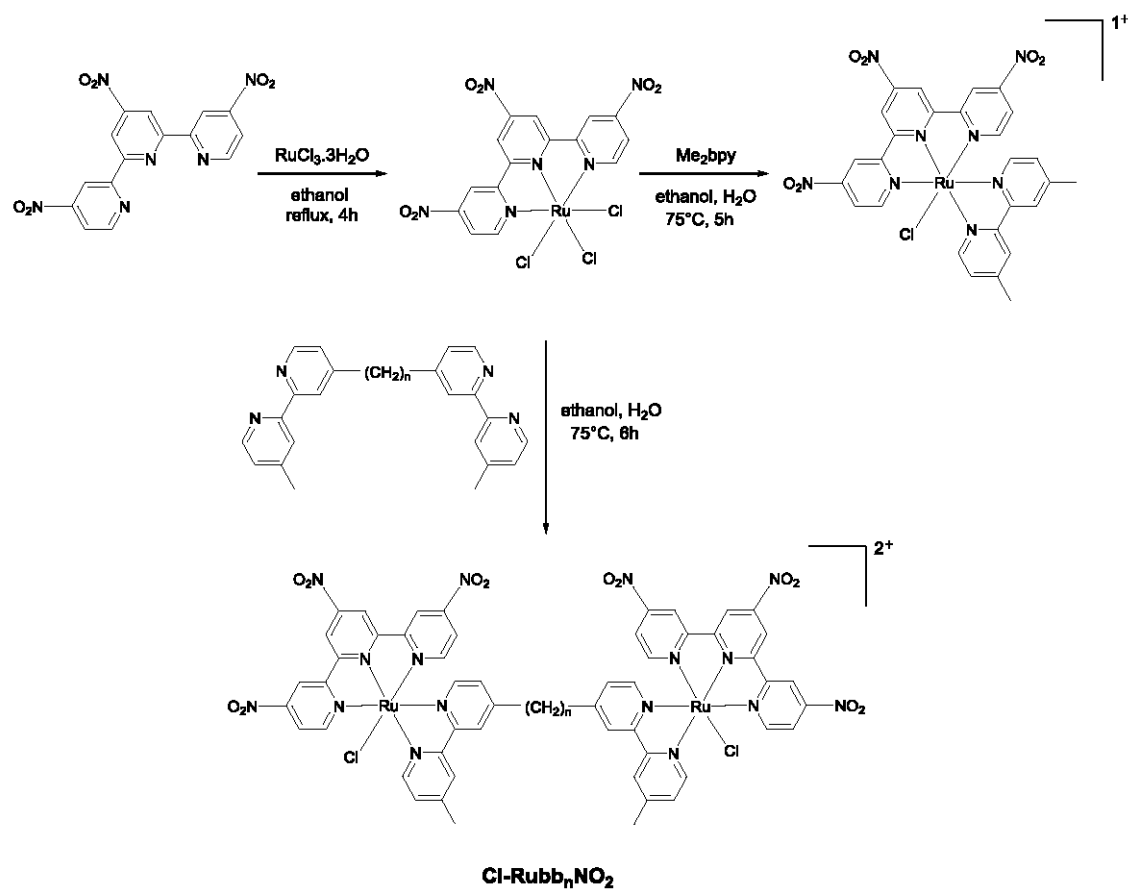
The mononuclear complex was prepared using an analogous method to that reported for $[\{\text{Ru}(\text{tpy})\text{Cl}\}_2(\mu\text{-bbH}_2\text{N}_n)]\text{Cl}_4$ from $[\text{Ru}\{(\text{NO}_2)_3\text{tpy}\}\text{Cl}_3]$ (50 mg, 0.086 mmol) and the bbN_{16} ligand (49 mg, 0.086 mmol) to obtain $[\text{Ru}\{(\text{NO}_2)_3\text{tpy}\}(\text{Cl})(\text{bbH}_2\text{N}_{16})]\text{Cl}_3$ as dark violet-brown solid. Typical yield ~ 24%. **$[\text{Ru}\{(\text{NO}_2)_3\text{tpy}\}(\text{Cl})(\text{bbH}_2\text{N}_{16})](\text{PF}_6)\text{Cl}_2$** Anal. Calcd. for $[\text{Ru}\{(\text{NO}_2)_3\text{tpy}\}(\text{Cl})(\text{bbH}_2\text{N}_{16})](\text{PF}_6)\text{Cl}_2 \cdot 0.5\text{C}_3\text{H}_6\text{O}$: C, 47.9%; H, 4.67%; N, 12.5%. Found: C, 47.7%; H, 4.47%; N, 12.6%. ^1H NMR (400 MHz, CD_3CN): δ 9.95 (m, 1H); 9.56 (d, $J = 3.4$ Hz, 1H); 9.46 (m, 1H); 9.33-9.30 (m, 2H); 8.66 (m, 1H); 8.50-8.41 (m, 2H); 8.33 (m, 1H); 8.26-8.22 (m, 2H); 8.17 (m, 1H); 8.03-7.96 (m, 5H); 7.44-7.41 (m, 2H); 7.27-7.24 (m, 1H); 6.97-6.89 (m, 3H); 4.28-4.26 (m,

2H); 3.76-3.71 (m, 2H); 2.84-2.78 (m, 4H); 2.46-2.39 (m, 3H); 2.34 (s, 3H); 1.65-1.08 (m, 20H). ^{13}C NMR (CD_3CN): δ 168.0, 161.5, 161.0, 160.0, 159.3, 158.4, 158.1, 157.9, 156.1, 155.1, 154.7, 153.5, 153.3, 153.1, 152.8, 152.5, 152.1, 151.8, 150.1, 129.4, 128.4, 127.6, 127.3, 126.6, 125.6, 123.9, 122.8, 122.5, 122.2, 121.9, 115.8, 113.0, 66.8, 50.1, 49.6, 30.4, 29.8, 28.0, 27.6, 21.5, 20.0 and 14.7.

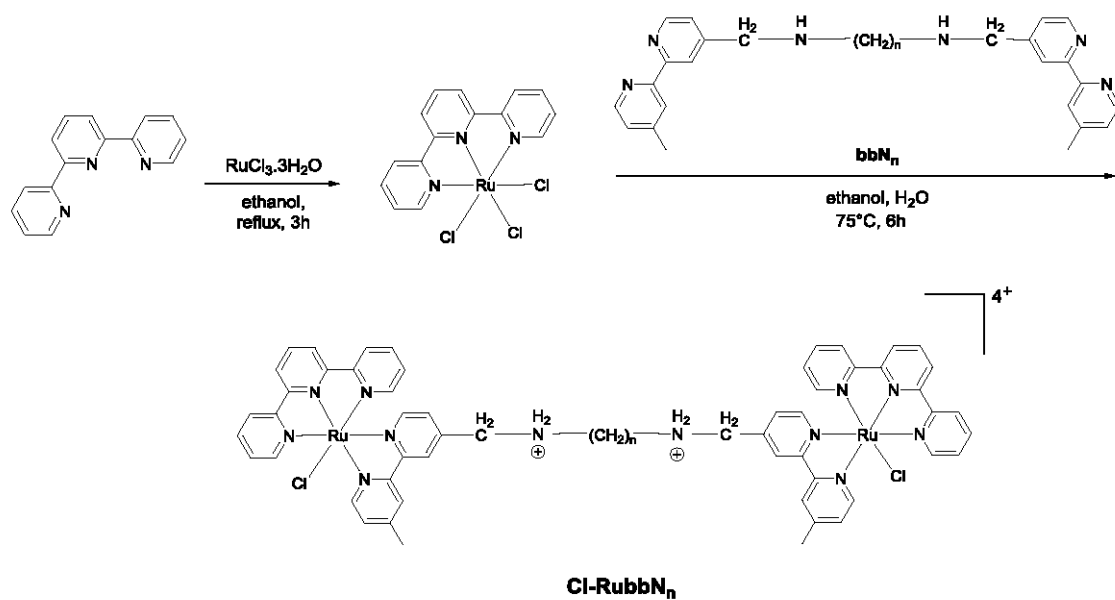
2.3. Results

2.3.1. Synthesis

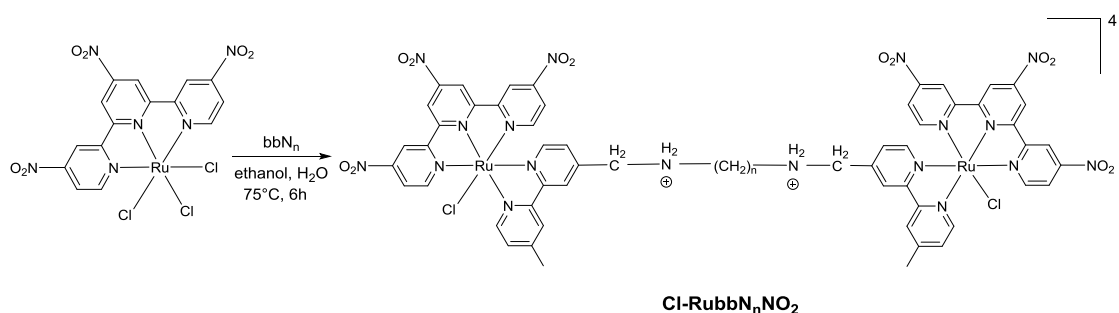
The syntheses of the mononuclear $[\text{Ru}(\text{tpy})(\text{bpy})\text{Cl}]^+$ and the dinuclear complexes $[\{\text{Ru}(\text{tpy})\text{Cl}\}_2(\mu\text{-bb}_n)]^{2+}$ (Cl-Rubb_n for n = 7, 10, 12, 14 and 16) have been previously reported.^{24,25} In this study, the family of dinuclear complexes has been extended through the synthesis of Cl-Rubb_nNO₂, Cl-RubbN_n, and Cl-RubbN_nNO₂ complexes, as shown in Schemes 2.1, 2.2 and 2.3. For the Cl-RubbN_n complexes, the procedure used for the synthesis of the Cl-Rubb_n complexes resulted in poor yield and purity for the Cl-RubbN_n complexes. To obtain satisfactory yields the bbN_n ligand was dissolved in ethanol/water and heated to 60 °C before the $[\text{Ru}(\text{tpy})\text{Cl}_3]$ was added, and then the mixture refluxed for a longer time period than was necessary for the synthesis of Cl-Rubb_n. $[\text{Ru}\{(\text{NO}_2)_3\text{tpy}\}\text{Cl}_3]$ was prepared in a similar manner to that previously reported for $[\text{Ru}(\text{tpy})\text{Cl}_3]$,²⁶ and upon addition of Me₂bpy yielded $[\text{Ru}\{(\text{NO}_2)_3\text{tpy}\}(\text{Me}_2\text{bpy})\text{Cl}]\text{Cl}$ in good yield. The synthesis of the new chlorido-containing dinuclear complexes Cl-Rubb_nNO₂ and Cl-RubbN_nNO₂ were achieved using similar procedures.



Scheme 2.1



Scheme 2.2



Scheme 2.3

2.3.2. Anticancer activity

The *in vitro* cytotoxicities of the ruthenium complexes and the control platinum complexes cisplatin and carboplatin were determined against the MCF-7 and MDA-MB-231 breast cancer cell lines, and the results are summarised in Table 2.1. Cisplatin showed moderate cytotoxicity against both cell lines, while carboplatin was essentially inactive. Although IC₅₀ values reported for cisplatin against MCF-7 cells can vary considerably, the results obtained for both control platinum complexes against both cell lines are consistent with previous studies.^{23,27-29} The dinuclear ruthenium complexes Cl-Rubb_n, for n = 10, 12 and 14, were more active than cisplatin against both cell lines. Interestingly, Cl-Rubb₁₂ was the most active, with the ruthenium complexes having the shortest linking chain (Cl-Rubb₇) and longest linking chain (Cl-Rubb₁₆) being the least active. Addition of nitro substituents onto the tpy rings of Cl-Rubb₁₂ and Cl-Rubb₁₆ decreased the activity of the ruthenium complexes, particularly in the case of the highly active Cl-Rubb₁₂. The replacement of two methylene groups by two amine groups in the ligand bridge for Cl-Rubb₇ (giving Cl-RubbN₇) and Cl-Rubb₁₆ (Cl-RubbN₁₆) decreased the activity of the former but had no effect on the latter complex that contained the longer linking chain. However, it was also noted that the replacement of the Me₂bpy ligand in [Ru{(NO₂)₃tpy}(Me₂bpy)Cl]⁺ by the bbN₁₆ ligand to form the mononuclear complex Cl-RubbN₁₆NO₂mono did significantly increase the activity in both cancer cell

lines. In the one example examined, the combination of amine groups in the linking ligand and nitro substituents on the *tpy* ligands for $\text{Cl-Ru(bbbN)}_3\text{NO}_2$ had little effect on the cytotoxicity with the MCF-7 cells but decreased the activity against the MDA-MB-231 cell line.

Table 2.1. The IC_{50} values of the metal complexes against the MCF-7 and MDA-MB-231 breast cancer cell lines, defined as the concentration (μM) of the complex required to inhibit cell growth by 50%.

Metal Complex	IC_{50} (μM)	
	MCF-7	MDA-MB-231
Cisplatin	34 ± 2	31 ± 3
Carboplatin	273 ± 7	451 ± 8
Cl-Rubb ₇	29 ± 4	24 ± 5
Cl-Rubb ₁₀	8 ± 3	14 ± 3
Cl-Rubb ₁₂	8 ± 4	9 ± 4
Cl-Rubb ₁₄	7 ± 4	13 ± 1
Cl-Rubb ₁₆	27 ± 5	24 ± 6
[Ru{(NO ₂) ₃ tpy}(Me ₂ bpy)]	48 ± 4	105 ± 7
Cl-RubbN ₇	68 ± 3	35 ± 4
Cl-RubbN ₁₆	27 ± 2	31 ± 4
Cl-Rubb ₁₂ NO ₂	42 ± 5	35 ± 4
Cl-Rubb ₁₆ NO ₂	36 ± 2	32 ± 2
Cl-RubbN ₁₆ NO ₂	31 ± 2	36 ± 2
Cl-RubbN ₁₆ NO ₂ mono	27 ± 2	26 ± 2

2.3.3. *Aquation and GMP binding*

Previous studies with mononuclear ruthenium(II) complexes that contain a chlorido ligand have shown that the first step in the binding to guanosine 5'-monophosphate disodium salt (GMP), a simple model for DNA, is aquation. Consistent with previous studies,²⁴ aquation of $[\text{Ru}(\text{tpy})(\text{Me}_2\text{bpy})\text{Cl}]^+$ was found to be relatively fast, with 50% of the ruthenium complex being converted to the corresponding aqua form in approximately 60 minutes. Similarly, 50% aquation of each ruthenium centre in the dinuclear complexes Cl-Rubb_n and Cl-RubbN_n was shown by ¹H NMR spectroscopy to occur in approximately 120 minutes (see Figure 2.3). The aquation then proceeds to equilibrium, where approximately 90% of the ruthenium complex exists in the aqua form. The inclusion of amine groups into the linking ligand had no significant effect on the rate or equilibrium position of aquation.

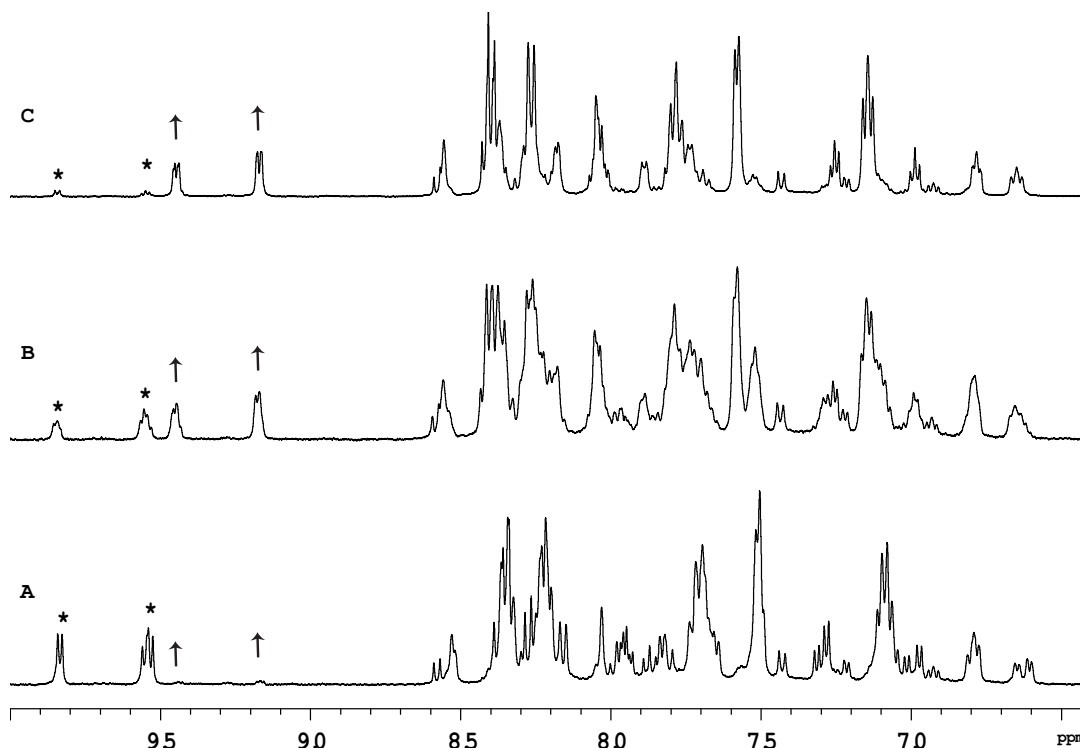


Figure 2.3. Aromatic region of the ^1H NMR spectrum of Cl-RubbN_{16} in D_2O as a function of time, after 5 minutes (A), 120 minutes (B) and 27 hours (C). The asterisk indicates the decrease in the $\text{H6-Me}_2\text{bpy}$ resonances of the Cl-RubbN_{16} complex, while the arrow shows the increase in the $\text{H6-Me}_2\text{bpy}$ resonances from the $\text{D}_2\text{O-RubbN}_{16}$ complex.

Figure 2.4 shows the ^1H NMR spectrum of Cl-RubbN_{16} as a function of time after dissolution in D_2O and the addition of 2 equivalents of GMP. After 120 minutes, the spectrum of the Cl-RubbN_{16} is essentially identical to that in the absence of GMP, as shown in Figure 2.3, with approximately 50% of the dinuclear complex aquated but with no covalent binding to GMP observed. As evidenced by the increasing intensity of the resonance at 5.36 ppm, assigned to the sugar $\text{H1}'$ of GMP bound to a ruthenium centre, the aquated form of Cl-RubbN_{16} slowly reacts with GMP, reaching an equilibrium of approximately 33% bound in 24 hours. Similar results were obtained with the Cl-Rubb_n complexes.

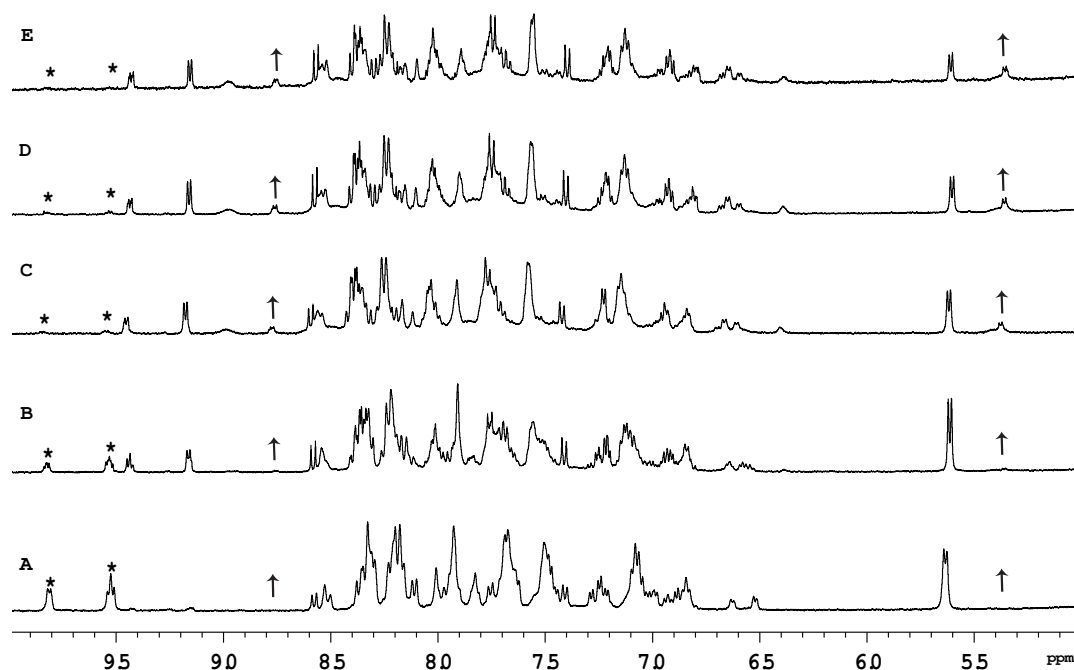


Figure 2.4. Aromatic region of the ^1H NMR spectrum of the $\text{Cl-RubbN}_{16} + \text{GMP}$ in D_2O as a function of time, after 10 minutes (A), 120 minutes (B), 450 minutes (C), 25 hours (D) and 76 hours (E). The asterisk indicates the decrease in H6- Me_2bpy resonances of the Cl-RubbN_{16} complex, while the arrows shows the increase of the peak for the H6- Me_2bpy protons of the GMP bound ruthenium complex (8.76 ppm) and the sugar H1' of the bound GMP (5.36 ppm).

Figure 2.5 shows the ^1H NMR spectrum of $[\text{Ru}\{(\text{NO}_2)_3\text{tpy}\}(\text{Me}_2\text{bpy})\text{Cl}]^+$ at various time points after the ruthenium complex was dissolved in D_2O . Unlike the corresponding non-nitrated complex $[\text{Ru}(\text{tpy})(\text{Me}_2\text{bpy})\text{Cl}]^+$, where $> 95\%$ of the ruthenium complex was converted into the aqua form well within 24 hours, 60% of the $[\text{Ru}\{(\text{NO}_2)_3\text{tpy}\}(\text{Me}_2\text{bpy})\text{Cl}]^+$ remained unchanged after 24 hours. This indicates that the incorporation of the nitro substituent on the tpy ligand significantly slowed the aquation reaction. Even after 216 hours, 25% of the original $[\text{Ru}\{(\text{NO}_2)_3\text{tpy}\}(\text{Me}_2\text{bpy})\text{Cl}]^+$ remained in the chlorido form. Interestingly, however, 10% of the $[\text{Ru}\{(\text{NO}_2)_3\text{tpy}\}(\text{Me}_2\text{bpy})\text{Cl}]^+$ was rapidly converted into another form after

being dissolved. This new complex then appeared to slowly aquate. Based upon the observations of Fallahpour *et al.*,³⁰ it is proposed that one of the three nitro substituents on the tpy ligand is reduced to an amine. This new “(NO₂)₂(NH₂)-tpy” complex then slowly aquates.

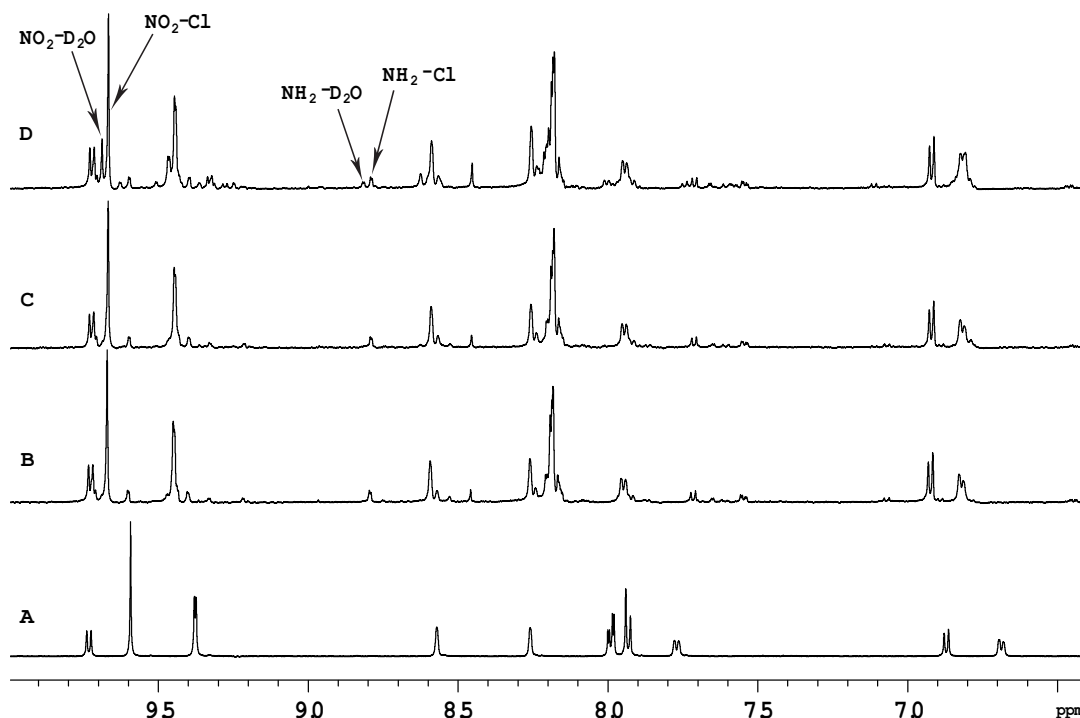


Figure 2.5. Aromatic region of the ¹H NMR spectrum of [Ru{(NO₂)₃tpy}(Me₂bpy)Cl]⁺ in CD₃OD (A) and in D₂O as a function of time, after 30 minutes (B), 4 hours (C) and 24 hours (D). NO₂-Cl indicates the non-aquated complex {H3' and H5' of (NO₂)₃tpy} and NO₂-D₂O represents the aquated form, while NH₂-Cl {H3 and H3" of (NO₂)₃tpy} and NH₂-D₂O represent the putative “(NO₂)₂(NH₂)-tpy” complexes.

2.3.4. Cyclic voltammetry of $[Ru\{(NO_2)_3tpy\}(Me_2bpy)Cl]^+$

Electrochemical measurements were carried out on the $[Ru\{(NO_2)_3tpy\}(Me_2bpy)Cl]^+$ and $[Ru(tpy)(Me_2bpy)Cl]^+$ complexes to assess the electronic effect of the nitro substituents on the ruthenium centre, and the electrode potentials are listed in Table 2.2.

(see Figure A1 in Appendix)

Table 2.2. Electrode potentials for $[Ru(L)(Me_2bpy)Cl]Cl$ in acetonitrile (in V vs Ag/AgCl; working electrode = glassy carbon).

Process ^a	L = tpy	L = (NO ₂) ₃ tpy
Oxidation E _a	0.94 ^b	1.24 (sh)
	1.28	1.33
Reduction E _c	-1.36	-0.40 (sh)
	-1.54	-0.52 (sh)
		-0.66
		-1.17 (sh)
		-1.45

^a All peaks irreversible unless otherwise stated; potentials are given for forward peaks; anodic (E_a) for oxidations and cathodic (E_c) for reductions. ^b Reversible; E_{1/2} = 0.90 V

The electrochemical response of the $[Ru(tpy)(Me_2bpy)Cl]^+$ complex as a hexafluorophosphate salt has previously been investigated;³¹ and the results here are consistent with that report: two ligand-based reductions are observed in the cathodic

region (tpy/tpy⁻ followed by Me₂bpy/Me₂bpy⁻), while the anodic region shows a reversible Ru(III/II) peak at +0.90 V. In the present case, an irreversible peak is also seen at +1.28 V, corresponding to oxidation of the chloride counter-ion. The [Ru{(NO₂)₃tpy}(Me₂bpy)Cl]⁺ complex shows several important changes compared to the non-nitrated parent complex. Three closely-spaced reductions appear at low potentials in the cathodic region (-0.4 to -0.7 V), followed by further irreversible peaks at more negative potentials. Previous work on the electrochemical behaviour of nitrated bipyridines and their platinum complexes has shown analogous cathodic behaviour: for example [Pt{4,4'-(NO₂)₂bpy}Cl₂] displayed two closely-spaced reductions, and the LUMOs for that complex were shown to be localised largely on the “NO₂-py” units.³² Further reduction of the complex occurred at -1.05 V,³³ very close to the potential of -1.06 V observed for the first reduction (bpy/bpy⁻) of the non-nitrated complex [Pt(bpy)Cl₂] under the same conditions.³² Based on these observations, the first three cathodic peaks for [Ru{(NO₂)₃tpy}(Me₂bpy)Cl]Cl are assigned here to reductions involving the NO₂-py moieties. The next two peaks are assigned to further reduction of the (NO₂)₃tpy ligand and reduction of the Me₂bpy ligand, probably in that order.

Most importantly, the nitro substituents are observed to exert a strong effect on the ruthenium centre, as the anodic peak corresponding to the Ru(III/II) couple is shifted positively by at least 300 mV, to the point where it coincides with oxidation of the chloride counter-ion (and is irreversible). This large positive shift indicates that the nitro substituents cause a significant decrease in the electron density on the ruthenium centre, making oxidation to Ru(III) more difficult.

2.4. Discussion

The results of this study show that the dinuclear ruthenium(II) complexes Cl-Rubb_n have potential as drugs against breast cancer. The most active complex, Cl-Rubb₁₂, was almost four-times more active than cisplatin. Furthermore, Cl-Rubb₁₂ is more active than the mononuclear [Ru(apy)(tpy)Cl]⁺ and dinuclear [{Ru(bpy)₂Cl}₂{μ-BL}]²⁺ complexes previously reported by other groups,^{22,23} and of similar activity to the most active dinuclear ruthenium-arene complex linked by a bis(pyridinone)alkane chain reported by Mendoza-Ferri *et al.*²¹ Interestingly, the Cl-Rubb_n complexes with the shortest (Cl-Rubb₇) or the longest linking chain (Cl-Rubb₁₆) were the least active against both breast cancer cell lines. Insertion of three nitro substituents onto the tpy ligand of Cl-Rubb₁₂ significantly decreased the activity against both breast cancer cell lines. Incorporation of amine groups into the linking bridging ligand of Cl-Rubb₇ decreased the activity, whereas, it had little effect on the activity of Cl-Rubb₁₆.

In previous studies with chlorido-containing dinuclear ruthenium(II) complexes,^{21,22,24,34} the cytotoxicity has always increased as the number of methylene groups in the flexible alkane chain increased. Interestingly, in the present study the Cl-Rubb₁₆ complex was the least active of the Cl-Rubb_n complexes. The decreased activities of Cl-Rubb₇ and Cl-Rubb₁₆, compared to Cl-Rubb₁₂ suggest two competing factors govern the anticancer activity. While it is yet to be confirmed, it is assumed that the major mechanism of anticancer activity is related to DNA binding, analogous to the corresponding dinuclear platinum complexes. Increasing the number of methylene groups in the linking chain should increase the lipophilicity of the dinuclear complex, and hence the ease with which it can pass through the cellular membrane. While aquation is the necessary first step in DNA binding, as determined by the GMP binding

experiments, all the Cl-Rubb_n complexes exhibited similar rates of aquation and percentage of the aqua form at equilibrium. Consequently, the relative cytotoxicity results could imply that the range of possible DNA cross-linked adducts formed have significantly different biological outcomes, and/or the anticancer activity is controlled by both covalent and reversible binding to DNA. For the corresponding inert Rubb_n complexes, the DNA binding affinity decreases with increasing methylene groups in the linking chain.³⁵ Furthermore, based purely upon polycation condensation of polyanionic DNA, it would also be expected that the cytotoxicity of the Cl-Rubb_n complexes would decrease with increasing chain length.

The inclusion of three nitro substituents on the tpy ligand significantly increased the IC₅₀ value for the more cytotoxic Cl-Rubb₁₂ but had a relatively small effect with the less cytotoxic Cl-Rubb₁₆. It was determined that the [Ru{(NO₂)₃tpy}(Me₂bpy)Cl]⁺ complex aquated significantly more slowly than the non-nitrated parent complex [Ru(tpy)(Me₂bpy)Cl]⁺. This observation is consistent with the results from the cyclic voltammetry study, from which it was concluded that there was a significant reduction in the electron density on the ruthenium centre for the trinitrated complex, compared to the non-nitrated parent complex. The reduced electron density on the ruthenium centre of [Ru{(NO₂)₃tpy}(Me₂bpy)Cl]⁺ would increase the energy barrier for the removal of the chlorido ligand from the metal centre, thereby decreasing the rate of the aquation reaction. Aquation was shown to be the first step in the coordination of the ruthenium complexes with DNA. Consequently, the Cl-Rubb_nNO₂ complexes would not form as many covalent adducts with DNA over the time period of the cytotoxicity assays, compared to their non-nitrated parent complexes. This suggests that the observed cytotoxicity of the Cl-Rubb_nNO₂ complexes would largely be due to their reversible, non-covalent, binding to DNA. Furthermore, it is reasonable to expect that the chlorido

form of the complex would more easily cross a cellular membrane than the more highly positively-charged aquated species. Based upon these assumptions, it could be tentatively concluded that the activity of Cl-Rubb₁₆ was predominantly due to reversible binding to DNA, while the activity of Cl-Rubb₁₂ was due to a combination of covalent and reversible binding to DNA.

Although the inclusion of one or more secondary amines into the bridging ligand of multinuclear platinum complexes significantly increases their cytotoxicity,¹ the incorporation of amine groups into the ligand bridge of Cl-Rubb_n did not increase the cytotoxicity. For the multinuclear platinum complexes, incorporation of an amine group or an inert am(m)ineplatinum(II) centre into the bridge enhances cellular accumulation and increases the affinity for DNA.^{1,8,36} The corresponding inert Rubb_n dinuclear ruthenium complexes (that do not contain labile chlorido ligands) enter L1210 murine leukaemia cells by passive diffusion, with a minor contribution from protein-mediated active transport.³⁵ Consequently, incorporation of amine groups into the ligand bridge could decrease the cellular uptake of the Cl-Rubb_n complexes, and thereby result in the observed lower activity for Cl-RubbN₇ relative to Cl-Rubb₇. However, it was also noted that Cl-RubbN₁₆ was equally as active (albeit weakly) as Cl-Rubb₁₆. This could suggest that the inclusion of an amine in the bridging ligand of a Cl-Rubb_n complex does increase the reversible binding affinity for DNA, thereby compensating for the lower cellular uptake.

2.5. Conclusions

In conclusion, the results of this study support the idea of developing a new class of anticancer agent by transferring from platinum to ruthenium the concept of gaining advantages in efficacy through the use of multinuclear complexes, as proposed by Mendoza-Ferri *et al.*²¹ Dinuclear ruthenium complexes - containing a single chlorido ligand on each metal centre - were synthesised and found to be significantly more active than cisplatin against two breast cancer cell lines. The anticancer activity appears to be due to a combination of covalent and reversible binding with DNA. The IC₅₀ results indicated that the Cl-Rubb₁₂ complex was the most active of the dinuclear complexes. The superior activity of Cl-Rubb₁₂ might be due to the best compromise between lipophilicity (for cellular uptake) and the cytotoxic effects of the covalent adducts formed with DNA. Given the vast array of ligands that can be utilised for the Cl-Rubb_n complexes, it should be possible to optimise cellular uptake and the kinetics of DNA binding, and thereby produce dinuclear ruthenium(II) complexes with significant clinical potential.

2.6. References

1. N. Farrell in *Platinum-Based Drugs in Cancer Therapy*; ed. L. R. Kelland and N. Farrell, Humana Press: Totowa, NJ, 2000, pp 321-338.
2. B. A. J. Jansen, J. van der Zwan, H. den Dulk, J. Brouwer and J. Reedijk, *J. Med. Chem.*, 2001, **44**, 245.
3. N. Farrell, Y. Qu, L. Feng and B. van Houten, *Biochemistry*, 1990, **29**, 9522.

4. Y. Qu, H. Rauter, A. P. S. Fontes, R. Bandarage, L. R. Kelland and N. Farrell, *J. Med. Chem.*, 2000, **43**, 3189.
5. N. Farrell, Y. Qu and M. P. Hacker, *J. Med. Chem.*, 1990, **33**, 2179.
6. P. Perego, L. Gatti, C. Caserini, R. Supino, D. Colangelo, R. Leone, S. Spinelli, N. Farrell and F. Zunino, *J. Inorg. Biochem.*, 1999, **77**, 59.
7. A. Riccardi, D. Meco, C. Ferlini, T. Servidei, G. Carelli, G. Segni, C. Manzotti and R. Riccardi, *Cancer Chemother. Pharmacol.*, 2001, **47**, 498.
8. J. D. Roberts, J. Peroutka, G. Beggiolin, C. Manzotti, L. Piazzoni and N. Farrell, *J. Inorg. Biochem.*, 1999, **77**, 47.
9. C. Manzotti, G. Pratesi, E. Menta, R. Di Domenico, E. Cavalletti, H. H. Fiebig, L. R. Kelland, N. Farrell, D. Polizzi, R. Supino, G. Pezzoni and F. Zunino, *Clin. Cancer Res.*, 2000, **6**, 2626.
10. P. Di Blasi, A. Bernareggi, G. Beggiolin, L. Piazzoni, E. Menta and M. L. Formento, *Anticancer Res.*, 1998, **18**, 3113.
11. G. Pratesi, P. Perego, D. Polizzi, S. C. Righetti, R. Supino, C. Caserini, C. Manzotti, F. C. Giuliani, G. Pezzoni, S. Tognella, S. Spinelli, N. Farrell and F. Zunino, *Brit. J. Cancer*, 1999, **80**, 1912.
12. S. Y. Sharp and L. R. Kelland, *Curr. Opin. Oncol., Endocr. Metab. Invest. Drugs*, 2000, **2**, 353.
13. A. Hegmans, Y. Qu, L. R. Kelland, J. D. Roberts and N. Farrell, *Inorg. Chem.*, 2001, **40**, 6108.

14. H. Rauter, R. Di Domenico, E. Menta, A. Oliva, Y. Qu and N. Farrell, *Inorg. Chem.*, 1997, **36**, 3919.
15. G. Scagilotti, S. Novello, L. Crino, F. De Marinia, M. Tonato, C. Noberasco, G. Selvaggi, F. Massoni, B. Gatti and G. Camboni, *Lung Cancer*, 2003, **41**, S223.
16. A. H. Calvert, H. Thomas, N. Colombo, M. Gore, H. Earl, L. Sena, G. Camboni, P. Liati and C. Sessa, *Eur. J. Cancer*, 2001, **37**, S260.
17. D. I. Jodrell, T. R. J. Evans, W. Steward, D. Cameron, J. Prendiville, C. Aschele, C. Noberasco, M. Lind, J. Carmichael, N. Dodds, G. Camboni, B. Gatti and F. De Braud, *Eur. J. Cancer*, 2004, **40**, 1872.
18. C. Sessa, G. Capri, L. Gianni, F. Peccatori, G. Grasselli, J. Bauer, M. Zucchetti, L. Vigano, A. Gatti, C. Minoia, P. Liati, S. Van den Bosch, A. Bernareggi, G. Camoboni and S. Marsoni, *Ann. Oncol.*, 2000, **11**, 977.
19. J. T. Hartmann and H.-P. Lipp, *Expert Opin. Pharmacother.*, 2003, **4**, 889.
20. P. M. Calvert, M. S. Highley, A. N. Hughes, E. R. Plummer, A. S. T. Azzabi, M. W. Verrill, M. G. Camboni, E. Verdi, A. Bernareggi, M. Zucchetti, A. M. Robinson, J. Carmichael and A. H. Calvert, *Clin. Cancer Res.*, 1999, **5**, 3796s.
21. M. G. Mendoza-Ferri, C. G. Hartinger, M. A. Mendoza, M. Groessl, A. E. Egger, R. E. Eichinger, J. B. Mangrum, N. P. Farrell, M. Maruszak, P. J. Bednarski, F. Klein, M. A. Jakupiec, A. A. Nazarov, K. Severin and B. Keppler, *J. Med. Chem.*, 2009, **52**, 916.
22. T. Yamada, Y. Noguchi, M. Nakai, O. Yamauchi, Y. Nakabayashi, T. Sato, Y. Tami, M. Chikuma and Y. Mino, *Inorg. Chim. Acta*, 2013, **394**, 190.

23. E. Corral, A. C. G. Hotze, H. den Dulk, A. Leczkowska, A. Rodger, M. J. Hannon and J. Reedijk, *J. Biol. Inorg. Chem.*, 2009, **14**, 439.
24. Y. Mulyana, J. G. Collins and F. R. Keene, *J. Incl. Phenom. Macrocycl. Chem.*, 2011, **71**, 371.
25. Y. Mulyana, D. K. Weber, D. P. Buck, C. A. Motti, J. G. Collins and F. R. Keene, *Dalton Trans.*, 2011, **40**, 1510.
26. P. A. Adcock, F. R. Keene, R. S. Smythe and M. R. Snow, *Inorg. Chem.*, 1984, **23**, 2336.
27. L. Dvorak, I. Popa, P. Starha and Z. Travnicek, *Eur. J. Inorg. Chem.*, 2010, 3441.
28. S. Gama, F. Mendes, F. Marques, I. C. Santos, M. F. Carvalho, I. Correia, J. C. Pessoa, I. Santos and A. Paulo, *J. Inorg. Biochem.*, 2011, **105**, 637.
29. A. J. Pope, C. Bruce, B. Kysela and M. J. Hannon, *Dalton Trans.*, 2010, **39**, 2772.
30. R.-A. Fallahpour, M. Neuburger and M. Zehnder, *New J. Chem.*, 1999, 43.
31. N. Yoshikawa, T. Matsumura-Inoue, N. Kanehisa, Y. Kai, H. Takashima and K. Tsukahara, *Analytical Sciences*, 2004, **20**, 1639.
32. P. R. Murray, S. Crawford, A. Dawson, A. Delf, C. Findlay, L. Jack, E. J. L. McInnes, S. Al-Musharafi, G. S. Nichol, I. Oswald and L. J. Yellowlees, *Dalton Trans.*, 2012, **41**, 201.

33. E. J. L. McInnes, A. J. Welch and L. J. Yellowlees, *Chem. Commun.*, 1996 2393.
34. M.-G. Mendoza-Ferri, C. G. Hartinger, R. E. Eichinger, N. Stolyarova, K. Severin, M. A. Jakupec, A. A. Nazarov and B. K. Keppler, *Organometallics*, 2008, **27**, 2405.
35. M. J. Pisani, P. D. Fromm, R. J. Clarke, Y. Mulyana, H. Körner, K. Heimann, J. G. Collins and F. R. Keene, *ChemMedChem.*, 2011, **6**, 848.
36. H. Silva, F. Frezard, E. J. Peterson, P. Kabolizadeh, J. J. Ryan and N. P. Farrell, *Mol. Pharmaceutics*, 2012, **9**, 1795.
37. J.-H. Guh, W.-L. Chang, J. Yang, S.-L. Lee, S. Wei, D. Wang, S. K. Kulp and C.-S. Chen, *J. Med. Chem.*, 2010, **53**, 2552.
38. M. Pandrala, F. Li, M. Feterl, Y. Mulyana, J. M. Warner, L. Wallace, F. R. Keene and J. G. Collins, *Dalton Trans.*, 2013, **42**, 4686.
39. F. H. Case, *J. Org. Chem.*, 1962, **27**, 640.
40. I. Sasaki, M. Imberdis, A. Gaudemer, B. Drahi, D. Azhari and E. Amouyal, *New J. Chem.*, 1994, **18**, 759.
41. B. M. Peek, G. T. Ross, S. W. Edwards, G. J. Meyer, T. J. Meyer and B. W. Erickson, *Int. J. Peptide Protein Res.*, 1991, **38**, 114.
42. D. Bao, B. Millare, W. Xia, B. G. Steyer, A. A. Gerasimenko, A. Ferreira, A. Contreras and V. I. Vullev *J. Phys. Chem. A*, 2009, **113**, 1259.

CHAPTER 3

***Tri- and tetra-nuclear
polypyridylruthenium(II) complexes as
antimicrobial agents***

3.1. Introduction

As discussed in chapter 1, infectious diseases remain a leading cause of death worldwide, and as there is also an increasing emergence of drug-resistant bacteria.¹ It is clear that there is a need for new antimicrobial agents. Dwyer and his co-workers first reported the antimicrobial potential of mononuclear iron and ruthenium complexes containing polypyridyl ligands.^{2,3} However, while these complexes exhibited excellent activity against drug-sensitive strains, they were significantly less active against current drug-resistant strains.⁴ In an attempt to increase the activity of inert polypyridylruthenium complexes against drug-resistant bacteria, our group has examined the antimicrobial properties of inert and chlorido-containing dinuclear ruthenium and iridium metal analogues.⁴⁻⁶ The inert dinuclear Ru_2b_n complexes showed excellent activity, with minimum inhibitory concentrations (MIC) of 1 and 2 $\mu\text{g/mL}$ for the Ru_2b_{12} and Ru_2b_{16} complexes against a range of Gram positive and Gram negative bacterial strains, and they maintained the activity against drug-resistant strains such as methicillin-resistant *Staphylococcus aureus* (denoted as MRSA).⁴ Furthermore, preliminary toxicity assays against human red blood cells and a human monocytic leukemia cell line (THP-1) indicated that the Ru_2b_n complexes were not significantly toxic to human cells.⁴

The inert dinuclear Ru_2b_n complexes with an overall charge of 4+ can interact reversibly with various intra-cellular receptors such as proteins and nucleic acids to stop bacterial cell replication. Ru_2b_{16} was shown to condense ribosomes when they existed as polysomes, and it was postulated that the condensation of polysomes would halt protein production and thereby inhibit bacterial growth.⁷ Although it would be expected that complexes which have a higher positive charge would condense polysomes more

efficiently, cellular uptake experiments with mononuclear and dinuclear polypyridylruthenium(III) complexes (3+ and 6+ respectively) demonstrated that they could not easily cross the cellular membrane, and hence they showed no antimicrobial activity.^{6,8} An alternative approach of increasing the charge of the dinuclear ruthenium complexes is to synthesise tri- and tetra-nuclear species. While the tri- and tetra-nuclear ruthenium complexes will be more positively charged, 6+ and 8+ respectively, they will also be more lipophilic than the dinuclear counterparts due to the additional non-polar linking ligands. Preliminary experiments with the tri- and tetra-nuclear complexes of Rubb₇ demonstrated the potential of this approach.⁴ The Rubb₇-tri and Rubb₇-tetra complexes were 2-4 times more active against a range of bacteria than the corresponding dinuclear Rubb₇.

Over the last decade there has been considerable interest in developing inert dinuclear ruthenium(II) complexes as nucleic acid binding probes, anticancer agents and cellular imaging agents.⁹⁻¹⁸ More recently, there has been increasing interest in using higher nuclearity ruthenium complexes as anticancer agents.¹⁹⁻²¹ Predominantly, research has focused on ruthenium clusters or cages, as these bulky complexes may preferentially accumulate in tumours due to the enhanced permeability and retention effect.¹⁸⁻²⁰ Alternatively, while several tri- and tetra-nuclear copper(II) complexes with modest antimicrobial activities have been reported,^{22,23} there have been very few studies on the potential of tri- or tetra-nuclear ruthenium complexes as antimicrobial agents.

The aims of this chapter were to synthesise the tri- and tetra-nuclear analogues of the most active dinuclear complexes, Rubb₁₂ and Rubb₁₆, and examine their antimicrobial activities, log P values, cellular uptake and time-kill curves. Additionally, due to the modular nature of the synthesis of these complexes, it was possible to synthesise both linear and non-linear tetranuclear complexes. The structures of the

multinuclear complexes and the important precursor complex $\text{Rubb}_n\text{-Cl}_2$, which was also examined for antimicrobial activity, are shown in Figure 3.1.

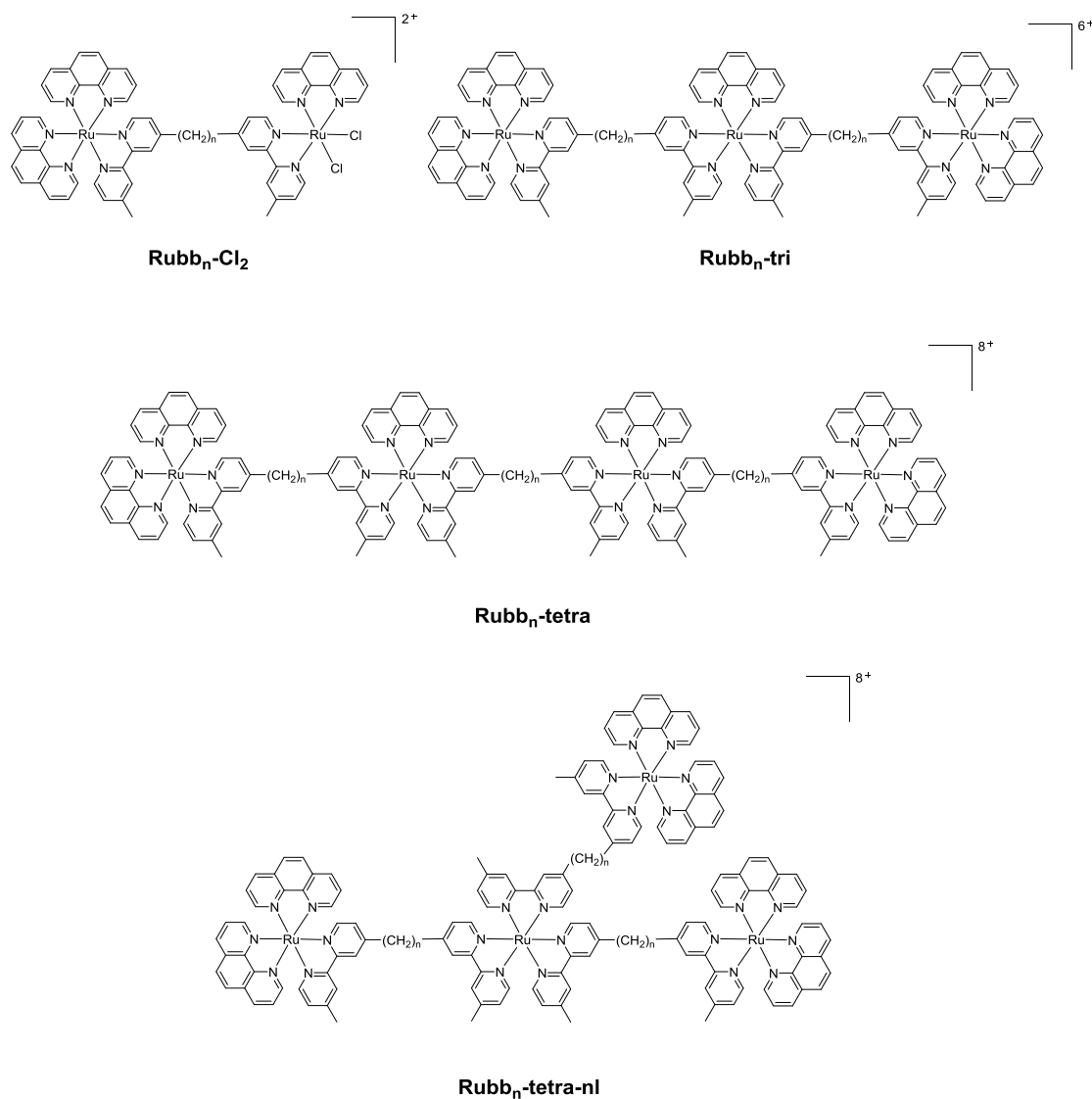


Figure 3.1. Chlorido-containing dinuclear complexes ($\text{Rubb}_n\text{-Cl}_2$), and the inert trinuclear ($\text{Rubb}_n\text{-tri}$) and tetranuclear (linear $\text{Rubb}_n\text{-tetra}$ and non-linear $\text{Rubb}_n\text{-tetra-nl}$) ruthenium(II) complexes.

3.2. *Experimental*

The antimicrobial assays were carried out by the author under the guidance of A/Prof Jeffery Warner, School of Veterinary and Biomedical Sciences, James Cook University, Townsville, QLD 4811, Australia. The fluorescence microscopic studies were carried out by the author under the guidance of Prof. Elizabeth J. Harry, The itthree institute, University of Technology Sydney, NSW 2007, Australia.

3.2.1. *Physical measurements*

^1H NMR and ^{13}C NMR spectra were recorded on a Varian Advance 400 MHz spectrometer at room temperature in D_2O {99.9%, Cambridge Isotope Laboratories (CIL)}, CDCl_3 (99.8%, CIL), CD_3CN (>99.8%, Aldrich), or CD_3OD (>99.8%, Aldrich). UV absorbance was measured on a Jenway 6300 spectrophotometer. Microanalyses were performed by the Microanalytical Unit, Research School of Chemistry, Australian National University, Canberra.

3.2.2. *Materials and methods*

Tetraethylammonium chloride, 2-methoxyethanol, lithium chloride, potassium hexafluorophosphate (KPF_6) and ammonium hexafluorophosphate (NH_4PF_6) were purchased from Aldrich and used as supplied; Amberlite[®] IRA-402 (chloride form) anion-exchange resin, SP-Sephadex C-25 cation exchanger and Sephadex[®] LH-20 were obtained from GE Health Care Bioscience. Cation-adjusted Mueller Hinton broth (CAMHB) was purchased from Fluka, Gillingham, UK; the control antibiotics gentamicin and ampicillin were purchased from Oxoid, Australia. The syntheses of ligands bb_n ($n = 10, 12$ and 16), $[\text{Ru}(\text{phen})_2(\text{py})_2]\text{Cl}_2$, $(\text{phenH}^+)[\text{Ru}(\text{phen})\text{Cl}_4]$ and *cis*- $[\text{Ru}^{\text{II}}(\text{DMSO})_4\text{Cl}_2]$ were performed according to reported literature methods.^{23, 39-41}

3.2.3. *Bacterial strains*

All bacterial strains are classified as C2 risk group and must be handled within a PC2 laboratory. Two *Staphylococcus aureus* (Gram positive) isolates, a methicillin-susceptible *S. aureus* strain (ATCC 25923), a clinical multidrug-resistant MRSA strain (a wild clinical strain from the JCU culture collection) and two Gram negative isolates *Escherichia coli* (ATCC 25922) and *Pseudomonas aeruginosa* (ATCC 27853) were used for *in vitro* antimicrobial studies.

3.2.4. *MIC and MBC determination*

The MIC tests were conducted by the broth micro-dilution method in duplicate as outlined in the CLSI guidelines.⁴³ The MBC tests were performed in duplicate according to the standard microbiological techniques protocol.⁴⁴ The bacteria were grown on Mueller Hinton agar and suspended in growth medium CAMHB. Bacterial inocula were adjusted to a turbidity equivalent to that of a 0.5 McFarland standard and diluted to a final concentration of $4-8 \times 10^5$ cfu/mL. Compounds tested were dissolved and serially diluted in cation-adjusted Mueller–Hinton broth (CAMHB; Fluka, Gillingham, UK) in sterile 96-well flat-bottom plates to a final volume of 100 μ L in each well. An equal volume of inocula was added to each well, making a final concentration range of the compounds tested, including the control antibiotics gentamicin and ampicillin (Oxoid, Australia), of between 0.25 and 128 μ g/mL. MICs were recorded after 16–18 h and 20–22 h of incubation at 37 °C. Colony counts of the inocula were performed for determination of the MBC. After MIC results were noted, the incubation was continued for another 4 h, the wells with no visible growth were taken into colony counting and the concentration of compounds that produced a 99.9% kill relative to the starting inoculum was recorded as the MBC.

MIC/MBC values were determined by serial dilution in accordance with the CLSI guidelines. MIC/MBC values are not reported with an error value, however, it is understood that the error is ± 1 dilution value. However, they were converted to μM to compare the values with IC_{50} values obtained against eukaryotic cell lines.

3.2.5. Cellular uptake

The cellular uptake of the ruthenium complexes was measured by monitoring the UV absorbance of the complexes remaining in the supernatant of the cultures after incubation for various periods of time. Bacterial inocula in log phase were adjusted to a cell concentration from $1\text{--}5 \times 10^7$ cfu/mL. Aliquots (2 mL) of the adjusted inocula were placed in glass culture tubes and 50 μL of stock solution (330 mg/L) of the ruthenium complex was added to give a final concentration of 8 mg/L. Control flasks containing 50 mL of each bacterial suspension were set up as blank samples to obtain UV calibration curves for each complex. Culture tubes and control flasks were incubated with agitation at 150 rpm at 37 °C for 0.5, 1, 1.5 or 2 h. At the end of incubation, the culture tubes were centrifuged (*S. aureus* and MRSA at 6000 g; *E. coli* and *P. aeruginosa* at 17000 g) at 4 °C for 10 min. Supernatants (1.6 mL) were carefully transferred to 2 mL tubes and the UV absorbance of the remaining ruthenium complex was measured at $\lambda = 488$ nm. Volumes (10, 30, 40, 50 and 65 μL) of a stock solution (330 mg/L) of each complex were added to 2 mL aliquots of the supernatant from each control bacterial suspension (untreated with drug) to acquire a UV-concentration linear correlation chart for calibration. The uptake of the complexes was calculated by using the calibration curve obtained from control bacterial aliquots. By using the measured UV-absorbance of the ruthenium complex remaining in the supernatant, the concentration of the drug in the supernatant was calculated from the calibration curve.

The concentration of the drug taken up by the cells was calculated by subtracting the drug concentration in supernatant from the initial concentration added to the broth.

3.2.6. *Lipophilicity (log P) determination*

The partition coefficients (log P) were measured using the shake-flask technique: each ruthenium complex (at 0.1 mM) was dissolved in the water phase and an equal volume of *n*-octanol was added. The two phases were mutually saturated by shaking overnight at ambient temperature and then were allowed to separate on standing. The concentration of the metal complex in each phase was determined spectrophotometrically at $\lambda = 450$ nm.

3.2.7. *Time-kill curve studies*

The time-kill assays were carried out by Sebastian Primrose at James Cook University. Time-kill assays were performed according to the basic microbiological techniques protocol.⁴⁴ Bacterial inocula in log phase were diluted to 10^5 – 10^6 cfu/mL and 5 mL aliquots were added into glass culture tubes. Compounds were dissolved in distilled water to make stock solutions at a concentration of $500 \times \text{MIC}$. Stock solutions (5, 10 and 20 μL) were added into the glass tubes to obtain the desired concentrations of $0.5 \times \text{MIC}$, MIC and $2 \times \text{MIC}$. Ampicillin and gentamicin were used as positive controls. Culture tubes were then incubated in a shaking incubator (Bioline model BL 4720, Edwards Instrument Company, Narellen, New South Wales, Australia) at 150 rpm at 37 °C. Viable bacteria were counted after 0, 0.5, 1.5, 3, 6, 12 and 24 h of incubation. Colony counts were performed by taking 100 μL of culture and making 10-fold serial dilutions in PBS then plating each onto trypticase soy agar (TSA II) + 5% sheep blood

agar (Oxoid, Australia). Plates were incubated for 18 h at 37 °C and viable counts were calculated to give cfu/mL. Each time–kill experiment was carried out in triplicate.

3.2.8. *Electrochemistry*

Cyclic voltammetry was carried out using an eDAQ EA161 potentiostat operated via an eDAQ ED401 e-corder. A glassy carbon working electrode, platinum wire counter electrode and Ag/AgCl reference electrode were used. Ferrocene was used as an internal reference check.⁴⁵ HPLC grade acetonitrile was used as solvent and the supporting electrolyte was 0.1 M tetra-*n*-butylammonium tetrafluoroborate.

3.2.9. *Wide-field fluorescent microscopy*

Bacterial strains and growth conditions

As the *E. coli* strain MG1665 was used in a previous study of the intracellular localisation of Rubb₁₆, the present study was also carried out using this bacterium. The bacterial strain was grown on Luria Broth (LB) agar plates at 37 °C. A bacterial culture was obtained by inoculating bacteria in LB media and incubating overnight in a shaking incubator in a water bath at 37 °C. The overnight culture was then diluted to a suspension with an optical density at λ 600 nm (OD₆₀₀) of approximately 0.05. A bacterial log phase culture was obtained by continuing the incubation of this suspension for approximately 2 h until the OD₆₀₀ reached 0.5.

MIC assay

The minimum inhibitory concentration (MIC) of Rubb₁₂-tetra against *E. coli* MG1665 was determined as described in section 3.2.4.

Drug treatment and staining protocols

A Rubb₁₂-tetra stock solution was prepared in Milli-Q water at a concentration of 128 mg/L. Rubb₁₂-tetra was added to the log phase bacterial culture and incubated for 1 h. The concentrations of Rubb₁₂-tetra used in this study ranged from 0.5×MIC to 2×MIC. After incubation with Rubb₁₂-tetra, the cells were washed twice with a phosphate buffer solution before further treatment or preparation for slides. For the co-localisation experiment with DAPI, Rubb₁₂-tetra treated *E. coli* cells were incubated with DAPI at room temperature for 15-30 min before being loaded onto agarose pads on slides for microscopy. The concentrations of DAPI used in the co-localisation assays were 20 mg/L.

Live cell microscopy

All live cell microscopy was performed by placing cells on 2% (w/v) agarose pads (prepared with identical media to that in which the cells were grown) within a 65 µL Gene Frame (Thermo Fisher Scientific). Luminescent images were obtained using a Zeiss Axioplan 2 fluorescence microscope (Carl Zeiss) as described previously.^{46,47} DAPI fluorescence and Rubb₁₂-tetra phosphorescence were visualised with filter sets 02 and 488015 (Carl Zeiss), respectively. Images were analysed and processed using AxioVision version 4.8 (Carl Zeiss).

3.2.10. Synthesis of metal complexes

All newly synthesised final products were characterised by ¹H NMR, ¹³C NMR, microanalyses and mass spectroscopy. All intermediate products were characterised by ¹H NMR and microanalyses.

[Ru(phen)₂(bb_n)](PF₆)₂, (Rubb_n-mono)

The mononuclear ruthenium(II) complexes Rubb_n-mono were synthesised as previously described (n = 7 and 16),²⁴ with typical yields being 50-60%. The ¹H NMR spectrum of Rubb₁₆-mono was consistent with that previously reported.²⁴

[Ru(phen)₂(bb₁₂)](PF₆)₂·2H₂O Anal. Calcd. for C₅₈H₆₂N₈F₁₂O₂P₂Ru: C, 53.8%; H, 4.83%; N, 8.7%. Found: C, 53.9%; H, 4.80%; N, 8.5%. ¹H NMR (400 MHz, CD₃CN): δ 8.63 (d, *J* = 8.0 Hz, 2H); 8.52 (dd, *J* = 8.2 Hz, 3.3 Hz, 2H); 8.40 (s, 2H); 8.35 (s, 2H); 8.26-8.17 (m, 8H); 7.88-7.85 (m, 2H); 7.78 (dd, *J* = 8.1 Hz, 5.1 Hz, 2H); 7.56-7.51 (m, 2H); 7.50-7.46 (m, 2H); 7.22-7.17 (m, 2H); 7.10 (t, *J* = 9.0 Hz, 2H); 2.76 (t, *J* = 7.6 Hz, 2H); 2.67 (t, *J* = 7.2 Hz, 2H); 2.51 (s, 3H); 2.41 (s, 3H); 1.70-1.56 (m, 4H); 1.35-1.17 (m, 16H).

[Ru(phen)₂(bb₁₀)](PF₆)₂·3H₂O Anal. Calcd. for C₅₆H₆₀N₈F₁₂O₃P₂Ru: C, 52.4%; H, 4.71%; N, 8.7%. Found: C, 52.2%; H, 4.47%; N, 8.5%. ¹H NMR (400 MHz, CD₃CN): δ 8.63 (d, *J* = 8.0 Hz, 2H); 8.48 (dd, *J* = 5.3 Hz, 4.7 Hz, 2H); 8.40 (s, 2H); 8.35 (s, 2H); 8.27-8.16 (m, 8H); 7.87 (d, *J* = 4.8 Hz, 2H); 7.81-7.75 (m, 2H); 7.57-7.51 (m, 2H); 7.48 (t, *J* = 6.4 Hz, 2H); 7.22-7.17 (m, 2H); 7.12-7.08 (m, 2H); 2.76 (t, *J* = 7.4 Hz, 2H); 2.68 (t, *J* = 7.5 Hz, 2H); 2.50 (s, 3H); 2.41 (s, 3H); 1.70-1.59 (m, 4H); 1.36-1.24 (m, 12H).

[{Ru(phen)₂}(μ-bb_n){Ru(phen)Cl₂}]Cl₂, (Rubb_n-Cl₂)

[Ru(phen)₂(bb₁₂)](PF₆)₂ (450 mg, 0.35 mmol), (phenH⁺)[Ru(phen)Cl₄] (216 mg, 0.35 mmol) and lithium chloride (280 mg) were dissolved in dry DMF (28 mL) and the mixture was stirred at 150 °C for 8 h in the dark under a nitrogen atmosphere. After cooling the reaction mixture to room temperature, acetone (80 mL) was added and the product precipitated as a dark brown material, which was kept with the mother liquor in

the fridge for 16 h. The precipitate was then filtered and washed with acetone (40 mL), dried under *vacuo* and redissolved in ethanol (20 mL). Solid NH_4PF_6 (200 mg) was added to the ethanol solution, resulting in the precipitation of the PF_6^- salt of the complex, which was then filtered and washed with ethanol (2×20 mL) and diethyl ether (2×20 mL) to afford a dark brown solid. The complex was purified on a Sephadex LH-20 column (2 cm diam. \times 30 cm) using acetone as the eluent. The major first band (brown) was collected and acetone was evaporated to obtain $[\{\text{Ru}(\text{phen})_2\}(\mu\text{-bb}_{12})\{\text{Ru}(\text{phen})\text{Cl}_2\}](\text{PF}_6)_2$ as dark brown solid. **$[\{\text{Ru}(\text{phen})_2\}(\mu\text{-bb}_{12})\{\text{Ru}(\text{phen})\text{Cl}_2\}](\text{PF}_6)_2 \cdot 0.5\text{NH}_4\text{PF}_6$** . Anal. Calcd. for $\text{C}_{70}\text{H}_{68}\text{N}_{10.5}\text{Cl}_2\text{F}_{15}\text{P}_{2.5}\text{Ru}_2$: C, 49.7%; H, 4.05%; N, 8.7%. Found: C, 49.6%; H, 3.67%; N, 8.3%. ^1H NMR (400 MHz, CD_3CN): δ 8.64 (d, $J = 8.1$ Hz, 4H); 8.54 (d, $J = 8.3$ Hz, 4H); 8.41-8.34 (m, 2H); 8.28-8.22 (m, 4H); 8.21-8.17 (m, 4H); 7.89-7.85 (m, 4H); 7.81-7.76 (m, 2H); 7.55 (dd, $J = 7.8$ Hz, 5.1 Hz, 4H); 7.48 (t, $J = 5.0$ Hz, 4H); 7.13-7.08 (m, 4H); 2.79-2.72 (m, 4H); 2.52 (s, 6H); 1.70-1.58 (m, 4H); 1.39-1.20 (m, 16H).

$[\{\text{Ru}(\text{phen})_2\}(\mu\text{-bb}_{16})\{\text{Ru}(\text{phen})\text{Cl}_2\}](\text{PF}_6)_2$ and $[\{\text{Ru}(\text{phen})_2\}(\mu\text{-bb}_{10})\{\text{Ru}(\text{phen})\text{Cl}_2\}](\text{PF}_6)_2$ complexes were synthesised as reported above for $[\{\text{Ru}(\text{phen})_2\}(\mu\text{-bb}_{12})\{\text{Ru}(\text{phen})\text{Cl}_2\}](\text{PF}_6)_2$.

$[\{\text{Ru}(\text{phen})_2\}(\mu\text{-bb}_{16})\{\text{Ru}(\text{phen})\text{Cl}_2\}](\text{PF}_6)_2 \cdot 3\text{CH}_2\text{Cl}_2 \cdot \text{C}_3\text{H}_6\text{O}$. Anal. Calcd. for $\text{C}_{80}\text{H}_{86}\text{N}_{10}\text{Cl}_8\text{F}_{12}\text{OP}_2\text{Ru}_2$: C, 48.5%; H, 4.38%; N, 7.1%. Found: C, 48.2%; H, 4.66%; N, 6.7%. ^1H NMR (400 MHz, CD_3CN): δ 8.64 (d, $J = 8.1$ Hz, 4H); 8.53 (d, $J = 7.9$ Hz, 4H); 8.42-8.34 (m, 2H); 8.27-8.22 (m, 4H); 8.21-8.16 (m, 4H); 7.89-7.85 (m, 4H); 7.79 (dd, $J = 7.9$ Hz, 5.0 Hz, 2H); 7.55 (dd, $J = 8.0$ Hz, 5.1 Hz, 4H); 7.48 (t, $J = 5.2$ Hz, 4H); 7.13-7.08 (m, 4H); 2.79-2.73 (m, 4H); 2.51 (s, 6H); 1.69-1.60 (m, 4H); 1.39-1.19 (m, 24H).

$[\{\text{Ru}(\text{phen})_2\}(\mu\text{-bb}_{10})\{\text{Ru}(\text{phen})\text{Cl}_2\}](\text{PF}_6)_2 \cdot \text{NH}_4\text{PF}_6 \cdot 2\text{CH}_2\text{Cl}_2$ Anal. Calcd. for $\text{C}_{70}\text{H}_{70}\text{N}_{11}\text{Cl}_6\text{F}_{18}\text{P}_3\text{Ru}_2$: C, 43.9%; H, 3.68%; N, 8.1%. Found: C, 43.8%; H, 3.54%; N,

7.9%. ^1H NMR (400 MHz, CD_3CN): δ 8.65 (d, $J = 7.9$ Hz, 4H); 8.54 (d, $J = 7.7$ Hz, 4H); 8.42-8.34 (m, 2H); 8.28-8.16 (m, 8H); 7.90-7.84 (m, 4H); 7.82-7.75 (m, 2H); 7.55 (dd, $J = 8.3$ Hz, 5.3 Hz, 4H); 7.48 (t, $J = 5.1$ Hz, 4H); 7.14-7.07 (m, 4H); 2.80-2.72 (m, 4H); 2.51 (s, 6H); 1.72-1.58 (m, 4H); 1.42-1.21 (m, 12H).

The PF_6^- salts were converted to chloride salts with Amberlite IRA- 402 (chloride form) anion-exchange resin. The PF_6^- salt of the complex was taken up in methanol (25 mL) and resin added and the mixture stirred at room temperature for 1-2 h until the solution was clear, the resin was then filtered and methanol was evaporated and the resultant solid dried in an oven at 70 °C for 16 h to obtain a dark brownish orange solid of $[\{\text{Ru}(\text{phen})_2\}(\mu\text{-bb}_n)\{\text{Ru}(\text{phen})\text{Cl}_2\}]\text{Cl}_2$ ($\text{Rubb}_n\text{-Cl}_2$), typical yields were 60-65 %, based on the synthetic starting material $[\text{Ru}(\text{phen})_2(\text{bb}_n)](\text{PF}_6)_2$.

$[\{\text{Ru}(\text{phen})_2\}(\mu\text{-bb}_n)\{\text{Ru}(\text{phen})\}(\mu\text{-bb}_n)\{\text{Ru}(\text{phen})_2\}]\text{Cl}_6$, ($\text{Rubb}_n\text{-tri}$)

In a typical reaction, both the starting materials $[\{\text{Ru}(\text{phen})_2\}(\mu\text{-bb}_{16})\{\text{Ru}(\text{phen})\text{Cl}_2\}](\text{PF}_6)_2$ (125 mg, 0.075 mmol) and $[\text{Ru}(\text{phen})_2(\text{bb}_{16})](\text{PF}_6)_2$ (98 mg, 0.075 mmol) were dissolved in ethanol–water (1:1, 60 mL) and the mixture refluxed at 80 °C in the dark under a nitrogen atmosphere for 4 h. The colour of the reaction mixture slowly turned from dark brown to dark red during the course of the reaction. The reaction mixture was cooled to room temperature and the solvent was evaporated under reduced pressure to obtain a dark orange solid, the resulting solid was converted to the chloride salt by stirring it in methanol using Amberlite IRA- 402 (chloride form) anion-exchange resin for 1-2 h, after filtration of the resin, methanol was evaporated and the resultant chloride salt was dissolved in water (10 mL) and loaded onto an SP Sephadex C-25 cation exchange column (2 cm diam. \times 25 cm), the column was washed with water and eluted with 0.6 M and then 0.8 M NaCl solutions to remove mono- and

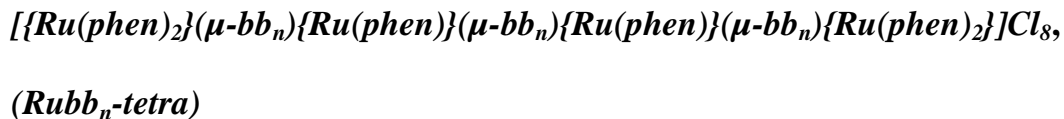
di-nuclear impurities. The desired trinuclear complex was eluted with 1 M NaCl solution containing 20% acetone. After removing the acetone, solid KPF_6 was added to the eluate and the complex was extracted into dichloromethane (2×30 mL). The organic layer was washed with water (20 mL), dried over anhydrous Na_2SO_4 , and evaporated to dryness to obtain the PF_6^- salt of the complex. The complex was further purified on Sephadex LH-20 (2 cm diam. \times 30 cm) using acetone as the eluent. The major first orange band was collected and the acetone removed and the product crystallised using acetonitrile-toluene to obtain a bright red–orange solid of $[\{\text{Ru}(\text{phen})_2\}(\mu\text{-bb}_{16})\{\text{Ru}(\text{phen})\}(\mu\text{-bb}_{16})\{\text{Ru}(\text{phen})_2\}](\text{PF}_6)_6$. **$[\{\text{Ru}(\text{phen})_2\}(\mu\text{-bb}_{16})\{\text{Ru}(\text{phen})\}(\mu\text{-bb}_{16})\{\text{Ru}(\text{phen})_2\}](\text{PF}_6)_6$.** Anal. Calcd. for $\text{C}_{136}\text{H}_{140}\text{N}_{18}\text{F}_{36}\text{P}_6\text{Ru}_3$: C, 51.0%; H, 4.41%; N, 7.9%. Found: C, 51.2%; H, 4.29%; N, 7.8%. ^1H NMR (400 MHz, CD_3CN): δ 8.67–8.60 (m, 5H); 8.57–8.49 (m, 5H); 8.43–8.34 (m, 8H); 8.29–8.17 (m, 18H); 7.88 (m, 5H); 7.82–7.76 (m, 5H); 7.59–7.51 (m, 8H); 7.48 (m, 5H); 7.14–7.07 (m, 5H); 2.82–2.72 (m, 8H); 2.57 (s, 3H); 2.51 (s, 6H); 2.47 (s, 3H); 1.72–1.59 (m, 8H); 1.39–1.17 (m, 48H). ^{13}C NMR (CD_3CN): δ 157.82, 157.76, 157.5, 155.7, 155.4, 153.57, 153.53, 153.48, 152.3, 152.1, 151.2, 148.8, 148.6, 137.55, 137.42, 131.9, 129.0, 128.9, 128.2, 126.86, 126.76, 125.7, 124.9, 35.6, 30.8, 30.4, 30.3, 30.2, 30.0, 29.9, 28.7, 21.4 and 21.0. TOF MS (ESI+): most abundant ion found for $[\text{M-4PF}_6]^{4+}$, m/z 654.94. Calc. for $\text{Ru}_3[\text{C}_{136}\text{H}_{140}\text{N}_{18}](\text{PF}_6)_2^{4+}$, m/z 654.97; most abundant ion found for $[\text{M-3PF}_6]^{3+}$, m/z 921.59. Calc. for $\text{Ru}_3[\text{C}_{136}\text{H}_{140}\text{N}_{18}](\text{PF}_6)_3^{3+}$, m/z 921.61; most abundant ion found for $[\text{M-2PF}_6]^{2+}$, m/z 1454.87. Calc. for $\text{Ru}_3[\text{C}_{136}\text{H}_{140}\text{N}_{18}](\text{PF}_6)_4^{2+}$, m/z 1454.90.

$[\{\text{Ru}(\text{phen})_2\}(\mu\text{-bb}_{12})\{\text{Ru}(\text{phen})\}(\mu\text{-bb}_{12})\{\text{Ru}(\text{phen})_2\}](\text{PF}_6)_6$. Anal. Calcd. for $\text{C}_{128}\text{H}_{124}\text{N}_{18}\text{F}_{36}\text{P}_6\text{Ru}_3$: C, 49.8%; H, 4.05%; N, 8.2%. Found: C, 50.1%; H, 3.82%; N, 8.2%. ^1H NMR (400 MHz, CD_3CN): δ 8.66–8.61 (m, 5H); 8.56–8.50 (m, 5H); 8.42–8.34 (m, 8H); 8.28–8.16 (m, 18H); 7.91–7.85 (m, 5H); 7.81–7.76 (m, 5H); 7.58–7.52 (m, 8H);

7.50-7.45 (m, 5H); 7.13-7.08 (m, 5H); 2.81-2.71 (m, 8H); 2.57 (s, 3H); 2.51 (s, 6H); 2.47 (s, 3H); 1.71-1.59 (m, 8H); 1.41-1.17 (m, 32H). ^{13}C NMR (CD_3CN): δ 157.8, 157.7, 157.5, 155.8, 154.9, 153.6, 153.5, 153.3, 152.3, 152.1, 151.2, 148.8, 148.5, 137.5, 137.4, 131.8, 129.0, 128.9, 128.4, 126.8, 126.7, 125.7, 124.9, 35.6, 30.9, 30.7, 30.4, 30.2, 30.1, 30.0, 29.8, 28.9, 21.1 and 20.8. TOF MS (ESI⁺): most abundant ion found for $[\text{M}-4\text{PF}_6]^{4+}$, m/z 626.91. Calc. for $\text{Ru}_3[\text{C}_{128}\text{H}_{124}\text{N}_{18}](\text{PF}_6)_2^{4+}$, m/z 626.91; most abundant ion found for $[\text{M}-3\text{PF}_6]^{3+}$, m/z 884.21. Calc. for $\text{Ru}_3[\text{C}_{128}\text{H}_{124}\text{N}_{18}](\text{PF}_6)_3^{3+}$, m/z 884.21; most abundant ion found for $[\text{M}-2\text{PF}_6]^{2+}$, m/z 1399.78. calc. for $\text{Ru}_3[\text{C}_{128}\text{H}_{124}\text{N}_{18}](\text{PF}_6)_4^{2+}$, m/z 1399.30. **$[\{\text{Ru}(\text{phen})_2\}(\mu\text{-bb}_{10})\{\text{Ru}(\text{phen})\}(\mu\text{-bb}_{10})\{\text{Ru}(\text{phen})_2\}](\text{PF}_6)_6$** . Anal. Calcd. for $\text{C}_{124}\text{H}_{116}\text{N}_{18}\text{F}_{36}\text{P}_6\text{Ru}_3$: C, 49.1%; H, 3.86%; N, 8.3%. Found: C, 48.8%; H, 3.84%; N, 8.2%. ^1H NMR (400 MHz, CD_3CN): δ 8.68-8.61 (m, 5H); 8.57-8.50 (m, 5H); 8.42-8.33 (m, 8H); 8.28-8.16 (m, 18H); 7.90-7.85 (m, 5H); 7.81-7.76 (m, 5H); 7.57-7.52 (m, 8H); 7.51-7.45 (m, 5H); 7.13-7.08 (m, 5H); 2.82-2.70 (m, 8H); 2.56 (s, 3H); 2.51 (s, 6H); 2.47 (s, 3H); 1.73-1.58 (m, 8H); 1.43-1.22 (m, 24H). ^{13}C NMR (CD_3CN): δ 157.8, 157.74, 157.6, 155.6, 155.1, 153.56, 153.51, 153.3, 152.3, 152.1, 151.2, 148.8, 148.5, 137.54, 137.42, 131.8, 129.0, 128.9, 128.3, 126.8, 126.7, 125.7, 124.9, 35.6, 30.9, 30.8, 30.3, 30.2, 30.09, 30.01, 29.9, 29.6, 21.1 and 20.9. TOF MS (ESI⁺): most abundant ion found for $[\text{M}-4\text{PF}_6]^{4+}$, m/z 612.89. Calc. for $\text{Ru}_3[\text{C}_{124}\text{H}_{116}\text{N}_{18}](\text{PF}_6)_2^{4+}$, m/z 612.89; most abundant ion found for $[\text{M}-3\text{PF}_6]^{3+}$, m/z 865.52. Calc. for $\text{Ru}_3[\text{C}_{124}\text{H}_{116}\text{N}_{18}](\text{PF}_6)_3^{3+}$, m/z 865.50; most abundant ion found for $[\text{M}-2\text{PF}_6]^{2+}$, m/z 1370.76. calc. for $\text{Ru}_3[\text{C}_{124}\text{H}_{116}\text{N}_{18}](\text{PF}_6)_4^{2+}$, m/z 1370.74.

The chloride salts were obtained by stirring the PF_6^- salts in methanol with Amberlite IRA- 402 (chloride form) anion-exchange resin for 1-2 h until the solution was clear. The resin was removed by filtration, and the orange-red solution was evaporated and the solid dried in an oven at 70 °C for 16 h to obtain a dark red solid of $[\{\text{Ru}(\text{phen})_2\}(\mu\text{-bb}_{10})\{\text{Ru}(\text{phen})\}(\mu\text{-bb}_{10})\{\text{Ru}(\text{phen})_2\}](\text{PF}_6)_6$.

$\text{bb}_n\{\text{Ru}(\text{phen})\}(\mu\text{-bb}_n)\{\text{Ru}(\text{phen})_2\}\text{Cl}_6$ ($\text{Rubb}_n\text{-tri}$), typical yields were 25-30%, based on the synthetic starting material $[\text{Ru}(\text{phen})_2(\text{bb}_n)](\text{PF}_6)_2$.



In a typical reaction, $[\{\text{Ru}(\text{phen})_2\}(\mu\text{-bb}_{16})\{\text{Ru}(\text{phen})\text{Cl}_2\}](\text{PF}_6)_2$ (95 mg, 0.057 mmol) was dissolved in ethanol–water (1:1, 50 mL) and bb_{16} ligand (32 mg, 0.057 mmol) was added and the reaction mixture heated at reflux for 4 h in the dark under a nitrogen atmosphere. The colour of the reaction slowly turned from dark brown to dark red during the course of the reaction. The reaction mixture was cooled to room temperature and the solvent was evaporated under reduced pressure to obtain a dark orange-red solid, which was then converted to the chloride salt by stirring in methanol with Amberlite IRA- 402 (chloride form) anion-exchange resin. After filtration of the resin, the methanol was evaporated to obtain the chloride salt which was dissolved in water (10 mL) and loaded onto an SP-Sephadex C-25 cation exchange column (2 cm diam. \times 25 cm), the column washed with water and eluted with 0.6 M and then 0.8 M NaCl solutions to remove the impurities. The desired tetranuclear complex was eluted with a 1 M NaCl solution containing 30 % acetone. After removing the acetone, solid KPF_6 was added to the eluate followed by extraction into DCM (2×20 mL). The organic layer was washed with water (20 mL), dried over anhydrous Na_2SO_4 , and evaporated to dryness to obtain the PF_6^- salt of the complex. The complex was further purified using Sephadex LH-20 with acetone as the eluent. The major first orange band was collected, the acetone evaporated and the resultant solid crystallised from acetonitrile-toluene to yield a bright red–orange precipitate of $[\{\text{Ru}(\text{phen})_2\}(\mu\text{-bb}_{16})\{\text{Ru}(\text{phen})\}(\mu\text{-bb}_{16})\{\text{Ru}(\text{phen})\}(\mu\text{-bb}_{16})\{\text{Ru}(\text{phen})_2\}](\text{PF}_6)_8$. **$[\{\text{Ru}(\text{phen})_2\}(\mu\text{-bb}_{16})\{\text{Ru}(\text{phen})\}(\mu\text{-bb}_{16})\{\text{Ru}(\text{phen})\}(\mu\text{-bb}_{16})\{\text{Ru}(\text{phen})_2\}](\text{PF}_6)_8$**

bb₁₆}{Ru(phen)}(μ-bb₁₆){Ru(phen)₂}(PF₆)₈. Anal. Calcd. for C₁₈₆H₁₉₈N₂₄F₄₈P₈Ru₄: C, 51.5%; H, 4.61%; N, 7.8%. Found: C, 51.4%; H, 4.42%; N, 7.8%. ¹H NMR (400 MHz, CD₃CN): δ 8.66-8.52 (m, 16H); 8.42-8.34 (m, 10H); 8.30-8.18 (m, 18H); 7.91-7.86 (m, 8H); 7.83-7.77 (m, 8H); 7.55 (m, 12H); 7.51-7.46 (m, 6H); 7.11 (m, 6H); 2.76 (m, 12H); 2.57 (s, 3H); 2.51 (s, 12H); 2.47 (s, 3H); 1.74-1.58 (m, 12H); 1.43-1.14 (m, 72H). ¹³C NMR (CD₃CN): δ 157.8, 157.75, 156.9, 155.6, 153.55, 153.50, 153.46, 152.2, 152.1, 151.2, 148.8, 148.5, 137.5, 137.4, 131.85, 131.82, 128.9, 128.8, 128.7, 128.2, 126.8, 126.7, 125.6, 124.9, 35.6, 30.8, 30.7, 30.4, 30.3, 30.24, 30.19, 30.05, 30.01, 29.8, 29.7, 21.1 and 20.6. TOF MS (ESI+): most abundant ion found for [M-6PF₆]⁶⁺, *m/z* 577.36. Calc. for Ru₄[C₁₈₆H₁₉₈N₂₄](PF₆)₂⁶⁺, *m/z* 577.33; most abundant ion found for [M-4PF₆]⁴⁺, *m/z* 938.55. Calc. for Ru₄[C₁₈₆H₁₉₈N₂₄](PF₆)₄⁴⁺, *m/z* 938.48; most abundant ion found for [M-3PF₆]³⁺, *m/z* 1299.40. Calc. for Ru₄[C₁₈₆H₁₉₈N₂₄](PF₆)₅³⁺, *m/z* 1299.63. **[{Ru(phen)₂}(μ-bb₁₂){Ru(phen)}(μ-bb₁₂){Ru(phen)}(μ-bb₁₂){Ru(phen)₂}(PF₆)₈.** Anal. Calcd. for C₁₇₄H₁₇₄N₂₄F₄₈P₈Ru₄: C, 50.2%; H, 4.21%; N, 8.1%. Found: C, 50.2%; H, 4.35%; N, 8.0%. ¹H NMR (400 MHz, CD₃CN): δ 8.68-8.50 (m, 16H); 8.43-8.33 (m, 10H); 8.29-8.22 (m, 10H); 8.21-8.16 (m, 8H); 7.88 (m, 8H); 7.82-7.75 (m, 8H); 7.59-7.52 (m, 12H); 7.48 (m, 6H); 7.10 (m, 6H); 2.75 (m, 12H); 2.59 (s, 3H); 2.51 (s, 12H); 2.46 (s, 3H); 1.71-1.57 (m, 12H); 1.43-1.21 (m, 48H). ¹³C NMR (CD₃CN): δ 157.79, 157.73, 155.6, 153.55, 153.52, 153.48, 152.29, 152.17, 151.2, 148.8, 148.5, 137.52, 137.41, 131.85, 131.81, 128.95, 128.91, 128.86, 128.1, 126.8, 126.7, 125.7, 124.9, 35.6, 30.8, 30.6, 30.35, 30.27, 30.23, 30.16, 30.04, 29.9, 29.8, 29.7, 21.1 and 20.5. TOF MS (ESI+): most abundant ion found for [M-6PF₆]⁶⁺, *m/z* 549.47. Calc. for Ru₄[C₁₇₄H₁₇₄N₂₄](PF₆)₂⁶⁺, *m/z* 549.28; most abundant ion found for [M-5PF₆]⁵⁺, *m/z* 688.18. Calc. for Ru₄[C₁₇₄H₁₇₄N₂₄](PF₆)₃⁵⁺, *m/z* 688.13; most

abundant ion found for $[M-4PF_6]^{4+}$, m/z 896.73. Calc. for $Ru_4[C_{174}H_{174}N_{24}](PF_6)_4^{4+}$, m/z 896.40.

$[Ru(phen)_2](\mu-bb_{10})\{Ru(phen)\}(\mu-bb_{10})\{Ru(phen)\}(\mu-bb_{10})\{Ru(phen)_2\}(PF_6)_8$.

Anal. Calcd. for $C_{168}H_{162}N_{24}F_{48}P_8Ru_4$: C, 49.4%; H, 4.00 %; N, 8.2%. Found: C, 49.4%; H, 3.92%; N, 8.0%. 1H NMR (400 MHz, CD_3CN): δ 8.68-8.51 (m, 16H); 8.41-8.33 (m, 10H); 8.28-8.22 (m, 10H); 8.21-8.15 (m, 8H); 7.87 (m, 8H); 7.81-7.76 (m, 8H); 7.54 (m, 12H); 7.50-7.46 (m, 6H); 7.12 (m, 6H); 2.78 (m, 12H); 2.56 (s, 3H); 2.51 (s, 12H); 2.45 (s, 3H); 1.73-1.56 (m, 12H); 1.45-1.22 (m, 36H). ^{13}C NMR (CD_3CN): δ 157.8, 157.7, 155.6, 153.56, 153.51, 153.46, 152.3, 152.2, 151.2, 148.8, 148.5, 137.5, 137.4, 131.8, 131.6, 128.94, 128.89, 128.82, 128.2, 126.8, 126.7, 125.6, 124.9, 35.6, 30.9, 30.6, 30.3, 30.2, 30.16, 30.08, 30.01, 29.9, 29.8, 29.7, 21.1 and 20.8. TOF MS (ESI+): most abundant ion found for $[M-5PF_6]^{5+}$, m/z 671.40. Calc. for $Ru_4[C_{168}H_{162}N_{24}](PF_6)_3^{5+}$, m/z 671.29; most abundant ion found for $[M-4PF_6]^{4+}$, m/z 875.77. Calc. for $Ru_4[C_{168}H_{162}N_{24}](PF_6)_4^{4+}$, m/z 875.36; most abundant ion found for $[M-3PF_6]^{3+}$, m/z 1215.32. Calc. for $Ru_4[C_{168}H_{162}N_{24}](PF_6)_5^{3+}$, m/z 1215.47.

The chloride salts were obtained by stirring the PF_6^- salts in methanol with Amberlite IRA- 402 (chloride form) anion-exchange resin. The resin was removed by filtration, and the orange-red solution was evaporated and dried in an oven at 70 °C for 16 h to obtain dark red $[Ru(phen)_2](\mu-bb_n)\{Ru(phen)\}(\mu-bb_n)\{Ru(phen)\}(\mu-bb_n)\{Ru(phen)_2\}Cl_8$ ($Rubb_n$ -tetra), typical yields were 20-25%, based on the synthetic starting material $[Ru(phen)_2](\mu-bb_n)\{Ru(phen)Cl_2\}(PF_6)_2$.

$[Ru(\mu-bb_n)_3]\{Ru(phen)_2\}_3Cl_8$, ($Rubb_n$ -tetra-nl)

In a typical reaction, a mixture of $[Ru(phen)_2(bb_{16})](PF_6)_2$ (229 mg, 0.174 mmol) and *cis*- $[Ru^{II}(DMSO)_4Cl_2]$ (28 mg, 0.057 mmol) was heated to reflux in ethanol–water (1:1,

20 mL) for 5-6 h under the nitrogen atmosphere. The reaction mixture was cooled to room temperature and the solvent evaporated to obtain an orange solid which was converted to the chloride salt by stirring in methanol with Amberlite IRA- 402 (chloride form) anion-exchange resin. After filtration of the resin and removal of methanol, the solid was dissolved in water (10 mL) and loaded onto an SP-Sephadex C-25 cation exchange column (2 cm diam. \times 25 cm), eluted with water and then with 0.6 M and then 0.8 M NaCl solutions to remove the impurities. The desired non-linear tetranuclear complex was eluted with a 1 M NaCl solution containing 30 % acetone. After removing the acetone, solid KPF_6 was added to the eluate followed by extraction into DCM (2×20 mL). The organic layer was washed with water (20 mL), dried over anhydrous Na_2SO_4 , and evaporated to dryness to obtain the PF_6^- salt of the complex. The complex was further purified using Sephadex LH-20 with acetone as the eluent, the major first orange band was collected and the acetone evaporated to yield a bright red–orange solid of $[\{\text{Ru}(\mu\text{-bb}_{16})_3\}\{\text{Ru}(\text{phen})_2\}_3](\text{PF}_6)_8$. **$[\{\text{Ru}(\mu\text{-bb}_{16})_3\}\{\text{Ru}(\text{phen})_2\}_3](\text{PF}_6)_8$** . Anal. Calcd. for $\text{C}_{186}\text{H}_{198}\text{N}_{24}\text{F}_{48}\text{P}_8\text{Ru}_4$: C, 51.5%; H, 4.61%; N, 7.8%. Found: C, 51.2%; H, 4.66%; N, 7.7%. ^1H NMR (400 MHz, CD_3CN): δ 8.67-8.62 (m, 8H); 8.57-8.51 (m, 8H); 8.44-8.36 (m, 10H); 8.26-8.22 (m, 10H); 8.21-8.18 (m, 8H); 7.92-7.84 (m, 8H); 7.82-7.76 (m, 8H); 7.58-7.52 (m, 12H); 7.49-7.45 (m, 6H); 7.14-7.07 (m, 6H); 2.74 (m, 12H); 2.64 (s, 3H); 2.54 (s, 12H); 2.44 (s, 3H); 1.73-1.57 (m, 12H); 1.44-1.16 (m, 72H). ^{13}C NMR (CD_3CN): δ 157.8, 157.7, 156.9, 156.5, 156.3, 155.7, 154.8, 153.7, 153.57, 153.53, 153.49, 152.3, 152.2, 151.2, 148.8, 148.6, 137.5, 137.4, 131.8, 129.0, 128.9, 128.8, 128.2, 126.8, 126.7, 125.7, 124.9, 35.6, 30.9, 30.6, 30.48, 30.40, 30.3, 30.2, 30.1, 30.04, 29.96, 29.91, 28.5, 21.1 and 20.7. TOF MS (ESI+): most abundant ion found for $[\text{M-8PF}_6]^{8+}$, m/z 396.77. Calc. for $\text{Ru}_4[\text{C}_{186}\text{H}_{198}\text{N}_{24}]^{8+}$, m/z 396.76; most abundant ion found for $[\text{M-7PF}_6]^{7+}$, m/z 474.10. Calc. for $\text{Ru}_4[\text{C}_{186}\text{H}_{198}\text{N}_{24}](\text{PF}_6)_1^{7+}$, m/z 474.14; most

abundant ion found for $[M-5PF_6]^{5+}$, m/z 721.90. Calc. for $Ru_4[C_{186}H_{198}N_{24}](PF_6)_3^{5+}$, m/z 721.79. **$[Ru(\mu-bb_{12})_3]\{Ru(phen)_2\}_3(PF_6)_8 \cdot 4H_2O$** . Anal. Calcd. for $C_{174}H_{182}N_{24}F_{48}O_4P_8Ru_4$: C, 49.3%; H, 4.33%; N, 7.9%. Found: C, 48.9%; H, 4.36%; N, 7.6%. 1H NMR (400 MHz, CD_3CN): δ 8.68-8.63 (m, 8H); 8.56-8.52 (m, 8H); 8.42-8.34 (m, 10H); 8.28-8.22 (m, 10H); 8.21-8.17 (m, 8H); 7.90-7.86 (m, 8H); 7.84-7.78 (m, 8H); 7.57-7.52 (m, 12H); 7.50-7.46 (m, 6H); 7.13-7.08 (m, 6H); 2.77 (m, 12H); 2.62 (s, 3H); 2.52 (s, 12H); 2.45 (s, 3H); 1.71-1.56 (m, 12H); 1.41-1.14 (m, 48H). ^{13}C NMR (CD_3CN): δ 157.8, 157.7, 156.8, 156.2, 156.0, 155.6, 154.5, 153.9, 153.6, 153.4, 152.3, 152.2, 151.2, 148.8, 148.6, 137.5, 137.4, 131.8, 129.0, 128.95, 128.89, 128.2, 126.8, 126.7, 125.7, 124.9, 35.6, 30.9, 30.7, 30.4, 30.3, 30.2, 30.1, 30.06, 30.02, 29.9, 29.3, 28.3, 21.2 and 21.1. TOF MS (ESI+): most abundant ion found for $[M-8PF_6]^{8+}$, m/z 375.75. Calc. for $Ru_4[C_{174}H_{174}N_{24}]^{8+}$, m/z 375.71; most abundant ion found for $[M-7PF_6]^{7+}$, m/z 450.00. Calc. for $Ru_4[C_{174}H_{174}N_{24}](PF_6)_1^{7+}$, m/z 450.10; most abundant ion found for $[M-6PF_6]^{6+}$, m/z 549.16. Calc. for $Ru_4[C_{174}H_{174}N_{24}](PF_6)_2^{6+}$, m/z 549.28; most abundant ion found for $[M-5PF_6]^{5+}$, m/z 688.18. Calc. for $Ru_4[C_{174}H_{174}N_{24}](PF_6)_3^{5+}$, m/z 688.13. **$[Ru(\mu-bb_{10})_3]\{Ru(phen)_2\}_3(PF_6)_8 \cdot 4H_2O$** . Anal. Calcd. for $C_{168}H_{170}N_{24}F_{48}O_4P_8Ru_4$: C, 48.6%; H, 4.13%; N, 8.1%. Found: C, 48.5%; H, 4.37%; N, 7.7%. 1H NMR (400 MHz, CD_3CN): δ 8.69-8.62 (m, 8H); 8.57-8.52 (m, 8H); 8.44-8.31 (m, 10H); 8.29-8.22 (m, 10H); 8.21-8.16 (m, 8H); 7.91-7.85 (m, 8H); 7.82-7.76 (m, 8H); 7.58-7.52 (m, 12H); 7.51-7.46 (m, 6H); 7.13-7.07 (m, 6H); 2.76 (m, 12H); 2.60 (s, 3H); 2.54 (s, 12H); 2.44 (s, 3H); 1.72-1.60 (m, 12H); 1.42-1.20 (m, 36H). ^{13}C NMR (CD_3CN): δ 157.8, 157.7, 157.0, 156.9, 156.4, 155.9, 155.6, 155.3, 153.57, 153.52, 153.4, 153.3, 152.3, 152.1, 151.2, 150.8, 148.8, 148.5, 137.5, 137.4, 131.8, 128.96, 128.90, 128.2, 126.8, 126.7, 125.7, 124.9, 35.6, 30.96, 30.91, 30.6, 30.2, 30.08, 30.01, 29.8, 29.3, 28.3, 21.2 and 20.9. TOF MS (ESI+): most abundant ion found for $[M-$

$5\text{PF}_6]^{5+}$, m/z 671.36. Calc. for $\text{Ru}_4[\text{C}_{168}\text{H}_{162}\text{N}_{24}](\text{PF}_6)_3^{5+}$, m/z 671.29; most abundant ion found for $[\text{M}-4\text{PF}_6]^{4+}$, m/z 875.45. Calc. for $\text{Ru}_4[\text{C}_{168}\text{H}_{162}\text{N}_{24}](\text{PF}_6)_4^{4+}$, m/z 875.36; most abundant ion found for $[\text{M}-3\text{PF}_6]^{3+}$, m/z 1215.60. Calc. for $\text{Ru}_4[\text{C}_{168}\text{H}_{162}\text{N}_{24}](\text{PF}_6)_5^{3+}$, m/z 1215.47; most abundant ion found for $[\text{M}-2\text{PF}_6]^{2+}$, m/z 1895.85. Calc. for $\text{Ru}_4[\text{C}_{168}\text{H}_{162}\text{N}_{24}](\text{PF}_6)_6^{2+}$, m/z 1895.69.

The chloride salts were obtained by stirring the PF_6^- salts in methanol with Amberlite IRA- 402 (chloride form) anion-exchange resin. The resin was removed by filtration, and the orange-red solution was evaporated and dried in oven at 70 °C for 16 h to obtain dark red $[\{\text{Ru}(\mu\text{-bb}_n)_3\}\{\text{Ru}(\text{phen})_2\}_3]\text{Cl}_8$ (Rubb_n-tetra-nl), typical yields were 25-35 %, based on the synthetic starting material $[\text{Ru}(\text{DMSO})_4\text{Cl}_2]$.

3.3. Results

3.3.1. Synthesis

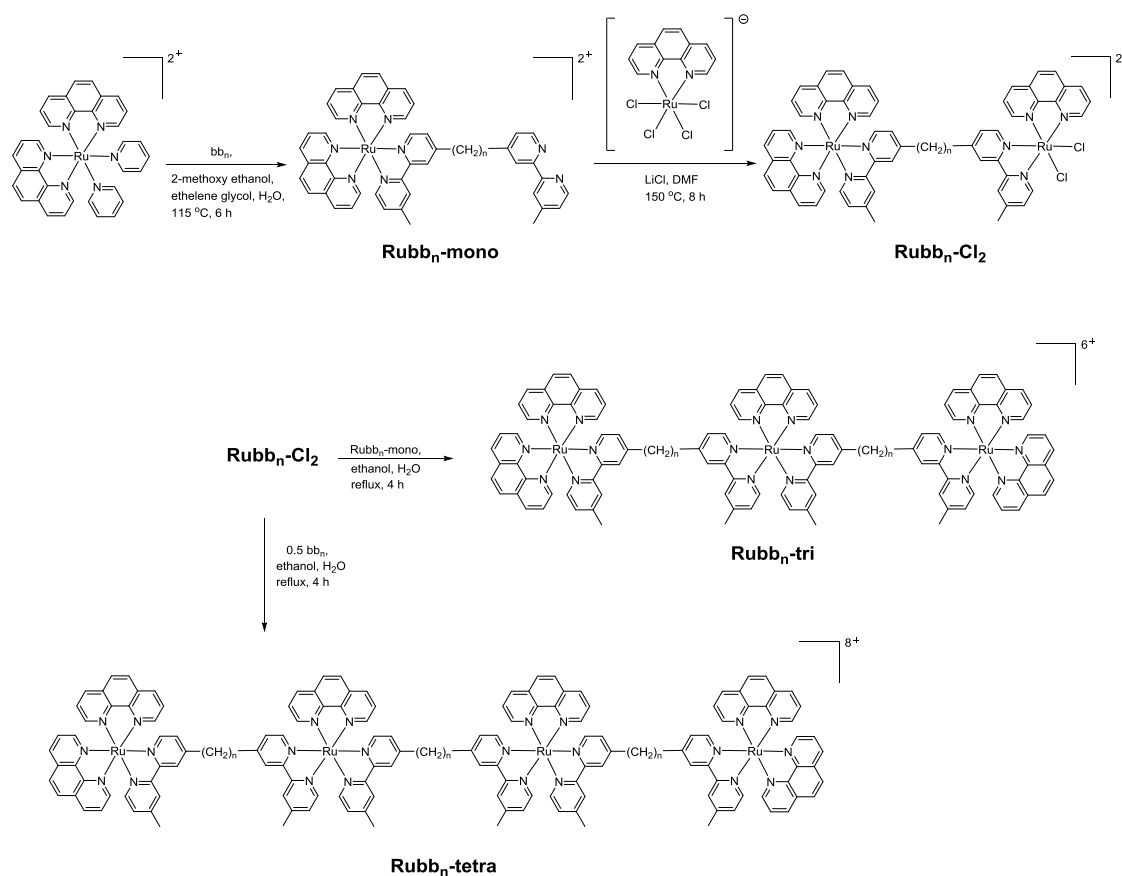
The synthesis of flexibly-linked dinuclear (Rubb_n-Cl₂), trinuclear (Rubb_n-tri), tetranuclear (Rubb_n-tetra) and non-linear tetranuclear (Rubb_n-tetra-nl) ruthenium complexes incorporating bb_n bridging ligands has been achieved in fair yield, as shown in Schemes 3.1 and 3.2. The chlorido-containing dinuclear species (Rubb_n-Cl₂) were synthesised by reacting the mononuclear complex, Rubb_n-mono, with $(\text{phenH}^+)[\text{Ru}(\text{phen})\text{Cl}_4]$ in DMF at reflux temperature. The characterisation of the chlorido complexes was carried out by NMR spectroscopy and they were used as precursors for the synthesis of the tri- and tetra-nuclear complexes.

The trinuclear and tetranuclear (both linear and non-linear) complexes were characterised by microanalysis, NMR (^1H and ^{13}C) and high resolution electrospray ionisation mass spectroscopy methods. Consistent with the observations previously

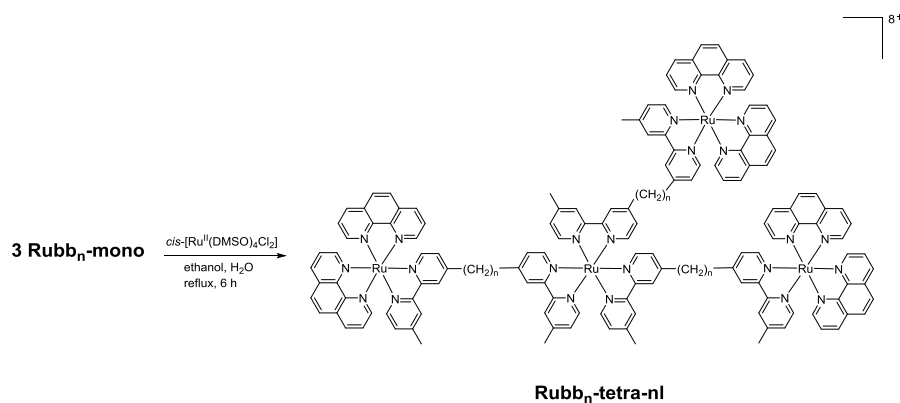
reported for Rubb₇-tetra,²⁴ satisfactory ESI-MS could not be obtained for the linear tetranuclear complexes when they were dissolved in acetonitrile. However, good mass spectra could be obtained using acetone as the solvent. The synthesis of non-linear complexes was achieved by the reaction between the mononuclear complex, Rubb_n-mono, and *cis*-[Ru^{II}(DMSO)₄Cl₂]. The reaction was carried out in ethanol-water at reflux temperatures for 5-6 hours, whereupon all the DMSO and chlorido ligands were replaced by the free '2,2'-bpy' entities of Rubb_n-mono complexes. All the inert complexes (tri, tetra, tetra-nl species) were purified by cation exchange on an SP Sephadex C-25 column, whereas the chlorido-containing complexes (Rubb_n-Cl₂) were purified by size exclusion on an Sephadex LH-20 column.

It is noted that geometric isomers will exist for the oligonuclear complexes in this study. In the bridging ligands bb_n, the 2,2'-bipyridine coordinating moieties are unsymmetrically substituted – one pyridine entity with a methyl group in the 4-position and the other with the bridging methylene chain. Accordingly, for cases where there are two bb_n ligands attached to one metal centre – as is the case for the central ruthenium in the trinuclear complexes and the two central ruthenium centres in the linear tetranuclear species – the chain-bearing pyridine entities may bear either relative 'trans' or one of two possible 'cis' orientations (one symmetrical in the sense that the centre will have C₂ point group symmetry – denoted *s-cis* – and the other has C₁ point group symmetry – denoted *u-cis*). For the trinuclear case (Rubb_n-tri) there are three isomers possible based on the central metal centre (*trans*, *s-cis* and *u-cis*), and six isomers based on the two internal metal centres (*trans,trans*; *s-cis,s-cis*; *u-cis,u-cis*; *trans,s-cis*; *trans,u-cis*; *s-cis,u-cis*) for the linear tetranuclear case (Rubb_n-tetra). For the dinuclear Rubb_n-Cl₂ complexes the two chlorido ligands may bear either a *cis,cis* or a *cis,trans* relationship to the chain-bearing pyridine entity, so that there are two isomers. Finally, in the case of

the non-linear tetranuclear complexes, $\text{Ru}_{\text{bb}_n}\text{-tetra-nl}$, the central Ru centre has three bb_n ligands attached so that the chain-bearing pyridine entities may bear either a facial or meridional orientation to one another – giving rise to two isomers (*fac* and *mer*). In the case of *fac/mer* geometric isomerism, the *mer* isomer is thermodynamically preferred for statistical reasons (3/1) but the *mer/fac* ratio is often considerably greater than that because of steric congestion in the *fac* form.²⁵ In the present case for the tetra-nl species, 2D NMR studies (COSY and ROESY) indicated the existence of both isomers with the *fac* isomer comprising about 5% (*mer/fac* = 19/1). The separation of possible geometrical isomers was not attempted for any of the complex systems in this study at this stage, and would represent a significant challenge in a number of these cases.



Scheme 3.1



Scheme 3.2

In agreement with previous studies, the Rubb_n-Cl₂ complexes hydrolysed when they were dissolved in water.^{26,27} The aromatic region of the ¹H NMR spectrum of a Rubb_n-Cl₂ complex dissolved in water was extremely complicated suggesting a mixture of [Rubb_n(OH₂)Cl]⁺ and [Rubb_n(OH₂)₂]²⁺ species, as has been previously observed for the hydrolysis of [*cis*-Ru(bpy)₂Cl₂].²⁷ Consistent with this proposal, the addition of

AgNO_3 to a $\text{Ru}_{\text{bb}_n}\text{-Cl}_2$ complex that had been in an aqueous solution for two days did induce some changes in the NMR spectrum. However, even after the addition of AgNO_3 , the aromatic region in the NMR spectrum was still very complex. This could indicate that both the *cis*- and *trans*-diaqua species were formed, as has been noted in the acid hydrolysis of $[\text{Ru}(\text{CO}_3)(\text{bpy})_2]$.²⁸

3.3.2. *Electrochemistry*

Cyclic voltammetry was used to determine the redox potentials for the multinuclear complexes with $n = 12$ (see

Table 3.1). All complexes showed a single, reversible Ru(II/III) oxidation peak at $\approx +1.27$ V *vs* Ag/AgCl , and a series of ligand-based reductions, consistent with the well-established behaviour of tris(bidentate) polypyridylruthenium complexes^{29,30} (see Figure A2 in Appendix). It was thought that differences might be discernible in the potentials, particularly the reduction patterns, given the subtle structural variations in the different metal centres in the multinuclear complexes. For example it has been established that in the homoleptic complexes $[\text{Ru}(\text{phen})_3]^{2+}$ and $[\text{Ru}(\text{Me}_2\text{bpy})_3]^{2+}$, the Me_2bpy ligand is slightly more difficult to reduce than phen due to the electron-donating effect of the methyl groups, and this also translates to an effect on the Ru(II) centre, which undergoes oxidation more readily.^{30,31} Either terminal of the bb_{12} ligand could be expected to mimic a Me_2bpy ligand, as has been observed for the complex $[\{(\text{bpy})_2\text{Ru}\}_2(\text{bb}_2)]^{4+}$, which shows very similar redox potentials to the mononuclear complex $[\text{Ru}(\text{bpy})_2(\text{Me}_2\text{bpy})]^{2+}$.³² In the present case, no significant differences were observed in the oxidation potentials of the complexes, even for the non-linear tetranuclear complex, in which the central ruthenium differs somewhat more from the others. The reduction patterns were also quite similar, with each complex showing two

closely-spaced reductions. A third clear reduction peak was observed for Rubb₁₂, though this was distorted by adsorption. This three-reduction set is consistent with the pattern reported for both mononuclear $[\text{Ru}(\text{L})_2(\text{Me}_2\text{bpy})]^{2+}$ (L= bpy, phen) and dinuclear $[\{\text{Ru}(\text{bpy})_2\}_2(\text{bb}_n)]^{4+}$ ($n = 2,3$).³²⁻³⁴ For the tri- and tetra-nuclear complexes only a small peak was evident at potentials where a third reduction might be expected, and a desorption peak was generally observed in the re-oxidation scan. Adsorption of reduction products has previously been noted for other multinuclear ruthenium bipyridyl complexes.^{35,36} The results indicate that redox differences between the complexes are negligible and unlikely to underpin any differences in biological activity.

Table 3.1. Electrode potentials for Ru(II) complexes in CH₃CN (in V vs Ag/AgCl; working electrode = glassy carbon; counter electrode = platinum wire; electrolyte = 0.1 M tetra-*n*-butylammonium tetrafluoroborate; internal standard = ferrocene).

Complex	Oxidation {E _{1/2} Ru(II/III)}	Reductions (E _{pc}) ^a
Rubb ₁₂	1.26	-1.33, -1.52, -1.92
Rubb ₁₂ -tri	1.28	-1.32, -1.49, -1.85 ^b
Rubb ₁₂ -tetra	1.26	-1.33, -1.50, -1.84 ^b
Rubb ₁₂ -tetra-nl	1.27	-1.32, -1.49, -1.85 ^b

a) irreversible/semi-reversible; cathodic peak given. b) weak

3.3.3. Antimicrobial activity

The minimum inhibitory concentrations (MIC) for the di-, tri- and tetra-nuclear ruthenium complexes against four bacterial strains (*Staphylococcus aureus* (*S. aureus*),

methicillin-resistant *S. aureus* (MRSA), *Escherichia coli* (*E. coli*) and *Pseudomonas aeruginosa* (*P. aeruginosa*)} have been determined and the results are summarised in Table 3.2. The results demonstrate that some of the ruthenium(II) complexes in the present study have significant antimicrobial activity against both classes of bacteria, and most of the complexes are more active against Gram positive bacteria than the Gram negative strains. Of particular note, the inert tri- and tetra-nuclear ruthenium complexes showed better antimicrobial activity than the corresponding dinuclear ruthenium(II) complexes (Rubb_n), particularly when the MIC values are given on a molar basis. Interestingly, the non-linear tetranuclear ruthenium(II) complexes ($\text{Rubb}_n\text{-tetra-nl}$) were two-fold less active than the dinuclear Rubb_n complexes. Of all the complexes, $\text{Rubb}_{12}\text{-tri}$, $\text{Rubb}_{16}\text{-tri}$, $\text{Rubb}_{12}\text{-tetra}$ and $\text{Rubb}_{16}\text{-tetra}$ are the most active compounds, and are up to four-times more active than the dinuclear counterparts against Gram positive and slightly more active against the Gram negative strains. Furthermore, $\text{Rubb}_{12}\text{-tri}$, $\text{Rubb}_{16}\text{-tri}$, $\text{Rubb}_{12}\text{-tetra}$ and $\text{Rubb}_{16}\text{-tetra}$ are 4-8 times more active than the previously reported $\text{Rubb}_7\text{-tri}$ and $\text{Rubb}_7\text{-tetra}$ complexes.⁴ Even though the overall charge of the linear and non-linear version of the tetranuclear complexes is the same (8+), the non-linear tetranuclear ruthenium complexes ($\text{Rubb}_n\text{-tetra-nl}$) are less active when compared to the corresponding linear species, suggesting that the linearity could play an important role in inhibiting bacterial growth. The dinuclear ruthenium(II) complexes with two chlorido ligands ($\text{Rubb}_n\text{-Cl}_2$) also showed good activity, but are fractionally less active than the tri- and tetra-nuclear complexes. In general, complexes with the bb_{12} linking ligand were the most active against *S. aureus*, MRSA, and *E. coli*, with the complexes having the shortest (bb_{10}) and longest (bb_{16}) linking chain being the least active. However, against *P. aeruginosa*, complexes with the bb_{16} linking ligand showed better activity.

Table 3.2. MIC values (μM) for the ruthenium complexes after 16-18 hours of incubation against Gram positive and Gram negative bacterial strains.

Compounds	Gram positive		Gram negative	
	<i>S. aureus</i>	MRSA	<i>E. coli</i>	<i>P. aeruginosa</i>
Rubb ₁₂	0.6	0.6	2.5	20.1
Rubb ₁₆	1.2	1.2	2.4	9.8
Rubb ₁₀ -tri	0.8	1.7	1.7	13.5
Rubb ₁₂ -tri	0.4	0.8	1.6	13.1
Rubb ₁₆ -tri	0.4	0.8	3.1	12.6
Rubb ₁₀ -tetra	1.2	2.5	2.5	19.9
Rubb ₁₂ -tetra	0.3	0.6	1.2	9.7
Rubb ₁₆ -tetra	0.3	0.6	2.3	9.2
Rubb ₁₀ -tetra-nl	2.5	2.5	5.0	19.9
Rubb ₁₂ -tetra-nl	1.2	1.2	4.9	19.4
Rubb ₁₆ -tetra-nl	1.1	2.3	4.6	18.5
Rubb ₁₀ -Cl ₂	5.9	5.9	5.9	46.9
Rubb ₁₂ -Cl ₂	1.4	1.4	2.9	23.0
Rubb ₁₆ -Cl ₂	1.4	2.8	5.5	44.2
Ampicillin	< 0.7	183.0	11.4	> 366.0
Gentamicin	< 0.5	66.9	1.0	0.5

Due to their greater lipophilicity (see Table 3.5), it was considered that the antimicrobial activity of the tri- and tetra-nuclear complexes could decrease to a greater extent with longer incubation times than would the dinuclear complexes. Table 3.3 summarises the MIC values for the ruthenium complexes when the assays were carried out over a 20-22 hour timeframe. The MIC values for the tri- and tetra-nuclear complexes increased by as much as four-fold for some of the complexes, when compared to the 16-18 hour values. Alternatively, the dinuclear complexes Rubb₁₂ and Rubb₁₆ only exhibited a maximum two-fold decrease in activity across the four bacteria. These observations suggest that the tri- and tetra-nuclear complexes rapidly accumulate within the bacteria, thereby decreasing the concentration in the incubation broth. However, even at the longer incubation time Rubb₁₂-tetra and Rubb₁₆-tetra are the most active of all the ruthenium complexes tested.

Table 3.3. MIC values (μM) for the ruthenium complexes after 20-22 hours of incubation against Gram positive and Gram negative bacterial strains.

Compound	Gram positive		Gram negative	
	<i>S. aureus</i>	MRSA	<i>E. coli</i>	<i>P. aeruginosa</i>
Rubb ₁₂	1.3	2.5	5.0	40.3
Rubb ₁₆	1.2	2.4	4.9	19.6
Rubb ₁₀ -tri	1.7	3.4	3.4	27.0
Rubb ₁₂ -tri	1.6	1.6	3.3	26.3
Rubb ₁₆ -tri	1.6	1.6	6.3	25.1
Rubb ₁₀ -tetra	2.5	5.0	5.0	19.9
Rubb ₁₂ -tetra	0.6	1.2	2.4	9.7
Rubb ₁₆ -tetra	1.1	1.1	2.3	9.2
Rubb ₁₀ -tetra-nl	5.0	5.0	9.9	19.9
Rubb ₁₂ -tetra-nl	1.2	2.4	4.9	19.4
Rubb ₁₆ -tetra-nl	2.3	2.3	4.6	18.5
Rubb ₁₀ -Cl ₂	5.9	11.7	5.9	46.9
Rubb ₁₂ -Cl ₂	2.9	1.4	5.7	23.0
Rubb ₁₆ -Cl ₂	2.8	2.8	11.0	44.2
Ampicillin	< 0.7	183.0	11.4	> 366.0
Gentamicin	< 0.5	66.9	1.0	0.5

The minimum bactericidal concentrations (MBC) of a selection of the ruthenium complexes were determined after the MIC values were obtained for the 20-22 hour incubation experiment. The results are summarised in Table 3.4. As the MBC values are generally $\leq 2 \times \text{MIC}$ for the 20-22 hour incubation, it can be concluded that the tri- and tetra-nuclear complexes are bactericidal rather than bacteriostatic.

Table 3.4. MBC values (μM) for a selection of the ruthenium complexes against Gram positive and Gram negative bacterial strains.

Compound	Gram positive		Gram negative	
	<i>S. aureus</i>	MRSA	<i>E. coli</i>	<i>P. aeruginosa</i>
Rubb ₁₂	2.6	2.5	10.1	40.3
Rubb ₁₂ -tri	3.3	3.3	6.6	52.6
Rubb ₁₆ -tri	1.6	6.3	12.6	50.3
Rubb ₁₂ -tetra	1.2	1.2	2.4	19.4
Rubb ₁₆ -tetra	2.3	2.3	4.6	37.0

3.3.4. *Log P*

Lipophilicity is a significant factor that affects the biological activity of any metal complex, as it is generally correlated to the capacity of the drug to penetrate through the cell membrane. The standard octanol-water partition coefficient ($\log P$) was determined for the mononuclear species $[\text{Ru}(\text{phen})_2(\text{Me}_2\text{bpy})]^{2+}$ and Rubb_n (as control experiments), Rubb_n-tri, Rubb_n-tetra and Rubb_n-tetra-nl complexes, and the results are summarised in Table 3.5. From the results, the trinuclear ruthenium complexes are more

lipophilic than the tetranuclear ruthenium complexes. For the dinuclear Rubb_n complexes, the antimicrobial activity was directly related to the log P, with activity increasing with increasing lipophilicity. However, although the trinuclear complexes were more lipophilic than their corresponding linear tetranuclear complexes, they were less active. This suggests lipophilicity is an important determinant of activity, but only to the level that allows the ruthenium complex to easily diffuse across the cellular membrane.

Table 3.5. Octanol-water partition coefficients (log P) for the ruthenium complexes. Maximum experimental error is ± 0.2 .

Metal complex	Charge	log P
$[\text{Ru}(\text{phen})_2(\text{Me}_2\text{bpy})]^{2+}$	+ 2	-2.9
Rubb_{12}	+ 4	-2.9
Rubb_{16}	+ 4	-1.9
$\text{Rubb}_{10}\text{-tri}$	+ 6	-1.3
$\text{Rubb}_{12}\text{-tri}$	+ 6	-1.0
$\text{Rubb}_{16}\text{-tri}$	+ 6	-0.8
$\text{Rubb}_{10}\text{-tetra}$	+ 8	-1.7
$\text{Rubb}_{12}\text{-tetra}$	+ 8	-1.6
$\text{Rubb}_{16}\text{-tetra}$	+ 8	-0.95
$\text{Rubb}_{10}\text{-tetra-nl}$	+ 8	-1.9
$\text{Rubb}_{12}\text{-tetra-nl}$	+ 8	-1.4
$\text{Rubb}_{16}\text{-tetra-nl}$	+ 8	-1.1

3.3.5. Cellular accumulation

The cellular accumulations of the tri- and tetra-nuclear ruthenium complexes in *S. aureus*, MRSA, *E. coli*, and *P. aeruginosa* were determined by measuring the concentration of the complex remaining in the culture supernatant after removing the bacteria by centrifugation. The concentration of the ruthenium complex in the supernatant was calculated from an absorbance calibration curve obtained by adding known concentrations of the ruthenium complex to a blank supernatant. As the absorbance of the ruthenium complexes varied with the different broths and supernatants for each bacterial strain, a calibration curve was determined for each complex in the supernatant of each bacterial strain. The uptake of complexes into bacterial strains was measured at various incubation time points, however the uptake did not significantly change with incubation time after 30 minutes. Figure 3.2 shows the uptake of the ruthenium complexes into the bacteria after 30 minutes. Surprisingly, the uptake of the complexes is slightly higher for the Gram negative bacteria than the Gram positive. The accumulation of Rubb₁₆-tri was the highest in both Gram positive and Gram negative bacteria. For all the complexes lower levels of accumulation were observed for *S. aureus*, compared to the other bacteria. For both the Gram positive and Gram negative bacteria, the cellular accumulation of the tetranuclear metal complexes was slightly lower than with the trinuclear counterparts. Surprisingly, the uptake of Rubb₁₂-tetra-nl is greater than Rubb₁₂-tetra and Rubb₁₂-tri.

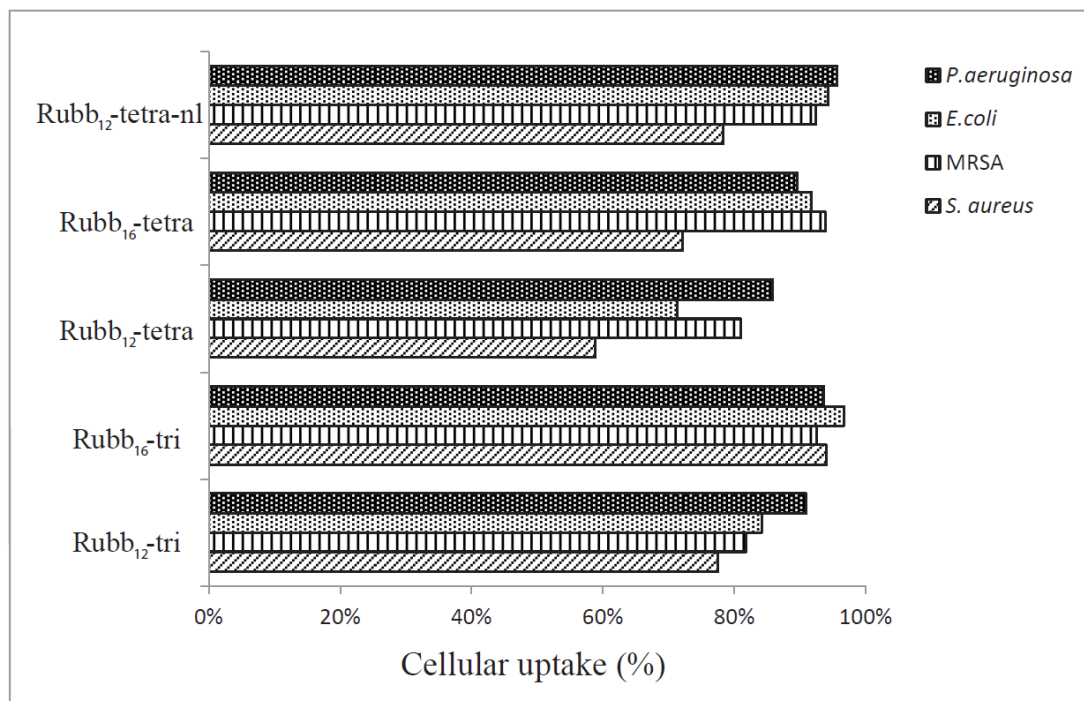


Figure 3.2. Cellular uptake of the ruthenium complexes into four bacteria after a 30 minute incubation. The experimental error is $\leq 5\%$.

3.3.6. Time-kill curve examination

As the Rubb₁₂-tri and Rubb₁₂-tetra complexes displayed better antimicrobial activity than their bb₁₆ analogues, time-kill curve experiments were performed to determine if the ruthenium complexes were bactericidal, and if so, the time required to kill 99.9% of the bacteria. In order to compare the results to those previously obtained with Rubb₁₂ and Rubb₁₆,⁵ the time-kill assays were carried out using *S. aureus*, MRSA, *E. coli* and *P. aeruginosa*. Time-kill curves for ampicillin and gentamicin were also determined for comparison. As seen in Figure 3.3 and Figure 3.4, the results confirm the bactericidal nature of Rubb₁₂-tri and Rubb₁₂-tetra, as $2 \times \text{MIC}$ was sufficient to kill 99.9% of the bacterial population of the bacteria. Interestingly, both Rubb₁₂-tri and Rubb₁₂-tetra kill 99.9% of the Gram negative bacteria (3-4 hours) more quickly than the Gram positive species (4-6 hours).

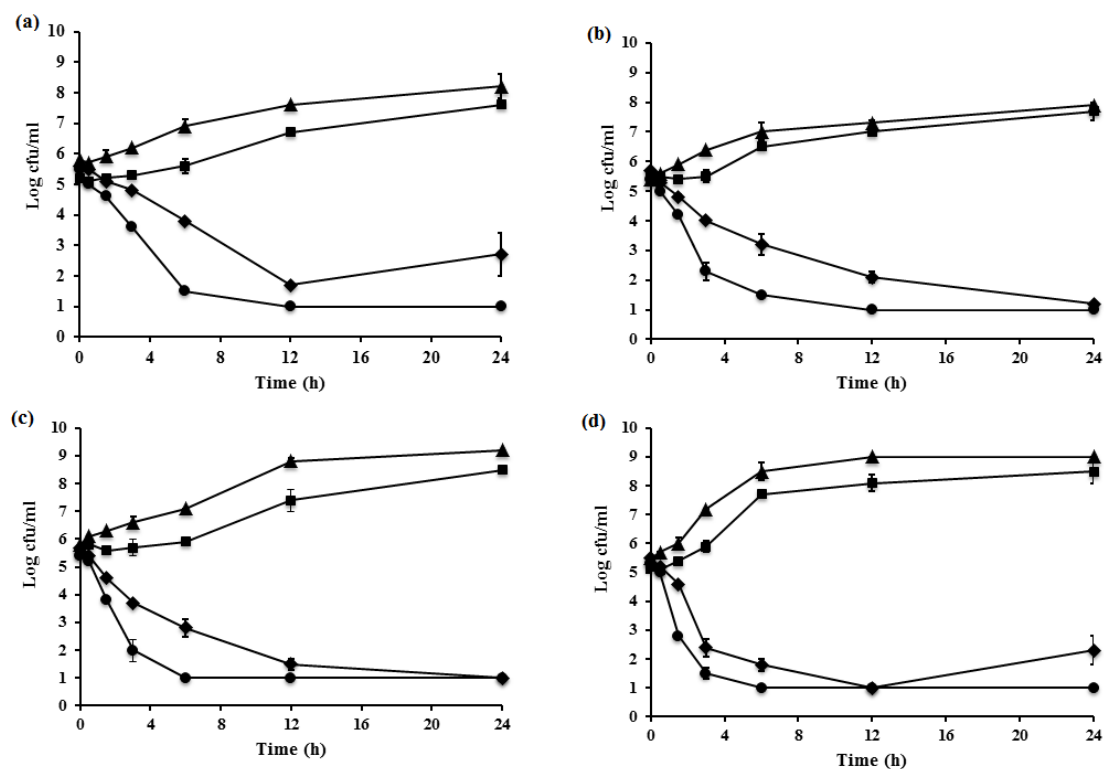


Figure 3.3. Time-kill curves for Rubb₁₂-tri against two Gram positive and two Gram negative strains, (a) against *S. aureus*, (b) against MRSA, (c) against *E. coli* and (d) against *P. aeruginosa*. Diamonds, growth control; squares, 0.5xMIC; triangles, 1xMIC; and circles, 2xMIC.

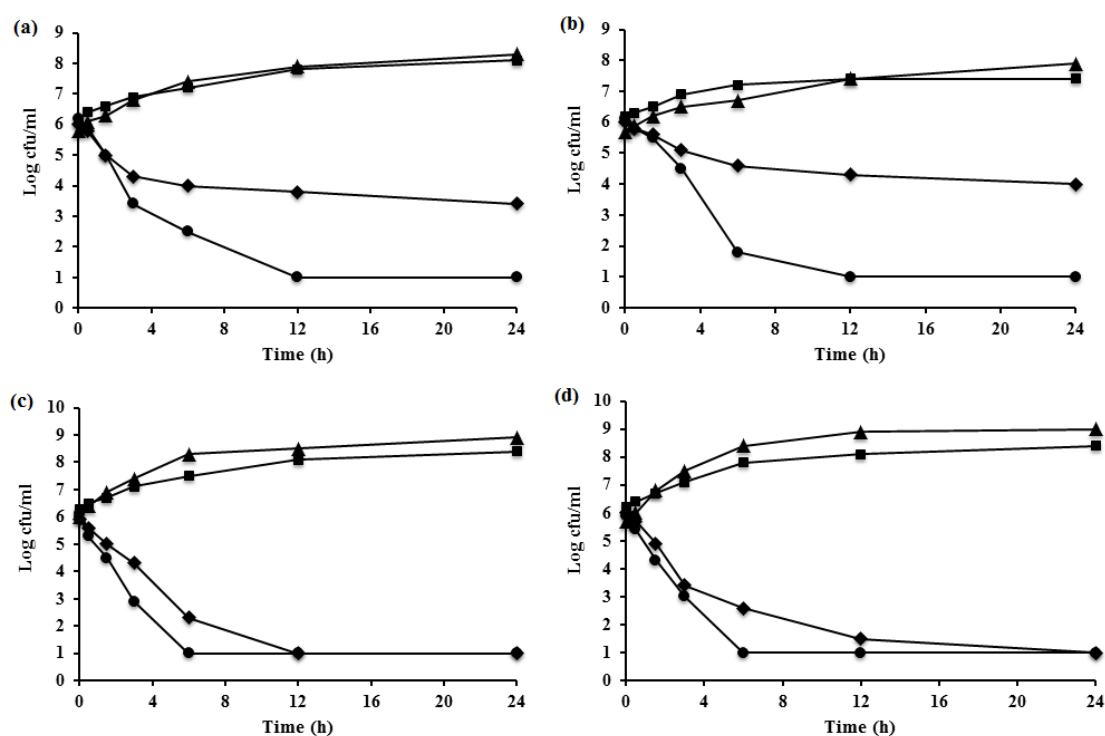


Figure 3.4. Time-kill curves for Rubb₁₂-tetra against two Gram positive and two Gram negative strains, (a) against *S. aureus*, (b) against MRSA, (c) against *E. coli* and (d) against *P. aeruginosa*. Triangles, growth control; squares, 0.5×MIC; diamonds, 1×MIC; and circles, 2×MIC.

3.3.7. Intra-bacterium localisation by wide-field fluorescent microscopy

As time did not permit a complete analysis of the results, only a preliminary analysis is presented. Wide-field fluorescence microscopic studies were carried out to determine the effect of Rubb₁₂-tetra on the growth of bacteria. As the *E. coli* strain used for microscopic studies was different from the particular strains used in the other studies presented in this thesis, the MIC of Rubb₁₂-tetra against *E. coli* MG1665 was determined, and found to be 9.6 μ M. *E. coli* cells were then incubated with Rubb₁₂-tetra at 0.5 \times MIC, 1 \times MIC, 2 \times MIC at 37 $^{\circ}$ C for 1 hour, then the cells were washed twice

with a phosphate buffer solution and incubated with DAPI at room temperature for 15-30 min before being loaded onto agarose pads on slides for microscopy. Similarly to the results obtained with Rubb₁₆, Rubb₁₂-tetra also localised at the ribosomes and particularly when they existed as polysomes. As shown in Figure 3.5, the nucleoid of the cells has condensed and become strand-like in appearance when treated with Rubb₁₂-tetra at $2 \times \text{MIC}$. This effect increased with the concentration of the Rubb₁₂-tetra complex and the incubation time. No significant overlap of the DAPI and Rubb₁₂-tetra luminescence was observed, suggesting that the Rubb₁₂-tetra complex is not localised at the chromosomal DNA. On the basis that the Rubb₁₂-tetra phosphorescence is not quenched upon DNA binding, the results suggests that the observed DNA condensation could be due to a change in the osmotic pressure due to the solvation of the 8+ charged Rubb₁₂-tetra complex within the cell. However, further studies are required to confirm this proposal.

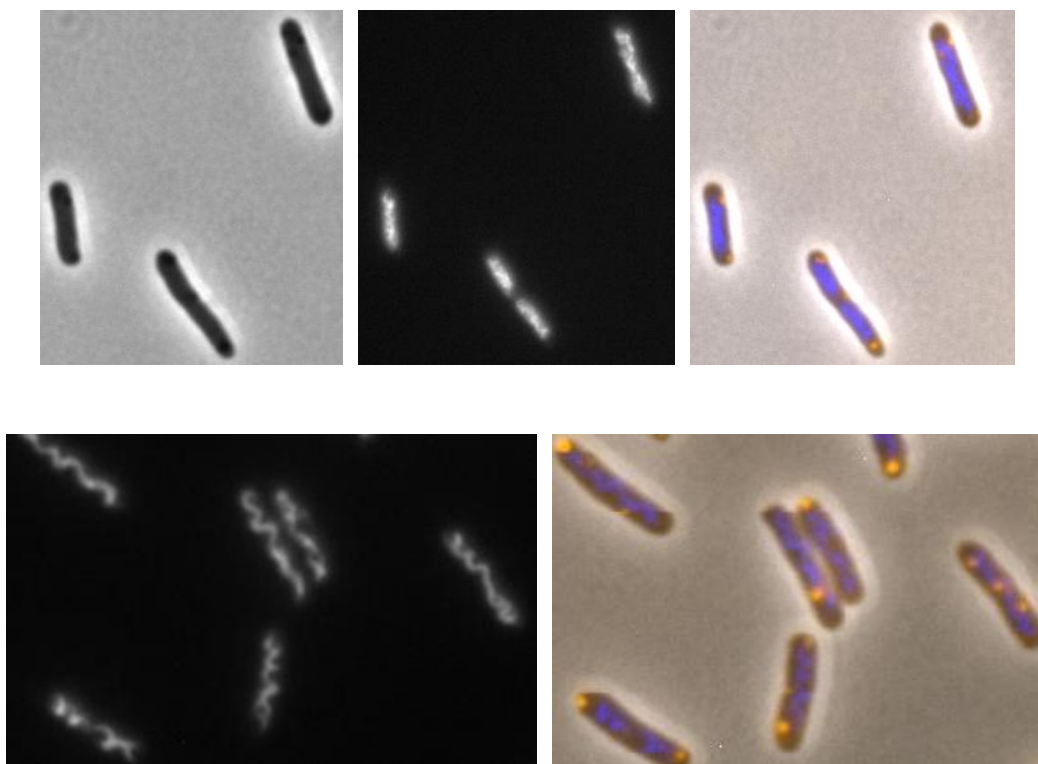


Figure 3.5. Fluorescence microscopy images of *E. coli* MG1665 cells at their mid-log phase incubated with Rubb₁₂-tetra at $0.5 \times \text{MIC}$ {top panel; left-hand side phase-contrast, middle fluorescence – DAPI (in black & white for greater contrast), right-hand side merged DAPI (blue) and Rubb₁₂-tetra phosphorescence (yellow)} and $2 \times \text{MIC}$ {lower panel; left-hand side fluorescence – DAPI (in black & white for greater contrast), right-hand side merged DAPI (blue) and Rubb₁₂-tetra phosphorescence (yellow)}.

3.4. Discussion

It was previously shown that dinuclear ruthenium(II) complexes (Rubb_n) exhibit excellent antimicrobial properties in terms of MIC values, cellular uptake, time-kill curves and show low toxicity towards human cells.⁴ In order to further improve the antimicrobial properties, in this chapter, the tri- and tetra-nuclear ruthenium(II) analogues of the most active dinuclear complexes, Rubb₁₂ and Rubb₁₆ were synthesised and their *in vitro* susceptibility, lipophilicity, time-kill curves and cellular accumulation

examined. The results of the MIC assays indicate that the linear tetranuclear complexes, $\text{Rubb}_n\text{-tetra}$, are consistently more active across the four bacteria used in this study than Rubb_{12} and Rubb_{16} . Alternatively, the trinuclear analogues of Rubb_{12} and Rubb_{16} are slightly more active against some bacteria than the corresponding dinuclear complexes, but slightly less active in others. In a similar manner to Rubb_{12} and Rubb_{16} , the tri- and tetra-nuclear linear complexes maintain their activity against MRSA compared to *S. aureus*, and are bactericidal. The non-linear tetranuclear complexes, $\text{Rubb}_n\text{-tetra-nl}$, are consistently less active than their linear counterparts and Rubb_{12} and Rubb_{16} . Significantly, whereas $\text{Rubb}_{10}\text{-tri}$ was generally more active than $\text{Rubb}_{10}\text{-tetra}$, the activity of $\text{Rubb}_n\text{-tetra}$ was greater than $\text{Rubb}_n\text{-tri}$ for $n = 12$ and 16 over the four bacterial strains used in the study. The time-kill curve studies on $\text{Rubb}_{12}\text{-tri}$ and $\text{Rubb}_{12}\text{-tetra}$ showed that the antimicrobial activity of these complexes against both Gram positive and Gram negative bacteria was dependent on concentration and also confirmed their bactericidal nature as $2 \times \text{MIC}$ concentration was sufficient to kill 99.9% of bacterial population. Interestingly, both complexes kill Gram negative bacteria more quickly than Gram positive bacteria. Microscopic studies showed the localisation of $\text{Rubb}_{12}\text{-tetra}$ at ribosomes particularly when they existed as polysomes. Furthermore, the nucleoid of the bacteria became condensed with a strand-like appearance when treated with $\text{Rubb}_{12}\text{-tetra}$ at $2 \times \text{MIC}$, this could be due to an osmotic pressure effect induced by the accumulation of metal complex in the bacteria. However, further studies and analysis are required to confirm this proposal.

The lipophilicity of the ruthenium complexes, as determined by $\log P$, increased in the order $\text{Rubb}_n < \text{Rubb}_n\text{-tetra} < \text{Rubb}_n\text{-tri}$, with all tri- and tetra-nuclear complexes being significantly more lipophilic than Rubb_{16} . As the ruthenium complexes enter bacterial cells by passive diffusion,³⁷ it is not surprising that the cellular accumulation

experiments demonstrated that the tri- and tetra-nuclear complexes rapidly accumulate to high concentrations within the bacteria. However, the extent of the cellular accumulation of the tri- and tetra-nuclear complexes in the Gram negative bacteria, particularly *P. aeruginosa*, is surprising. The results of this study demonstrate that the lower toxicity of the dinuclear complexes towards *P. aeruginosa* is probably not strongly correlated to the cellular accumulation – as it was previously concluded – but rather to a lower intrinsic ability to kill *P. aeruginosa* cells. Preliminary pharmacokinetic experiments with mice have indicated that Rubb₁₂ and Rubb₁₆ are rapidly cleared from the blood;³⁸ consequently, the greater lipophilicity and greater cellular uptake may be advantageous for *in vivo* antimicrobial studies.

Interestingly, the one non-linear tetranuclear complex examined in cellular accumulation experiments, Rubb₁₂-tetra-nl, showed greater accumulation than the corresponding linear complex Rubb₁₂-tetra. Despite Rubb₁₂-tetra-nl being slightly more lipophilic than Rubb₁₂-tetra, it would be expected that the linear complex would cross a cell membrane more easily than a non-linear complex. However, as the ruthenium complexes enter bacterial cells by passive diffusion,³⁸ the level of the cellular accumulation is a function of the binding of the ruthenium complex to intra-cellular receptors, such as nucleic acids and proteins. Despite the relatively greater accumulation of Rubb₁₂-tetra-nl compared to Rubb₁₂-tetra, the linear complex exhibited greater activity. Previous studies have shown that because of the flexibility of the alkane chain in the bb_n ligand, both ruthenium metal centres in the Rubb_n complexes can closely associate with the DNA minor groove.³⁹ Similarly, the linear tetranuclear complexes could also follow the curvature of the DNA groove allowing close association of the four ruthenium centres with the DNA backbone. Alternatively, due to the three-

dimensional shape of the non-linear tetranuclear complexes, the interactions with DNA would be substantially different and a different biological response would be expected.

3.5. Conclusions

There has been increasing interest in trinuclear and higher nuclearity ruthenium complexes as anticancer agents.¹⁹⁻²¹ However, there have been very few studies on the potential of tri- or tetra-nuclear ruthenium complexes as antimicrobial agents. The present study indicates that these multinuclear complexes are highly active antimicrobial agents. Consequently, using the Rubb_n scaffold as a starting point, oligonuclear ruthenium complexes can be synthesised which vary by almost two orders of magnitude in lipophilicity, but contain a higher charge and remain water-soluble. Furthermore, the higher nuclearity complexes would be expected to display different nucleic acid binding or condensation potential and exhibit different pharmacokinetic profiles.

3.6. References

1. H. W. Boucher, G. H. Talbot, J. S. Bradley, J. E. Jr Edwards, D. Gilbert, L. B. Rice, M. Scheld, B. Spellberg and J. Bartlett, IDSA Report on Development Pipeline 2009, **48**, 1.
2. F. P. Dwyer, E. C. Gyarfás, W. P. Rogers and J. H. Koch, *Nature*, 1952, **170**, 190.
3. F. P. Dwyer, I. K. Reid, A. Shulman, G. M. Laycock and S. Dixon, *Aust. J. Exp. Biol. Med. Sci.* 1969, **47**, 203.
4. F. Li, Y. Mulyana, M. Feterl, J. Warner, J. G. Collins and F. R. Keene, *Dalton Trans.*, 2011, **40**, 5032.
5. F. Li, M. Feterl, Y. Mulyana, J. M. Warner, J. G. Collins and F. R. Keene, *J. Antimicrob. Chemother.*, 2012, **67**, 2686.
6. M. Pandrala, F. Li, M. Feterl, Y. Mulyana, J. M. Warner, L. Wallace, F. R. Keene and J. G. Collins, *Dalton Trans.*, 2013, **42**, 4686.
7. F. Li, E. J. Harry, A. L. Bottomley, M. D. Edstein, G. W. Birrell, C. E. Woodward, F. R. Keene and J. G. Collins, *Chem. Sci.*, **2014**, 5, 685.
8. M. Pandrala, F. Li, L. Wallace, P. J. Steel, B. Moore II, J. Autschbach, J. G. Collins, and F. R. Keene, *Aust. J. Chem*, 2013, **66**, 1065.
9. M. J. Hannon, *Pure and Applied Chemistry*, 2007, **79**, 2243.
10. B. M. Zeglis, V. C. Pierre and J. K. Barton, *Chem. Commun.* 2007, 4565.

11. F. R. Keene, J. A. Smith and J. G. Collins, *Coord. Chem. Rev.*, 2009, **253**, 2021.
12. M. R. Gill and J. A. Thomas, *Chem. Soc. Rev.*, 2012, **41**, 3179.
13. P. Lincoln and B. Nórdén, *Chem. Commun.*, 1996, 2145.
14. J. Malina, M. J. Hannon and V. Brabec, *Chem. Eur. J.*, 2008, **14**, 10408.
15. M. R. Gill, J. Garcia-Lara, S. J. Foster, C. Smythe, G. Battaglia and J. A. Thomas, *Nat. Chem.*, 2009, **1**, 662.
16. U. McDonnell, J. M. C. A. Kerchoffs, R. P. M. Castineiras, M. R. Hicks, A. C. G. Hotze, M. J. Hannon and A. Rodger, *Dalton Trans.*, 2008, **5**, 667.
17. X.-L. Zhao, Z.-S. Li, Z.-B. Zheng, A.-G. Zhang and K.-Z. Wang, *Dalton Trans.*, 2013, **42**, 5764.
18. D. R. Boer, L. Wu, P. Lincoln and M. Coll, *Angew. Chem., Int. Ed.*, 2014, **53**, 1949.
19. A. K. Renfrew, *Metallomics*, 2014, **6**, 1324.
20. B. Therrien, G. Süß-Fink, P. Govindaswamy, A. K. Renfrew and P. J. Dyson, *Angew. Chem., Int. Ed.*, 2008, **47**, 3773.
21. G. Süß-Fink, *Dalton Trans.*, 2010, **39**, 1673.
22. X. Li, X.-J. Li, Z.-Y. Wu and C.-W. Yan, *New J. Chem.*, 2012, **36**, 2472.
23. W. Luo, X.-G. Meng, G.-Z. Chen and Z.-P. Ji, *Inorg. Chim. Acta*, 2009, **362**, 551.

24. Y. Mulyana, D. K. Weber, P. D. Buck, C. A. Motti, J. G. Collins and F. R. Keene, *Dalton Trans.*, 2011, **40**, 1510.
25. N. C. Fletcher, M. Nieuwenhuyzen and S. Rainey *J. Chem. Soc., Dalton Trans.*, 2001, 2641.
26. P. M. van Vliet, J. G. Haasnoot and J. Reedijk, *Inorg. Chem.*, 1994, **33**, 1934.
27. E. A. Seddon and K. R. Seddon, *The Chemistry of Ruthenium*, 1984, Elsevier, Amsterdam.
28. M. G. Sauaia, E. Tfouni, R. H. de Almeida Santos, M. T. do Prado Gambardella, M. P. F. M. Del Lama, L. F. Guimaraes and R. S. da Silva, *Inorg. Chem. Commun.*, 2003, **6**, 864.
29. A. Juris, V. Balzani, F. Barigelletti, S. Campagna, P. Belser and A. Von Zelewsky, *Coord. Chem. Rev.* 1988, **84**, 85.
30. Y. Kawanishi, N. Kitamura, and S. Tazuke, *Inorg. Chem.* 1989, **28**, 2968.
31. A. B. P. Lever, *Inorg. Chem.* 1990, **29**, 1271.
32. A. Macatangay, G. Y. Zheng, D. P. Rillema, D. C. Jackman and J. W. Merkert, *Inorg. Chem.* 1996, **35**, 6823.
33. A. Bouskila, B. Drahi, E. Amouyal, I. Sasaki and A. Gaudemer *J. Photochem. Photobiol. A*, 2004, **163**, 381.
34. M. Furue, N. Kuroda and S. Nozakura, *Chem. Lett.* 1986, 1209.
35. M. Cavazzini, S. Quici, C. Scalera, F. Puntoriero, G. La Ganga and S. Campagna, *Inorg. Chem.* 2009, **48**, 8578.

36. M. Staffilani, E. Höss, U. Giesen, E. Schneider, F. Hartl, H-P. Josel and L. De Cola, *Inorg. Chem.*, 2003, **42**, 7789.
37. F. Li, M. Feterl, J. M. Warner, F. R. Keene and J. G. Collins, *J. Antimicrob. Chemother.*, 2013, **68**, 2825.
38. F. Li, PhD thesis, “Inert dinuclear polypyridylruthenium(II) complexes as antimicrobial agents”, University of New South Wales, Australia, 2013.
39. J. L. Morgan, C. B. Spillane, J. A. Smith, P. D. Buck, J. G. Collins and F. R. Keene, *Dalton Trans.*, 2007, 4333.
40. X. Hua and A. V. Zelewsky, *Inorg. Chem.*, 1995, **34**, 5791.
41. T. Tagano, *Inorg. Chim. Acta*, 1992, **195**, 221.
42. I. P. Evans, A. Spencer and G. Wilkinson, *J. Chem. Soc. Dalton Trans.* 1973, 204.
43. Clinical and Laboratory Standards Institute. *Performance Standards for Antimicrobial Susceptibility Testing: Nineteenth Informational Supplement M100-S19*. CLSI, Wayne, PA, USA, 2009.
44. M. Motyl, K. Dorso, J. Barrett and R. Giacobbe, *Current Protocols in Pharmacology*. New York: John Wiley & Sons, 2005; 13A.3.1–22.
45. D. Bao, B. Millare, W. Xia, B. G. Steyer, A. A. Gerasimenko, A. Ferreira, A. Contreras and V. I. Vullev *J. Phys. Chem. A*, 2009, **113**, 1259.
46. P. C. Peters, M. D. Migocki, C. Thoni and E. J. Harry, *Mol. Microbiol.*, 2007, **64**, 487.

47. S. Moriya, R. A. Rashid, C. D. Andrade Rodrigues and E. J. Harry, *Mol. Microbiol.*, 2010, **76**, 634.

CHAPTER 4

***Clinical potential of polypyridylruthenium(II)
complexes***

4.1. Introduction

In the previous chapter it was established that the oligonuclear ruthenium complexes linked by the bb_n ligand have significant activity against the Gram positive bacteria *S. aureus* and MRSA and the Gram negative species *E. coli* and *P. aeruginosa*. However, in order to further assess their clinical potential it is important to examine their activities against a wider range of bacteria; and in particular, to clinical isolates that are of current concern. In recent years, the Infectious Diseases Society of America (IDSA) has identified a group of antibiotic-resistant bacteria that are capable of “escaping” the biocidal action of antibiotics and represent new paradigms in pathogenesis, transmission and resistance.^{1,2} These bacteria of particular concern - *Enterococcus faecium*, *Staphylococcus aureus*, *Klebsiella pneumoniae*, *Acinetobacter baumannii*, *Pseudomonas aeruginosa* and *Enterobacter* species - have been classified by the IDSA as the ESKAPE pathogens.^{1,2} According to the IDSA, the ESKAPE pathogens cause a wide range of hospital-acquired infections (nosocomial infections) and are increasingly resistant to many of the antimicrobial drugs.¹⁻⁴ This chapter reports the results of MIC assays of Rubb_n -tri and Rubb_n -tetra for $n = 12$ and 16 against seventeen clinical isolates, including eleven bacteria classified as ESKAPE pathogens.

While it is critical that any new antimicrobial agent be active against bacteria, it is also important that the drug has significantly lower toxicity towards humans and/or animals. The positively-charged ruthenium complexes could selectively target bacterial cells over eukaryotic cells due to the greater presence of negatively-charged components (phospholipids, such as phosphatidyl-glycerol, teichoic acids and lipopolysaccharides) in the bacterial membrane and cell wall.⁵ In contrast, the high content of zwitterionic phosphatidyl-choline in the outer membrane leaflet of healthy eukaryotic cells confers an overall neutral charge on these cells that results in a greatly reduced capacity for

electrostatic interactions. A previous pharmacokinetic study carried out within our group demonstrated that Rubb_{12} accumulated in the liver and kidney of mice administered with the ruthenium complex.⁶ Consequently, in order to examine the toxicity of the oligonuclear ruthenium complexes against eukaryotic cells the toxicity of Rubb_n -tri and Rubb_n -tetra for $n = 12$ and 16 was assayed against liver (Hep-G2) and kidney (BHK and HEK-293) cells.

In addition to high antimicrobial activity, – and low toxicity towards eukaryotic cells – it is also vital that a potential drug can maintain a suitable concentration in blood for an appropriate time period after administration.⁷⁻⁹ Consequently, a pharmacokinetic analysis – *viz.* serum concentration as a function of time and organ accumulation – of Rubb_{12} -tetra and Rubb_{16} was carried out and compared to the profiles obtained previously for Rubb_{12} .

4.2. Experimental

The antimicrobial and pharmacokinetic studies were carried out by the author under the guidance of A/Prof Jeffery Warner, School of Veterinary and Biomedical Sciences, James Cook University, Townsville, QLD 4811, Australia.

4.2.1. Selection of bacteria

Thirty-five clinical isolates were selected from the James Cook University culture collection, and their susceptibility to 17 clinically-used antimicrobial drugs was determined using standard disk diffusion assays. From these assays, and CLSI guidelines,¹² seventeen bacterial strains were selected that represented a balance between Gram positive and Gram negative, and within this classification isolates that were classed as susceptible or resistant to the current range of antimicrobial drugs. As the oligonuclear ruthenium complexes appear to be more effective against Gram positive bacteria,^{10,13} a greater number of Gram negative strains was selected. All five Gram positive strains were resistant to one or more antimicrobial drugs. For the twelve Gram negative species, six were classified as susceptible and six were resistant to the antimicrobial drugs (see Table 4.1).

Table 4.1. Based upon CLSI guidelines and the zone of inhibitions obtained for each bacteria against a range of antibiotic drugs, the Gram positive and Gram negative strains are classified as either susceptible or resistant to one or more antibiotics used in this study.

Antibiotics used in the disk diffusion assay.	Gram positive bacterial strains resistant to one or more antibiotics.	Gram negative bacterial strains that were resistant to one or more antibiotics.	Gram negative bacterial strains that were sensitive to all the antibiotics.
Penicillin, Oxacillin, Vancomycin, Tetracyclin, Erythromycin, Trimethoprim plus Sulphamethoxazole Linezolid, Ampicillin, Gentamicin, Ceftazidime, Tobramycin, Cefepime, Meropenem, Ciprofloxacin, Levofloxacin, Cefpodoxime, Amikacin.	<i>S. aureus</i> , MRSA strain #1, MRSA strain #2, <i>Enterococcus faecium</i> and VRE.	<i>Citrobacter freundii</i> , <i>Enterobacter cloacae</i> (H/F), <i>Enterobacter aerogenes</i> , <i>Klebsiella pneumonia</i> ESBL, <i>Proteus vulgaris</i> , and <i>Serratia marcescens</i> .	<i>E. Coli</i> (piglet isolate), <i>Enterobacter gergoviae</i> (D/E), <i>P. aeruginosa</i> (biofilm producer), <i>Acinetobacter venetianus</i> , <i>Providencia rettgeri</i> , and <i>Morganella morganii</i> .

4.2.2. Minimum inhibitory concentration (MIC) determination

The MIC analyses were conducted in duplicate by the broth micro-dilution method, as outlined in Chapter 3, Section 3.2.4.

4.2.3. Eukaryotic cell culture

The determination of the toxicities of the ruthenium complexes towards eukaryotic cell lines was carried out by Xin Li, a PhD student in our group. The BHK (baby hamster kidney), HEK-293 (human embryonic kidney) and Hep-G2 (human liver carcinoma) cell lines were used in this study. All cell lines were generously supplied by Australian Army Malaria Institute (Enoggera, QLD, Australia), and originated from the American Type Culture Collection (ATCC, Manassas, VA). All cell lines were cultured in 75 mL culture flasks in RPMI-1640 (Roswell Park Memorial Institute 1640) culture media supplemented with 10% fetal bovine serum, 4 mM L-glutamine and 1.5 g/L sodium bicarbonate at 37 °C in an atmosphere of 5% humidified CO₂. Cells used in the study were in the logarithmic growth phase. Cells were grown to 70% confluence, and then trypsinised with 0.25% trypsin-0.02% EDTA.

4.2.4. Cytotoxicity

The cytotoxicities of the ruthenium complexes were determined using the Alamar Blue cytotoxicity assays as previously described.¹⁴ All data were from at least three independent experiments and the IC₅₀ determined using GraphPad Prism 6.0 (GraphPad Software, San Diego, USA).

4.2.5. Animals

Mixed-sex in-bred BALB/c mice aged 9-12 weeks were obtained from the small animal house located at the School of Veterinary and Biomedical Sciences, James Cook University, Townsville, Australia. Food and water were available *ad libitum* throughout the studies. All the experiments were undertaken after obtaining ethics approval from the Ethics Committee at James Cook University.

4.2.6. Pharmacokinetic studies

Rubb₁₆ and Rubb₁₂-tetra were dissolved in sterile PBS solution at the appropriate concentrations to obtain the desired doses. Drug solutions, approximately 200 µL, were administered to the mice according to their body weight to achieve doses of 16 mg/kg. The intramuscular (i.m) route of administration was used in all the cases. Drug solutions were administered as boluses to the mice intramuscularly in both thighs through a 26.5-gauge needle.

4.2.7. Sampling

In all the studies, three mice were sampled at each time point. Blood was sampled at 0.5, 1, 3, 6, 12 and 24 hours after dosing of the ruthenium complexes through the intramuscular (i.m.) route. For the Rubb₁₆ complex, brain, heart, lung, liver, kidney, spleen and gastrocnemius were collected from mice 6 hours after a single dose of 16 mg/kg. For the Rubb₁₂-tetra complex, liver, kidney and gastrocnemius were collected after 0.5, 1, 3, 6, 12 and 24 hours after a single dose of 16 mg/kg.

Blood was collected from the mice by cardiac puncture immediately after they were sacrificed and then transferred to 1.7 mL eppendorf micro-centrifuge tubes. The

samples were kept in a fridge at 4 °C until the blood was completely clotted and then the serum was separated by centrifugation at 3,000 g for 5 min. Tissues were washed with sterile PBS and weighed. Serum and tissue samples were stored at -20 °C until analysis.

4.2.8. Sample preparation and digestion

Blood serum samples were thawed and diluted 20-fold in Milli-Q water for ICP-MS analysis. Organ samples were digested using a microwave oven (Milestone Starter D). Fresh samples were placed in a digestion vessel, SupraPure double-distilled HNO₃ (3 mL), AR Grade H₂O₂ (1 mL) and Milli-Q water (4 mL) added and the mixture was left in the fume hood for 2 h to digest the organ. The vessel was then loaded into the microwave oven, and heated to 180 °C for 10 min. After cooling, the digested samples were quantitatively transferred into a 100 mL volumetric flask and diluted to the mark using Milli-Q water. These solutions were diluted 2-fold before ICP-MS analysis.

4.2.9. Concentration determination of ruthenium metal by ICP-MS

Sample analysis was carried out using a Bruker 820-MS Inductively Coupled Plasma Mass Spectrometer (ICP-MS). A ruthenium standard (1000 mg/L ruthenium in 2% HCl) was used for calibration. The concentrations of ⁹⁹Ru and ¹⁰¹Ru were measured and the ¹⁰¹Ru isotope was used for quantification. A 20 ppb solution of the ruthenium standard was used to calibrate the instrument, indium was used as an internal standard to correct for the instrument drift and matrix effects. A 5 ppb independent ruthenium standard was used as the quality control sample.

4.3. Results

4.3.1. Antimicrobial activity

The minimum inhibitory concentrations (MIC) for the various ruthenium complexes against the selected clinical isolates have been determined and the results are summarised in Table 4.2, Table 4.3 and Table 4.4. The results demonstrate that the ruthenium complexes have significant antimicrobial activity against most of the bacteria. All of the Gram positive bacteria are highly susceptible to the ruthenium complexes. As expected, the ruthenium complexes displayed lower and more variable activities against the Gram negative bacteria. Based upon CLSI guidelines for each of the twelve Gram negative species and the most active of the ruthenium complexes against each bacterium,¹² four strains would be classified as susceptible, five strains as intermediate and three strains as resistant to the ruthenium complexes (see Table 4.5).

In general, the Rubb_n -tri and Rubb_n -tetra complexes showed better antimicrobial activity than the Rubb_n and chlorido-containing dinuclear ruthenium(II) complexes. Interestingly, for the Rubb_n -tri and Rubb_n -tetra complexes, the complexes linked by the bb_{12} ligand showed better activities than the complexes linked by the bb_{16} ligand. For the dinuclear Rubb_n complexes, Rubb_{16} was found to be of equal or better activity than Rubb_{12} against all bacteria examined in this study.

Table 4.2. MIC values (μM) for the ruthenium complexes against five Gram positive bacterial strains resistant to one or more antibiotics.

Bacterial strain	Rubb ₁₂	Rubb ₁₆	Rubb ₁₂ -tri	Rubb ₁₆ -tri	Rubb ₁₂ -tetra	Rubb ₁₆ -tetra	^a Cl-Rubb ₁₄	^b Cl ₂ -Rubb ₁₂
<i>S. aureus</i>	1.3	0.6	0.4	0.8	0.6	0.6	0.7	1.4
MRSA #1	1.3	0.6	0.8	1.6	0.6	0.6	1.5	1.4
MRSA #2	0.6	0.6	0.4	0.8	0.6	1.2	1.5	0.7
<i>Enterococcus faecium</i>	1.3	0.3	0.8	0.8	0.6	1.2	3.0	1.4
VRE	0.6	0.6	0.8	0.8	0.6	1.2	1.5	0.7

^a Cl-Rubb₁₄ = [$\{\text{Ru}(\text{tpy})\text{Cl}\}_2\{\mu\text{-bb}_{14}\}\text{Cl}\}]^{2+}$.

^b Cl₂-Rubb₁₂ = [$\{\text{Ru}(\text{phen})_2\}(\mu\text{-bb}_{12})\{\text{Ru}(\text{phen})\text{Cl}_2\}\text{Cl}_2\}]^{2+}$.

Table 4.3. MIC values (μM) for the ruthenium complexes against Gram negative bacterial strains that were resistant to one or more antibiotics.

Bacterial strain	Rubb ₁₂	Rubb ₁₆	Rubb ₁₂ -tri	Rubb ₁₆ -tri	Rubb ₁₂ -tetra	Rubb ₁₆ -tetra	^a Cl-Rubb ₁₄	^b Cl ₂ -Rubb ₁₂
<i>Citrobacter freundii</i>	2.5	2.4	1.6	3.1	1.2	1.2	6.0	2.9
<i>Enterobacter cloacae</i> (H/F)	5.0	4.9	3.3	3.1-6.2	2.4	2.3-4.6	23.8	5.8
<i>Enterobacter aerogenes</i>	5.0	4.9	3.3	6.2	2.4	4.6	23.8	11.5
<i>Klebsiella pneumoniae</i> ESBL	10.0	4.9	13.1	6.2	4.8	4.6	23.8	23.0
<i>Proteus vulgaris</i>	10.0	4.9	6.6	6.2	2.4	4.6	11.9	11.5
<i>Serratia marcescens</i>	40.3	19.5	26.2	12.5	9.6	9.2	47.6	46.0

^a Cl-Rubb₁₄ = [$\{\text{Ru}(\text{tpy})\text{Cl}\}_2\{\mu\text{-bb}_{14}\}$]²⁺.

^b Cl₂-Rubb₁₂ = [$\{\text{Ru}(\text{phen})_2\}(\mu\text{-bb}_{12})\{\text{Ru}(\text{phen})\text{Cl}_2\}$]²⁺.

Table 4.4. MIC values (μM) for the ruthenium complexes against Gram negative bacterial strains that were sensitive to all the antibiotics.

Bacterial strain	Rubb ₁₂	Rubb ₁₆	Rubb ₁₂ -tri	Rubb ₁₆ -tri	Rubb ₁₂ -tetra	Rubb ₁₆ -tetra	^a Cl-Rubb ₁₄	^b Cl ₂ -Rubb ₁₂
<i>E. Coli</i> (piglet isolate)	2.5	2.4	1.6	3.1	0.6	2.3	3.0	1.4
<i>Enterobacter gergoviae</i> (D/E)	1.3	1.2	0.8	1.6	0.6	1.2	6.0	2.9
<i>P. aeruginosa</i> (biofilm producer)	20.1	9.8	13.1	12.5	4.8	9.2	11.9	5.8
<i>Acinetobacter venetianus</i>	2.5	2.4	1.6	1.6	0.6	1.2	6.0	2.9
<i>Providencia rettgeri</i>	40.3	39.0	26.2	25.0	19.2	37.0	95.1	91.9
<i>Morganella morganii</i>	40.3	39.0	26.2	25.0	19.2	18.5	>95.1	46.0

^a Cl-Rubb₁₄ = [$\{\text{Ru}(\text{tpy})\text{Cl}\}_2\{\mu\text{-bb}_{14}\}$]²⁺.

^b Cl₂-Rubb₁₂ = [$\{\text{Ru}(\text{phen})_2\}(\mu\text{-bb}_{12})\{\text{Ru}(\text{phen})\text{Cl}_2\}$]²⁺.

Table 4.5. Based upon CLSI guidelines and the MIC values of the ruthenium complexes, the Gram negative strains used in the study can be classified as susceptible, intermediate or resistant to the ruthenium complexes.

Susceptible	Intermediate	Resistant
<i>E.Coli</i> (piglet isolate)	<i>Proteus vulgaris</i>	<i>Providencia rettgeri</i>
<i>Citrobacter freundii</i>	<i>Enterobacter aerogenes</i>	<i>Serratia marcescens</i>
<i>Acinetobacter venetianus</i>	<i>Klebsiella pneumoniae</i> ESBL	<i>Morganella morganii</i>
<i>Enterobacter gergoviae</i> (D/E)	<i>P.aeruginosa</i> (biofilm producer)	----
<i>Enterobacter cloacae</i> (H/F)	----	----

4.3.2. Toxicity against eukaryotic cells

The cytotoxicities of the tri- and tetra-nuclear complexes against liver and kidney cell lines (BHK, HEK-293 and Hep-G2) were determined and compared to the values previously obtained for the Rubb_n dinuclear complexes.¹⁵ The results are summarised in Table 4.6. All ruthenium complexes were toxic against the three cell lines, and particularly the cancer cell line Hep-G2. The complexes containing the bb_{12} -linking ligand were less toxic than those that contained the bb_{16} -linking ligand, with Rubb_{12} generally being the least toxic and Rubb_{16} -tetra the most toxic of the compounds.

Table 4.6. The IC₅₀ values of the ruthenium complexes against the BHK, HEK-293 and Hep-G2 cell lines after a 72 hour incubation. IC₅₀ is defined as the concentration (μM) of the complex required to inhibit cell growth by 50%. Errors were calculated from the standard deviation (SD) of the data set.

Complexes	BHK	HEK-293	Hep-G2
Rubb ₁₂	54.3 ± 3.2	15.1 ± 2.8	5.2 ± 2.0
Rubb ₁₂ -tri	21.2 ± 1.7	8.8 ± 0.7	7.4 ± 3.9
Rubb ₁₆ -tri	9.7 ± 1.2	7.8 ± 3.8	3.1 ± 0.5
Rubb ₁₂ -tetra	13.1 ± 1.9	6.4 ± 1.4	5.2 ± 1.3
Rubb ₁₆ -tetra	6.4 ± 0.2	5.1 ± 0.8	3.5 ± 0.5
Rubb ₁₂ -Cl ₂	21.4 ± 0.9	10.4 ± 0.5	15.2 ± 0.5
Rubb ₁₆ -Cl ₂	18.4 ± 2.2	13.9 ± 1.2	9.2 ± 0.5
Cisplatin	170.3 ± 30.5	115.0 ± 20.8	13.5 ± 0.5

4.3.3. Time-course cytotoxicity assays

As the incubation time (16-18 hour) used to determine the antimicrobial activities (MIC values) of the ruthenium complexes was much shorter than the incubation time (72 hour) used in the cytotoxicity assays, the IC₅₀ values for Rubb₁₂-tri and Rubb₁₂-tetra were determined as a function of time against the eukaryotic cell lines. Rubb₁₂-tri and Rubb₁₂-tetra were selected for extended studies as they are more active against bacteria and less toxic towards eukaryotic cells than the Rubb₁₆-tri and Rubb₁₆-tetra complexes.

The cytotoxicities of Rubb₁₂-tri and Rubb₁₂-tetra were determined at 4, 8, 24, 48 and 72 hours and the results are summarised in Table 4.7. As would be expected, the IC₅₀ values increased significantly with decreasing incubation time.

Table 4.7. The IC₅₀ values (μM) of Rubb₁₂-tri and Rubb₁₂-tetra against the BHK, HEK-293 and Hep-G2 cell lines as a function of time. Errors were calculated from the standard deviation (SD) of the data set.

Complex	Cell line	Time (hours)				
		4 h	8 h	24 h	48 h	72 h
Rubb ₁₂	BHK	190.9±36.5	103.8±8.5	70.5±26.4	57.5±7.1	54.3±3.2
	HEK-293	90.8±17.9	90.48±34.3	50.9±19.9	24.9±1.1	15.1±2.8
	Hep-G2	103.2±3.8	109.7±29.3	61.7±5.5	15.8±10.4	5.2±2.0
Rubb ₁₂ -tri	BHK	116.2±37.8	119.7±14.9	51.2±1.9	24.0±1.3	25.4±0.5
	HEK-293	90.5±13.4	65.5±5.6	36.1±6.7	10.4±0.8	8.5±1.5
	Hep-G2	72.0±10.10	61.7±6.5	45.3±3.7	8.9±1.7	6.5±2.3
Rubb ₁₂ -tetra	BHK	50.2±0.2	48.1±1.9	27.7±0.6	16.9±0.6	10.6±0.3
	HEK-293	43.6±3.6	36.4±3.9	21.7±1.1	10.3±1.7	7.9±1.8
	Hep-G2	47.6±0.4	47.4±4.7	33.8±1.1	11.8±3.8	6.4±1.5

4.3.4. Pharmacokinetic studies

In a previous study within our group it was established that intramuscular injection of Rubb₁₂, compared to subcutaneous or intravenous injections, provided the highest serum concentrations over the first three hours after administration of the ruthenium complex.⁶ Consequently, the intramuscular injection route was used for the administration of the ruthenium complexes in the studies.

The maximum tolerated dose (MTD) of Rubb₁₆ and Rubb₁₂-tetra when administered by intramuscular injection was determined to be ≥ 32 mg/kg and > 16 mg/kg respectively. A single dose of 16 mg/kg of Rubb₁₆ or Rubb₁₂-tetra was administered and the serum concentration of the ruthenium complexes as a function of time was determined by ICP-MS for up to 24 hours after dosing. Although it is acknowledged that it is possible that ruthenium complex could be degraded in mice after administration, the accumulations are based upon the ruthenium complex remaining intact. The results are shown in Figure 4.1. The highest concentration of Rubb₁₆ and Rubb₁₂-tetra detected in the serum was at the first time point monitored after administration (0.5 hour), with the concentration then declining for the next 5 hours before remaining relatively constant to the final time point at 24 hours. Although there were only relatively small differences, the serum concentration of Rubb₁₂-tetra, in mg/L, was higher at all time points monitored than for Rubb₁₆. However, in terms of μM , the serum concentrations of Rubb₁₆ and Rubb₁₂-tetra were similar (within experimental error) at all time points after administration.

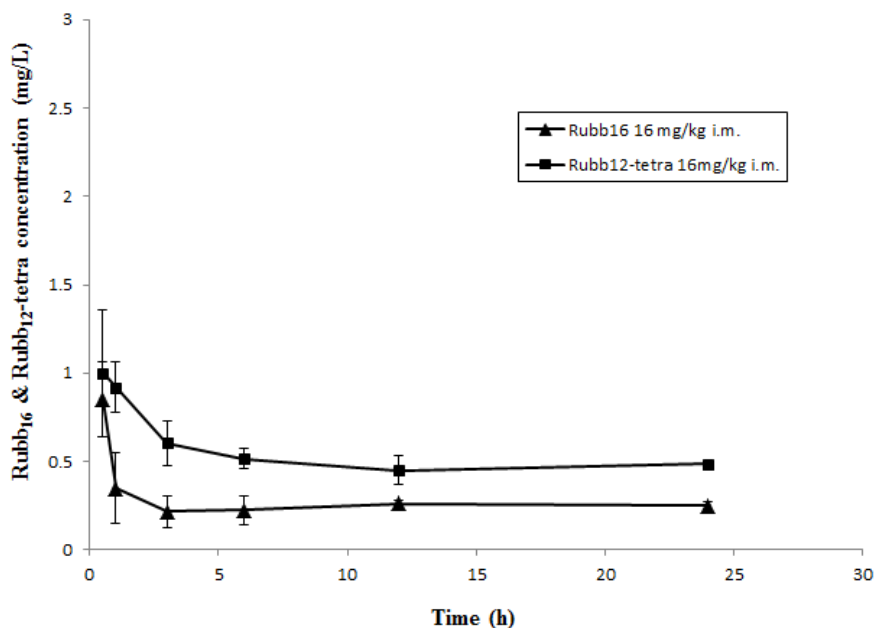


Figure 4.1. The serum level of Rubb₁₆ and Rubb₁₂-tetra after the administration of a single dose of 16 mg/kg by the i.m. route.

4.3.5. *Tissue distribution and accumulation of Rubb₁₆ and Rubb₁₂-tetra as a function of time.*

The distribution of Rubb₁₆ in a range of organs six hours after the ruthenium complex was administered was determined, and the results are shown in Figure 4.2 and Figure 4.3. As was previously observed for Rubb₁₂, the primary site of accumulation is the liver, with the kidney, spleen, heart and lungs also exhibiting measurable quantities of ruthenium. Accumulation of Rubb₁₆ in muscle tissue was very high. As Rubb₁₆ was found to accumulate to the greatest degree in the liver, kidneys and at the site of the injection (i.e. gastrocnemius), the accumulation of Rubb₁₂-tetra was only determined for these organs, but as a function of time after administration (see Figure 4.3 and Figure 4.4). Although the accumulation of Rubb₁₂-tetra in liver at six hours in mg/kg after administration of the ruthenium complex was greater than was observed for Rubb₁₆, the concentrations of Rubb₁₆ and Rubb₁₂-tetra were similar (within experimental error).

Both Rubb₁₆ and Rubb₁₂-tetra accumulated to a similar degree in the liver and kidney of the mice. Accumulation of both the complexes was very high at the site of the injection.

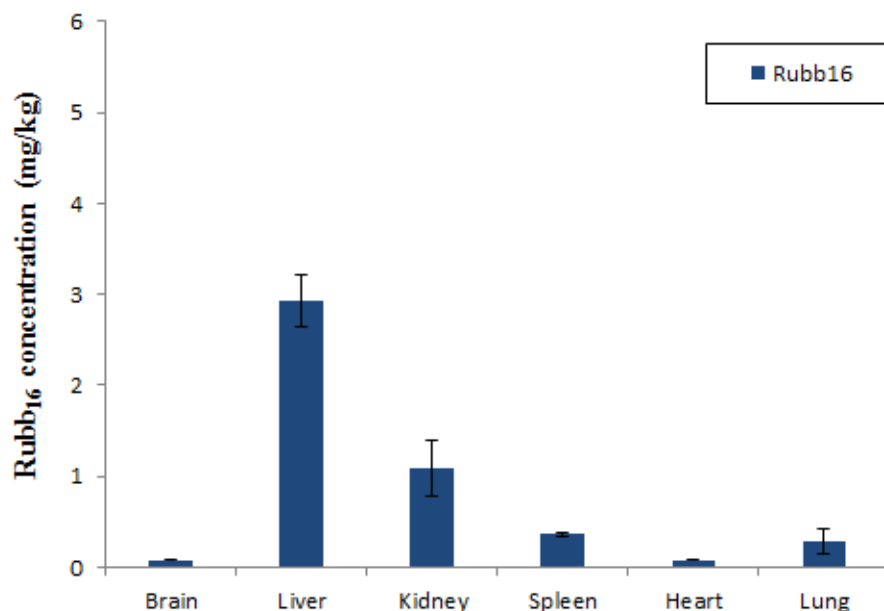


Figure 4.2. Tissue accumulation of Rubb₁₆ in various organs at 6 hours after a single dose of 16 mg/kg by i.m. injection in mice.

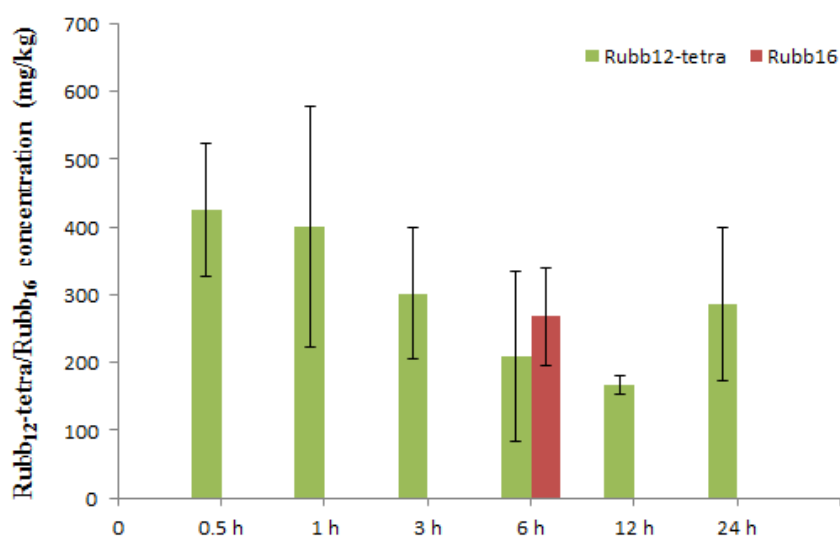


Figure 4.3. Accumulation of Rubb₁₂-tetra (as function of time) and Rubb₁₆ (after 6 hours) in gastrocnemius after a single dose of 16 mg/kg by i.m. injection of Rubb₁₂-tetra/Rubb₁₆ in mice.

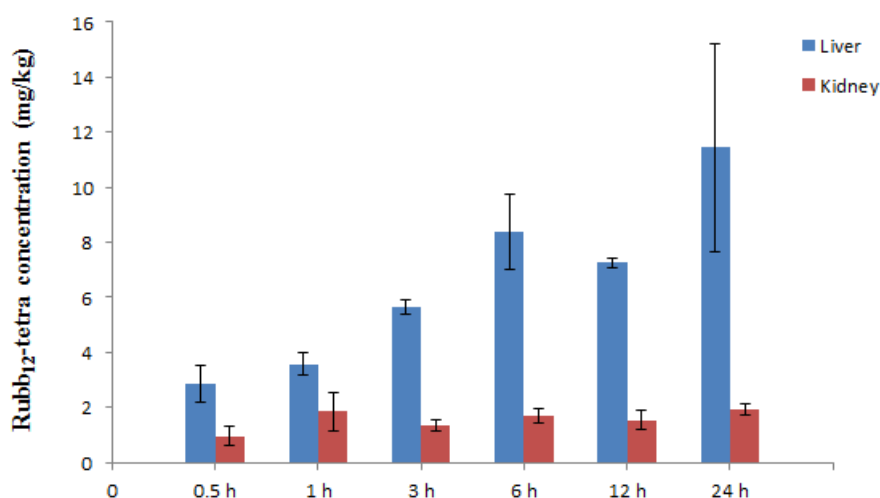


Figure 4.4. Tissue accumulation of Rubb₁₂-tetra in liver and kidney as function of time after a single dose of 16 mg/kg by i.m. injection of Rubb₁₂-tetra in mice.

4.4. Discussion

The results presented in chapter 3 demonstrated that the inert tri- and tetra-nuclear ruthenium(II) complexes linked by the bb_n ligand (Rubb_n-tri and Rubb_n-tetra) exhibit excellent antimicrobial properties in terms of their MIC and MBC values. The results presented in this chapter demonstrate that Rubb₁₂-tri and Rubb₁₂-tetra in particular are active against a wider variety of Gram positive bacteria than the two bacterial strains used in the screening assays (*S. aureus* and MRSA), as discussed in chapter 3, but show variable activity towards Gram negative species.

Of the Gram negative isolates, three are classified as being resistant to all the ruthenium complexes used in this study - *Providencia rettgeri*, *Serratia marcescens* and *Morganella morganii*. By comparison, the *Providencia rettgeri* and *Morganella morganii* isolates were susceptible to all the antimicrobial drugs used in the disk diffusion assays, and *Serratia marcescens* was susceptible to all but one of the antimicrobial drugs. While the data does not allow definitive conclusions to be drawn

on the reason for the resistance of these three Gram negative species to the ruthenium complexes, it is noted that they all belong to the *Enterobacteriaceae* family of bacteria. However, it is noted that *E. coli* is also a member of the *Enterobacteriaceae* family. The outer membrane of Gram negative bacteria provides an additional barrier to the uptake of drugs, compared to Gram positive species. Furthermore, Gram negative bacteria generally contain lipopolysaccharides (LPS) in the outer leaflet of the outer membrane, which further hinders access of an antimicrobial agent to the cytoplasm of bacteria. In general, antimicrobial agents can cross the outer membrane using either a lipid-mediated pathway or diffusion porins for more hydrophilic drugs.¹⁶ General diffusion porins are proteins that create hydrophilic, size exclusion, pores through the outer membrane.¹⁶ It is possible that the differential activities of the ruthenium complexes to the Gram negative bacteria could be due the differences in the LPS and specific porins between the various strains.

The results presented in this chapter also demonstrated that the Rubb_n-tri and Rubb_n-tetra complexes are toxic to liver and kidney cells. However, even when comparing the 72 hour cytotoxicity data with the 16-18 hour antimicrobial MIC values, it is clear that the ruthenium complexes are more toxic to bacteria than the eukaryotic cells examined in this study. For the BHK and HEK-293 cell lines, the dinuclear Rubb₁₂ complex was less toxic than the tri- and tetra-nuclear species. Against the Hep-G2 liver cell line, all ruthenium complexes showed similar toxicity. In order to more appropriately compare the toxicity of the ruthenium complexes between bacterial and eukaryotic cells, the IC₅₀ values were determined as a function of time. Interestingly, after a 24 hour incubation the toxicities of Rubb₁₂, Rubb₁₂-tri and Rubb₁₂-tetra towards the Hep-G2 cells were similar to those against the BHK and HEK-293 cell lines. However, Rubb₁₂ was still slightly less toxic than the tri- and tetra-nuclear analogues

against the three cell lines. Table 4.8 compares the toxicity of Rubb₁₂, Rubb₁₂-tri and Rubb₁₂-tetra against the three eukaryotic cell lines for a 24 hour incubation to the average MIC of the five Gram positive strains examined in this chapter and the average of the five Gram negative strains classified as susceptible to the ruthenium complexes in this chapter. The di-, tri- and tetra-nuclear inert complexes are approximately 50-times more toxic to Gram positive bacteria than liver and kidney cells. Consistent with the MIC results presented in chapter 3, the activity of the oligonuclear ruthenium complexes against Gram negative species was lower, with Rubb₁₂, Rubb₁₂-tri and Rubb₁₂-tetra only being approximately 25-times more toxic against strains classified as susceptible than against the eukaryotic cells.

Table 4.8. Comparison of the selective toxicity (SI) of the ruthenium complexes to the BHK, HEK-293 and Hep-G2 cell lines to the antimicrobial activity against the average MIC value of the five Gram positive {G (+)} strains examined in this chapter and the average of the five Gram negative {G (-)} strains classified as susceptible to the ruthenium complexes in this chapter. SI is defined as the ratio of the IC₅₀ (at 24 hours) to the MIC.

	BHK		HEK-293		Hep-G2	
Complex	G (+)	G (-)	G (+)	G (-)	G (+)	G (-)
$\Delta\Delta$ -Rubb ₁₂	69	26	50	18	60	22
Rubb ₁₂ -tri	80	29	56	20	71	25
Rubb ₁₂ -tetra	46	26	36	20	56	31

Toxicity of the metal complexes could be related to their cellular uptake. The lower toxicity of the dinuclear complex is possibly due to its lower lipophilicity, with the log P values for Rubb₁₂, Rubb₁₂-tri and Rubb₁₂-tetra being -2.9, -1.0 and -1.6 respectively.¹⁰ Interestingly, even though the trinuclear species is more lipophilic than the tetranuclear complex, it was generally less toxic to the eukaryotic cells. This demonstrates the importance of the cationic charge of the ruthenium complex in the mechanism of the observed toxicity towards eukaryotic cells.

In the initial studies on the antimicrobial potential of polypyridyl ruthenium complexes, Dwyer and co-workers found that the minimum lethal dose of mononuclear complexes, Δ -[Ru(phen)₃](ClO₄)₂ and Δ -[Ru(bpy)₃]I₂, when administered by intraperitoneal injection were > 18.4 mg/kg and 15.7-16.8 mg/kg respectively.¹⁷ Although a different administration route was used in this study, the results suggest that Rubb₁₆ and Rubb₁₂-tetra are slightly less toxic than the simple mononuclear complexes. However, the results from this study indicate Rubb₁₆ and Rubb₁₂-tetra are slightly more toxic than was previously determined for Rubb₁₂ (MTD \geq 64 mg/kg by intramuscular administration).⁶

Pharmacokinetic experiments indicated that the highest concentration of Rubb₁₆ and Rubb₁₂-tetra detected in the serum was at the first time point monitored after administration (0.5 hour), with the concentration then declining for the next 2.5 hours before remaining relatively constant to the final time point at 24 hours. Unfortunately, the highest concentration obtained for either Rubb₁₆ or Rubb₁₂-tetra was only \leq 1 mg/L. As the MIC values for Rubb₁₆ and Rubb₁₂-tetra against the most susceptible of the bacterial strains are 1-2 mg/L it can be concluded that these ruthenium complexes would be unlikely to show any antibacterial efficacy *in vivo* when administered at 16 mg/kg. As high levels of accumulation were observed at the site of injection, it could be

concluded that the low serum concentration of Rubb₁₆ and Rubb₁₂-tetra could be due to their slow release from the muscle to the blood. However, further studies would be required to confirm this proposal. Figure 4.5 (reproduced from the PhD thesis of F. Li, a former PhD student in our group) shows the serum concentration of Rubb₁₂ as a function of time after administration of the ruthenium complex by intramuscular injection. Although the experiments were not conducted at a dose of 16 mg/kg it is clear that the serum concentrations of Rubb₁₂ are much higher than was achieved with either Rubb₁₆ or Rubb₁₂-tetra. This indicates that the pharmacokinetics is significantly affected by the lipophilicity of the ruthenium complex. After administration, the ruthenium complex partitions from the muscle into the blood, then from the blood the ruthenium complex is distributed to the tissues, eventually reaching a steady state concentration in the blood for a period of time up to at least 24 hours. Comparing the two dinuclear complexes, it is observed that Rubb₁₆ reaches a steady-state concentration in serum more quickly than does Rubb₁₂. These results highlight a drug design point that increasing the lipophilicity of a potential anticancer or antimicrobial agent may increase the *in vitro* activity of a compound, as measured by IC₅₀ or MIC, but could decrease the *in vivo* efficacy.

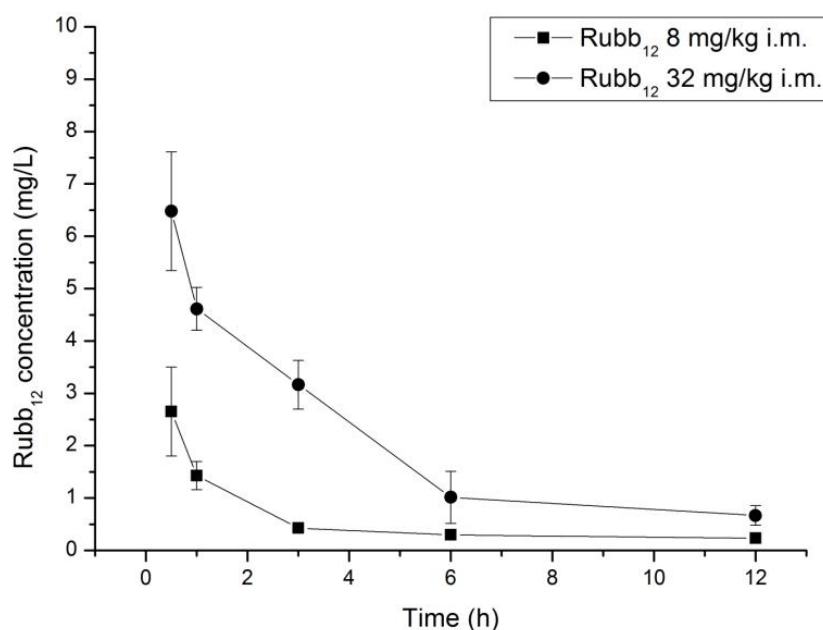


Figure 4.5. The serum level of Rubb₁₂ after the administration of a single dose of 8 mg/kg or 32 mg/kg by the i.m. route. (Figure reproduced from the PhD thesis of F. Li, UNSW, 2013).

4.5. Conclusions

The antimicrobial activities of the tri- and tetra-nuclear ruthenium complexes against a wider range of clinically relevant bacteria and their toxicity to liver and kidney cells were examined in this study. In addition the serum level concentration and tissue accumulation of Rubb₁₆ and Rubb₁₂-tetra in mice were also examined. The results of this study demonstrate that, Rubb_n complexes are highly active against Gram positive bacteria and against Gram negative bacteria they were less active. Compared to the tri- and tetra-nuclear complexes, the dinuclear Rubb₁₂ complex was less toxic to liver and kidney cells. The *in vivo* experiments demonstrate that the serum level concentrations of both Rubb₁₆ and Rubb₁₂-tetra were less than the MIC values against Gram positive and Gram negative bacteria, and both the complexes accumulated mainly in liver and kidney after dosing.

4.6. References

1. L. B. Rice, *J. Infect. Dis.*, 2008, **197**, 1079.
2. H. W. Boucher, G. H. Talbot, J. S. Bradley, J. E. Edwards, D. Gilbert, L. B. Rice, M. Scheld, B. Spelberg and J. Bartlett, *Clin. Infect. Dis.*, 2009, **48**, 1.
3. J. N. Pendleton, S. P. Gorman and B. F. Gilmore, *Expert. Rev. Anti Infect. Ther.*, 2013, **11**, 297.
4. M. Hassani, *Clin. Res. Infect. Dis.*, 2014, **1**, 1005.
5. A. J. Mason, A. Marquette and B. Bechinger, *Biophys. J.* 2007, **93**, 4289.
6. F. Li, *PhD thesis*, University of New South Wales, Australia, 2013.
7. M. Frik, A. Martínez, B. T. Elie, O. Gonzalo, D. R. de Mingo, M. Sanaú, R. S. Delgado, T. Sadhukha, S. Prabha, J. W. Ramos, I. Marzo and M. Contel, *J. Med. Chem.*, 2014, **57**, 9995.
8. A. Weiss, R. H. Berndsen, M. Dubois, C. Müller, R. Schibli, A. W. Griffioen, P. J. Dyson and P. N. Sliwinska, *Chem. Sci.*, 2014, **5**, 4742.
9. D. M. Fisher, R. R. Fenton and J. R. Aldrich-Wright, *Chem. Commun.*, 2008, 5613.
10. A. K. Gorle, M. Feterl, J. M. Warner, L. Wallace, F. R. Keene and J. G. Collins, *Dalton Trans.*, 2014, **43**, 16713.
11. Y. Mulyana, D. K. Weber, D. P. Buck, C. A. Motti, J. G. Collins and F. R. Keene, *Dalton Trans.*, 2011, **40**, 1510.
12. Twenty-First Informational Supplement, CLSI, Wayne, PA, USA, 2009, **31**, M100-S21.
13. F. Li, Y. Mulyana, M. Feterl, J. Warner, J. G. Collins and F. R. Keene, *Dalton Trans.*, 2011, **40**, 5032.

14. J. O'Brien, I. Wilson, T. Orton and F. Pognan, *Eur. J. Biochem.*, 2000, **267**, 5421.
15. X. Li, A. K. Gorle, T. D. Ainsworth, K. Heimann, C. E. Woodward, J. G. Collins and F. R. Keene, *Dalton Trans.*, 2015, **44**, 3594.
16. A.H. Delcour, *Biochim. Biophys. Acta.*, 2009, **1794**, 808.
17. F. P. Dwyer, E. C. Gyarfas, W. P. Rogers and J. H. Koch, *Nature*, 1952, **170**, 190.

CHAPTER 5

***Mononuclear polypyridylruthenium(II)
complexes with high membrane permeability in
Gram negative bacteria - in particular
Pseudomonas aeruginosa.***

5.1. Introduction

As discussed in chapters 1 & 3, infectious diseases remain a leading cause of death worldwide and a developing resistance to antimicrobial drugs is a significant threat to humans.¹ While there has been modest success in developing new drugs against Gram positive bacteria, the therapeutic options for Gram negative species are extremely limited.^{2,3} Furthermore, there are very few drugs for Gram negative species in the development pipeline. Of the Gram negative species, the Infectious Diseases Society of America noted that infections caused by *Pseudomonas aeruginosa* were emerging as a particular worldwide concern.¹ Indeed, *P. aeruginosa* is responsible for 10-15% of nosocomial (hospital-acquired) infections worldwide.⁴ *P. aeruginosa* is naturally resistant to antimicrobials due to the low permeability of its outer membrane.^{5,6} The outer membrane limits the movement of small molecules into the cell for all Gram negative bacteria: however, it is particularly significant for *P. aeruginosa*, where – for example – the outer membrane permeability is 10-to 100-fold lower than that of *Escherichia coli*.⁷

A variety of ruthenium complexes have shown good activity against Gram positive bacteria, but generally poor activity against Gram negative species.⁸⁻¹⁰ In an attempt to extend and enhance the activity of polypyridylruthenium(II) complexes, particularly against current drug-resistant bacterial strains, our group has examined the antimicrobial properties of various mono- and oligo-nuclear polypyridylruthenium(II) complexes (see Figure 5.1).^{11,12} These complexes showed excellent activity against drug-sensitive Gram positive bacterial strains such as *S. aureus*, and maintained the activity against drug-resistant strains such as MRSA.^{11,12} However, although the ruthenium complexes showed good activity against the Gram negative strain *E. coli*,

they exhibited relatively poor activity against *P. aeruginosa*.^{11,12} It was also shown that the mononuclear complex $[\text{Ru}(\text{Me}_4\text{phen})_3]^{2+}$ (Me_4phen = 3,4,7,8-tetramethyl-1,10-phenanthroline) and the dinuclear complexes which showed excellent activity towards Gram positive bacteria (Rubb_{12} and Rubb_{16}) readily accumulated in the bacterial cell.¹³ However, these mono- and di-nuclear complexes do not readily accumulate in *P. aeruginosa* and show low activity towards this species. To improve the cellular uptake and thereby increase the activities of ruthenium complexes against *P. aeruginosa* – while maintaining activity against Gram positive strains – the antimicrobial properties of inert tri- and tetra-nuclear polypyridyl ruthenium(II) complexes ($\text{Rubb}_n\text{-tri}$ and $\text{Rubb}_n\text{-tetra}$) were studied in chapter 3. The tri- and tetra-nuclear complexes were more active than the dinuclear complexes against the Gram positive strains. However, while the cellular uptake of the tri- and tetra-nuclear complexes into *P. aeruginosa* was vastly improved compared to the dinuclear complexes, no improvement in activity was observed. Taken together; the results suggest that *P. aeruginosa* is more sensitive to the mononuclear complexes than to complexes with higher nuclearity. However, simply increasing the lipophilicity of a mononuclear complex does not necessarily improve the cellular uptake. Our group has previously demonstrated that the uptake of $[\text{Ru}(\text{phen})_2(\text{bb}_7)]^{2+}$ ($\log P = -0.7$; phen = 1,10-phenanthroline) in *P. aeruginosa* is not significantly improved compared to $[\text{Ru}(\text{Me}_4\text{phen})_3]^{2+}$, and is actually lower than the less lipophilic dinuclear complex Rubb_{16} ($\log P = -1.9$).¹³

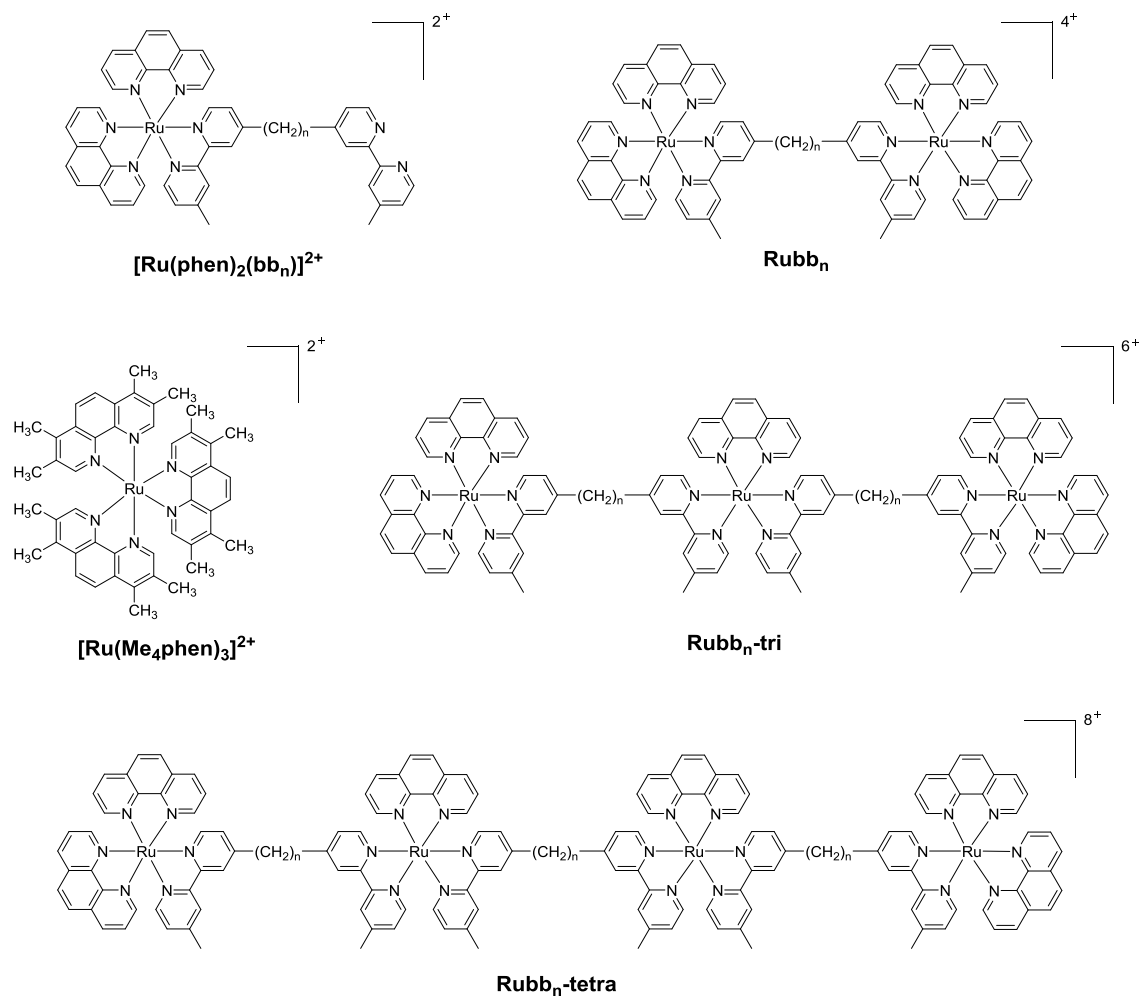


Figure 5.1. Structure of $[\text{Ru}(\text{phen})_2(\text{bb}_n)]^{2+}$, Rubb_n , $[\text{Ru}(\text{Me}_4\text{phen})_3]^{2+}$, $\text{Rubb}_n\text{-tri}$ and $\text{Rubb}_n\text{-tetra}$.

The aim of the research presented in this chapter was to increase the cellular accumulation of mononuclear ruthenium complexes in *P. aeruginosa*, by utilising the lipophilicity of the bb_n ligand, but rather than having a “dangling” bb_n chain, the aim was to use bb_n as a tetradentate ligand to produce $[\text{Ru}(\text{phen})(\text{bb}_n)]^{2+}$: the two accessible geometric isomeric forms of the complex, *cis*- α - $[\text{Ru}(\text{phen})(\text{bb}_n)]^{2+}$ and *cis*- β - $[\text{Ru}(\text{phen})(\text{bb}_n)]^{2+}$ are shown in Figure 5.2 (a, b). While $[\text{Ru}(\text{phen})(\text{bb}_n)]^{2+}$ would be expected to have similar or greater lipophilicity than the most active mononuclear complex, $[\text{Ru}(\text{Me}_4\text{phen})_3]^{2+}$, the two isomeric forms have a different physical shape, and

hence could interact with biological receptors in a different manner. This chapter describes the synthesis of these $[\text{Ru}(\text{phen})(\text{bb}_n)]^{2+}$ complexes, the separation of their geometric isomers and an examination of their antimicrobial activity, cellular accumulation in four bacteria and their affinity for DNA. In addition, fluorescence microscopy was used to examine the uptake of *cis*- α - $[\text{Ru}(\text{phen})(\text{bb}_{12})]^{2+}$ into live *P. aeruginosa*.

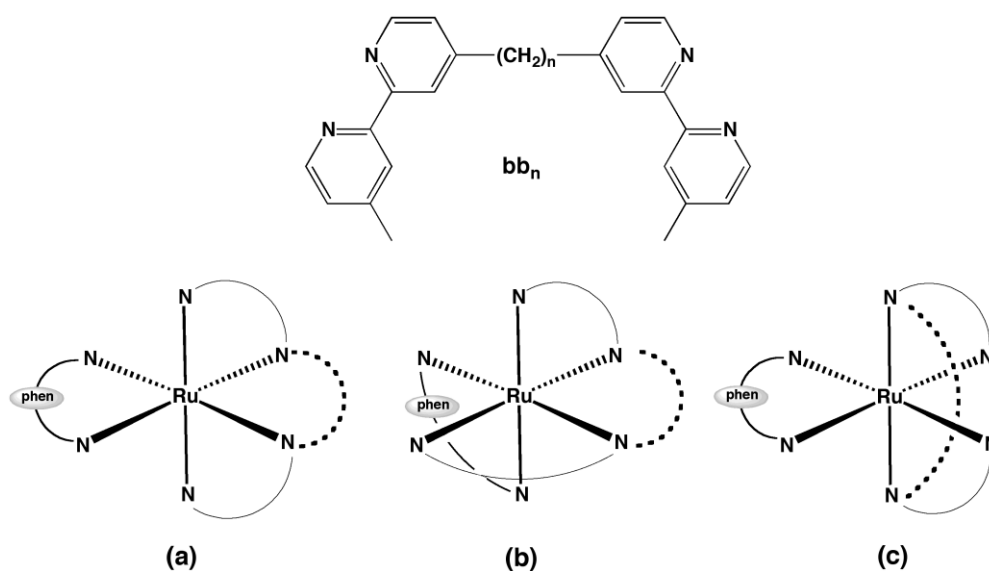


Figure 5.2. The ligand bb_n , and the possible isomeric forms of the mononuclear complex $[\text{Ru}(\text{phen})(\text{bb}_n)]^{2+}$ with bb_n as a tetradentate ligand: (a) *cis*- α isomer, (b) *cis*- β isomer and (c) a form in which the central polymethylene chain spans the trans positions. The isomers shown in (a) and (c) have C_2 point group symmetry, whereas the *cis*- β isomer is asymmetric (C_1).

5.2. *Experimental*

The antimicrobial assays were carried out by the author under the guidance of A/Prof Jeffery Warner, School of Veterinary and Biomedical Sciences, James Cook University, Townsville, QLD 4811, Australia.

5.2.1. *Physical measurements*

^1H NMR and ^{13}C NMR spectra were recorded on a Varian Advance 400 MHz spectrometer at room temperature in D_2O {99.9%, Cambridge Isotope Laboratories (CIL)}, CDCl_3 (99.8%, CIL), CD_3CN (> 99.8%, Aldrich) or CD_3OD (> 99.8%, Aldrich). UV absorbance was measured on a Jenway 6300 spectrophotometer. Mass spectroscopic analysis was performed by the RSC Mass Spectrometry Facility, Research School of Chemistry, Australian National University, Canberra. Microanalyses were performed by the Microanalytical Unit, Research School of Chemistry, Australian National University, Canberra.

5.2.2. *Materials and methods*

Potassium hexafluorophosphate (KPF_6), ammonium hexafluorophosphate (NH_4PF_6) and 1,10-phenanthroline were purchased from Aldrich and used as supplied; Amberlite[®] IRA-402 (chloride form) anion-exchange resin and SP-Sephadex C-25 cation exchanger were obtained from GE Health Care Bioscience. Cation-adjusted Mueller Hinton broth (CAMHB) was purchased from Fluka, Gillingham, UK; the control antibiotics gentamicin and ampicillin were purchased from Oxoid, Australia. The syntheses of ligands bb_n ($n = 10$ and 12) and *cis*- $[\text{Ru}(\text{DMSO})_4\text{Cl}_2]$ were performed according to previously reported methods.^{25,26} The complex *cis,cis*- $[\text{RuCl}_2(\text{DMSO})_2(\text{phen})]$ was

prepared as previously described.²⁷ The ^1H NMR spectrum was consistent with that previously reported.

5.2.3. *Bacterial strains*

The same panel of bacterial strains as mention in Chapter 3, Section 3.2.3 was used for the *in vitro* antimicrobial studies in this chapter.

5.2.4. *MIC determination*

The MIC analyses were conducted by the broth micro-dilution method in duplicate, as outlined in Chapter 3, Section 3.2.4.

5.2.5. *DNA binding studies*

Experiments were carried out in PBS buffer at pH = 7.4. The ratio of the UV absorbance of CT DNA solution at 260 nm and 280 nm was greater than 1.8, indicating the CT DNA was sufficiently free from protein. The DNA concentration of the stock solution (2.35×10^{-3} M) was determined by UV absorbance using a molar absorption coefficient of $13,300 \text{ M}^{-1} \text{ cm}^{-1}$ per base pair at 260 nm. Absorption titration experiments were carried out by keeping the concentration of the ruthenium complex constant (2.5×10^{-5} M) and varying the CT DNA concentration from 0 to 5.0×10^{-5} M. Absorbance values were recorded after each successive addition of CT DNA solution.

5.2.6. *Cellular uptake*

The cellular uptake experiments were carried out according to procedure described in Chapter 3, Section 3.2.5.

5.2.7. *Epifluorescent microscopy*

Epifluorescent microscopy images were obtained using an epifluorescent microscope (AxioImager.Z1, Zeiss, Germany), equipped with a digital camera (AxioCamMRm, Zeiss, Germany). A *P. aeruginosa* inoculum in log phase was adjusted to a 0.5 Macfarland standard and incubated in CAMHB broth containing *cis*- α -[Ru(phen)(bb₁₂)]Cl₂ (at 8 or 32 μ g/mL – 1 or 4 x MIC) for 2 hours. After incubation, 1 mL of the bacterial suspension was centrifuged at 6000 g at 4 °C for 5 minutes and the pellet washed four times and then re-suspended in a final volume of 50 μ L of PBS solution. A sample of the suspension was prepared for viewing by epifluorescence microscopy. Briefly, the bacteria were dried on the Superfrost[®] Plus glass slides (Menzel-Glaser, Germany) and mounted using mounting media (Vectashield, Vector Laboratories, USA). Slides were examined at 63 \times magnification using filter set 45 (Zeiss, Germany) (excitation BP 560/40 nm and emission BP 630/75).

5.2.8. *Lipophilicity (log P) determination*

The log P values were determined according to the procedure described in Chapter 3, Section 3.2.6.

5.2.9. *Syntheses*

All newly synthesised materials were characterised by ¹H NMR, microanalyses and mass spectroscopy. All known materials were characterised by ¹H NMR and were found to be consistent with that previously reported.

[Ru(phen)(bb_n)](PF₆)₂

A solution of *cis,cis*-[RuCl₂(DMSO)₂(phen)] (200 mg, 0.39 mmol), the appropriate bb_n ligand (0.47 mmol) in N₂-purged ethylene glycol (35 mL) was heated to 130-140 °C and stirred under an N₂ atmosphere for 2 h. The colour of the reaction mixture turned from light green to bright orange during the course of the reaction. The reaction mixture was cooled to room temperature and water (10 mL) was added to the bright orange solution, which was then loaded onto a SP Sephadex C-25 cation exchange column (3 cm diam. × 20 cm). The column was washed with water and the desired mononuclear complex was eluted with aqueous 0.3 M NaCl solution. Solid KPF₆ was added to the eluate and the complex was extracted into dichloromethane (2 × 30 mL). The organic layer was washed with water (20 mL), dried over anhydrous Na₂SO₄, and evaporated to dryness to obtain the PF₆⁻ salt of the complex. The complex was further purified by recrystallisation with acetonitrile/diethyl ether to obtain a bright red–orange solid of [Ru(phen)(bb_n)](PF₆)₂. Typical yields were ~20-25 %

[Ru(phen)(bb₁₂)](PF₆)₂. Anal. Calcd. for C₄₆H₅₀N₆F₁₂P₂Ru : C, 51.3%; H, 4.68%; N, 7.8%. Found: C, 51.2%; H, 4.73%; N, 8.0%. TOF MS (ESI⁺): most abundant ion found for [M-2PF₆]²⁺, *m/z* 394.16. Calc. for Ru[C₄₆H₅₀N₆]²⁺, *m/z* 394.15; most abundant ion found for [M-1PF₆]¹⁺, *m/z* 933.27. Calc. for Ru[C₄₆H₅₀N₆](PF₆)₁¹⁺, *m/z* 933.28. ¹H NMR characterisation was carried out for the purified geometrical isomers, see below.

[Ru(phen)(bb₁₀)](PF₆)₂. Anal. Calcd. for C₄₄H₄₆N₆F₁₂P₂Ru: C, 50.3%; H, 4.42%; N, 8.0%. Found: C, 50.0%; H, 4.28%; N, 8.0%. TOF MS (ESI⁺): most abundant ion found for [M-2PF₆]²⁺, *m/z* 380.15. Calc. for Ru[C₄₄H₄₆N₆]²⁺, *m/z* 380.14; most abundant ion found for [M-1PF₆]¹⁺, *m/z* 905.24. Calc. for Ru[C₄₄H₄₆N₆](PF₆)₁¹⁺, *m/z* 905.25. ¹H NMR characterisation was carried out for the purified geometrical isomers (see below).

Separation of Geometric isomers

[Ru(phen)(bb_n)](PF₆)₂ (35 mg, for n = 10, 12) was converted to the chloride salt by stirring in methanol with Amberlite IRA-402 (chloride form) anion-exchange resin for 1 h. After removal of the resin by filtration, the methanol filtrate was evaporated and the resultant chloride salt was dissolved in water (20 mL) and loaded onto a SP Sephadex C-25 cation exchange column (1.5 cm diam. × 90 cm), the symmetrical and unsymmetrical isomers were eluted as two separate bands using aqueous 0.075 M sodium toluene-4-sulfonate solution as eluent. Solid KPF₆ was added to the eluents and the complexes were extracted into dichloromethane (2 × 20 mL). The organic layer was washed with water (20 mL), dried over anhydrous Na₂SO₄, and evaporated to dryness to obtain the PF₆⁻ salt of the complex. The isomers were further purified by recrystallisation with acetonitrile/diethyl ether.

[Ru(phen)(bb₁₂)](PF₆)₂.

Cis-α-isomer. ¹H NMR (400 MHz, CD₃CN): δ 8.60 (dd, *J* = 1.2 Hz, 8.2 Hz, 2H, H4/H7); 8.37 (bs, 2H, bipy3); 8.34 (d, *J* = 1.5 Hz, 2H, bipy3'); 8.25 (s, 2H, H5/H6); 8.20 (dd, *J* = 1.1 Hz, 5.2 Hz, 2H, H2/H9); 7.73 (dd, *J* = 5.2 Hz, 8.2 Hz, 2H, H3/H8); 7.64 (d, *J* = 5.7 Hz, 2H, bipy6'); 7.30 (d, *J* = 5.7 Hz, 2H, bipy6); 7.27 (dd, *J* = 1.7 Hz, 5.8 Hz, 2H, bipy5'); 7.04 (dd, *J* = 1.0 Hz, 5.8 Hz, 2H, bipy5); 2.84 (dd, *J* = 6.7 Hz, 4H, CH₂ bipy); 2.48 (s, 6H, CH₃ bipy); 1.66-1.58 (m, 4H, CH₂ bipy); 1.18-1.04 (m, 16H, 8 × CH₂).

Cis-β-isomer. ¹H NMR (400 MHz, CD₃CN): δ 8.63 (dd, *J* = 1.2 Hz, 4.8 Hz, 1H, H7 [or H4]); 8.61 (dd, *J* = 1.2 Hz, 4.8 Hz, 1H, H4 [or H7]); 8.38 (bs, 1H, bipy3); 8.32 (bs, 1H, bipy3'); 8.31 (m, 2H, bipy3&3'); 8.26 (s, 2H, H5/H6); 8.22 (dd, *J* = 1.3 Hz, 5.3 Hz, 1H, H2 [or H9]); 8.16 (dd, *J* = 1.3 Hz, 5.3 Hz, 1H, H9 [or H2]); 7.79-7.72 (m, 2H, H3/H8);

7.68 (d, $J = 5.8$ Hz, 1H, bipy6); 7.39-7.35 (m, 2H, bipy6&6'); 7.31 (dd, $J = 1.7$ Hz, 5.4 Hz, 1H, bipy5); 7.16 (m, 1H, bipy6'); 7.14-7.09 (m, 2H, bipy5'); 7.06 (dd, $J = 1.2$ Hz, 5.6 Hz, 1H, bipy5); 2.90 (t, $J = 12.6$ Hz, 2H, CH_2 bipy); 2.86-2.78 (m, 2H, CH_2 bipy); 2.56 (s, 3H, CH_3 bipy); 2.47 (s, 3H, CH_3 bipy); 1.82-1.68 (m, 4H, CH_2 bipy); 1.38-1.18 (m, 16H, $8 \times CH_2$).

[Ru(phen)(bb₁₀)](PF₆)₂.

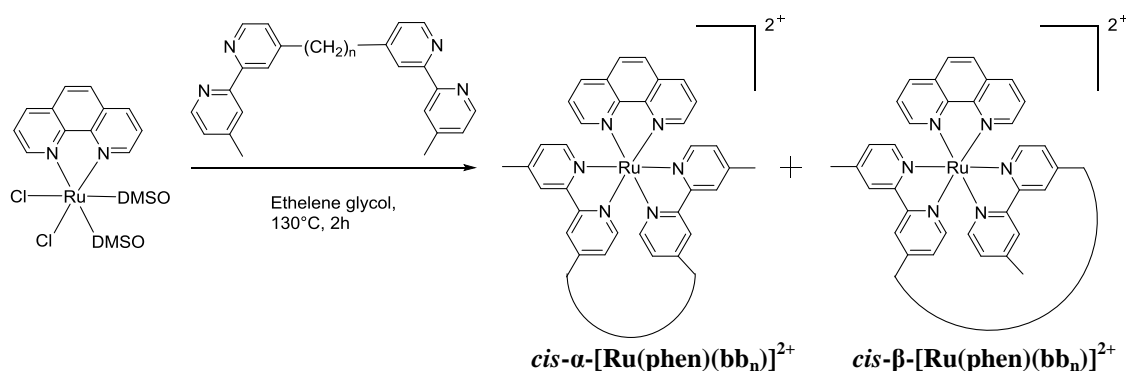
Cis- α -isomer. ¹H NMR (400 MHz, CD₃CN): δ 8.61 (dd, $J = 1.2$ Hz, 8.2 Hz, 2H, H4/H7); 8.36 (bs, 2H, bipy3); 8.31 (d, $J = 1.5$ Hz, 2H, bipy3'); 8.26 (s, 2H, H5/H6); 8.23 (dd, $J = 1.1$ Hz, 5.2 Hz, 2H, H2/H9); 7.73 (dd, $J = 5.2$ Hz, 8.3 Hz, 2H, H3/H8); 7.60 (d, $J = 5.8$ Hz, 2H, bipy6'); 7.27 (d, $J = 5.7$ Hz, 2H, bipy6); 7.23 (dd, $J = 1.5$ Hz, 5.7 Hz, 2H, bipy5'); 7.03 (dd, $J = 1.0$ Hz, 5.8 Hz, 2H, bipy5); 2.83 (t, $J = 6.5$ Hz, 4H, CH_2 bipy); 2.48 (s, 6H, CH_3 bipy); 1.66-1.53 (m, 4H, CH_2 bipy); 1.16-1.01 (m, 12H, $6 \times CH_2$).

Cis- β -isomer. ¹H NMR (400 MHz, CD₃CN): δ 8.66-8.61 (m, 2H, H4/H7); 8.33-8.28 (m, 4H, bipy3&3'); 8.28 (s, 2H, H5/H6); 8.26-8.22 (m, 2H, H2/H9); 7.80 (m, 1H, H3 [or H8]); 7.75 (m, 1H, H8 [or H3]); 7.64 (d, $J = 5.8$ Hz, 1H, bipy6); 7.46 (d, $J = 5.7$ Hz, 1H, bipy6'); 7.39 (d, $J = 5.6$ Hz, 1H, bipy6); 7.34 (m, 1H, bipy5); 7.22 (dd, $J = 1.3$ Hz, 5.9 Hz, 1H, bipy5'); 7.14 (dd, $J = 1.1$ Hz, 5.8 Hz, 1H, bipy5'); 7.09 (dd, $J = 1.0$ Hz, 5.7 Hz, 1H, bipy5); 6.85 (d, $J = 6.0$ Hz, 1H, bipy6'); 2.93-2.86 (m, 2H, CH_2 bipy); 2.84-2.77 (m, 2H, CH_2 bipy); 2.56 (s, 3H, CH_3 bipy); 2.47 (s, 3H, CH_3 bipy); 1.71-1.56 (m, 4H, CH_2 bipy); 1.36-1.10 (m, 12H, $6 \times CH_2$).

5.3. Results

5.3.1. Synthesis

The synthesis of a series of mononuclear $[\text{Ru}(\text{phen})(\text{bb}_n)]^{2+}$ complexes containing the flexible bb_n ligand has been achieved with good yields, as shown in Scheme 5.1. The ruthenium complexes were prepared by refluxing *cis,cis*- $[\text{RuCl}_2(\text{DMSO})_2(\text{phen})]$ with the bb_n ligand in ethylene glycol, and purified by cation exchange chromatography on a SP Sephadex C-25 column using aqueous sodium chloride as the eluent, followed by recrystallisation from acetonitrile/diethyl ether. The *cis*- α and *cis*- β geometrical isomers of the mononuclear $[\text{Ru}(\text{phen})(\text{bb}_n)]^{2+}$ complexes were separated by cation exchange chromatography on a SP Sephadex C-25 column using sodium toluene-4-sulfonate as the eluent and a column length of ~1 metre. The complexes were characterised by microanalysis, NMR spectroscopy and high resolution electrospray ionisation mass spectrometry. Although the $[\text{Ru}(\text{phen})(\text{bb}_n)]^{2+}$ complexes were prepared to examine their antimicrobial activity in comparison with the previously reported Rubb_n and $[\text{Ru}(\text{Me}_4\text{phen})_3]^{2+}$ complexes, they could also be useful as DNA binding probes.¹⁴⁻¹⁷



Scheme 5.1

5.3.2. Geometric isomers

The phen ligand places constraints upon the coordination disposition of the bb_n ligand as a tetradentate, and there are actually three possible geometric isomers for the $[\text{Ru}(\text{phen})(\text{bb}_n)]^{2+}$ complexes – the symmetrical *cis*- α and unsymmetrical *cis*- β forms (see Figure 5.2 a, b respectively), as well as an additional “symmetrical” isomer in which the pyridine groups of two 2,2'-bipyridine moieties bearing the bridging methylene chain are coordinated in *trans* positions around the metal centre (see Figure 5.2 c). The ability of a bidentate ligand containing a polymethylene chain ($n \geq 10$) to function as a *trans*-spanning chelate ring has been reported in the literature,¹⁸ but is not common. Only one of the two possible symmetrical isomers $\{ \text{cis-}\alpha\text{-}[\text{Ru}(\text{phen})(\text{bb}_n)]^{2+} \}$ was observed in the ^1H NMR spectrum of the reaction mixture, indicating that the highly strained (based upon molecular modelling) alternative symmetrical isomer with the *trans*-spanning central ring was not formed, presumably because of steric crowding. The molecular models of the two geometric isomers that were formed are shown in Figure 5.3.

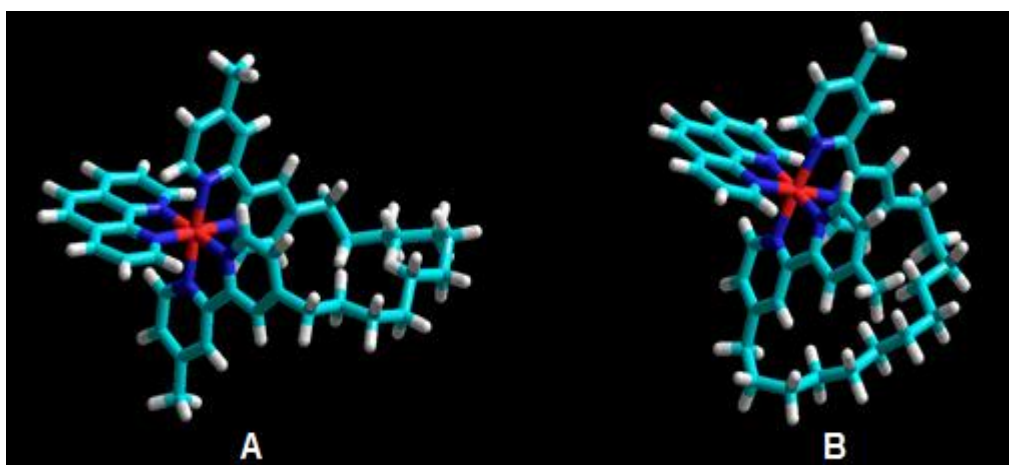


Figure 5.3. Molecular models of the isomers *cis*- α - $[\text{Ru}(\text{phen})(\text{bb}_{12})]^{2+}$ (A) and *cis*- β - $[\text{Ru}(\text{phen})(\text{bb}_{12})]^{2+}$ (B) produced with the HyperChem program. The colours of atoms are: Ru, red; C, cyan; H, white; N, blue.

The structures of the *cis*- α and unsymmetrical *cis*- β isomers were confirmed by NMR spectroscopy. As shown in Figure 5.4 C, only one symmetrical set of resonances is observed for both the phen and bb_n aromatic protons for the *cis*- α - $[\text{Ru}(\text{phen})(\text{bb}_n)]^{2+}$ structure. Alternatively, a near doubling of the number of resonances from the aromatic protons is observed for the unsymmetrical *cis*- β - $[\text{Ru}(\text{phen})(\text{bb}_n)]^{2+}$ structure (see Figure 5.4 B). The identity of the symmetric ruthenium complex was unambiguously determined by comparing ROE cross-peaks in ROESY spectra of the ruthenium complex with inter-proton distances obtained from molecular models of the *cis*- α - $[\text{Ru}(\text{phen})(\text{bb}_n)]^{2+}$ structure.

The relative proportions of the *cis*- α and *cis*- β isomers in the synthesis was dependent upon both the number of added equivalents of the bb_n ligand and the number of methylene groups in the bb_n ligand. For $[\text{Ru}(\text{phen})(\text{bb}_{12})]^{2+}$, the addition of four equivalents of the bb_{12} ligand to *cis,cis*- $[\text{RuCl}_2(\text{DMO})_2(\text{phen})]$ resulted in a 1:1 ratio of *cis*- α /*cis*- β , whereas when only 1.2 equivalents of bb_{12} ligand was used, the observed ratio was 1:2. For $[\text{Ru}(\text{phen})(\text{bb}_{10})]^{2+}$, 1.2 equivalents of bb_{10} resulted in a 1:1.5 ratio of *cis*- α /*cis*- β .

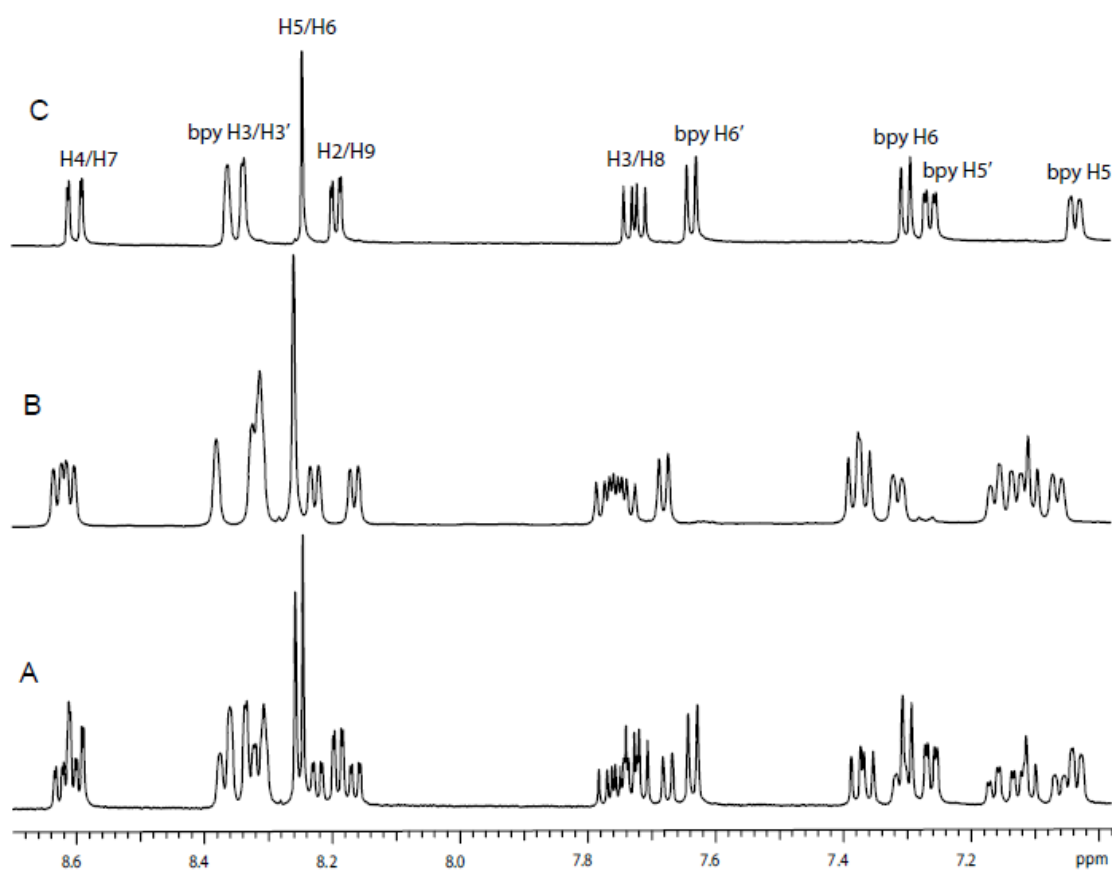


Figure 5.4. Aromatic region of the ^1H NMR spectra of the $[\text{Ru}(\text{phen})(\text{bb}_{12})]^{2+}$ complexes in CD_3CN . (A) mixture of the *cis*- α and *cis*- β isomers, (B) *cis*- β isomer and (C) *cis*- α isomer.

5.3.3. Antimicrobial activity

The minimum inhibitory concentrations (MIC) for the $[\text{Ru}(\text{phen})(\text{bb}_n)]^{2+}$ complexes against four bacterial strains $\{S. aureus, \text{MRSA}, E. coli \text{ and } P. aeruginosa\}$ were determined, and the results are summarised in Table 5.1. The results demonstrate that the $cis\text{-}\alpha\text{-}[\text{Ru}(\text{phen})(\text{bb}_{12})]^{2+}$ and $cis\text{-}\beta\text{-}[\text{Ru}(\text{phen})(\text{bb}_{12})]^{2+}$ complexes have significant antimicrobial activity against both classes of bacteria, but are more active against the Gram positive than the Gram negative species. Of particular note, the $cis\text{-}\alpha\text{-}[\text{Ru}(\text{phen})(\text{bb}_{12})]^{2+}$ complex is two-four times more active than the $cis\text{-}\beta\text{-}[\text{Ru}(\text{phen})(\text{bb}_{12})]^{2+}$ isomer against the Gram negative species, but both isomers show equal activity against the Gram positive bacteria. The $[\text{Ru}(\text{phen})(\text{bb}_{12})]^{2+}$ complexes are two to four-fold more active than the corresponding $[\text{Ru}(\text{phen})(\text{bb}_{10})]^{2+}$ species. While the $cis\text{-}\alpha\text{-}[\text{Ru}(\text{phen})(\text{bb}_{12})]^{2+}$ complex exhibited similar activity to that previously reported for $[\text{Ru}(\text{Me}_4\text{phen})_3]^{2+}$, dinuclear, trinuclear and tetranuclear ruthenium complexes against the Gram positive bacteria and *E. coli*, it was however more active against *P. aeruginosa*.^{10,12} In particular, it was four-fold more active than the $[\text{Ru}(\text{Me}_4\text{phen})_3]^{2+}$ complex.

Table 5.1. MIC values ($\mu\text{g/mL}$) for the ruthenium complexes after 16-18 hours of incubation against Gram positive and Gram negative bacterial strains.

Compounds	Gram positive		Gram negative	
	<i>S. aureus</i>	MRSA	<i>E. coli</i>	<i>P. aeruginosa</i>
<i>cis</i> - α -[Ru(phen)(bb ₁₀)] ²⁺	1	16	32	32
<i>cis</i> - β -[Ru(phen)(bb ₁₀)] ²⁺	1	16	32	32
<i>cis</i> - α -[Ru(phen)(bb ₁₂)] ²⁺	0.5	4	8	8
<i>cis</i> - β -[Ru(phen)(bb ₁₂)] ²⁺	0.5	4	16	32
[Ru(Me ₄ phen) ₃] ²⁺	0.5	4	8	32
[Ru(phen) ₂ (bb ₇)] ²⁺	4	16	16	32
[Ru(phen) ₂ (bb ₁₆)] ²⁺	16	16	64	64
Ampicillin	1	> 128	4	> 128
Gentamicin	< 0.5	32	0.5	1

5.3.4. Log P

Lipophilicity is one factor that affects the biological activity of any metal complex, as it is generally correlated to the capacity of the drug to penetrate through the cell membrane. The standard octanol-water partition coefficient (log P) was determined for the [Ru(phen)(bb_n)]²⁺ complexes and [Ru(Me₄phen)₃]²⁺, and the results are summarised in Table 5.2. As would be expected, the [Ru(phen)(bb₁₂)]²⁺ isomers are more lipophilic than their [Ru(phen)(bb₁₀)]²⁺ analogues. More significantly, the [Ru(phen)(bb₁₂)]²⁺ isomers are more lipophilic than [Ru(Me₄phen)₃]²⁺, of similar lipophilicity to Rubb₁₂-tri and less lipophilic than [Ru(phen)₂(bb₇)]²⁺.

Table 5.2. Octanol-water partition coefficients (log P) for the ruthenium complexes.

Metal complex	Charge	log P
$[\text{Ru}(\text{Me}_4\text{phen})_3]^{2+}$	+ 2	-1.35
* $[\text{Ru}(\text{phen})_2(\text{bb}_7)]^{2+}$	+2	-0.7
<i>cis</i> - α - $[\text{Ru}(\text{phen})(\text{bb}_{10})]^{2+}$	+ 2	-1.2
<i>cis</i> - β - $[\text{Ru}(\text{phen})(\text{bb}_{10})]^{2+}$	+ 2	-1.4
<i>cis</i> - α - $[\text{Ru}(\text{phen})(\text{bb}_{12})]^{2+}$	+ 2	-0.9
<i>cis</i> - β - $[\text{Ru}(\text{phen})(\text{bb}_{12})]^{2+}$	+ 2	-1.0
# Rubb_{12}	+ 4	-2.9
# Rubb_{16}	+ 4	-1.9
# Rubb_{10} -tri	+ 6	-1.3
# Rubb_{12} -tri	+ 6	-1.0
# Rubb_{16} -tri	+ 6	-0.8
# Rubb_{10} -tetra	+ 8	-1.7
# Rubb_{12} -tetra	+ 8	-1.6
# Rubb_{16} -tetra	+ 8	-0.95

* data from ref 16, # data from chapter 3.

5.3.5. Cellular accumulation

As explained in chapter 3, the cellular accumulations of the *cis*- α - $[\text{Ru}(\text{phen})(\text{bb}_{12})]^{2+}$ and *cis*- β - $[\text{Ru}(\text{phen})(\text{bb}_{12})]^{2+}$ complexes in *S. aureus*, MRSA, *E. coli* and *P. aeruginosa* were determined by measuring the concentration of the ruthenium complex remaining in the culture supernatant after removing the bacteria by centrifugation. Figure 5.5 shows the cellular accumulation of *cis*- α - $[\text{Ru}(\text{phen})(\text{bb}_{12})]^{2+}$ and *cis*- β -

$[\text{Ru}(\text{phen})(\text{bb}_{12})]^{2+}$ into the bacteria after 45 minutes of incubation, while Figure 5.6 shows the cellular accumulation as a function of time up to two hours. The *cis*- α - and *cis*- β - $[\text{Ru}(\text{phen})(\text{bb}_{12})]^{2+}$ isomers exhibited higher levels of accumulation in *P. aeruginosa* than with *E. coli*, unlike all other ruthenium complexes (mono- and oligo-nuclear) where accumulation in *E. coli* was consistently either similar to or greater than that with *P. aeruginosa*.^{12,13} Furthermore, both the *cis*- α and *cis*- β isomers of $[\text{Ru}(\text{phen})(\text{bb}_{12})]^{2+}$ exhibited much higher levels of accumulation than either $[\text{Ru}(\text{Me}_4\text{phen})_3]^{2+}$ or $[\text{Ru}(\text{phen})_2(\text{bb}_7)]^{2+}$ with *P. aeruginosa* (see Figure 5.6), but accumulated to similar levels with the tri- and tetra-nuclear Ru_{bb_n} complexes in this bacterium (see chapter 3).

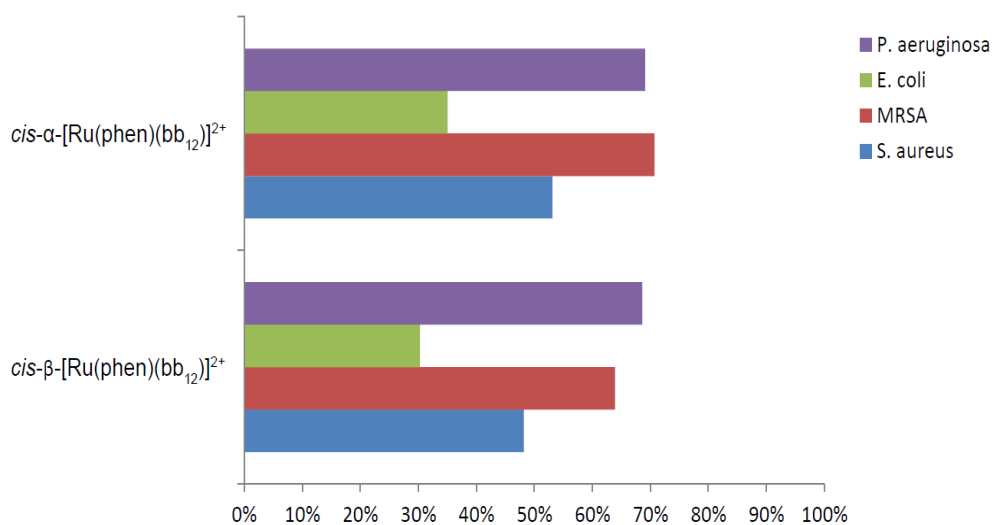


Figure 5.5. Cellular uptake of the *cis*- α - $[\text{Ru}(\text{phen})(\text{bb}_{12})]^{2+}$ and *cis*- β - $[\text{Ru}(\text{phen})(\text{bb}_{12})]^{2+}$ complexes into bacteria after incubation for 45 minutes. The experimental error in all cases is $\leq 5\%$.

Another interesting difference in the accumulation of the *cis*- α and *cis*- β isomers of $[\text{Ru}(\text{phen})(\text{bb}_{12})]^{2+}$ in *P. aeruginosa* was the observed decrease in accumulation over

longer time points, compared to the observed increase in accumulation of $[\text{Ru}(\text{Me}_4\text{phen})_3]^{2+}$ and $[\text{Ru}(\text{phen})_2(\text{bb}_7)]^{2+}$ over a two-hour period (see Figure 5.6).

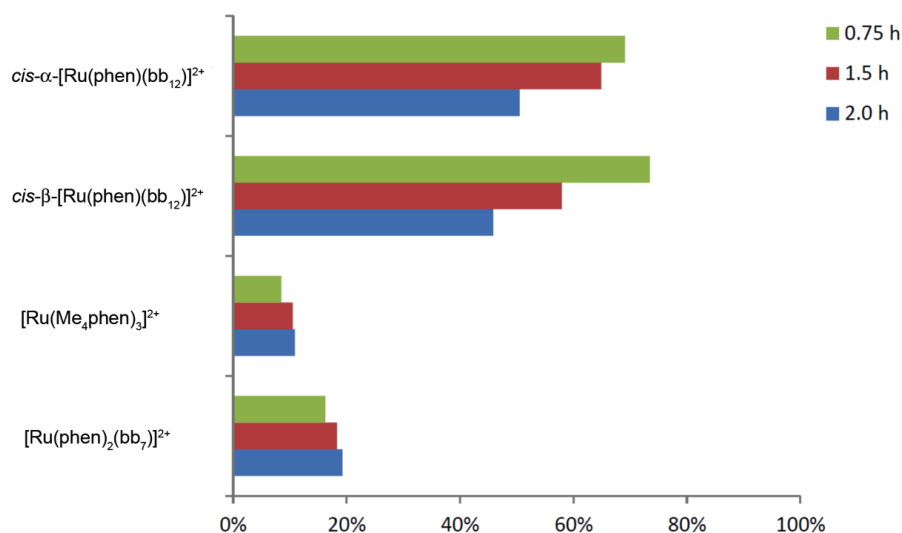


Figure 5.6. Cellular uptake of the $cis-\alpha\text{-}[\text{Ru}(\text{phen})(\text{bb}_{12})]^{2+}$, $cis-\beta\text{-}[\text{Ru}(\text{phen})(\text{bb}_{12})]^{2+}$, $[\text{Ru}(\text{Me}_4\text{phen})_3]^{2+}$ and $[\text{Ru}(\text{phen})_2(\text{bb}_7)]^{2+}$ into *P. aeruginosa* after incubation for 0.75, 1.5 and 2.0 hours. The experimental error is $\leq 5\%$.

5.3.6. Epifluorescence microscopy

In order to confirm the cellular uptake of the ruthenium complexes, the accumulation of $cis-\alpha\text{-}[\text{Ru}(\text{phen})(\text{bb}_{12})]^{2+}$ in *P. aeruginosa* was examined by epifluorescence microscopy. Figure 5.7 shows an epifluorescence microscopic image of *P. aeruginosa* incubated with $cis-\alpha\text{-}[\text{Ru}(\text{phen})(\text{bb}_{12})]^{2+}$ at 8 $\mu\text{g/mL}$ (MIC) for 2 hours. The figure shows that the ruthenium complex is taken up by the bacterium at MIC concentrations. Although the resolution is low, due to the small size of *P. aeruginosa*, the results suggest that the ruthenium complex is not localised within the bacterium (see the lower panel of Figure 5.7), with the $cis-\alpha\text{-}[\text{Ru}(\text{phen})(\text{bb}_{12})]^{2+}$ complex appearing to be evenly distributed throughout cytoplasm. However, when *P. aeruginosa* was incubated with

the ruthenium complex at $4 \times \text{MIC}$, which resulted in a stronger signal and greater contrast, the results do suggest that the ruthenium complex may be localised to a small extent in the bacterium (see Figure 5.8). The phosphorescence¹⁹ from the *cis*- α -[Ru(phen)(bb₁₂)]²⁺ appears to be slightly stronger at the cell poles, in a similar manner to what was observed in an earlier study with the dinuclear complex Rubb₁₆ in *E. coli*.²⁰ However, unlike the results observed with Rubb₁₆, where the dinuclear complex very selectively localised at the cell poles and at particular points in the middle of the cells,²⁰ the selective localisation with *cis*- α -[Ru(phen)(bb₁₂)]²⁺ appears to be much less pronounced. In the study with *E. coli* it was concluded that the Rubb₁₆ selectively bound the RNA of ribosomes, with the unbound chromosomal DNA occupying the remainder of the cytoplasm.²⁰ Based upon the comparison of the fluorescence microscopy results between Rubb₁₆ and *cis*- α -[Ru(phen)(bb₁₂)]²⁺, it is tentatively concluded that *cis*- α -[Ru(phen)(bb₁₂)]²⁺ does not show a significant selectivity for RNA compared to DNA.

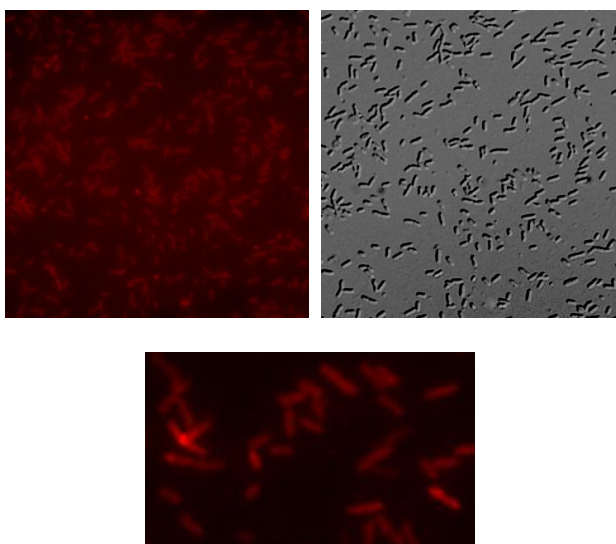


Figure 5.7. Epifluorescence microscopy images of a *P. aeruginosa* sample incubated with 8 $\mu\text{g/mL}$ *cis*- α -[Ru(phen)(bb₁₂)]²⁺ for 2 hours. The fluorescence

microscopy images are: top panel left-hand side phosphorescence, right-hand side phase-contrast, lower panel expansion of the ruthenium complex phosphorescence.

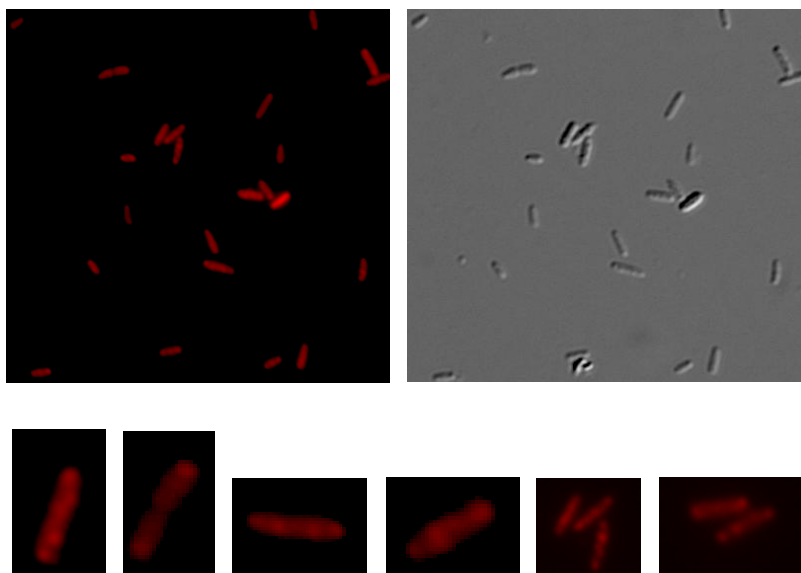


Figure 5.8. Epifluorescence microscopy images of a *P. aeruginosa* sample incubated with 32 $\mu\text{g/mL}$ *cis*- α -[Ru(phen)(bb₁₂)]²⁺ for 2 hours. The fluorescence microscopy images are: top panel left-hand side phosphorescence, right-hand side phase-contrast; lower panel expansions of the ruthenium complex phosphorescence.

5.3.7. Interaction with DNA

In order to determine if the *cis*- α -[Ru(phen)(bb_n)]²⁺ isomers bound DNA with greater affinity than the *cis*- β -[Ru(phen)(bb_n)]²⁺ analogues, the binding of the [Ru(phen)(bb_n)]²⁺ complexes to calf-thymus (CT) DNA was examined by UV-Vis spectroscopy. With increasing concentrations of DNA, the absorbance of the *cis*- α -[Ru(phen)(bb_n)]²⁺ and *cis*- β -[Ru(phen)(bb_n)]²⁺ complexes at 454 nm decreased by 6-10% (e.g. see Figure 5.9). The binding constant (K_b) of the ruthenium complexes with CT DNA was calculated

from the standard equation (Equation 1) using the ratio of slope to the intercept in plots of $[\text{DNA}]/(\epsilon_a - \epsilon_f)$ versus $[\text{DNA}]$.²¹

$$\text{Equation 1: } [\text{DNA}]/(\epsilon_a - \epsilon_f) = [\text{DNA}]/(\epsilon_b - \epsilon_f) + 1/K_b(\epsilon_b - \epsilon_f)$$

where ϵ_a , ϵ_b and ϵ_f are the apparent, free and bound molar absorption coefficients of the ruthenium complexes, $[\text{DNA}]$ is the CT-DNA concentration and K_b is the binding constant.

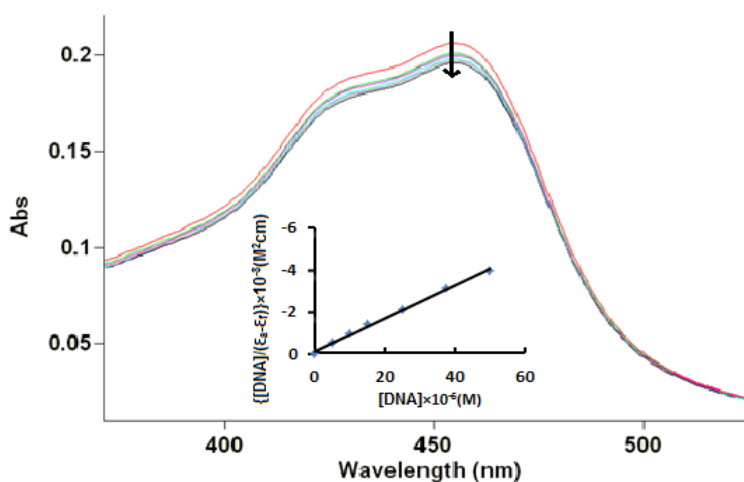


Figure 5.9. UV absorption spectra of $\text{cis-}\alpha\text{-[Ru(phen)(bb}_{12}\text{)]}^{2+}$ in the absence and presence of CT DNA with increasing DNA/complex ratios from 0:1 to 2:1. The arrow shows the changes upon increasing concentrations of CT DNA. Inset: plot of $[\text{DNA}]/(\epsilon_a - \epsilon_f)$ versus $[\text{DNA}]$.

All $[\text{Ru(phen)(bb}_n\text{)]}^{2+}$ complexes showed relatively strong binding to CT DNA, with binding constants of approximately $1 \times 10^6 \text{ M}^{-1}$ (see Table 5.3). However, no significant differences in the DNA binding affinities between the $\text{cis-}\alpha\text{-[Ru(phen)(bb}_n\text{)]}^{2+}$ and $\text{cis-}\beta\text{-[Ru(phen)(bb}_n\text{)]}^{2+}$ isomers were observed. In addition, $[\text{Ru(Me}_4\text{phen)}_3]^{2+}$ bound with similar or even slightly higher affinity than the $[\text{Ru(phen)(bb}_n\text{)]}^{2+}$ complexes.

Table 5.3. The CT DNA binding constants (K_b) of the $[\text{Ru}(\text{phen})(\text{bb}_n)]^{2+}$ complexes and $[\text{Ru}(\text{Me}_4\text{phen})_3]^{2+}$. Estimated maximum error is $\pm 20\%$.

Metal complex	$K_b \text{ (M}^{-1}\text{)}$
$[\text{Ru}(\text{Me}_4\text{phen})_3]^{2+}$	2.0×10^6
<i>cis</i> - α - $[\text{Ru}(\text{phen})(\text{bb}_{10})]^{2+}$	1.0×10^6
<i>cis</i> - β - $[\text{Ru}(\text{phen})(\text{bb}_{10})]^{2+}$	1.1×10^6
<i>cis</i> - α - $[\text{Ru}(\text{phen})(\text{bb}_{12})]^{2+}$	8.0×10^5
<i>cis</i> - β - $[\text{Ru}(\text{phen})(\text{bb}_{12})]^{2+}$	5.0×10^5

5.4. Discussion

Gram negative bacteria have an additional membrane compared to Gram positive species, and this second outer membrane functions as an effective barrier to antimicrobial drugs. One reason for the reduced permeability is that the outer leaflet of the outer membrane is composed of lipopolysaccharide (LPS), rather than the glycerophospholipids usually found in biological membranes.²² LPSs contain six or seven fatty acid chains, rather than the two chains in glycerophospholipids.²¹ As a consequence, a LPS-based bilayer has low fluidity, and hence even hydrophobic drugs partition poorly into the hydrophobic section of the bilayer. Furthermore, while many Gram negative bacteria have high-permeability porins (proteins that produce diffusion channels across membranes), *P. aeruginosa* has only low-efficiency porins suitable for small molecules.^{22,23} Consequently, the development of molecules that can easily cross

the membrane of *P. aeruginosa* is an important aspect in the development of new antimicrobial agents.

It has been previously shown by our group and other researchers that certain types of polypyridylruthenium(II) complexes exhibit good antimicrobial activity against Gram positive bacteria, but only variable activity against Gram negative species.⁸⁻¹² In particular, very few ruthenium(II) complexes, or complexes of other transition metals, have shown good activity against *P. aeruginosa* – a bacterium of current concern.^{1,4} In previous studies we have demonstrated that the mononuclear complexes $[\text{Ru}(\text{Me}_4\text{phen})_3]^{2+}$ or $[\text{Ru}(\text{phen})_2(\text{bb}_7)]^{2+}$ do not readily accumulate in *P. aeruginosa*, and only exhibit modest antimicrobial activities against this bacterium.¹³ Alternatively, tri- and tetra-nuclear complexes readily accumulate in *P. aeruginosa*, but also only exhibit modest activities against this species (chapter 3). The results of this study are significant in terms of the development of new antimicrobial agents in two ways: (1) the *cis*- α - and *cis*- β - $[\text{Ru}(\text{phen})(\text{bb}_{12})]^{2+}$ complexes readily accumulate in *P. aeruginosa* (and to a considerably greater extent than in *E. coli*), and the *cis*- α - $[\text{Ru}(\text{phen})(\text{bb}_{12})]^{2+}$ complex shows good activity against *P. aeruginosa*, albeit still with lower activity than with Gram positive species; and (2) more generally, this study suggests that in future development of metal-based antimicrobial agents, it could be advantageous to increase lipophilicity by incorporating alkane groups in an expanded chelate ring, such as in *cis*- α - $[\text{Ru}(\text{phen})(\text{bb}_{12})]^{2+}$, rather than through the addition of an alkyl chain or methyl groups on aromatic ligands.

The $[\text{Ru}(\text{phen})(\text{bb}_n)]^{2+}$ complexes can be synthesised in good yield and the geometric isomers easily separated. The $[\text{Ru}(\text{phen})(\text{bb}_n)]^{2+}$ complexes are slightly more lipophilic than $[\text{Ru}(\text{Me}_4\text{phen})_3]^{2+}$, but less lipophilic than $[\text{Ru}(\text{phen})_2(\text{bb}_7)]^{2+}$. However,

the $[\text{Ru}(\text{phen})(\text{bb}_n)]^{2+}$ complexes accumulate in *P. aeruginosa* to a considerably greater extent than either $[\text{Ru}(\text{Me}_4\text{phen})_3]^{2+}$ or $[\text{Ru}(\text{phen})_2(\text{bb}_7)]^{2+}$. This suggests that the differences in cellular uptake between these ruthenium complexes is not primarily related to lipophilicity, as judged by log P, but due to other structural characteristics that affect membrane permeability.

For both the *cis*- α - and *cis*- β - $[\text{Ru}(\text{phen})(\text{bb}_{12})]^{2+}$ isomers, the level of cellular accumulation in *P. aeruginosa* initially rose to high levels over 45 minutes, but then decreased to some extent over the next 75 minutes. Alternatively, for both $[\text{Ru}(\text{Me}_4\text{phen})_3]^{2+}$ and $[\text{Ru}(\text{phen})_2(\text{bb}_7)]^{2+}$, although the initial accumulation was considerably less than that observed with the *cis*- α - and *cis*- β - $[\text{Ru}(\text{phen})(\text{bb}_{12})]^{2+}$ isomers, no decrease in accumulation was observed at longer time points up to two hours. Although further studies are required, the results tentatively suggest that *P. aeruginosa* may be able to induce an effective efflux pump against the *cis*- α - and *cis*- β - $[\text{Ru}(\text{phen})(\text{bb}_{12})]^{2+}$ complexes.

It is not clear why *cis*- α - $[\text{Ru}(\text{phen})(\text{bb}_{12})]^{2+}$ is more active than *cis*- β - $[\text{Ru}(\text{phen})(\text{bb}_{12})]^{2+}$ against *P. aeruginosa*, as both isomers accumulated to a similar degree in the bacterium. Previous studies have demonstrated the di- and oligo-nuclear $\text{Ru}(\text{bb}_n)$ complexes target DNA and RNA in both bacterial and eukaryotic cells.^{20,24} Although further studies at higher magnification are required, the results from the initial epifluorescence microscopy study suggests that unlike the dinuclear ruthenium complex, $\text{Ru}(\text{bb}_{16})$, which shows a high degree of selectivity for ribosomes (RNA), the *cis*- α -isomer binds chromosomal DNA with similar affinity compared with ribosomal RNA. However, the results of the DNA binding studies for the $[\text{Ru}(\text{phen})(\text{bb}_n)]^{2+}$ complexes suggest that nucleic acid binding affinity is not likely to be the explanation

of the greater activity of $cis\text{-}\alpha\text{-}[\text{Ru}(\text{phen})(\text{bb}_{12})]^{2+}$, compared to $cis\text{-}\beta\text{-}[\text{Ru}(\text{phen})(\text{bb}_{12})]^{2+}$. While the overall DNA (and potentially RNA) binding affinities are similar, it is probable that the biological consequences of the DNA binding could be different (e.g. through different specific high affinity sites), and thereby result in different antimicrobial activities.

5.5. Conclusions

In conclusion, the results of this study indicate that the ruthenium(II) complex $cis\text{-}\alpha\text{-}[\text{Ru}(\text{phen})(\text{bb}_{12})]^{2+}$ can readily accumulate in *P. aeruginosa*, and to a far greater extent than in *E. coli*, and exhibit good antimicrobial activity against either of the bacteria. The results suggest that the structural differences between $cis\text{-}\alpha\text{-}[\text{Ru}(\text{phen})(\text{bb}_{12})]^{2+}$ and the mononuclear complexes previously studied $\{[\text{Ru}(\text{Me}_4\text{phen})_3]^{2+}$ and $[\text{Ru}(\text{phen})_2(\text{bb}_7)]^{2+}\}$ are significant in terms of interactions with the outer membrane of *P. aeruginosa*. As a consequence, and given that the structure can be readily modified, it is possible that ruthenium(II) complexes can be customised to particular bacteria. Perhaps, the results of this study suggest a new structural motif for metal-based antimicrobial drugs, paving the way forward for the development of new antimicrobial agents for Gram negative bacteria.

5.6. References

1. H. W. Boucher, G. H. Talbot, J. S. Bradley, J. E. Jr Edwards, D. Gilbert, L. B. Rice, M. Scheld, B. Spellberg and J. Bartlett, *IDSA Report on Development Pipeline*, 2009, **48**, 1.
2. E. A. Azzopardi, E. L. Ferguson and D. W. Thomas, *J. Antimicrob. Chemother.*, 2013, **68**, 257.
3. H. Nikaido and J.-M. Pagès, *FEMS Microbiol. Rev.*, 2012, **36**, 340.
4. T. Strateva and D. Yordanov, *J. Med. Microbiol.*, 2009, **58**, 1133.
5. Z. Drulis-Kawa, J. Gubernator, A. Dorotkiewicz-Jach, W. Doroskiewicz and A. Kozubek, *Int. J. Pharmaceutics*, 2006, **315**, 59.
6. H. P. Schweizer, *Expert Opin. Drug Discov.*, 2012, **7**, 633.
7. R. E. W. Hancock, *Clinical Infectious Diseases*, 1998, **27** (Suppl 1), S93.
8. A. Bolhuis, L. Hand, J. E. Marshall, A. D. Richards, A. Rodger and J. Aldrich-Wright, *Eur. J. Pharm. Sci.*, 2011, **42**, 313.
9. C. S. Devi, D. A. Kumar, S. S. Singh, N. Gabra, N. Deepika, Y. P. Kumar and S. Satyanarayana, *Eur. J. Med. Chem*, 2013, **64**, 410.
10. F. Li, Y. Mulyana, M. Feteri, J. Warner, J. G. Collins and F. R. Keene, *Dalton Trans.*, 2011, **40**, 5032.
11. M. Pandrala, F. Li, M. Feterl, Y. Mulyana, J. M. Warner, L. Wallace, F. R. Keene and J. G. Collins, *Dalton Trans.*, 2013, **42**, 4686.

12. A. K. Gorle, M. Feterl, J. M. Warner, L. Wallace, F. R. Keene and J. G. Collins, *Dalton Trans.*, 2014, **43**, 16713.
13. F. Li, M. Feterl, Y. Mulyana, J. M. Warner, J. G. Collins and F. R. Keene, *J. Antimicrob. Chemother.*, 2012, **67**, 2686.
14. B. M. Zeglis, V. C. Pierre and J. K. Barton, *Chem. Commun.*, 2007, 4565.
15. C. Metcalfe and J. A. Thomas, *Chem. Soc. Rev.*, 2003, **32**, 215.
16. F. R. Keene, J. A. Smith and J. G. Collins, *Coord. Chem. Rev.*, 2009, **253**, 2021.
17. M. R. Gill and J. A. Thomas, *Chem. Soc. Rev.*, 2012, **41**, 3179.
18. A. J. Pryde, E. L. Shaw and E. Weeks, *J. Chem. Soc., Chem. Commun.*, 1973, 947.
19. While microscopy techniques involving luminescence are conventionally referred to as “fluorescence microscopy”, in the case of polypyridylruthenium(II) complexes the luminescence is in fact phosphorescence as emission involves transition from a triplet excited state to a singlet ground state – whereas fluorescence involves transition between singlet excited and ground states.
20. F. Li, E. J. Harry, A. L. Bottomley, M. D. Edstein, G. W. Birrell, C. E. Woodward, F. R. Keene and J. G. Collins, *Chem. Sci.*, 2014, **5**, 685.
21. A. Srishailam, N. M. Gabra, Y. P. Kumar, K. L. Reddy, C. S. Devi, D. A. Kumar, S. S. Singh and S. Satyanarayana, *J. Photochem. Photobiol B: Biology*, 2014, **141**, 47.

22. H. Nikaido, *Science*, 1994, **264**, 382.
23. S. Tamber, E. Maier, R. Benz and R. E. W. Hancock, *J. Bacteriol.*, 2007, **189**, 929.
24. X. Li, A. K. Gorle, T. D. Ainsworth, K. Heimann, C. E. Woodward, J. G. Collins and F. R. Keene, *Dalton Trans.*, 2015, **44**, 3594.
25. Y. Mulyana, D. K. Weber, P. D. Buck, C. A. Motti, J. G. Collins and F. R. Keene, *Dalton Trans.*, 2011, **40**, 1510.
26. I. P. Evans, A. Spencer and G. Wilkinson, *J. Chem. Soc. Dalton Trans.* 1973, 204.
27. H. A. Hudali, J. V. Kingston and H. A. Tayim, *Inorg. Chem.*, 1979, **18**, 1391.
28. Clinical and Laboratory Standards Institute. *Performance Standards for Antimicrobial Susceptibility Testing: Nineteenth Informational Supplement M100-S19*. CLSI, Wayne, PA, USA, 2009.

CHAPTER 6

Conclusions and Future Perspectives

6.1. Conclusions

Ruthenium complexes have been widely examined for their use as therapeutic agents, and are considered as an alternative to existing platinum-based drugs.¹⁻⁶ This thesis has explored the potential of polypyridylruthenium(II) complexes as antimicrobial and anticancer agents.

A series of dinuclear ruthenium complexes - containing a single chlorido ligand on each metal centre (Cl-Rubb_n, Cl-RubbN_n, Cl-Rubb_nNO₂ and Cl-RubbN_nNO₂) were synthesised and characterised (chapter 2). Their anticancer activities against two breast cancer cell lines were examined. The Cl-Rubb_n complexes were found to be significantly more active than cisplatin against these cell lines. Aquation and GMP binding studies on these complexes revealed that the anticancer activity appears to be due to a combination of covalent and reversible binding with DNA. The IC₅₀ results indicated that the Cl-Rubb₁₂ complex was the most active of the dinuclear complexes. The superior activity of Cl-Rubb₁₂ might be due to the best compromise between lipophilicity (for cellular uptake) and the cytotoxic effects of the covalent adducts formed with DNA.

A series of inert tri- and tetra-nuclear ruthenium(II) complexes have been synthesised and characterised (chapter 3). These complexes were tested for their antimicrobial activity against Gram positive and Gram negative bacterial strains. Complexes with the bb₁₂ linking ligand were the most active against *S. aureus*, MRSA, and *E. coli*, with the complexes having the shortest (bb₁₀) and longest (bb₁₆) linking chain being the least active. However, against *P. aeruginosa*, complexes with the bb₁₆ linking ligand showed better activity. Surprisingly, the cellular uptake of these complexes is slightly higher for the Gram negative bacteria than the Gram positive. For

both the Gram positive and Gram negative bacteria, the cellular accumulation of the tetranuclear metal complexes was slightly lower than with the trinuclear counterparts, however, the uptake of Rubb₁₂-tetra-nl was greater than Rubb₁₂-tetra and Rubb₁₂-tri. The results confirmed the bactericidal nature of Rubb₁₂-tri and Rubb₁₂-tetra, as $2 \times \text{MIC}$ was sufficient to kill 99.9% of the bacterial population. Interestingly, both Rubb₁₂-tri and Rubb₁₂-tetra kill 99.9% of the Gram negative bacteria (3-4 hours) more quickly than the Gram positive species (4-6 hours).

Chapter 4 describes the antimicrobial activities of the polypyridylruthenium(II) complexes against a wider range of clinically relevant bacteria and their toxicity to liver and kidney cells. In addition, the serum level concentration and tissue accumulation of Rubb₁₆ and Rubb₁₂-tetra in mice were also examined. The results of this study demonstrate that the ruthenium complexes are highly active against Gram positive bacteria but they were less active against Gram negative bacteria. Compared to the tri- and tetra-nuclear complexes, the dinuclear Rubb₁₂ complex was less toxic to liver and kidney cells. The *in vivo* experiments demonstrate that the serum level concentrations of both Rubb₁₆ and Rubb₁₂-tetra were less than the MIC values against Gram positive and Gram negative bacteria, and both the complexes accumulated mainly in the liver and kidney after dosing.

In Chapter 5, it was shown that the mononuclear ruthenium(II) complex, *cis*- α -[Ru(phen)(bb₁₂)]²⁺, can readily accumulate in *P. aeruginosa*, and to a far greater extent than in *E. coli*, and exhibited good antimicrobial activity against either of the bacteria. The results suggest that the structural differences between *cis*- α -[Ru(phen)(bb₁₂)]²⁺ and the mononuclear complexes previously studied {[Ru(Me₄phen)₃]²⁺ and [Ru(phen)₂(bb₇)]²⁺} are significant in terms of interactions with the outer membrane of

P. aeruginosa.

The results of this study suggests that polypyridylruthenium(II) complexes have significant potential as therapeutic agents. The antimicrobial potential was confirmed through the screening of a range of the ruthenium complexes against a panel of clinical isolates. The results also confirmed the high activity of the ruthenium complexes towards Gram positive bacteria, but only variable activity against Gram negative species. It was originally proposed that tri- and tetra-nuclear ruthenium complexes linked by the bb_n ligand might be more active than their $Rubb_n$ dinuclear counterparts. The synthesised tri- and tetra-nuclear complexes were found to be more active than the dinuclear analogues, with $Rubb_{12}$ -tetra showing the best antimicrobial activity. Furthermore, $Rubb_{12}$ -tri exhibited the best selective toxicity towards bacteria, compared to eukaryotic cells. The increased lipophilicity of the tri- and tetra-nuclear complexes allowed them to accumulate in bacterial cells, particularly Gram negative species, to a greater degree than the $Rubb_n$ complexes. However, this suggests the lower antimicrobial activity of the ruthenium complexes towards Gram negative bacteria, may not be strongly correlated to the cellular accumulation, but rather to a lower intrinsic ability to kill the Gram negative cells. In addition, the pharmacokinetic study demonstrated that increasing the lipophilicity decreased the concentration of the ruthenium complex in the blood. For $Rubb_{12}$ -tetra, the blood serum concentration in mice was below MIC concentrations 30 minutes after administration. It is clear that the rate of transfer from muscle tissue to the blood is much slower than the rate of clearance from the blood to the organs, particularly the liver. These results highlight a possible disadvantage to the commonly used approach for increasing *in vitro* antimicrobial or anticancer activity – increasing the lipophilicity of the drug.

Although log P is commonly used to compare lipophilicity of potential drugs, the results of this study suggest that it should only be used to compare the lipophilicity of members of a closely related family of compounds. Thomas and co-workers have shown the DNA imaging potential of the dinuclear polypyridylruthenium(II) complex $[\{\text{Ru}(\text{phen})_2\}_2(\mu\text{-tpphz})]^{4+}$ {tpphz = tetrapyrrodo[3,2-*a*:2',3'-*c*:3'',2''-*h*:2''',3'''-*j*]phenazine}; however, the bipyridine analogue $[\{\text{Ru}(\text{bpy})_2\}_2(\mu\text{-tpphz})]^{4+}$ showed no uptake in live cells.⁷ Rubb₁₂ (log P = - 2.7) is significantly less lipophilic than $[\{\text{Ru}(\text{bpy})_2\}_2(\mu\text{-tpphz})]^{4+}$ (log P = -1.6), but still rapidly accumulates in bacterial or eukaryotic cells. This indicates that dinuclear, or oligonuclear, complexes linked by flexible alkane chain can cross cellular membranes more readily than ruthenium complexes linked by relatively bulky rigid linking ligands. Notwithstanding the above, incorporation of the bb_n chain into a chelate ring as with the ruthenium complex *cis*- α -[Ru(phen)(bb₁₂)]²⁺ demonstrated that the alkane chain does not need to be a linear extended structure that resembles the fatty acid chain of a phospholipid. The good cellular uptake and relatively high activity of *cis*- α -[Ru(phen)(bb₁₂)]²⁺ against both *E. coli* and *P. aeruginosa* suggests that this type of structure has good potential as an antimicrobial agent against Gram negative bacteria. Although it is yet to be established, it is possible that *cis*- α -[Ru(phen)(bb₁₂)]²⁺, like [Ru(Me₄phen)₃]²⁺, does not make the bacterial cell membrane permeable; but primarily exhibits antimicrobial activity through nucleic acid binding. Should this be proven, it could then be possible to balance membrane permeabilisation with nucleic acid binding in order to obtain ruthenium complexes with optimally high antimicrobial activity and low eukaryotic cell toxicity. The results of this thesis suggests that the Rubb_n class of polypyridylruthenium(II) complexes have the potential to be effective therapeutic agents. The anticancer activity of the Cl-Rubb_n complexes support the idea of developing a new class of anticancer

agent by transferring from platinum to ruthenium the concept of gaining advantages in efficacy through the use of multinuclear complexes, however, further studies are required to understand more about their anticancer properties.

6.2. Future perspectives

As described in chapter 2, the substitution of electron withdrawing groups on the tridentate ligand (tpy) and the inclusion of amine groups in the alkane chain of the bb_n bridging ligand decreased the anticancer activity of Cl-Rubb $_n$ complexes. Since the electron withdrawing groups have reduced the activity, it could be possible to increase the lipophilicity and thereby activity by introducing electron donating groups such as $-CH_3$ and $-OCH_3$ (instead of electron withdrawing groups such as $-NO_2$) on the tpy ligand of Cl-Rubb $_n$ complexes. Half-sandwich complexes developed by Sadler and co-workers have shown promising anticancer properties, these complexes use arene moieties as ligands.^{8,9} The replacement of tridentate 'tpy' ligand of Cl-Rubb $_n$ complexes with arene moieties (for e.g. *p*-cymene) could possibly enhance the anticancer properties of these complexes (see Figure 6.1).

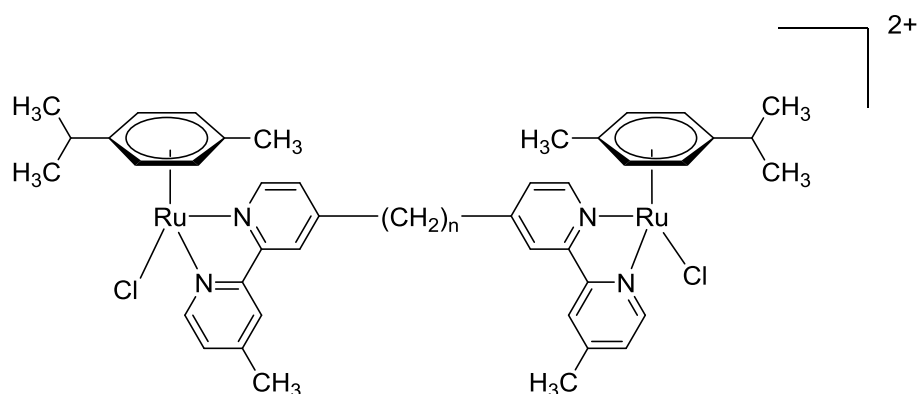


Figure 6.1. Dinuclear Cl-Rubb $_n$ complex containing arene moiety instead of tpy ligand.

The tri- and tetra-nuclear complexes are more toxic to bacteria than to eukaryotic cells. These complexes should be further investigated to identify their mode of entry into bacterial cells. As with the dinuclear Rubb_n complexes, if these tri- and tetra-nuclear complexes also enter the bacterial cells in an energy-independent manner and significantly depolarise and permeabilise the cellular membrane, then these complexes could be used in conjunction with antibiotics which have low cellular uptake properties. As these complexes are highly toxic to bacteria, it is possible that they could also display better activities against cancer cell lines. The *in vivo* experiments demonstrate that both Rubb_{16} and Rubb_{12} -tetra exhibit low serum level concentrations when compared to the MIC values against the bacterial strains due to the slow rate of release of these complexes from muscle into the blood. The dinuclear complex containing two chlorido ligands on one ruthenium centre, $\text{Cl}_2\text{-Rubb}_{12}$ (see Figure 6.2), showed good activity against bacteria with low levels of toxicity to eukaryotic cells. As this complex would be less lipophilic than Rubb_{12} -tetra, the rate of release of $\text{Cl}_2\text{-Rubb}_{12}$ from muscle into the blood could be better, resulting in improved serum level concentration.

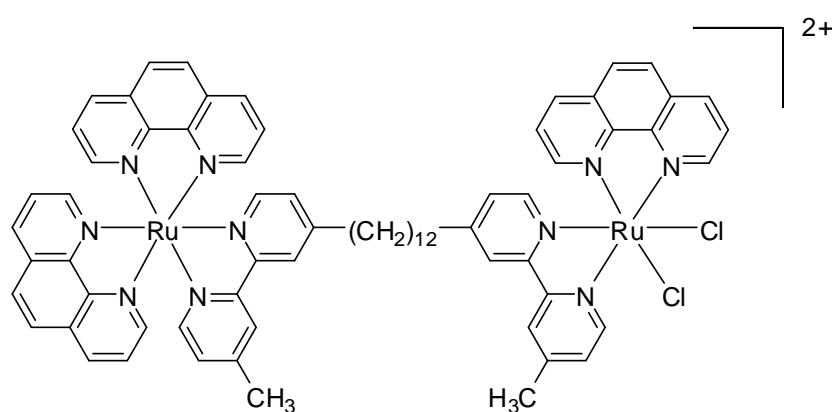


Figure 6.2. Dinuclear ruthenium complex, $\text{Cl}_2\text{-Rubb}_{12}$.

The mononuclear ruthenium complexes, $[\text{Ru}(\text{phen})(\text{bb}_n)]^{2+}$, described in chapter 5, showed excellent antimicrobial properties, in particular against Gram negative bacteria. These complexes could be further explored to obtain a better understanding of their mode of action against this class of bacteria. In order to develop these complexes as therapeutic agents, their *in vitro* toxicity to healthy eukaryotic cells and *in vivo* efficacy on a healthy animal model should be examined. The high toxicity of these complexes to bacteria indicates that they could be investigated for their potential anticancer properties as well. Finally, given that the structure can readily be modified, it is possible that these ruthenium(II) complexes can be developed as potential candidate for clinical usage.

6.3. References

1. C. S. Allardyce and P. J. Dyson, *Platin. Met. Rev.*, 2001, **45**, 62.
2. V. Brabec and O. Novakova, *Drug Resistance Updates*, 2006, **9**, 111.
3. J. Reedijk, *Platinum Met. Rev.*, 2008, **52**, 2.
4. I. Kostova, *Current Medicinal Chemistry*, 2006, **13**, 1085.
5. G. Süss-Fink, *Dalton Trans.*, 2010, **39**, 1673.
6. W. H. Ang and P. J. Dyson, *Eur. J. Inorg. Chem.*, 2006, 4003.
7. M. R. Gill, J. Garcia-Lara, S. J. Foster, C. Smythe, G. Battaglia and J. A. Thomas, *Nat. Chem.*, 2009, **1**, 662.
8. R. E. Aird, J. Cummings, A. A. Ritchie, M. Muir, R. E. Morris, H. Chen, P. J. Sadler and D. I. Jodrell. *Br. J. Cancer.*, 2002, **86**, 1652.
9. S. H. van Rijt and P. J. Sadler, *Drug Discov. Today*, 2009, **14**, 1089.

APPENDIX

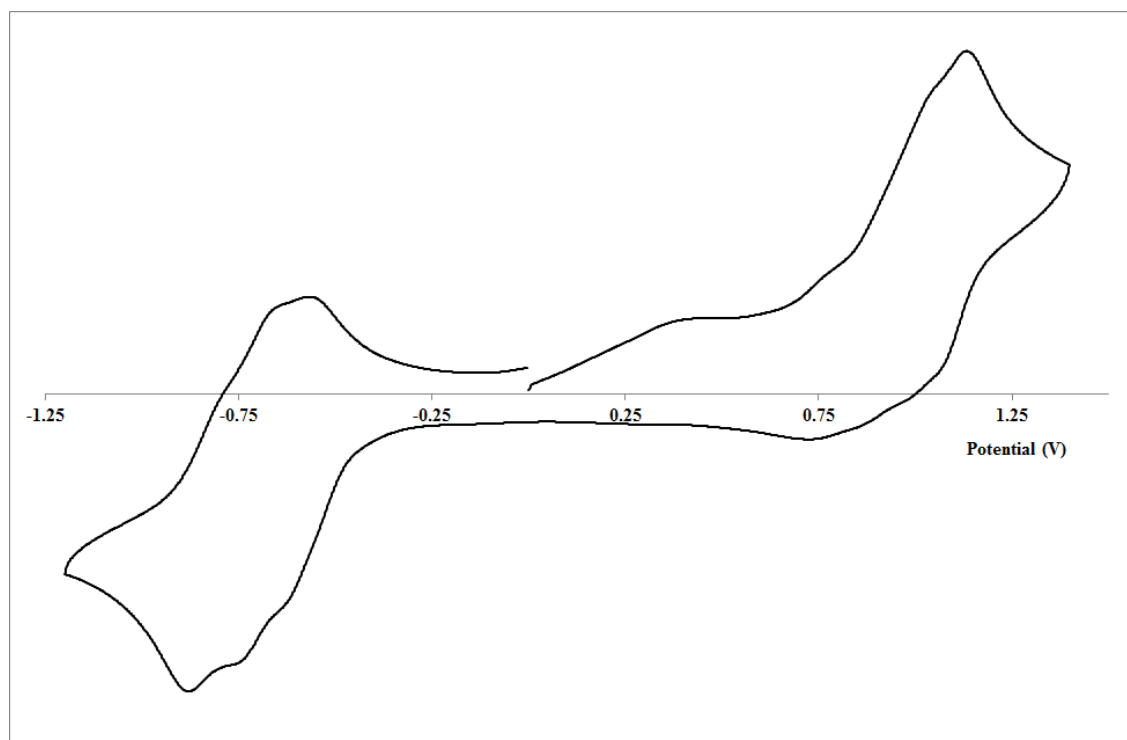


Figure A1. Cyclic voltammogram of $[\text{Ru}\{(\text{NO}_2)_3\text{tpy}\}(\text{Me}_2\text{bpy})\text{Cl}]\text{Cl}$ in acetonitrile.

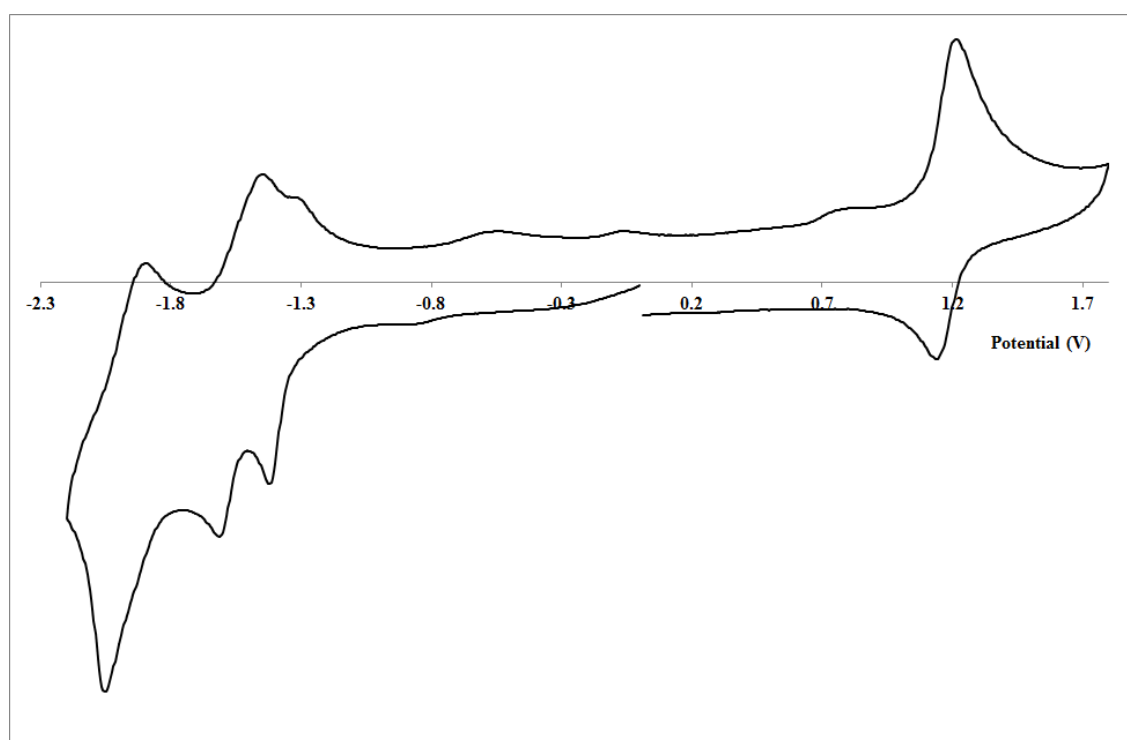


Figure A2. Cyclic voltammogram of Rubb_{12} in acetonitrile.